An Exploration Framework for Porphyry to Epithermal Transitions in the Toodoggone Mineral District (94E)

Farhad Bouzari, Thomas Bissig, Craig J.R. Hart, and Hildebrando Leal-Mejía

Geoscience BC Report 2019-08
MDRU Publication 424

Geoscience BC

MDRU
MINERAL DEPOSIT RESEARCH UNIT

THE UNIVERSITY OF BRITISH COLUMBIA

An Exploration Framework for Porphyry to Epithermal Transitions in the Toodoggone Mineral District (94E)

Farhad Bouzari, Thomas Bissig, Craig J.R. Hart, and Hildebrando Leal-Mejía

Geoscience BC* Report 2019-08

MDRU Publication 424

Keywords: porphyry deposits, epithermal deposits, Toodoggone, exploration, British Columbia

Suggested Citation:
Bouzari, F., Bissig, T., Hart, C.J.R., Leal-Mejía, H. (2019). An Exploration Framework for Porphyry to Epithermal Transitions in the Toodoggone Mineral District (94E). Geoscience BC Report 2019-08, MDRU Publication 424, 101 p.

Report prepared by MDRU†

Dept. Earth, Ocean and Atmospheric Sciences, The University of British Columbia
Vancouver, BC V6T 1Z4, Canada
Tel: +1-604-822-6136
Email: mdru@eoas.ubc.ca

Includes bibliographic references.
Electronic monograph issued in PDF format.
ISBN 978-0-88865-319-2

*Geoscience BC is an independent, non-profit organization that generates earth science in collaboration with First Nations, local communities, government, academia and the resource sector. Our independent earth science enables informed resource management decisions and attracts investment and jobs. Geoscience BC gratefully acknowledges the financial support of the Province of British Columbia.

†MDRU—Mineral Deposit Research Unit is an internationally-recognized collaborative venture between the mining industry and Earth, Ocean and Atmospheric Sciences Department at The University of British Columbia (UBC), established with assistance from the Natural Sciences and Engineering Research Council of Canada (NSERC), and devoted to solving mineral exploration-related problems.

Cover image: North Ridge, about 1750m a.s.l., looking northeast to the quartz-sericite altered areas that form rusty pale-brown outcrops. The Toodoggone River, at about 1050m a.s.l., forms the valley with Mount Katharin (2335m a.s.l.) on the opposing side of the valley. The Sofia porphyry copper prospect is located in the Toodoggone River valley about 3.3 km east of the North Ridge.

ABSTRACT

The Toodoggone district in the Stikine terrane of northeastern British Columbia is one of few mineral districts in BC and worldwide that host a significant number of preserved Early Jurassic high- and low-sulfidation epithermal-type deposits. These deposits are hosted by a thick (>2 km) succession of Early Jurassic sub-aerial andesitic and dacitic volcanic rocks of Toodoggone Formation. These and underlying strata were probably covered by thick successions (>4 km) of Jurassic and Cretaceous Bowser and Sustut basin clastic strata that protected and facilitated preservation of the epithermal deposits during subsequent, post-Late Cretaceous uplift.

New age relationships suggest that epithermal-type deposits formed contemporaneously with pluton emplacement and porphyry-type K-silicate alteration at depth. The Re-Os age (193.8 ± 0.8 Ma) of molybdenite from Baker mine mineralization overlaps with nearby K-feldspar-altered coarse-grained granodiorite (Duncan pluton) that gives a U-Pb zircon age of 193.4 ± 2.6 Ma. Similar temporal relationships are evident for epithermal-type mineralization at Alunite Ridge and the 189.6 ± 2.1 Ma K-silicate-altered granodiorite which hosts porphyry copper mineralization at the Sofia occurrence.

Field observations, alteration assemblages, vein types, trace metal concentrations and the evaluation of fluid inclusions indicate that some of the epithermal-type veins that were previously classified as low-sulfidation have alteration features indicative of shallow-level porphyry systems. Quartz-sericite-pyrite alteration lacking kaolinite occurs at Baker mine, Black Gossan and Sofia. White micas in sericite alteration at these localities are moderately crystalline (>1.75 index) and K-rich on the basis of SWIR data. Such alteration characteristics are also features of shallow-level porphyry systems. Occurrences of pyrophyllite with quartz-sericite alteration at the Brenda mine also indicate shallow porphyry alteration rather than typical advanced argillic related to epithermal environment.

The occurrence of quartz-magnetite±pyrite±chalcopyrite in drill holes at the Baker mine indicates a transition towards porphyry alteration just 100-150 m below the surface. Such K-silicate alteration also occurs in several valley cuts into the deeper exposed plutons in the district such as at Black Gossan, suggesting that porphyry-level alteration is exposed.

Fluid inclusion analysis indicate near-surface exposures of high temperature (up to 556 °C) and saline (up to 50 wt.% NaCl equiv.) fluids associated with quartz veins and K-silicate alteration at the Baker mine that are characteristic of deep level porphyry-type alteration. More importantly, these fluids occur only 100-200 m below the surface where lower temperature (<358°C) and dilute (<2.6% wt.% NaCl equiv.) fluids caused pervasive sericite alteration and gold-bearing quartz veins. This suggests that the quartz-sericite-pyrite alteration in the district is directly related to higher temperature porphyry-type alteration at depth. Similar low to moderate temperature and low-salinity fluids were also recognized with the sericite alteration at Black Gossan and Alunite Ridge.

The transition to a porphyry center is further supported by the high concentrations of Cu, Mo, W, and Sn (which are typically enriched in the core of porphyry system) relative to Sb, As, Ag, Li and Tl (which are typically enriched in shallow level above porphyry systems). A normalized-element ratio index, the MDRU Porphyry Index (MPIx) is developed and applied to the Toodoggone district. This index indicates that Sofia and Baker mines have a distinct porphyry character and that other deposits or prospects such as Shasta, Cliff Creek, Black Gossan and Alunite Ridge also have notable porphyry affinities.

Results from this study indicate that there are a range of mineralization types in the central Toodoggone district from the deep porphyry to shallow epithermal environments which formed episodically over the period from ca. 196 to 186 Ma. A new framework proposed herein indicates the potential for exploration of porphyry-type copper mineralization in areas previously known for epithermal mineralization.

INTRODUCTION

Porphyry copper and epithermal gold-silver deposits typically form in the upper parts of large magmatic-hydrothermal systems that result from fluids generated from the crystallization of intermediate composition calc-alkalic igneous magmas in island and continental margin arcs (Sillitoe, 2010). Distal expressions of hydrothermal activity may result in the formation of alteration up to 10 km from the site of porphyry mineralization (Titley et al., 1986; Cunningham et al., 2004; Halley et al., 2015). Spatial and temporal links between porphyry copper and epithermal gold-silver deposits are known to occur in several porphyry belts, such as those in the Philippines (Sillitoe and Gappe, 1984; Arribas et al., 1995; Hedenquist et al., 1998), and have increasingly supported a genetic association.

The Toodoggone mineral district in northern British Columbia (Fig. 1) is one of the few districts in BC that hosts significant high- and low-sulfidation epithermal-type mineral deposits and occurrences (Diakow et al., 1991, 1993; Duuring et al., 2009a and b). Past gold and silver production at the Baker, Shasta and Lawyers mines was exclusively from veins that were previously classified as quartz-adularia or low-sulfidation type (Duuring et al., 2009a). Exploration in the region has historically mostly focused on high-grade, low-tonnage, low-sulfidation epithermal gold-silver targets (Diakow et al., 1993).

Porphyry deposits such as Kemess preferentially occur, or are exposed, in the southern parts of the Toodoggone district whereas epithermal deposits dominate the central and northern parts (Diakow et al., 1991; Duuring et al., 2009a). This distribution has been linked to the preferential preservation of the epithermal deposits or conversely, deeper erosion of the southern part of the district. This has led previous workers to conclude that potential porphyry copper deposits in the central and northern parts of the Toodoggone district are likely located deeper, beneath the more than two kilometres of Toodoggone Formation strata (Duuring et al., 2009a).

To understand the regional metallogenic controls on ore deposit distribution and the relationships between porphyry and epithermal mineralization, the key mineral occurrences in the Toodoggone mineral district were evaluated in terms of their mineralization, alteration styles and exploration potential. Field observations are supported by more focussed studies on alteration mineral characteristics, vein type descriptions, geochemical footprint mapping, age relationships between mineralization and intrusive units, and characteristics of the hydrothermal fluids. These data are combined to provide new evidence that establishes a spatial link between the known mineralization in the Toodoggone district to the porphyry system (sensu Sillitoe, 2010). A new framework and strategic guidelines for improved exploration decision-making are also provided.

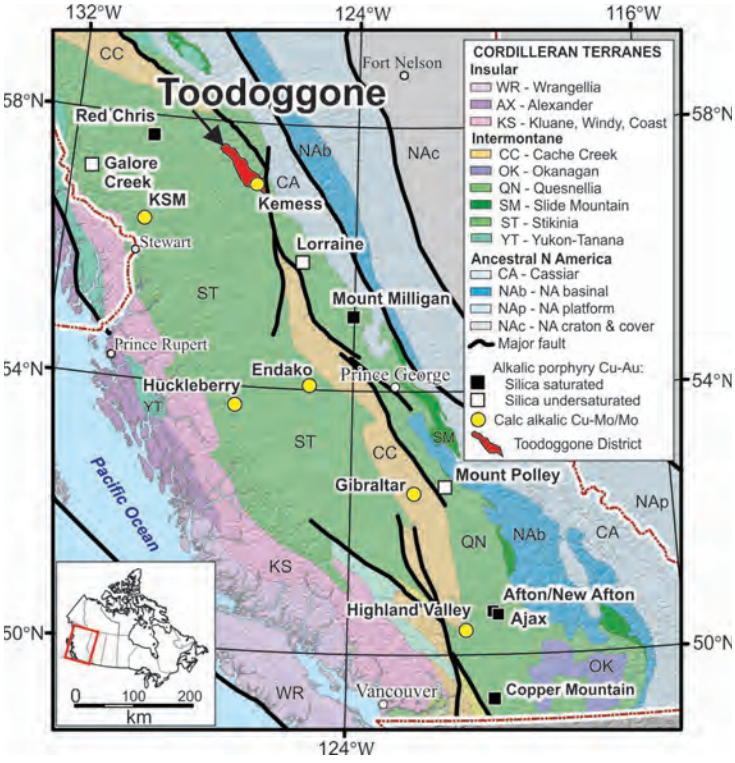

Figure 1: Location map of Cordilleran tectonic terranes, the Toodoggone mineral district and major porphyry copper deposits in British Columbia (modified after Bissig and Cooke, 2014).

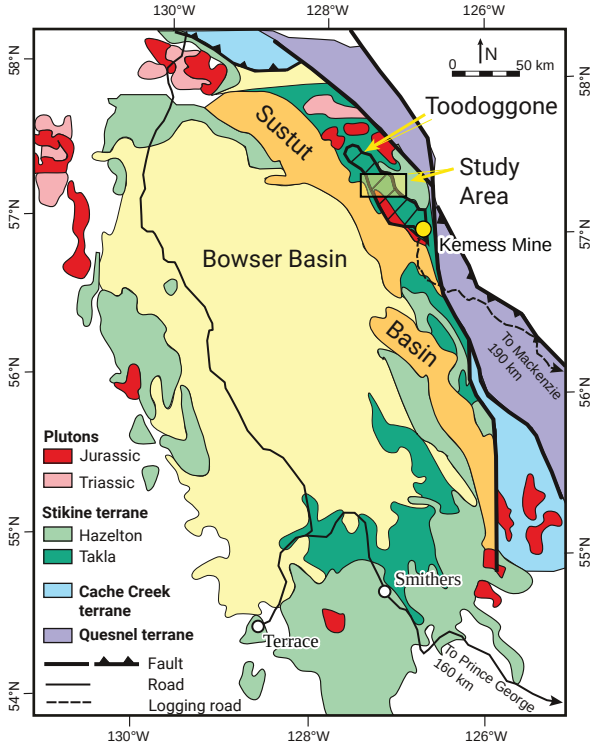

Figure 2: Terrane map of northern British Columbia showing tectonic elements of the Stikine terrane and location of the Toodoggone region (modified after Diakow et al., 1993).

GEOLOGICAL SETTING

The Toodoggone district (NTS 094E) in northern British Columbia is a 35 x 17 km, NW-trending mineral district located in the eastern part of the Stikine terrane (Fig. 1). Volcanic and sedimentary strata of the Early and Middle Jurassic Hazelton Group underlie much of the Toodoggone district and occupy an elongated structural depression of Late Triassic Takla Group volcanic rocks and less-exposed Permian Asitka Group carbonate units. Clastic sedimentary rocks of the Middle Jurassic to Cretaceous Bowser Lake Group are not exposed in the study area (Fig. 2) but thick, deformed sequences occur to the west and southwest of the Toodoggone district. These sediments, and those of the younger Sustut Group piggyback basin, were likely deposited above the Hazelton Group and protected the Toodoggone district rocks until their subsequent removal by erosion.

The stratigraphic succession in the study area, from oldest to youngest, includes: the Asitka Group, Takla Group, Hazelton Group and the Sustut Group (Table 1). The geology of the Toodoggone district is described in detail by Diakow (1990) and Diakow et al. (1993, 2005). A compilation geology map figure based on Diakow et al. (1993) and unpublished data is represented in Fig. 3, and a brief geological history is summarized below.

Stratigraphic Units

The oldest unit is the Lower Permian Asitka Group which includes limestone and lesser chert and felsic volcanic rocks. Rocks of the Asitka Group are exposed locally in fault-bounded wedges or roof pendants around the periphery of the Black Lake plutonic suite to the south of the Baker mine and southeast of Alunite Ridge (Fig. 3). Near the Baker mine, the Asitka Group sedimentary rocks are largely massive grey-white crystallized limestone that locally host skarn-type mineralization.

Takla Group rocks are lithologically and temporally similar to Late Triassic rocks referred to as Stuhini Group in the Stikine, and Takla Group in the Quesnel terrane. The Triassic rocks in the Toodoggone district, although part of Stikine, are referred to as Takla Group by Diakow et al., (1993), and are correlated with similar strata 30 km south in the McConnell Creek area. Takla Group rocks in the district are massive, dark green, coarse-grained porphyritic augite basalt, fine-grained aphyric basaltic andesite lava flows with subordinate interbeds of lapilli tuff and volcanic breccia. Locally, pillow lavas are interbedded with sandstone and conglomerate. Contacts of the Takla Group volcanic rocks with Jurassic sequences are generally faulted but locally a gently-dipping angular unconformity may be present (Diakow et al., 1993).

Lower to middle Jurassic Hazelton Group subaerial volcanic and volcaniclastic rocks of intermediate composition unconformably overlie the Takla Group. These rocks are assigned to the Toodoggone Formation which are equivalent to the Telkwa Formation of the Hazelton Group (Diakow et al., 1991). The Toodoggone formation is subdivided into seven stratigraphic members and grouped into lower (Duncan, Metsantan, and Saunders members) and upper (Junkers, Grave, Pillar and Bell members) volcanic cycles that are separated by an intra-formational eruptive hiatus (Table 1, Diakow et al., 1991, 2006). Subaerial andesite to dacite flows and tuff are the dominant

Table 1: Summarized stratigraphy of the study area in the central part of the Toodoggone district (from Diakow et al., 1993).

Period	Stratigraphy		Cycle		Member	Rock Type
Cretaceous	Sustut Group					Conglomerate
Middle and Upper Jurassic	Hiatus					
Lower Jurassic	Hazelton Group	Toodoggone Formation	Upper		Belle	Rhyolite ignimbrite
					Pillar	Basaltic andesit, andesite porphyry, lappili tuff
					Graves	Dacite ash-flow tuff, rhyolite flows
					Junkers	Basalt, andesite, and dacite lava flow
			Lower	Black Lake Intrusive	Saunders	Dacite ash-flows
					Metsantan	Andesite lava flows
					Duncan	Lapilli tuff, conglomerate
Upper Triassic	Takla (Stuhini) Group					Basalt and andesite flows
Lower Permian	Asitka Group					Massive limeston, chert, argillite

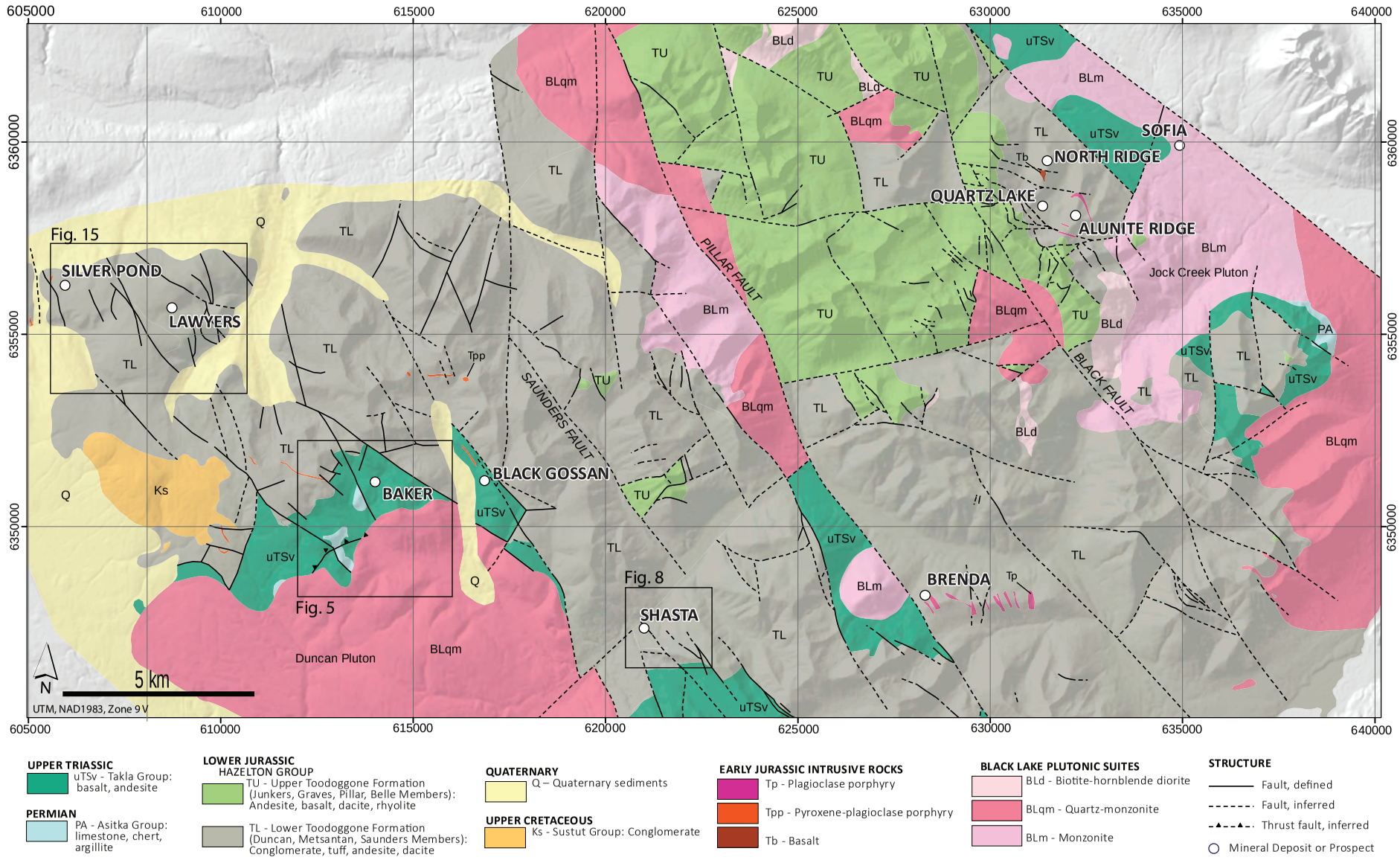

Figure 3: Geology map of the study area in the central part of the Toodoggone district (Compiled from Diakow et al., 1993 and unpublished maps).

rock types with rare basalt and rhyolite flows and subordinate volcanic siltstone to conglomerate and rare limestone lenses. These are cut by dark green, fine-grained porphyritic basalt dykes that are typically < 2 m wide and in turn by porphyritic andesite dykes that are up to 15 m wide.

Sustut Group strata are well-bedded Lower and Upper Cretaceous continental sedimentary rocks that were deposited and are best exposed in the Sustut basin to the west of the Toodoggone district. Sustut Group clastic sedimentary rocks within the study area occur as isolated outliers of conglomerate with siltstone and sandstone interbeds that rest unconformably upon the Toodoggone volcanic successions (Fig. 3).

Intrusive Rocks

Several porphyritic plutons and sub-volcanic stocks intrude the Toodoggone Formation strata. These intrusions are well-exposed in the southern and eastern regions but are presumably barely unroofed stocks with low relief in the western and central study area (Diakow et al., 1993). These Early Jurassic granitoids, designated the Black Lake Plutonic Suites (Woodsworth et al., 1988) form part of an arcuate belt of Late Triassic and Early to Middle Jurassic stocks and composite batholiths that are exposed intermittently along the eastern margin of the Bowser Basin. The Black Lake pluton is a pink granodiorite and quartz monzonite with coarse to medium-grained phenocrysts of plagioclase, orthoclase, quartz, hornblende and biotite.

Structures

Several steeply-dipping normal faults and a few strike-slip and thrust faults have disrupted the strata in the Toodoggone district. The dominant structures are steeply-dipping faults which define a prominent northwest-trending regional structural fabric. High-angle northeast-trending faults appear to truncate and displace northwest-trending faults and form steep valleys (Diakow et al., 1993). Strata of the Toodoggone Formation are not strongly deformed whereas older Asitka Group rocks are locally strongly deformed. These structural features, stratigraphic variations and unit distributions indicate that much of the volcanic activity occurred in an extensional environment. Abrupt thickening of the Toodoggone ash-flow units is attributed to local collapse along penecontemporaneous faults (Diakow et al., 1993). A longitudinal cross-section defines a symmetric, northwest-elongated depression (Fig. 4) with older rocks only exposed at the edges of the depression and younger rocks cropping out dominantly towards the centre. The Black Lake plutonic suite and several smaller bodies are either elongated or preferentially oriented to the northwest suggesting that the ascent of magma to subvolcanic levels was probably facilitated by extensional structures of similar orientation (Diakow et al., 1993).

FIELD AND LABORATORY TECHNIQUES

Access to the Toodoggone area is by air to the Sturdee or the Kemess mine airstrips, the latter located about 30 km to the south of the study area. Road access is available along the 400 km, seasonally maintained Omineca Resource Access Road from Mackenzie, the town nearest to the Toodoggone district. Within the study area, there is gravel road access to Baker, Brenda, Shasta, Black Gossan and Lawyers properties, whereas access to Alunite Ridge, Quartz Lake and Sofia is by foot or helicopter.

Fieldwork included visits to a number of prospects, past producers and mineral occurrences including: Silver Pond (S, N, Ridge), Lawyers (Cliff Creek, AGB zone); Baker; Black Gossan; Shasta; Brenda; Alunite Ridge and surrounding areas (N-Ridge, Quartz Lake) as well as Sofia. During fieldwork, alteration and mineralization features, vein types, and host rock relationships were examined at each prospect.

A total of 124 rock samples representing host rocks, alteration and mineralization were collected. All samples were slabbed and photographed at The University of British Columbia (UBC). Appendix 1 includes a list of samples, UTM locations and descriptions. Polished-thin sections were prepared for a sub-set

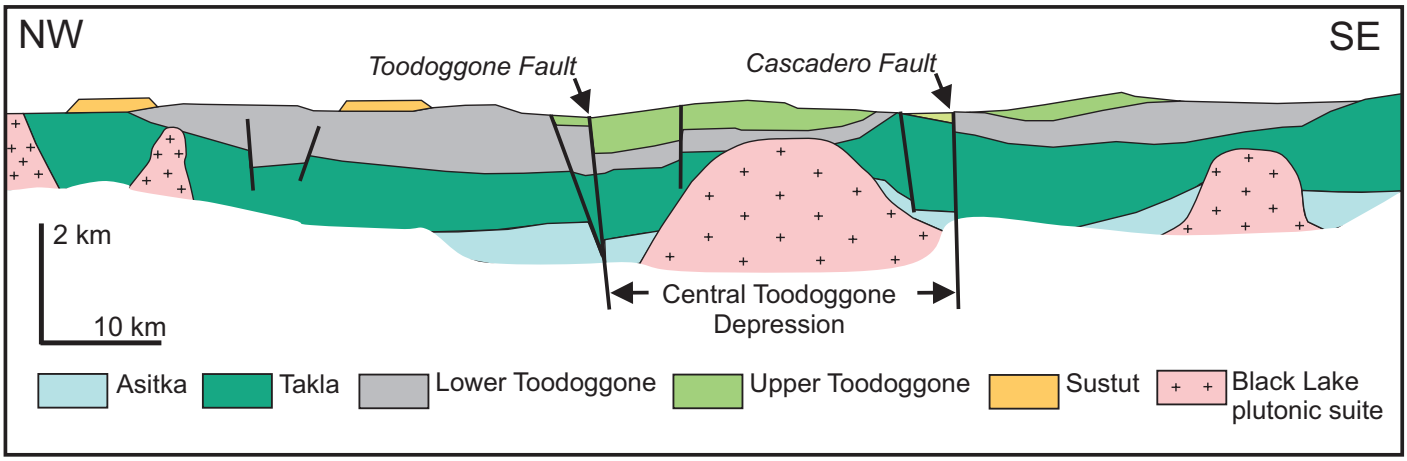

Figure 4: Schematic NW-SE cross section of the Toodoggone district showing main structural features and the Toodoggone central depression (from Diakow et al., 1993), the focus area for this study. The Toodoggone and Cascadero faults occur north and south of the study area, respectively, outside the area shown in Figure. 3.

of 22 samples that were evaluated at UBC using a petrographic microscope (Appendix 2).

Zircons from five samples were separated for U-Pb geochronology. Laser Ablation Inductively Coupled Plasma Mass Spectrometry (LA-ICP-MS) analyses were carried out using a Resonetics m50-LR 193 nm excimer laser coupled to an Agilent 7700x ICP-MS at the PCIGR labs at UBC. Details of analyses and zircon geochemistry of these and additional samples from the Toodoggone district are discussed elsewhere (Bouzari and Hart, 2019). A Re-Os age of one molybdenite sample from Baker mine was obtained from the University of Alberta. Details of the isotope study and results are provided in Appendix 3.

All samples were analyzed using the tabletop version of the Terraspec® by Analytical Spectral Devices (ASD) Inc., with full range VNIR and SWIR wavelengths for the range of 350-2500 nm. All SWIR analyses were completed at UBC. A sheet of mylar was used as a standard, and this sheet was scanned at the start and end of every sampling day. Calibration with the white reflectance disk was completed at the start of every sampling day, and re-calibrated every hour. The spectrum input was left at 100, and the white reference was set at 200. Spectra were visually inspected during collection, and where spectra were weak or aspectral, additional locations on the sample were scanned. Samples were processed with TSG (The Spectral Geologist) software for measuring spectral features such wavelength position and crystallinity. Mineral identification and spectra quality assessment (e.g., noise and molecular water contamination) were performed using the SpecWin software. Results are documented in Appendix 4.

A total of 74 samples were analyzed for trace elements at Bureau Veritas Minerals (Vancouver, BC) using a multi-acid digestion method and Ultra-trace ICP-ES/MS method (MA250) and for ore grade (MA401) to characterize the geochemical signature of host rock, alteration and mineralization. Gold was not included in the analyses. Note also that due to the digestion technique used, the most resistive minerals such as zircons may not be completely dissolved. The concentrations of HREE, Hf and Zr should be considered minimum concentrations. Geochemical reference materials and duplicate samples were used to check analytical quality assurance and control. Results are shown in Appendix 5.

Fluid inclusions were studied to characterize fluid inclusion type, assemblages, salinity and homogenization temperature. Double polished sections, ca. 100 µm, were prepared at Vancouver Petrographics for eight samples. Fluid inclusion thermometry was carried out on five selected samples at the MDRU Fluid Inclusion Laboratory at UBC, using an Olympus BX60 polarizing microscope coupled with a LINKAM THMGS600 heating/freezing stage. Salinity was calculated based on the melting temperature of ice (Tm ice) or halite (Tm salt) using Bodnar (1993) equations. Results of the fluid inclusion study are in Appendix 6.

MINERAL DEPOSITS AND PROSPECTS

The Toodoggone district contains several mineralization types including epithermal gold-silver, porphyry copper-molybdenum and skarn. During 1925-1926, placer gold was discovered in the area which attracted exploration activity to the region. During the 1960s, a regional geochemical survey led to the discovery of gold mineralization at Lawyers and Chappelle (now Baker) and copper mineralization at Kemess (Diakow et al., 1993). Gold has been the focus of exploration in the central parts of the Toodoggone district with main prospects including Silver Pond, Lawyers, Baker, Brenda, Quartz-Lake and Alunite Ridge (Fig. 3).

Field and petrographic observations of these prospects characterized the alteration and mineralization as a basis to evaluate ore genesis, mineral system context and exploration potential. In the following section, key observations are summarized for specific deposits or prospects. Sample locations and descriptions are in Appendix 1, and thin-section petrography descriptions for selected samples are in Appendix 2.

Baker Mine

The Baker mine (formerly known as Chappelle) exploited Au-Ag mineralization along NE striking-steeply dipping veins (Diakow et al., 1993; Duuring et al. 2009a). At least six precious metal

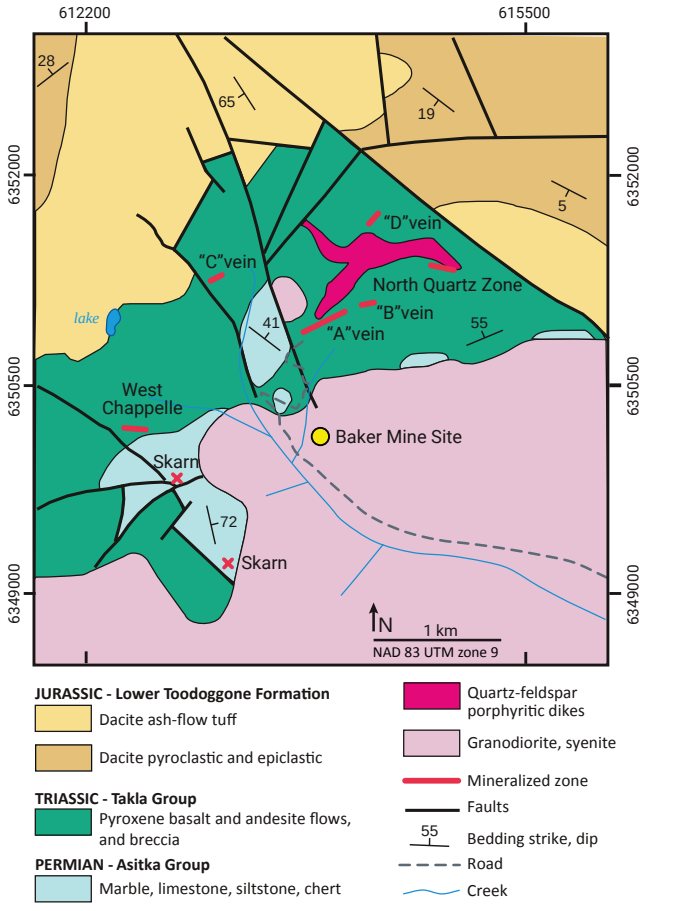

Figure 5: Geology of the Baker mine area (after Diakow, et al., 1993).

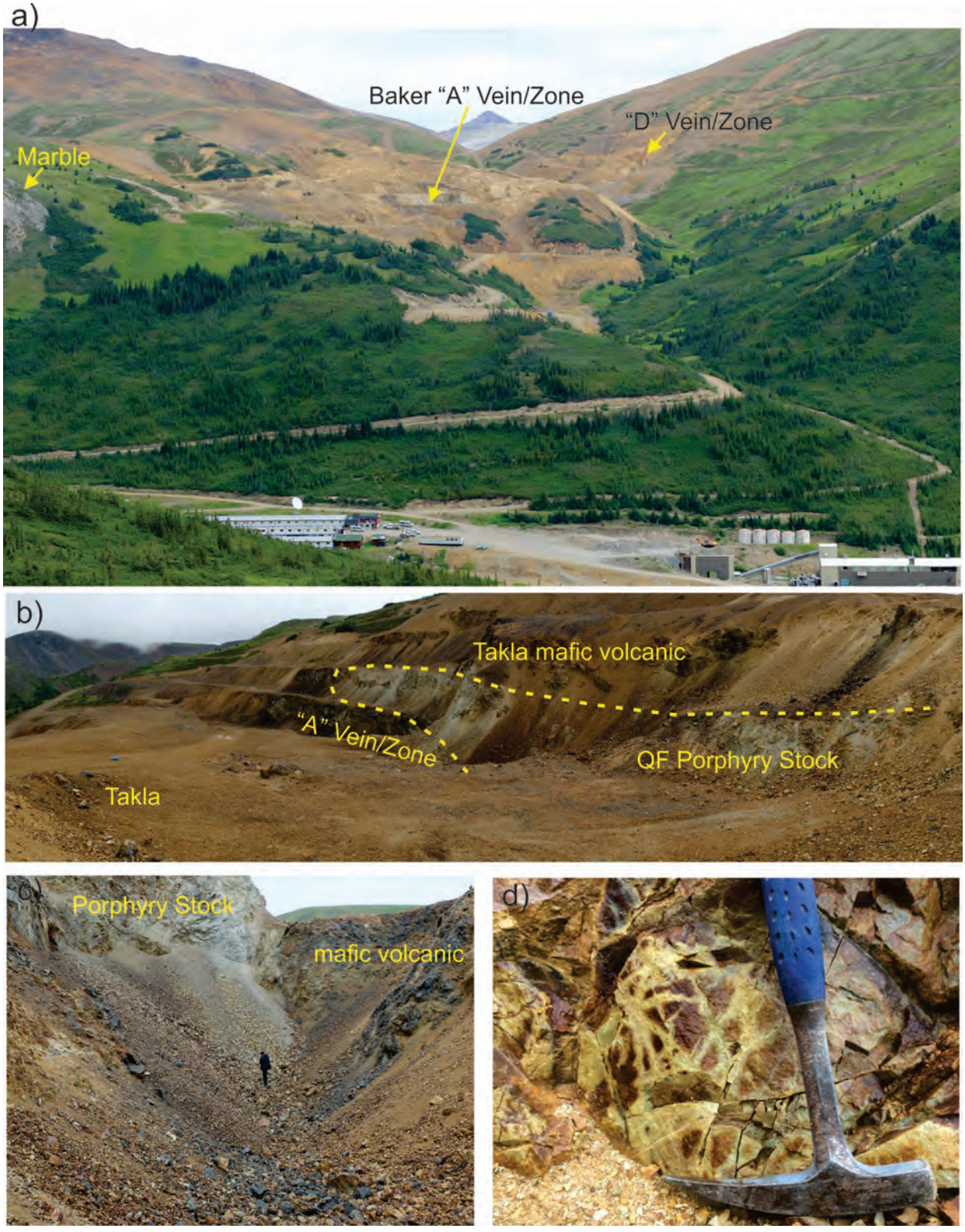

Figure 6: Host rocks, alteration and veins at Baker: a) Baker Mine, looking north showing the main ore zones. b) Baker main pit showing the quartz-feldspar porphyry (QFP) and volcanic host rocks. The main mineralization occurring near the contact of the porphyry and volcanic rocks. c) Small working pit showing the contact of the porphyry and volcanic rocks. d) Stockwork quartz-sericite alteration in the quartz-feldspar porphyry. e) Takla Group volcanic rock with pervasive chlorite alteration and disseminated pyrite replacing pyroxene phenocrysts. f) QFP with plagioclase and quartz phenocrysts and pervasive sericite alteration cut by grey quartz veins. g) QFP cut by a quartz-pyrite-molybdenite vein. Molybdenite occurs as darker phase near vein margin. h) Takla Group volcanic with intense veinlet-controlled and pervasive green sericite-chlorite alteration. i) A drill core sample of a porphyry unit from ~200 below surface showing pervasive K-feldspar alteration, secondary biotite after hornblende cut by banded quartz-magnetite-hematite veins (qtz-mag-hem) which are in turn cut by pyrite-chalcopyrite-epidote-chlorite veins (py-cp-ep-chl). j) A post mineral mafic dyke cuts the altered Takla volcanic rocks.

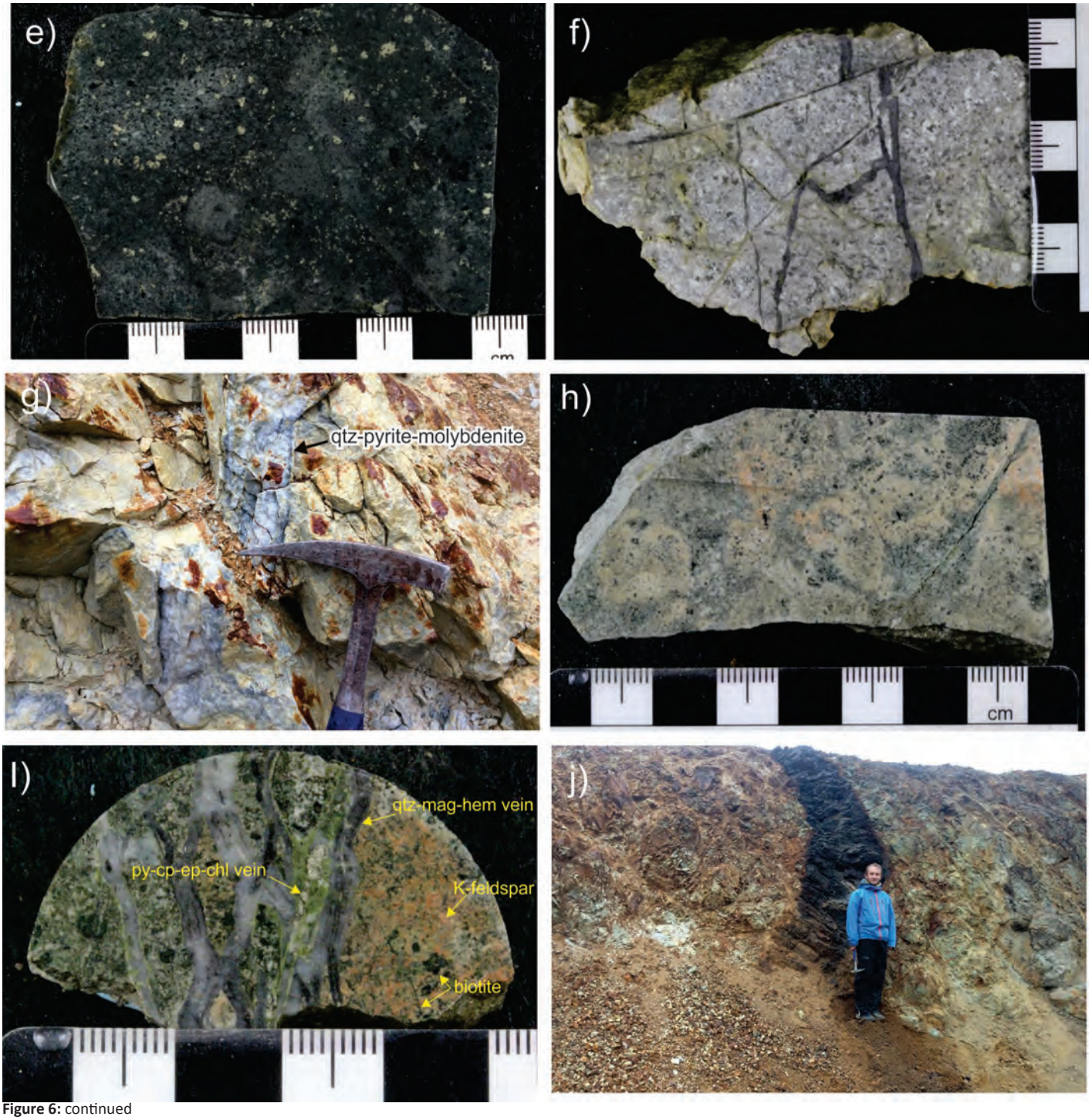

Figure 6: continued

bearing veins have been discovered, named A, B, C, D, North Quartz Zone and West Chappelle veins. Total production prior to 1997 was approximately 766,000 oz Ag and 41,000 oz Au (Minfile Production Detail Report, 2016) from two veins (A and B veins, Figures 5 and 6a). The B vein at Baker has been described as an up to 5 m wide, low-sulfidation quartz–sericite–calcite–kaolinite–pyrite–chalcopyrite–acanthite–sphalerite–galena–gold vein with chlorite-epidote wall-rock alteration (Duuring et al. 2009a).

Mineralization occurs within an uplifted block of Takla Group strata which is intruded by the Duncan pluton (Black Lake plutonic suite) in the south and overlain by strata of the Toodoggone Formation in the north, east and west. Mineralized zones are centered on a 1 km long and 100-200 m wide quartz-feldspar porphyry stock (Figures 5, 6a and b). The Takla Group host rock consists of basaltic to andesitic volcanic rock that have chlorite and epidote alteration (Fig. 6e). The quartz-feldspar porphyry (QFP) is characterized by abundant medium to fine-grained plagioclase and sub-rounded quartz phenocrysts in dull grey altered groundmass (Fig. 6f). Late mafic dykes cut the host rock and mineralization (Fig. 6J). Asitka Formation limestone

at the contact with the Duncan pluton in the southwest of the Baker mine (Fig. 5) has been recrystallized and contains skarn-type alteration with galena and sphalerite.

Stockworks of quartz-sericite-pyrite veins (Fig. 6d) and pervasive quartz-sericite-pyrite alteration (Fig. 6f) have obliterated much of the original texture of the porphyry stock (Fig. 6d). Milky to grey quartz veins, locally with irregular boundaries (Figures 6g and f), cut the quartz-feldspar porphyry. These veins contain molybdenite; coarse-grained typically close to the vein wall (Fig. 6g) and fine-grained with pyrite and traces of chalcopyrite near the center of the veins (Fig. 6f). The Takla Group volcanic rocks near the porphyry stock are affected by chlorite, green sericite, and epidote alteration (Fig. 6h) and disseminated pyrite and chalcopyrite. Moving away from the porphyry stock, the green sericite alteration diminishes whereas the epidote alteration increases with chlorite and disseminated pyrite for over 2 km.

Drill core from a 1987 drill campaign (Carter et al., 1988) intersected porphyry-style banded quartz-magnetite veins with associated pink, hematite-bearing feldspar alteration only a few 100 m below the known extent of the vein mineralization. These veins are cut by chalcopyrite-pyrite veins with chlorite and epidote alteration (Fig. 6l). Copper mineralization apparently was not the target of exploration at the time since chalcopyrite bearing rocks do not appear to have been systematically sampled or analysed for geochemistry.

The occurrence of quartz-feldspar porphyry stocks with quartz-sericite-pyrite alteration surrounded by chlorite-green sericite and chlorite-epidote alteration in the host basalt-andesite alteration is similar to the alteration type and zonation in porphyry deposits. Moreover, the quartz-magnetite and quartz-molybdenite-pyrite veins are comparable to the “A-type” and “B-type” vein in porphyry deposits, respectively (Gustafson and Hunt, 1975). These field relationships suggest that mineralization at Baker represents shallower parts of a porphyry deposit which are overprinted by intermediate-sulfidation epithermal (or sub-epithermal) mineralization.

Black Gossan

Black Gossan is a 1 km long and 300-400 m wide altered area that is ~3 km east of Baker mine. The geology of the Black Gossan area is similar to that of the Baker mine with the host rock of Takla Group volcanic rocks in contact with the Duncan pluton

Figure 7: Black Gossan rock and alteration: a) View of the Black Gossan looking south showing jarosite and clay-altered Takla Group volcanic rocks. b) Cut sample of Takla Group andesite with pervasive sericite alteration cut by quartz veins. c) Granodiorite near the bottom of the valley cut by K-feldspar vein. d) Granodiorite with K-feldspar alteration cut by quartz-magnetite vein.

and Toodoggone Formation (Fig. 3). The area is characterized by clay alteration and iron oxide, yellow jarositic weathered rocks (Fig. 7a). Alteration includes pervasive clay-sericite, and silicification. Narrow light grey quartz veinlets occur (Fig. 7b). At lower elevations ~200-300 m below the Black Gossan highest elevation, near the road cut, a small body of granodiorite is exposed; it is presumably part of the Black Lake plutonic suite (Duncan pluton). It is cut by veinlet controlled K-feldspar alteration (Fig. 7c) and locally contains quartz-magnetite veins (Fig. 7d).

Shasta

The Shasta deposit is located 8 km southeast of Baker mine. About 1 Moz Ag and 20,000 oz Au were produced in the early 1990s (Minfile Production Detail Report, 2016). Mineralization is hosted in two, up to 10 m wide vein and breccia zones. These include the Creek and JM zones which strike to the north and northwest, respectively (Fig. 8, and 9a, Thiersch et al., 1997). The host rocks are Lower Toodoggone Formation volcanic and epiclastic rocks which are in contact with a dacite dome with flanking tuff and breccias (Marsden and Moore, 1990). These range from very fine-grained to >4mm sized clast-bearing lithic-crystal tuffs with plagioclase, hornblende, and augite phenocrysts. The groundmass is largely altered to micro-crystalline quartz, fine-grained opaques and isotropic clays.

Field observations were from ore materials outside of the adits because the veins were inaccessible. From field and petrographic observations, the veins cut an early-stage K-feldspar alteration (Fig. 9b). Green to grey sericite alteration overprints the K-feldspar alteration (Fig. 8b). Locally, mineralization occurs as breccia zones with clasts of K-feldspar altered volcanic rock (Fig. 9c). Three vein types are recognized: 1) grey to white quartz-pyrite-chalcopyrite±galena±sphalerite veins (Figures 9c and 9d, 9a, 10a), 2) quartz-calcite-galena-sphalerite-acanthite±electrum (Fig. 9e and 9b, 10b) and 3) late calcite veins which cut earlier mineralized veins (Fig. 9f).

Both early potassic alteration and chalcopyrite-pyrite mineralization with massive grey quartz suggest that an early copper mineralizing event preceded the main precious metal mineralization. Much of the gold and silver mineralization is associated with galena at the onset of the last mineralizing stage (Thiersch et al. 1997). The early chalcopyrite-pyrite mineralizing event may be related to porphyry-style Cu mineralization. The quartz-pyrite-chalcopyrite stockwork veins that cut argillically-altered volcaniclastic rocks at the Silver Reef showing, ~1 km south of Shasta may represent this early stage of mineralization.

Brenda

The Brenda prospect is 8 km east of Shasta. The geology is dominated by Lower Toodoggone Formation volcanic rocks intruded by several small Early Jurassic stocks and dykes of

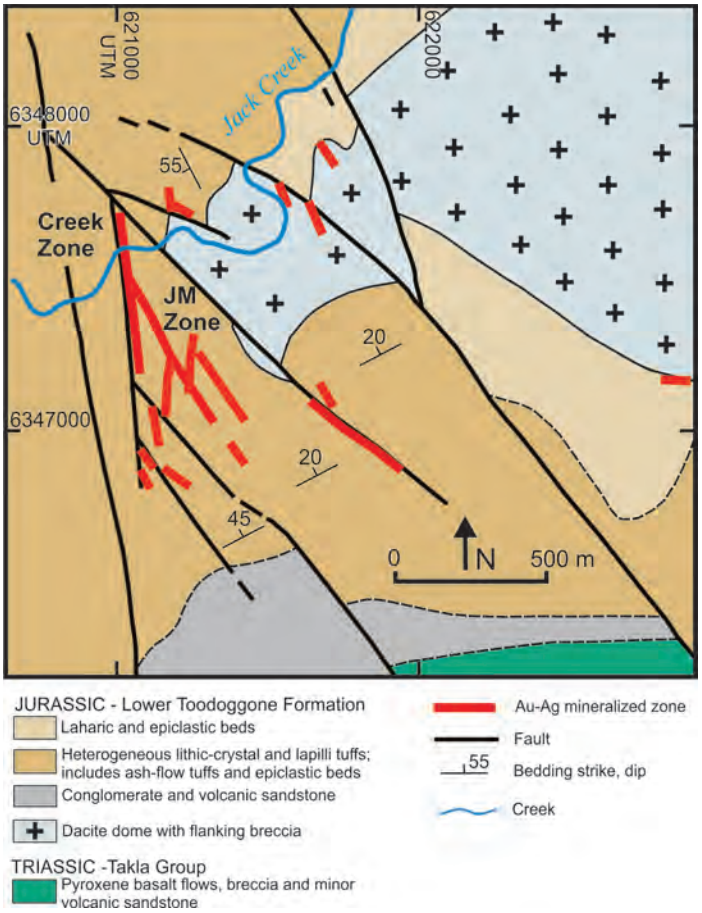

Figure 8: Geology map of the Shasta area (after Diakow, et al., 1993).

intermediate composition (Fig. 3). Alteration is centered on a porphyry body around the White Pass area ~350 m above the elevation of Jock Creek (Fig. 11a). The host rocks are intensely altered with remnants of quartz and plagioclase phenocrysts indicating that it is a quartz-plagioclase porphyry (Fig. 11b). These are cut by post-alteration hornblende-plagioclase porphyry of probable monzonitic composition (Fig. 11c). Alteration is variable and includes intense quartz-sericite-pyrite alteration with a buff grey appearance that is typical of an advanced argillic assemblage (Fig. 11b). Clay alteration is locally widespread, particularly on the north slopes, and where alunite is reported (Lane, 2017). Additionally, the Creek Zone, 2 km northwest of the White Pass area, features intensely quartz-pyrite-sericite altered plagioclase porphyritic rocks, with alunite alteration.

Intense quartz-sericite alteration is focussed in narrow, structurally-emplaced, elongated porphyry bodies. This suggests an advanced argillic alteration zone and it potentially represents the shallow parts of porphyry-style system at depth.

Alunite Ridge, North Ridge and Quartz Lake

The area around the small Quartz Lake, ~11 km northeast from Brenda and 3 km west of the Toodoggone River, contains several mineral occurrences including Quartz Lake, Alunite Ridge, North

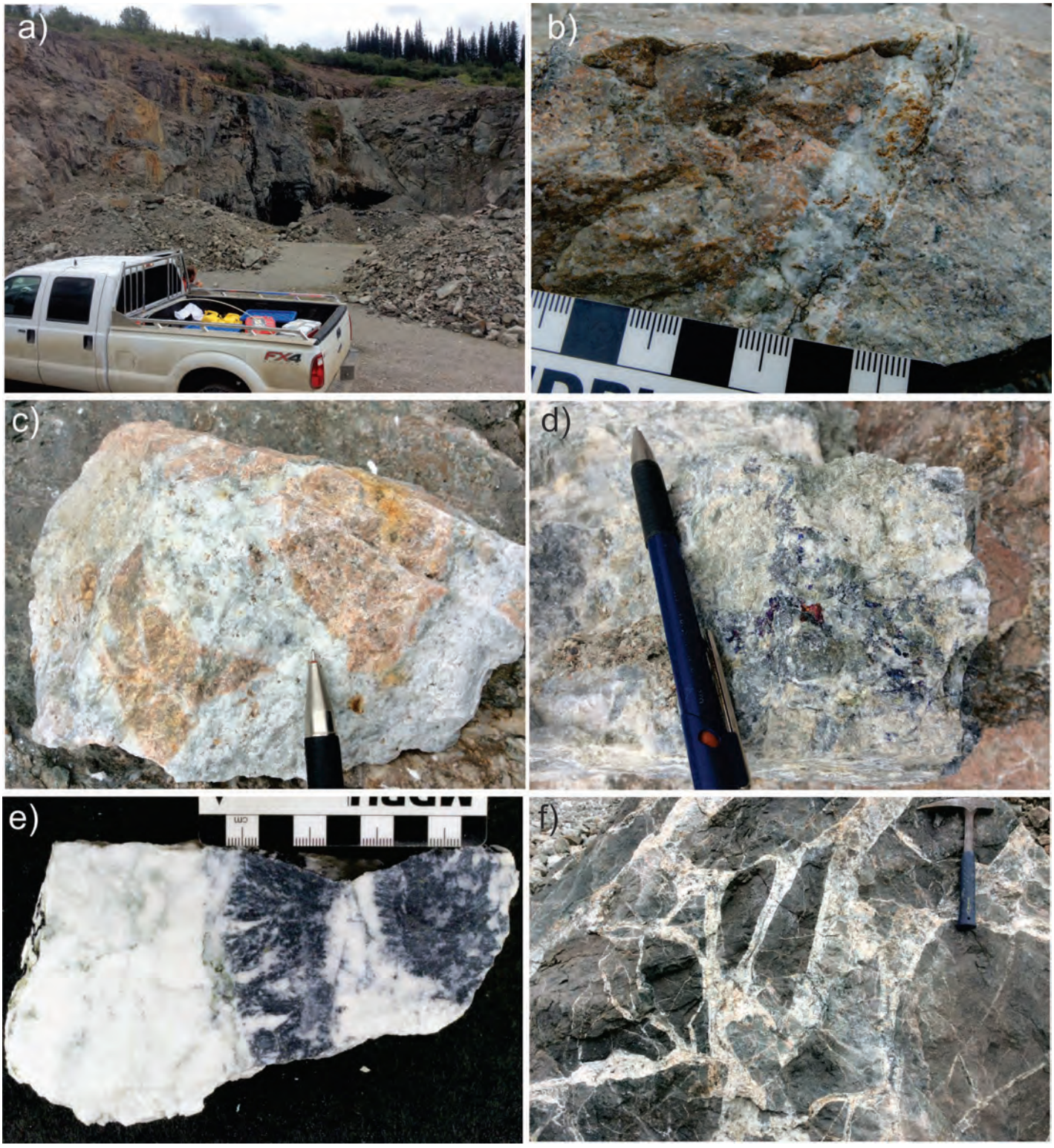

Figure 9: Shasta host rocks and alteration. a) Looking south towards the Creek Zone adit. The main mineralized zone is ~10 m wide and strikes to the southeast. b) Mineralized quartz-pyrite-chalcopyrite vein cutting at early K-feldspar alteration overprinted by green sericite alteration. c) Breccia ore with quartz-pyrite-chalcopyrite and clasts of K-feldspar altered volcanic rock. d) A boulder of the ore with early stage quartz-chalcopyrite (tarnished)-pyrite mineralization. e) Quartz-calcite-galena-sphalerite vein containing acanthite and electrum. f) Late stage carbonate-quartz vein.

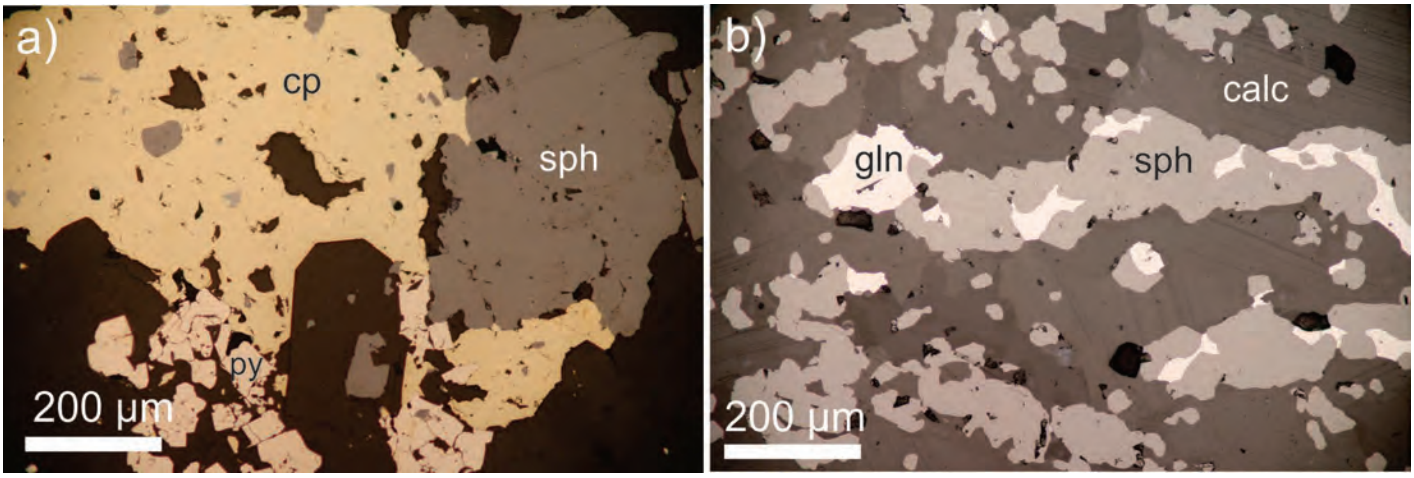

Figure 10: Reflected light photomicrographs showing example of vein types at Shasta: a) Early chalcopyrite-pyrite-sphalerite vein. b) later sphalerite-galena in a quartz-carbonate groundmass. cp = chalcopyrite, py = pyrite, sph = sphalerite, gln = galena, calc = calcite

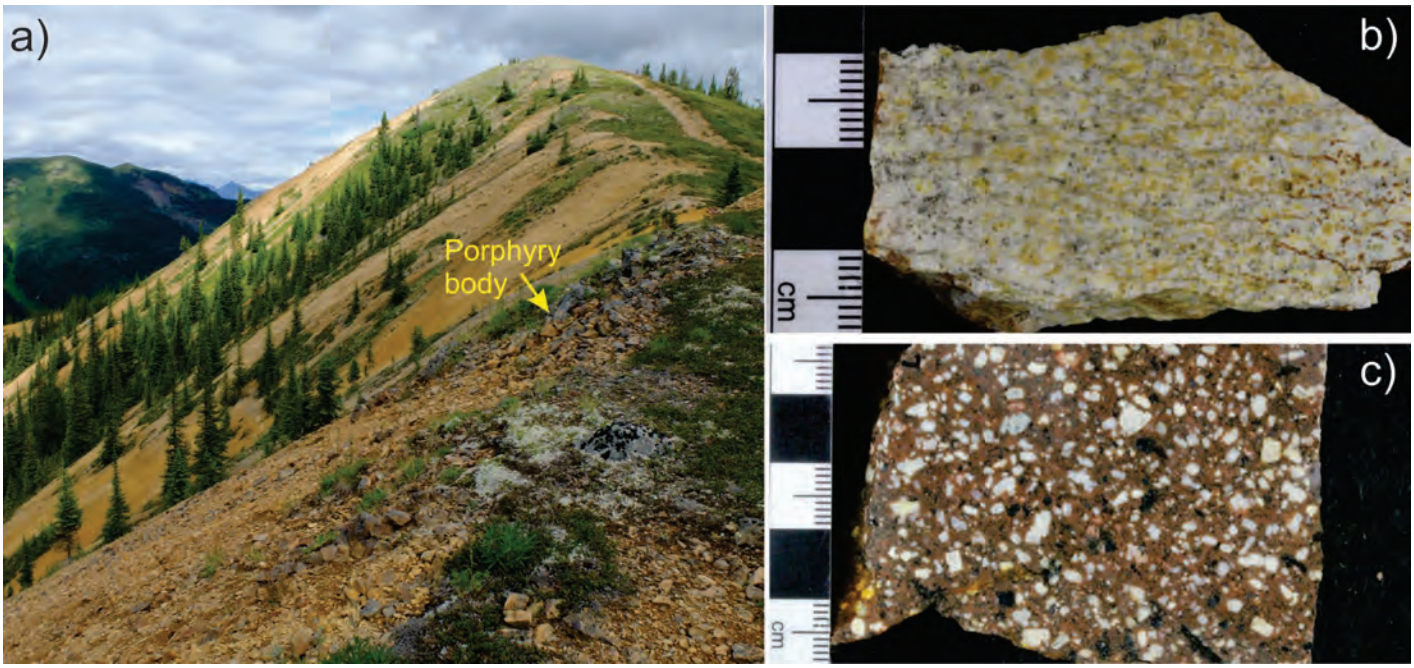

Figure 11: Brenda area rock types: a) Looking northeast to the main Brenda ridge showing the advanced argillic altered and oxidized host rocks. b) A fine-grained porphyry with small (<3 mm) plagioclase and quartz phenocrysts strongly affected by sericite-pyrite-clay alteration. c) Post-alteration, weakly-altered hornblende-plagioclase monzonite which cuts the alteration.

Ridge and Sickle Creek. The Alunite Ridge and North Ridge occur as two northeast-trending ridges with the Quartz Lake property in the valley between the two ridges. The Lower Toodoggone Formation andesitic lava flows, tuffs, breccia, and epiclastic rocks are intruded by small dykes and stocks of monzonite (Fig. 3). The Jock Creek monzonitic pluton forms a large body in the south and east.

Intense zones of alteration occur in northwest-trending zones about 200 m wide (Fig. 12). Gold mineralization occurs in a 10-15 m wide zone (Duuring et al., 2009a) in silicified rock with quartz-alunite alteration, locally with vuggy textures (Fig. 13a, b) and zones of buff-grey intense diaspore alteration (Fig. 13c, d). These are surrounded by quartz-sericite alteration (North Ridge) which locally contains pyrophyllite in zones that transition to the quartz alunite alteration (e.g., SW of North Ridge, Fig. 13e). The host volcanic and volcaniclastic rocks beyond the advanced argillic altered zones are affected by chlorite and pyrite alteration (Fig. 13f). Banded quartz veins with calcite and K-feldspar (Fig. 13g) host low sulfidation-type chalcopyrite-sphalerite-galena-pyrite mineralization 100-300 m from the advanced argillic altered zone at Alunite Ridge (Duuring et al., 2009a). Similar types of veins and mineralization, locally with amethystine quartz (Fig. 13i, j) occur at the base of the valley near Quartz Lake. Post-mineralization monzonite dykes cut the alteration (Fig. 13h).

Figure 12: North Ridge, about 1750m a.s.l., looking northeast to the quartz-sericite altered areas that form rusty pale-brown outcrops. The Toodoggone River at about 1050m a.s.l. form the valley with Mount Katharin (2335m a.s.l.) on the opposing side of the valley.

Sofia

The Sofia prospect is in the Toodoggone River valley about 3 km northeast of Alunite Ridge, at an elevation of 1050 m a.s.l. which is about 700 m lower than Alunite Ridge (Fig. 3). A 10 m wide yellow-rusted outcrop shows coarse equigranular granodiorite in contact with Takla Group volcanic rocks (Fig. 14a). Late aplite dykes cut both granodiorite and volcanic rock (Fig. 14c). The granodiorite has pervasive and veinlet related pink K-feldspar alteration. It has been cut by abundant quartz-magnetite veins (Fig. 14b). These veins are barren and only trace chalcopyrite occurs. The Takla Group volcanic rocks are strongly altered to chlorite and locally have abundant disseminated pyrite and minor chalcopyrite (Fig. 14d). The quartz-magnetite veins are comparable to M-veins that form during the early stages in deeper parts of the porphyry deposit K-silicate alteration (Arancibia and Clark, 1996).

Lawyers

The Lawyers system includes three mineralized zones: the Amethyst Gold Breccia (AGB), Cliff Creek and Duke's Ridge from which 3.7 Moz Ag and 0.17 Moz Au were produced between 1989 and 1992 (Minfile Production Detail Report, 2016). The Lawyers deposit is about 7 km northwest of the Baker mine and is hosted in the Lower Toodoggone Formation (Fig. 3). Host rocks are trachyandesite lava flows and dacitic tuff (Fig. 16a). The mineralization occurs within northwest-trending structures, 10-100 m wide and up to 1 km long (Fig. 15, 16b). The AGB and Duke's Ridge ore zones consist of vein and breccia bodies. The veins are chalcedonic with some hematite (Fig. 16c) with typically younger comb-texture amethyst (Fig. 16d). Mineralization includes fine-grained electrum, argentite, native gold and silver with minor chalcopyrite, sphalerite and galena (Diakow et al., 1993). Adularia occurs at the margin of the veins with ankerite and locally hematite dusting of host rock plagioclase phenocrysts (Fig. 16e).

At Cliff Creek, massive quartz vein material cuts dacitic host rocks that are altered to sericite-dickite-kaolinite. Early quartz is grey and contains pyrite, chalcopyrite and a fine-grained grey sulfide mineral. This material is cut by white quartz and amethyst (Fig. 16f). The chalcopyrite-pyrite assemblage, along with a lack of open space textures suggest elevated temperatures and potentially a deeper setting compared to the amethyst-bearing vein materials at Lawyers. This is also consistent with the observed alteration in the wallrock suggesting that the prospects in the Lawyers area could be distal expressions of a larger porphyry system.

Silver Pond

The Silver Pond area is located west and northwest of Cliff Creek and includes a number of Minfile occurrences. Of those, Silver Pond North, Silver Pond South and Silver Pond Ridge were visited. The most intense and widespread alteration is at Silver Pond North, 2 km west of Cliff Creek (Fig. 15, 16g). Host rocks

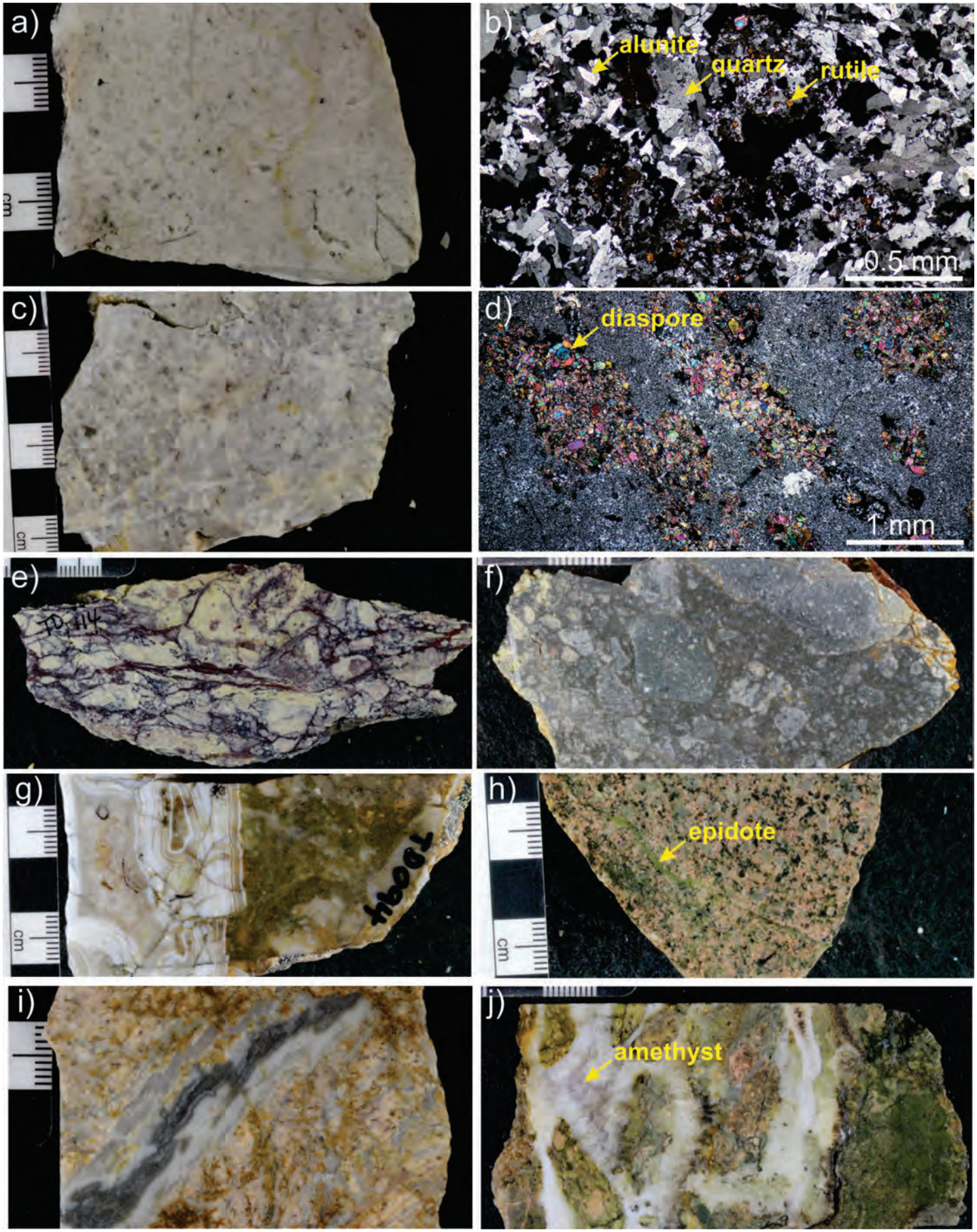
a)
b)
alunite
quartz
rutile
0.5 mm
c)
d)
diaspore
1 mm
e)
f)
g)
h)
epidote
i)
j)
amethyst

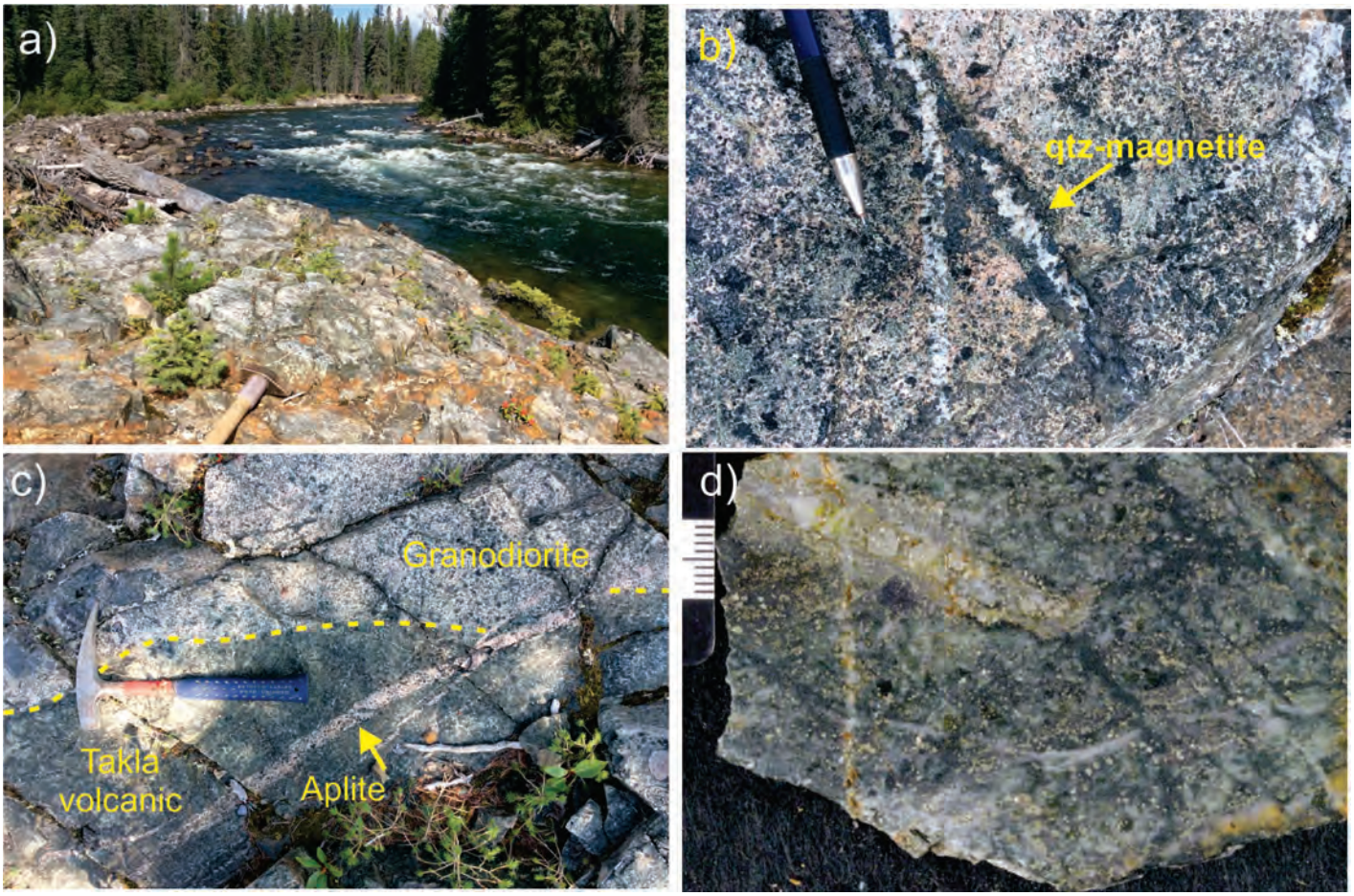

Figure 14: Sofia prospect and rock types. a) Sofia outcrop, ~10m wide, located in west side of the Toodoggone River valley showing rusted granodiorite host rock. b) Sofia granodiorite with pervasive pink K-feldspar alteration cut by quartz-magnetite veinlets. c) Sofia granodiorite in contact with Takla volcanic rock and cut by late aplite dike. d) Takla volcanic host rock with strong chlorite alteration and abundant disseminated pyrite and minor chalcopyrite mineralization.

Figure 13: (left)Alunite Ridge, North Ridge and Quartz Lake rocks: a) Sample of intensely silicified rock with abundant alunite from Alunite Ridge. b) Photomicrograph of quartz-alunite altered rock of Fig. 13a showing quartz and tabular alunite with some vuggy texture. c) Sample from Alunite Ridge with buff grey alteration composed of quartz-diaspore-sericite and dickite. d) Photomicrograph showing clusters of diaspore (high birefringence colors) in a fine-grained quartz-sericite-clay groundmass (grey). e) Sample from southwest of the North Ridge, with breccia textures showing pale yellow lustrous texture with intense quartz-sericite-pyrophyllite alteration. The protolith is unclear but is probably a dacitic volcanic rock. f) Sample of volcaniclastic rock of the Toodoggone Formation with pervasive chlorite alteration and disseminated pyrite in matrix. g) Sample of banded quartz vein from Alunite Ridge with chlorite alteration. h) Sample of monzonite dikes with epidote alteration from Alunite Ridge i) Banded white and grey quartz vein cutting silicified and chlorite-sericite altered rock from Quartz Lake (DDH SG-04-18 at 97 m). j) Late quartz vein with late amethyst at Quartz Lake (DDH SG-04-18 at 13 m).

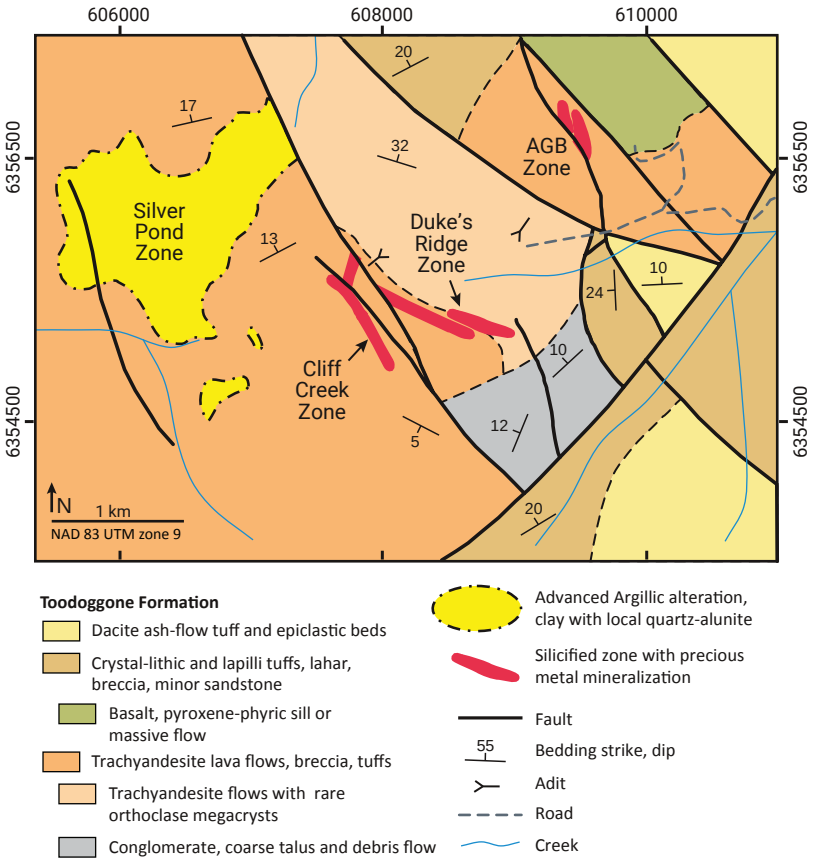

Figure 15: Geology of the Lawyers area (after Diakow, et al., 1993).

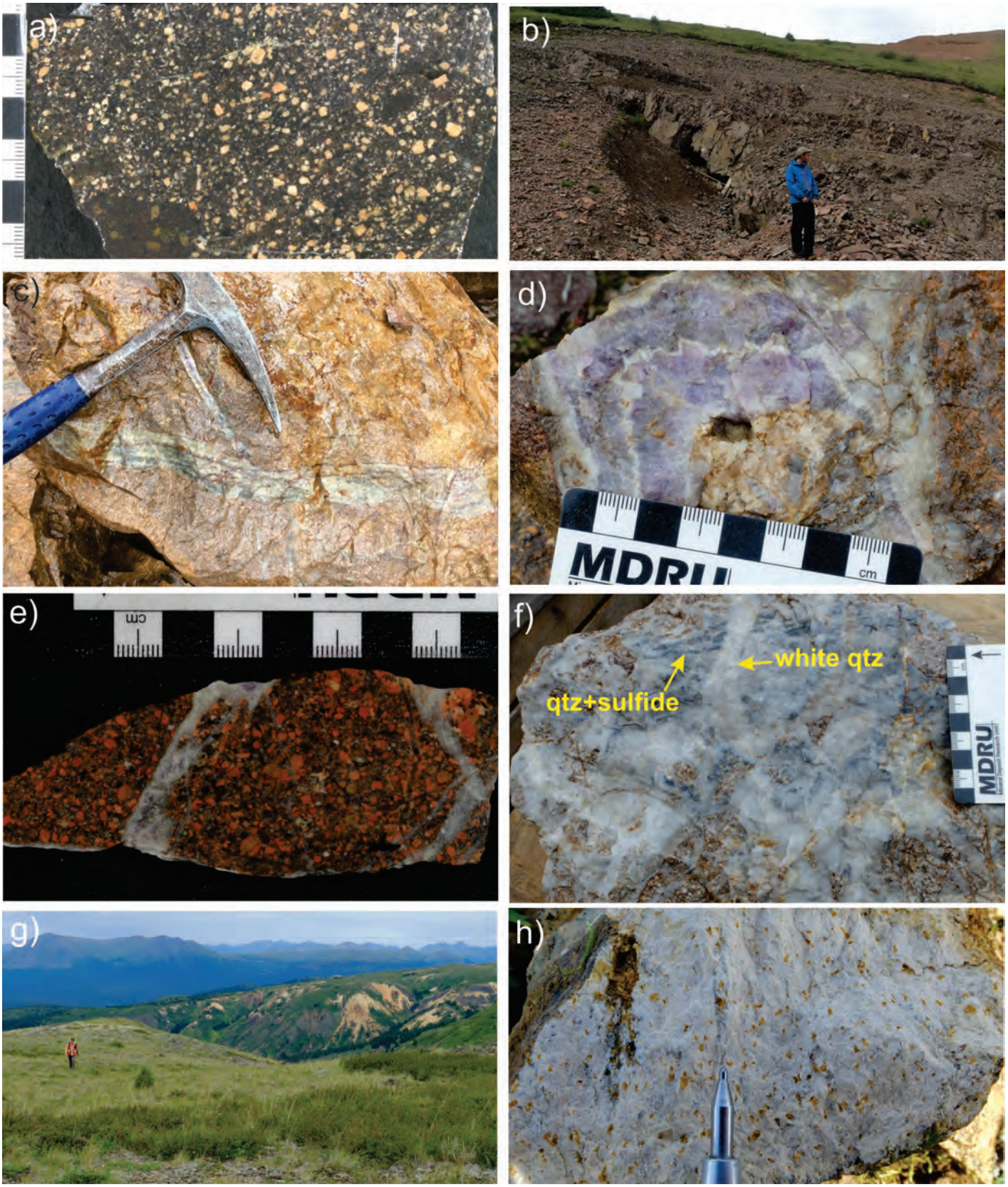

Figure 16: Lawyers and Silver Pond: a) Trachyandesite host rock of the Toodoggone Formation with abundant plagioclase phenocrysts and some clasts of similar rocks. b) Mineralized zone and small adit in Duke's Ridge. c) Banded chalcedony and hematite vein with ankerite-altered host rock (AGB zone). d) comb-textured amethyst vein. e) Amethyst vein cutting andesite with hematite-altered plagioclase phenocrysts. f) Sample of ore vein from Cliff Creek, showing early grey quartz vein with pyrite, chalcopyrite and a fine-grained grey sulfide phase cut by white quartz and amethyst. g) Looking north towards Silver Pond North, showing the extensive clay-altered area (yellow-reddish weathering outcrops). h) Sample of trachyandesitic tuff from Silver Pond North with fine-grained quartz and dickite alteration.

are dacitic tuffs that are intensely altered to chalcedonic quartz, dickite, and iron oxides (Fig. 16h). Pyrite is generally oxidized and locally clay alteration overprints quartz-sericite-pyrite alteration. The most intense alteration is related to subvertical roughly WNW-trending zones of higher permeability although the lateral extent of the alteration zone suggests that there is also be a stratigraphic control. Diakow et al. (1991) reported the presence of alunite and barite in the most intensely altered zones.

Silver Pond North alteration indicates an epithermal environment with a supergene overprint that results in sulfide oxidation and possibly clay alteration. However, the area lacks features that elsewhere are typical of paleosurfaces such as sub-horizontal chalcedonic silica zones, sinter deposits or steam-heated sugary quartz ± clay alteration. Alteration seems to be controlled by subvertical structures, vuggy residual quartz alteration is absent and quartz-alunite alteration is of modest extent. Thus, the area does not represent a well-developed lithocap in the classical sense (cf. Sillitoe, 2010).

AGE RELATIONSHIPS

Isotopic age determination from a number of volcanic host rocks, intrusive units and alteration phases of mineralized centers in the Toodoggone district are summarized by Diakow, et al. (2006) and Duuring et al. (2009a). New isotopic dates from the central Toodoggone area and a summary of previously published ages are in Table 2. This includes five new laser U-Pb zircon ages of the intrusive units (Fig. 18) and one Re-Os age of the molybdenite from the ore at the Baker deposit (Appendix 3).

Duncan Pluton, Baker Mine and Black Gossan Alteration

The Duncan pluton forms a large body, 20 x 5 km in the southwest of the Toodoggone district. Its northern part is exposed south of Baker mine (Fig. 3). Notable mineralization is not reported within or immediately adjacent to this pluton. Diakow et al., (2006) reported an Ar-Ar cooling age of 196.9 ± 2 Ma for this pluton on a sample from 10 km southeast of Baker near the Sturdee airstrip. Granodiorite in this area locally has K-feldspar veins and alteration. A sample from this outcrop (TD040) gave a weighted ^{206}Pb-^{238}U crystallization age of 202.3 ± 2.3 Ma (2σ errors, Fig. 17a). Phases of granodiorite probably related to the Duncan pluton are in contact with the limestone just south of the Baker mine. Both the limestone and the granodiorite show skarn type alteration. The granodiorite is altered to K-feldspar, diopside and epidote. A sample of granodiorite from this area (TD088) yielded a zircon U-Pb age of 197.9 ± 1.8 Ma (Fig. 17b). A small outcrop of highly K-silicate-altered granodiorite, occurs at the lower elevation of the Black Gossan. Zircons from this unit (TD051) yielded a U-Pb age of 193.4 ± 2.6 Ma (Fig. 17c). These data suggest that Duncan pluton probably is composed of several phases which were emplaced between at least ca. 202 and 193 Ma.

Sulfide mineralization at the Baker mine was dated using molybdenite from a quartz-molybdenite-pyrite±chalcopyrite vein within intensely quartz-sericite altered quartz-feldspar porphyry unit. Molybdenite (TD010) yielded a Re-Os age of 193.8 ± 0.8 Ma (Appendix 3). Thus, the mineralization at Baker is coeval, within error, with the emplacement of the granodiorite phase at nearby Black Gossan.

Table 2: Summary of age data from the central Toodoggone area.

Sample#	UTM E	UTM N	Area	Rock type	Alteration	Mineral	Method	Age (Ma)	Reference
			Alunite Ridge	Dacite dike		Zircon	U-Pb	188.7 ± 0.8	Diakow et al. (2006)
			Alunite Ridge		Adularia	Adularia	^{40}Ar-^{39}Ar	190.0 ± 1.3	Diakow et al. (2006)
			Alunite Ridge		Quartz-alunite	Alunite	^{40}Ar-^{39}Ar	196.9 ± 2.2	Diakow et al. (2006)
TD105	632239	6358266	Alunite Ridge	Syenite dike		Zircon	U-Pb	184.0 ± 2.4	This study
TD010	613957	6350793	Baker Mine	Quartz-Feldspar Porphyry	Sericite	Molybdenite	Re-Os	193.8 ± 0.8	This study
TD088	613053	6349593	Baker Mine, endoskarn	Granodiorite	diopside, K-feldspar, epidote	Zircon	U-Pb	197.9 ± 1.8	This study
TD051	616917	6350841	Black Gossan	Monzonite	K-feldspar	Zircon	U-Pb	193.4 ± 2.6	This study
			Brenda	Monzonite dike			^{40}Ar-^{39}Ar	187.3 ± 1.2	Diakow et al. (2006)
LW-011			Cliff Creek	Dacite tuff	K-feldspar	K-feldspar	^{40}Ar-^{39}Ar	189.7 ± 2.6	Clark and Williams-Jones (1991)
TD040	618768	6338922	Duncan pluton, Sturdee	Granodiorite		Zircon	U-Pb	202.3 ± 2.3	This study
			Duncan pluton, Sturdee	Granodiorite			^{40}Ar-^{39}Ar	196.9 ± 2	Diakow et al. (2006)
			Jock Creek Pluton	Monzonite		Zircon	U-Pb	196.7 ± 0.3	Diakow et al. (2006)
LW-037			Lawyer's AGB	Dacite tuff	K-feldspar	K-feldspar	^{40}Ar-^{39}Ar	188.2 ± 2.3	Clark and Williams-Jones (1991)
SH84-03			Shasta	Dacite tuff	K-feldspar	Adularia	^{40}Ar-^{39}Ar	186.7 ± 1.7	Clark and Williams-Jones (1991)
TD123	634963	6360017	Sofia	Granodiorite	K-feldspar	Zircon	U-Pb	189.6 + 2.1	This study

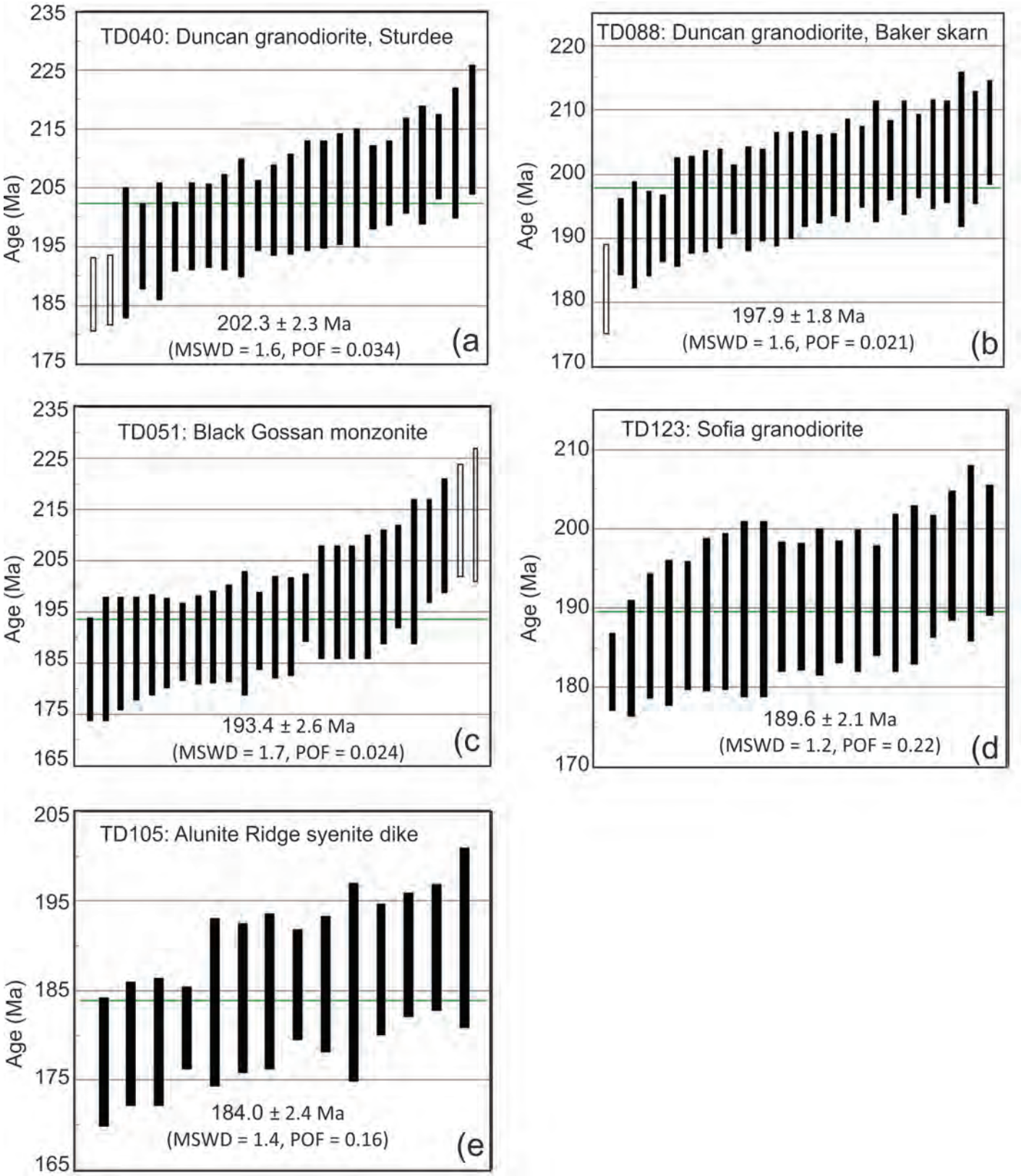

Figure 17: Plots of $^{206}Pb/^{238}U$ ages for zircon analyses from the Toodoggone intrusions. Error bars (including decay constant errors) for individual analyses are shown at the 2σ level. Assigned ages are based on a weighted $^{206}Pb/^{238}U$ age for each sample. Rejected analyses are shown as open bars. MSWD = mean square of weighted deviates; POF = probability of fit.

Jock Creek Pluton, Sofia Porphyry and Alunite Ridge Epithermal Mineralization

Porphyry-type copper alteration and mineralization at Sofia is exposed in a small outcrop of granodiorite, which, based on the district geology map (Fig. 3) is probably a phase of the Jock Creek pluton. This K-feldspar-altered Sofia granodiorite (TD123) yielded a U-Pb zircon age of 189.6 ± 2.1 Ma (Fig. 17d). Diakow et al., (2006) reported a U-Pb zircon age for the Jock Creek pluton about 4 km southeast of Sofia at 196.7 ± 0.3 Ma. The age of the Sofia granodiorite is similar (within error) to the ^{40}Ar-^{39}Ar age of alteration adularia from the low to intermediate-sulfidation type vein at Alunite Ridge at 190.0 ± 1.3 Ma (Diakow et al., 2006). Interestingly, the older phase of the Jock Creek pluton dated by Diakow et al. (196.7 ± 0.3 Ma) is similar to the alteration alunite age from the high-sulfidation mineralization at Alunite Ridge (196.9 ± 2.2, Diakow et al., 2006; Table 2). These data suggest multistage and coeval intrusive activity and locally porphyry mineralization at depth with the epithermal type mineralization near surface in the Sofia-Alunite Ridge area.

Magmatism continued after the initial porphyry-epithermal mineralization. A post-mineralization syenite dike (TH105) that cuts alteration at Alunite Ridge yields a zircon U-Pb age of 184.5 ± 2.0 Ma. A similar U-Pb zircon age of 188.7 ± 0.8 Ma is reported for a dacite dike at Alunite Ridge (Diakow et al., 2006).

Lawyers, Cliff Creek and Shasta Epithermal

^{40}Ar-^{39}Ar ages from K-feldspar at Lawyers AGB zone (188.2 ± 2.3 Ma), Cliff Creek (189.7 ± 2.6 Ma) and Shasta (186.7 ± 1.7 Ma) are reported by Clark and Williams-Jones (1991). The dates suggest that low to intermediate sulfidation-type epithermal gold mineralization may have continued into the Early Jurassic and outlasted the nearby Baker mine mineralization event.

ALTERATION CHARACTERISTICS FROM SHORT WAVE INFRARED SPECTROSCOPY (SWIR)

Shortwave Infrared (SWIR) spectroscopy can effectively identify alteration minerals in porphyry and epithermal environments (Halley et al., 2015). Spectrometers such as the TerraSpec™ can identify and characterize many mineral species, particularly phases containing -OH such as white micas, clays and chlorite.

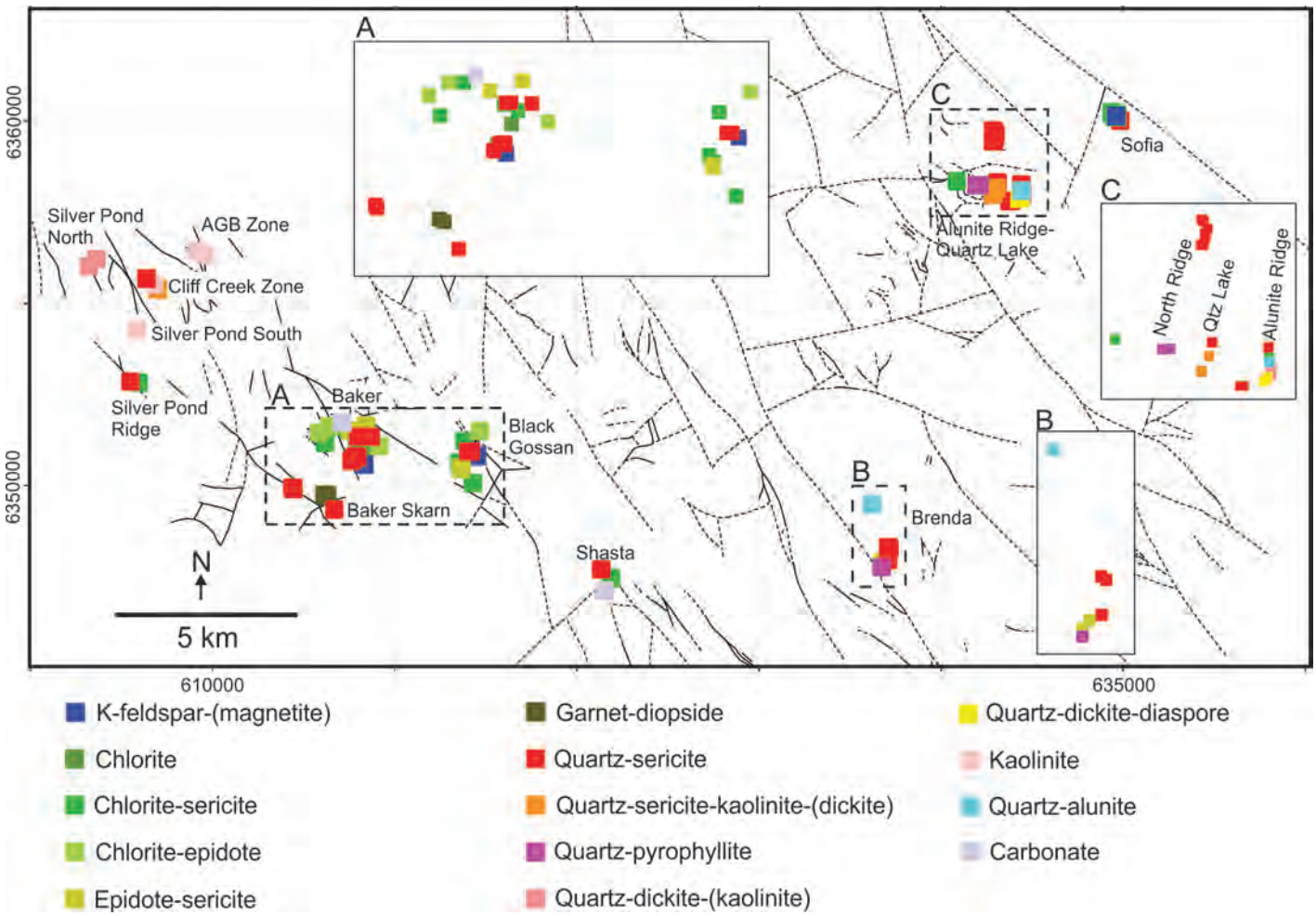

Figure 18: Map showing type and distribution of alteration as determined by SWIR and field observations in Toodoggone district

The distribution of these common alteration minerals can provide information on temperature and pH gradients in porphyry and allied deposits. Moreover, the subtle variations in mineral compositions can further provide a vector towards the mineralization centre.

Alteration Types

Details of alteration minerals identified by SWIR analyses are presented in Appendix 3. A summary of results that have been combined with some of the field observations are in Fig. 18. SWIR results from prospects sampled during this study identify sericite (illite, muscovite), pyrophyllite, clays (kaolinite, dickite), chlorite, epidote, carbonate, diaspore and alunite as main alteration phases.

At the Baker mine, the quartz-feldspar porphyry is altered to quartz-sericite with local chlorite whereas the Takla Group volcanic rocks are affected by chlorite, epidote and locally sericite (Fig. 18). Similar types of alteration occur at the Black Gossan occurrence with the chlorite-sericite alteration in Takla Group mafic rocks and quartz-sericite in porphyritic volcanic rocks. At Shasta, variable sericite, carbonate, and chlorite alteration is identified. The vein and breccia mineralization has quartz-sericite alteration and the wall rock has chlorite and carbonate alteration. At Brenda, the plagioclase porphyry body shows quartz-sericite and quartz-pyrophyllite alteration. Alunite was identified at Creek Zone, about 2 km north of the main zone indicating quartz-alunite at the periphery of the quartz-pyrophyllite alteration. The post mineral monzonite bodies have epidote-sericite alteration.

At Alunite Ridge, the volcanic host rocks are affected by quartz-sericite and quartz-sericite-kaolinite-(dickite), diaspore and alunite alteration. Quartz-sericite is the dominant alteration type on the north side of the North Ridge whereas pyrophyllite occurs on the southern part closer to the Quartz Lake. The samples suggest zoning from intense quartz-sericite to quartz-pyrophyllite, and then to quartz-alunite and diaspore from North Ridge to Alunite Ridge (Fig. 18). At Sofia, K-feldspar–magnetite alteration is overprinted by quartz-sericite and chlorite-sericite alterations.

SWIR analysis identified only kaolinite in Lawyers AGB zone whereas sericite and dickite occur at Cliff Creek suggesting higher temperature alteration assemblages. Similarly, the occurrence of dickite at Silver Pond North and sericite with chlorite at Silver Pond Ridge suggests higher temperature assemblages than those of AGB zone.

Alteration Mineral Variation

Type and the chemical composition of alteration minerals are controlled by temperature, pressure, composition and pH of hydrothermal fluids and composition of host rocks (Parry et al., 1984) and trends and patterns in these features can provide vectoring tools to identify zones of mineralization. White mica, chlorite and clays are common alteration minerals in porphyry systems and their variations are discussed below.

White Micas and Pyrophyllite: The white micas are a group of fine-grained phyllosilicates including true micas such as muscovite, phengite and paragonite, and also K-deficient micas or illite (Deer et al., 2003). The term “sericite” is a field term used for fine-grained white micas (Meyer and Hemley, 1967). The aluminum content of white micas reflects pH condition during alteration, and micas become increasingly aluminous at low pH environments whereas higher pH stabilizes Fe-Mg-rich phengite (Halley et al., 2015). The wavelength position of the AlOH absorption feature (2200 nm) is used to estimate white mica composition. Therefore, mapping the white mica composition shift from Fe-Mg-rich to K-rich provides clues to vectoring towards more acidic parts of the alteration system.

The crystallinity of the white micas has been used to characterize the temperature of alteration (Cohen, 2012, Halley et al., 2015). At higher temperatures (>300 °C), the white micas are more crystalline whereas at lower temperatures they are less crystalline, commonly K-deficient (e.g., illitic) and contain interlayered illite-smectite. The white mica crystallinity index is calculated based on the depth of the AlOH absorption band (2200 nm) of the SWIR spectra relative to the intensity of the water absorption band (1900 nm). The term ‘illite’ was used where the deep, water absorption band occurred in the sample. However, the boundary between illite and muscovite is arbitrary as these phases represent a single continuous solid solution (Cohen, 2011).

At Toodoggone, muscovite, illite and pyrophyllite were identified (Fig. 19a). Muscovite and illite were identified at Baker, Black Gossan, Shasta, Brenda and Alunite Ridge whereas at Cliff Creek and Silver Pond Ridge only illite was identified, and at North Ridge and Sofia muscovite alteration occur. Pyrophyllite was identified at Brenda and in southern parts of North Ridge. Muscovite and illite display AlOH 2200 nm variations from 2200 to 2230 nm. Muscovite and illite with paragonitic compositions (AlOH < 2205) are rare. Most of the white micas have muscovite or illite compositions (AlOH 2205-2210) suggesting an acidic environment of formation (Fig. 20a). Those with slightly phengitic compositions (AlOH > 2210) locally occur at Shasta, Silver Pond Ridge and Alunite Ridge. In these locations, the phengitic character of the white micas is probably controlled by specific host rocks (e.g., biotite-bearing monzonite dike at Alunite Ridge and Silver Pond Ridge) or accompanying carbonate alteration (e.g., Shasta).

Samples with white mica have a wide range of crystallinity (Fig. 21a). Most have low crystallinity (<1) however, higher crystalline white micas (>2) occur at Baker, Black Gossan and Sofia. At Baker

and Black Gossan the highly crystalline micas occur with strong quartz-sericite alteration of the intrusive porphyry, and at Sofia with the chlorite-sericite alteration. Thus, alteration at these prospects formed at higher temperatures potentially similar to those expected in a porphyry alteration assemblage. At Alunite Ridge the limited data suggests that white mica crystallinity increases towards the east and to the north (North Ridge).

Clays: Clay minerals, including montmorillonite, halloysite, kaolinite and dickite, have been identified largely at Lawyers-Silver Pond and Alunite Ridge (Fig. 19b). These minerals are absent at Baker, Black Gossan and Sofia where more crystalline white micas confirm comparatively higher temperature alteration. Occurrences of dickite at Cliff Creek and Silver Pond North suggest higher alteration temperatures than at the AGB

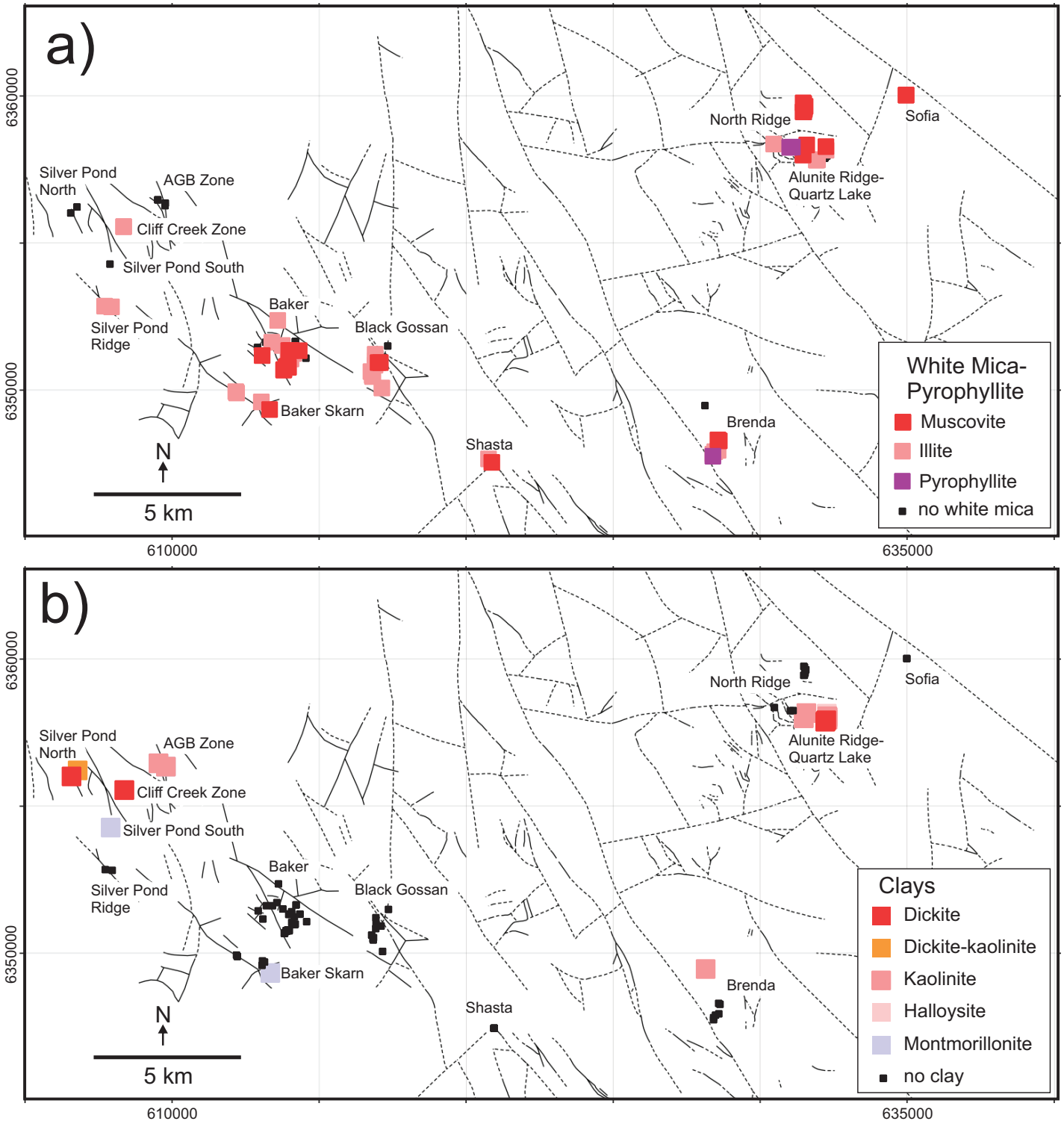

Figure 19: SWIR data showing distribution of white mica and pyrophyllite and clays in Toodoggone district.

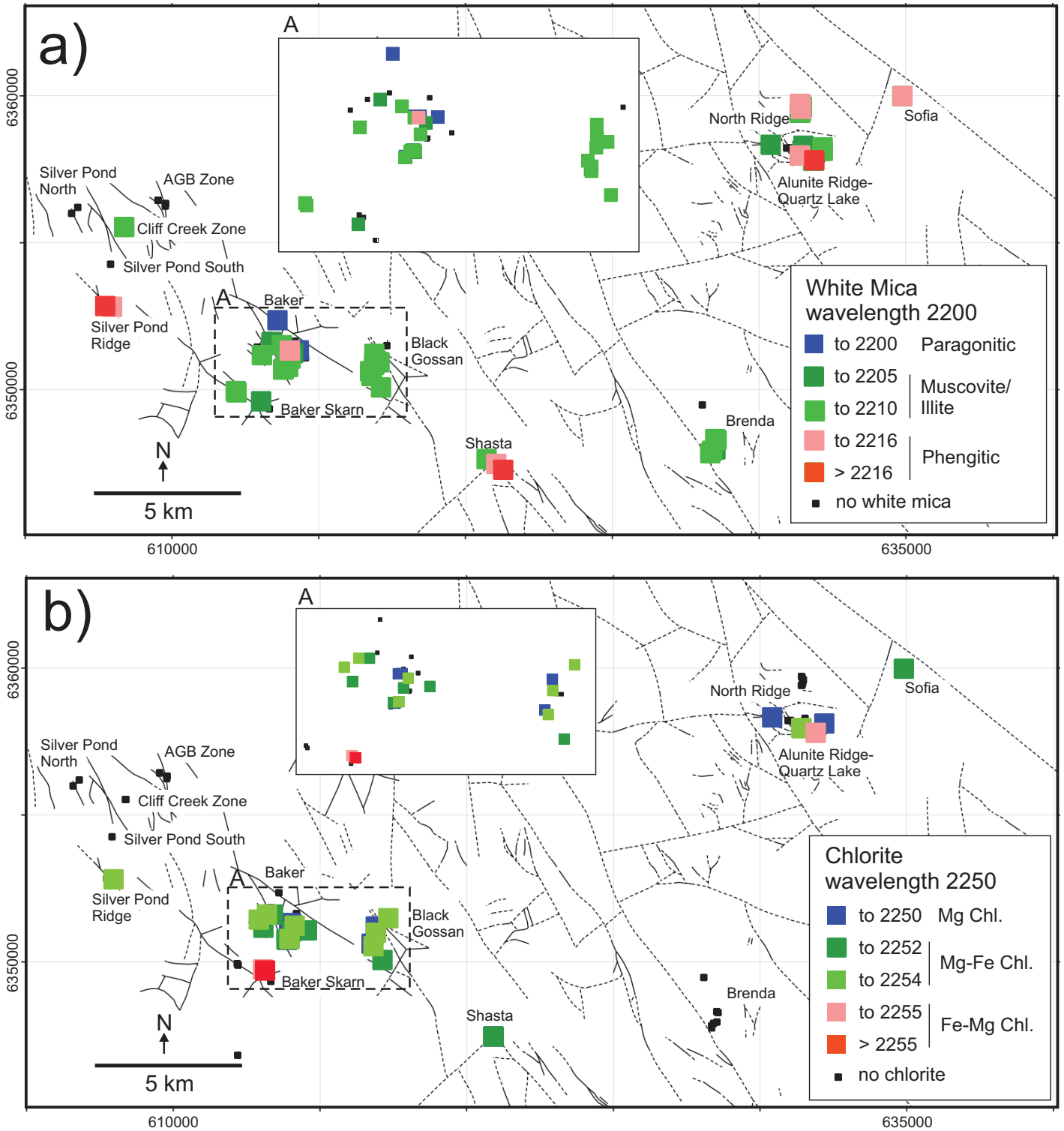

Figure 20: SWIR data showing variations of white mica and chlorite composition based on the 2200 and 2250 nm absorption feature, respectively.

zone. Similarly, dickite occurs in the eastern parts of the Alunite Ridge. All of these clay minerals show a very narrow range of crystallinity (around 1, Fig. 21b).

Chlorite: Chlorite occurs in mafic volcanic host rocks beyond the zones of sericite or advanced argillic alteration. Similar to white mica, the composition of chlorite reflects the chemical environment of alteration, such as pH, but is less sensitive to pH and temperature than white mica. The wavelength position of absorption of the 2250 nm spectral band is used to map changes in chlorite composition (Fig. 20b). Chlorite occurs at most prospects and shows intermediate Mg-Fe compositions. However, no distinct trends are visible but this may be due to the limited extent of sampling.

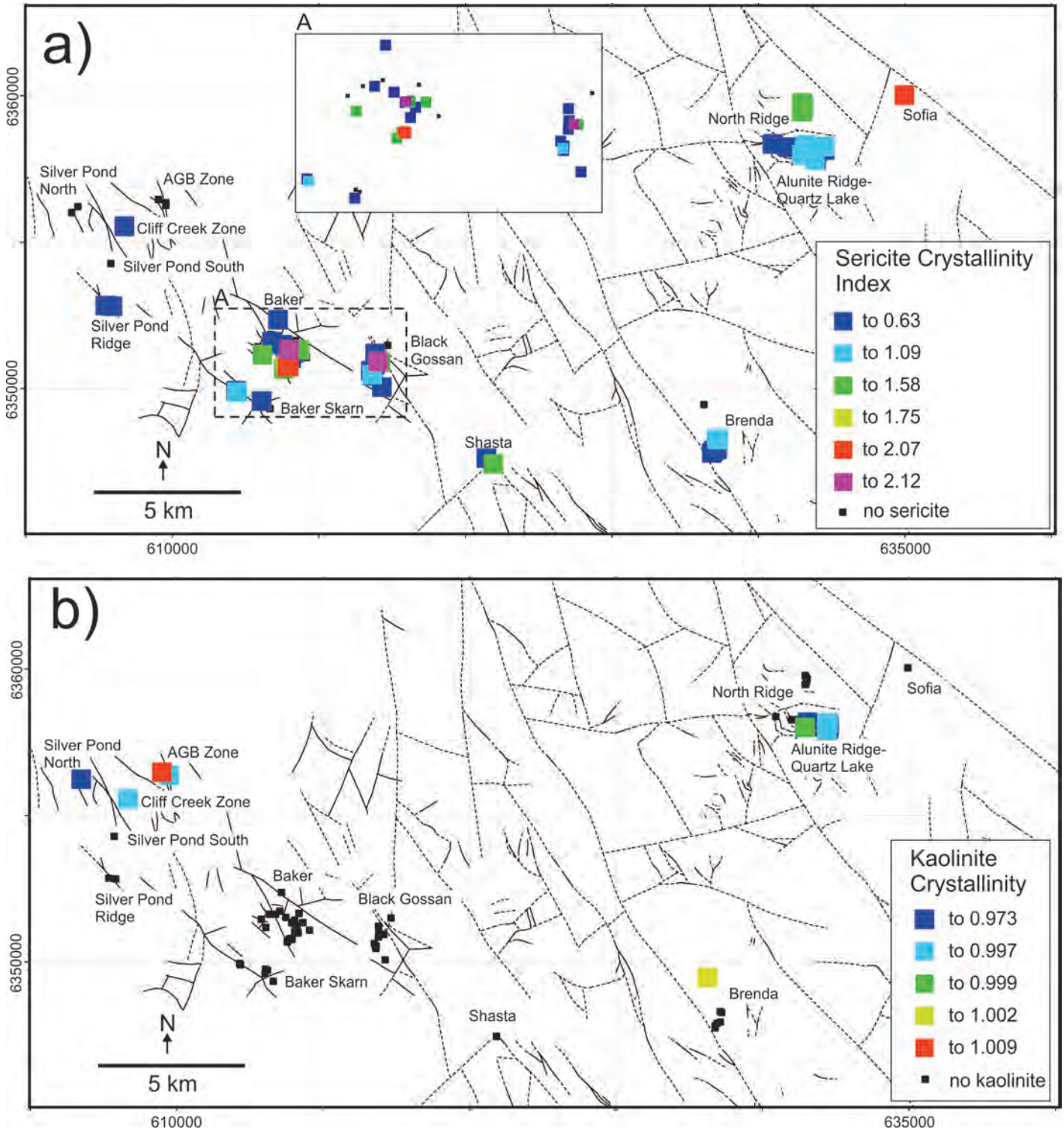

Figure 21: SWIR data showing crystallinity of sericite (muscovite, illite) and kaolinite group (kaolinite, dickite and halloysite).

GEOCHEMICAL CHARACTERISTICS

A total of 75 outcrop samples representing various rock types and alteration assemblages were analyzed for major and trace elements. Results are in Appendix 4. These rocks have been affected by variable, locally intense, alteration that destroys the original mineralogy. Therefore, major elements such as Si, Ca and Na are not reliable to characterize the pre-alteration host rocks. Immobile trace element composition of the samples, however, has been used to characterize the rock types and mineralization-related elements such as Cu, W, Sb have been used to characterize the geochemical footprint of each deposit or prospect.

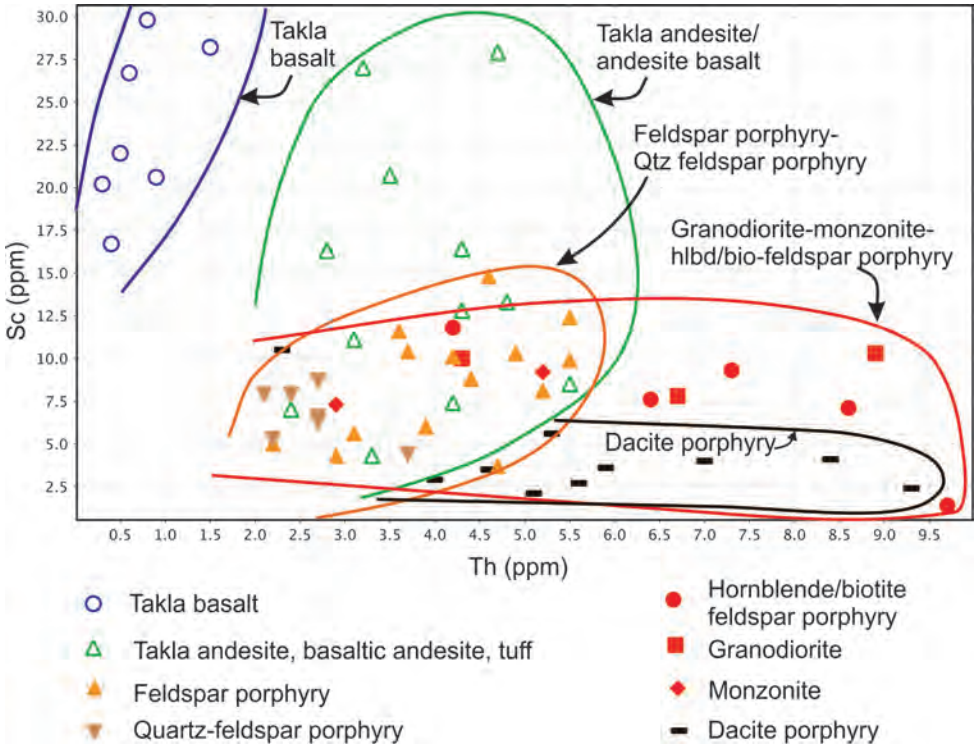

Figure 22: Th-Sc plot showing Toodoggone host rock types

Host Rock Composition

Volcanic and intrusive rocks in the Toodoggone district are characterized on the basis of their Th and Sc concentrations (Fig. 22). Trace element concentrations of all analyzed rocks vary between <1-10 ppm for Th and <1-30 ppm for Sc and show some distinct grouping. The mafic units of the Takla Group that are mapped as basalt show high Sc (>10 ppm) but low Th (<2 ppm) concentrations whereas the less mafic components, mapped as basaltic andesite, andesite and tuff, display variable Sc (3-28 ppm) and moderate Th (2-6 ppm) concentrations. Rocks of the Toodoggone Formation with distinct porphyry textures that contain feldspar phenocrysts that occur in Lawyers, Baker, Black Gossan, Brenda, Cliff Creek and Silver Pond North, have a similar range of Th concentrations compared to those of the Takla Group andesite but display distinctly lower Sc (<15 ppm) concentrations. The quartz-feldspar porphyry (QFP) unit at Baker which is strongly altered to quartz-sericite-pyrite is grouped with the feldspar porphyry unit in Fig. 22, but because the QFP has Th concentrations <4 ppm it might be possible to geochemically distinguish it from the feldspar porphyry unit. All of the other intrusive units mapped during this study, including granodiorite, monzonite and hornblende/biotite feldspar porphyry display a similar range of Sc to the feldspar porphyry unit (<12 ppm) but display variable Th concentration (3-10 ppm). Dacite porphyry, which is the main host rock at Alunite Ridge and North Ridge, is mapped as part of the Lower Toodoggone Formation (Fig. 3). This unit, however, shows Th and Sc compositions that are similar to the granodiorite or hornblende/biotite plagioclase porphyry unit, thus suggesting that dacite porphyry is a distinct phase of the Toodoggone Formation or potentially an intrusive unit.

Host Rock REE Composition

Trace element data were normalized to the compositions of C1 carbonaceous chondrite meteorites using the normalization values of Sun and McDonough (1989). Note, however, that HREE may be slightly underreported due to the analytical technique used. Normalized REE diagrams (Fig. 23a and b) show that all samples have patterns typical of subduction-related magmas, characterized by enrichments in light REE (LREE, e.g. La) relative to compatible heavy REE (HREE, e.g., Yb) (e.g., Gromet and Silver, 1987). Samples from the Takla Group mafic unit show the least LREE enrichment (grey highlight in Fig. 23a) suggesting an origin from a more primitive magma. The granodiorite, monzonite and units with porphyry textures, with the exception of dacite porphyry, show similar REE patterns to those of the Takla Group volcanic rocks. The quartz-feldspar porphyry shows slightly less LREE enrichment relative to feldspar porphyry (Fig. 23b).

Most samples show weak LREE enrichment (La/Sm]n = 1 to 6) and weak enrichment or depletion of MREE relative to HREE (Dy/Ybn = 0.6 to 1.5) suggesting that largely hornblende crystallization controlled the REE distribution. The dacite porphyry shows stronger depletion of MREE and HREE with Dy/Ybn = 0.4 to 0.7 suggesting that garnet crystallization likely caused this effect (Bissig et al., 2017) which may reflect crustal thickness (Kay and Mpodozis, 2001).

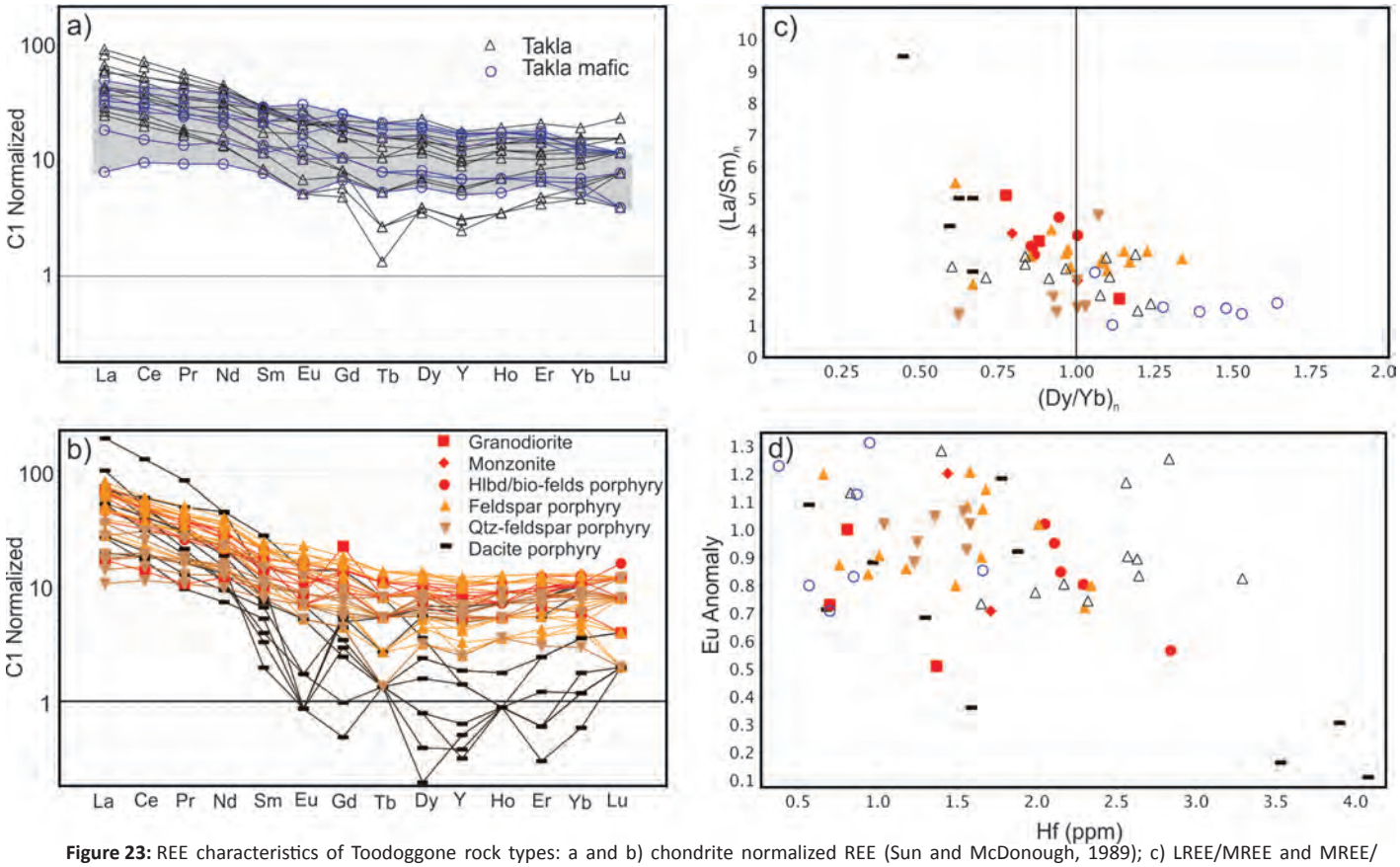

Figure 23: REE characteristics of Toodoggone rock types: a and b) chondrite normalized REE (Sun and McDonough, 1989); c) LREE/MREE and MREE/HREErelationships; d) Eu anomaly relative to Hf as a proxy for crystallization.

All rock units lack a significant Eu anomaly (Eun/Eu* > 0.5) or show a weak positive Eu anomaly (Fig. 23d). The Eu anomaly does not correlate with Hf content which is a proxy for crystal fractionation. These suggest that plagioclase fractionation was not significant (Burnham et al., 2015) and the magmatic oxidation state and/or magmatic water content was high (Lang and Titley, 1998; Richards, 2012; Loucks, 2014). The exception exists for the dacite porphyry which shows a variable Eu anomaly (Eun/Eu* = 0.1 to 1.2) correlating negatively with the Hf concentration suggesting the effect of crystal fractionation of probably a more evolved magma.

Mineralization Geochemical Footprint

Rock samples were analyzed for trace metals to further characterize the main mineralization and alteration assemblages. Distribution of the selected elements occurring with the mineralization are in Figures 23 to 27 and discussed below as a basis to compare the mineralization in the district and their position within the porphyry mineral system.

Copper mineralization with grades up to 0.7% occurs with the quartz veins with sericite alteration at Shasta and Cliff Creek. Weak copper mineralization (~0.05% Cu) occurs with K-feldspar and sericite-chlorite alteration at Sofia and Baker. Copper in surface samples collected from other prospects is commonly < 100 ppm. Molybdenum with concentrations of > 200 ppm occurs with the quartz-feldspar porphyry unit at Baker with phyllic alteration and to a lesser degree with the chlorite-altered Takla Group rocks. It also occurs with the copper mineralization at Shasta. Weak molybdenum mineralization (40-50 ppm) occurs with the quartz-sericite alteration at Black Gossan and with grey quartz veins at Cliff Creek (Fig. 24). Veins with sphalerite and galena at Shasta and Cliff Creek contain > 1% zinc and lead. Lead and zinc also occur with the skarn type mineralization at Baker. Takla Group volcanic rocks around the Baker mine and at Black Gossan have elevated (100-200 ppm) zinc concentrations (Fig. 25).

At Shasta and Cliff Creek, the galena, sphalerite, chalcopyrite mineralization contains > 200 ppm silver. At Brenda, the quartz-sericite altered porphyry unit contains ~50 ppm silver. At Lawyers AGB zone the banded quartz veins contain ~10 ppm silver. At Baker, rocks with quartz-pyrite veins and sericite or chlorite alteration contain low silver concentrations of ~5 ppm. At the Alunite Ridge, the quartz-sericite-dickite altered rocks, especially in the east, contain low silver (2-4 ppm) concentrations (Fig. 26). Host rocks cut by quartz-pyrite veins or with quartz-sericite-pyrite alteration at Baker and Black Gossan have arsenic concentrations of 30 to 90 ppm. Up to 80 ppm arsenic also occurs with the late pyrite veins with chlorite alteration at Sofia. Quartz-sericite-pyrite alteration at Alunite Ridge and Brenda has

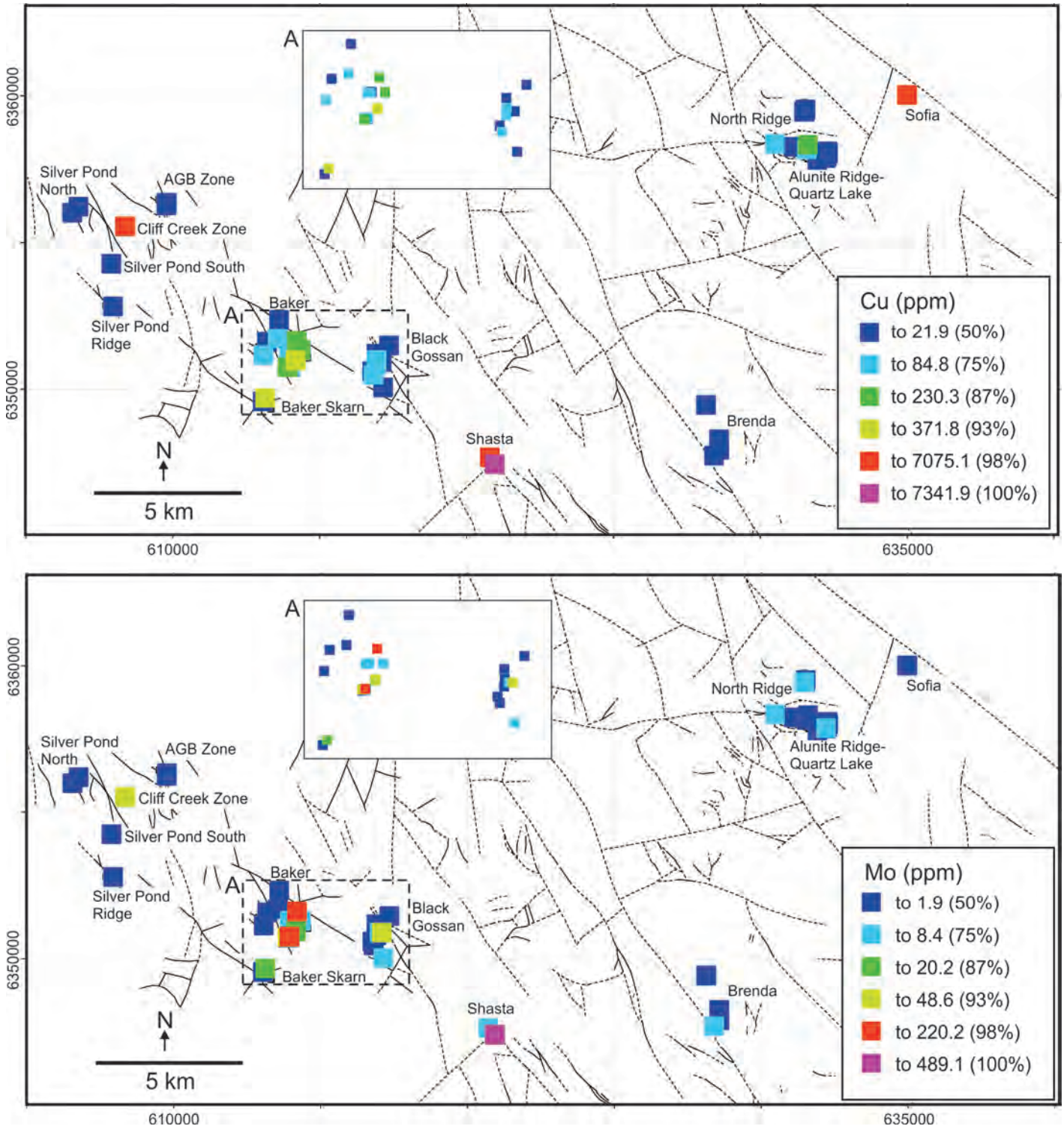

Figure 24: Maps showing concentration distribution of Cu and Mo in select mineralized surface rock samples.

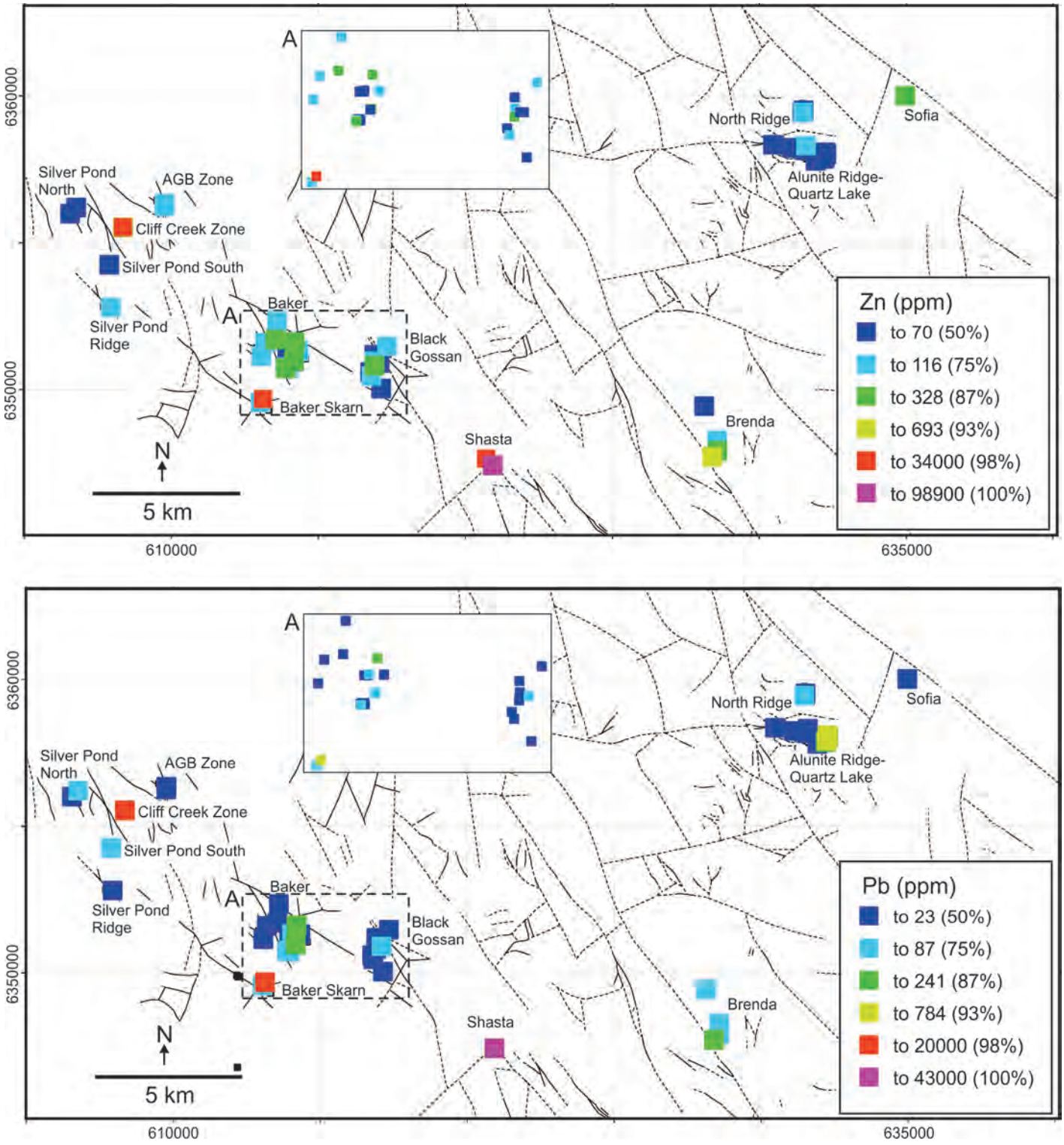

Figure 25: Maps showing concentration distribution of Zn and Pb in select mineralized surface rock samples.

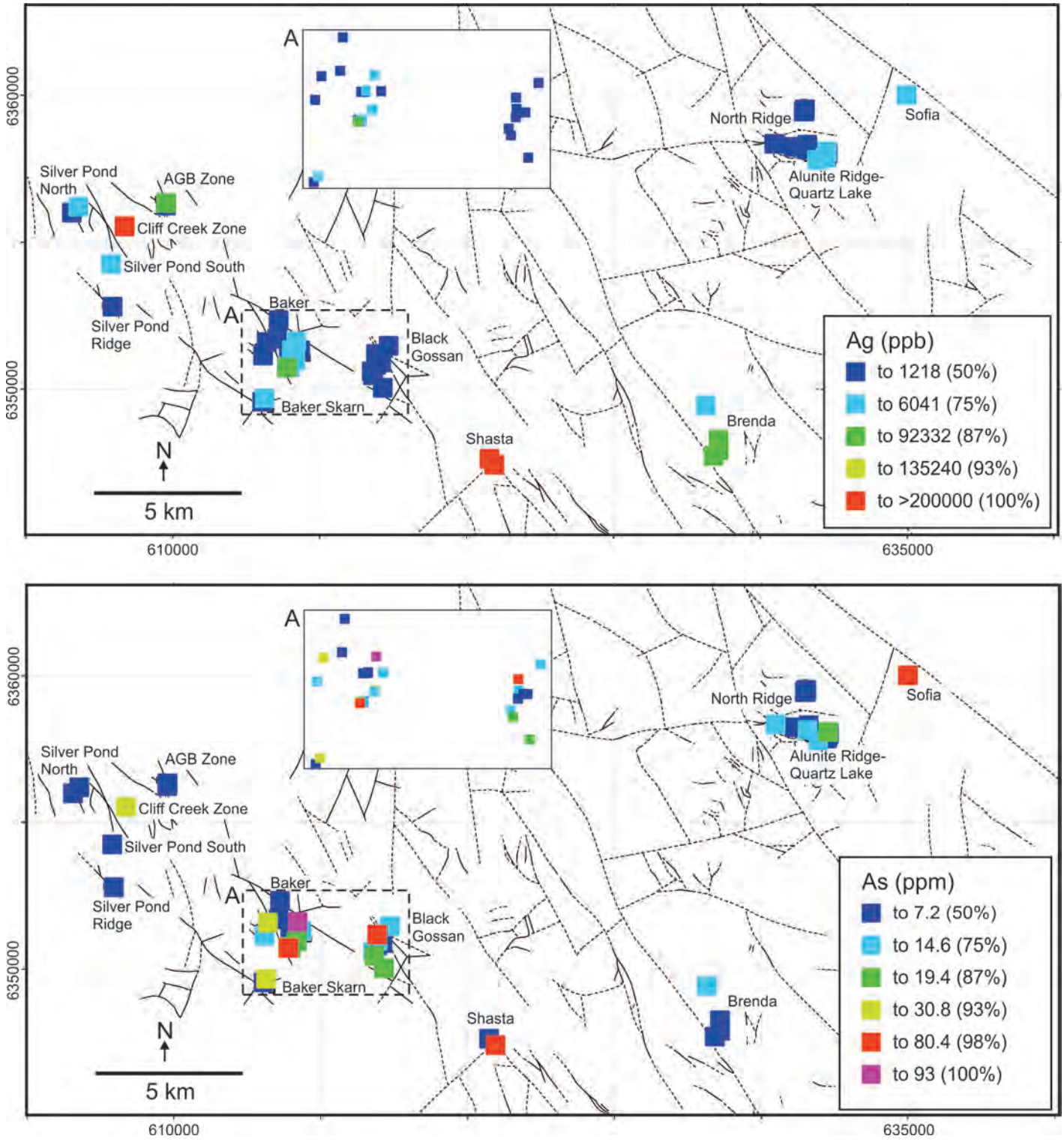

Figure 26: Maps showing concentration distribution of Ag and As in select mineralized surface rock samples.

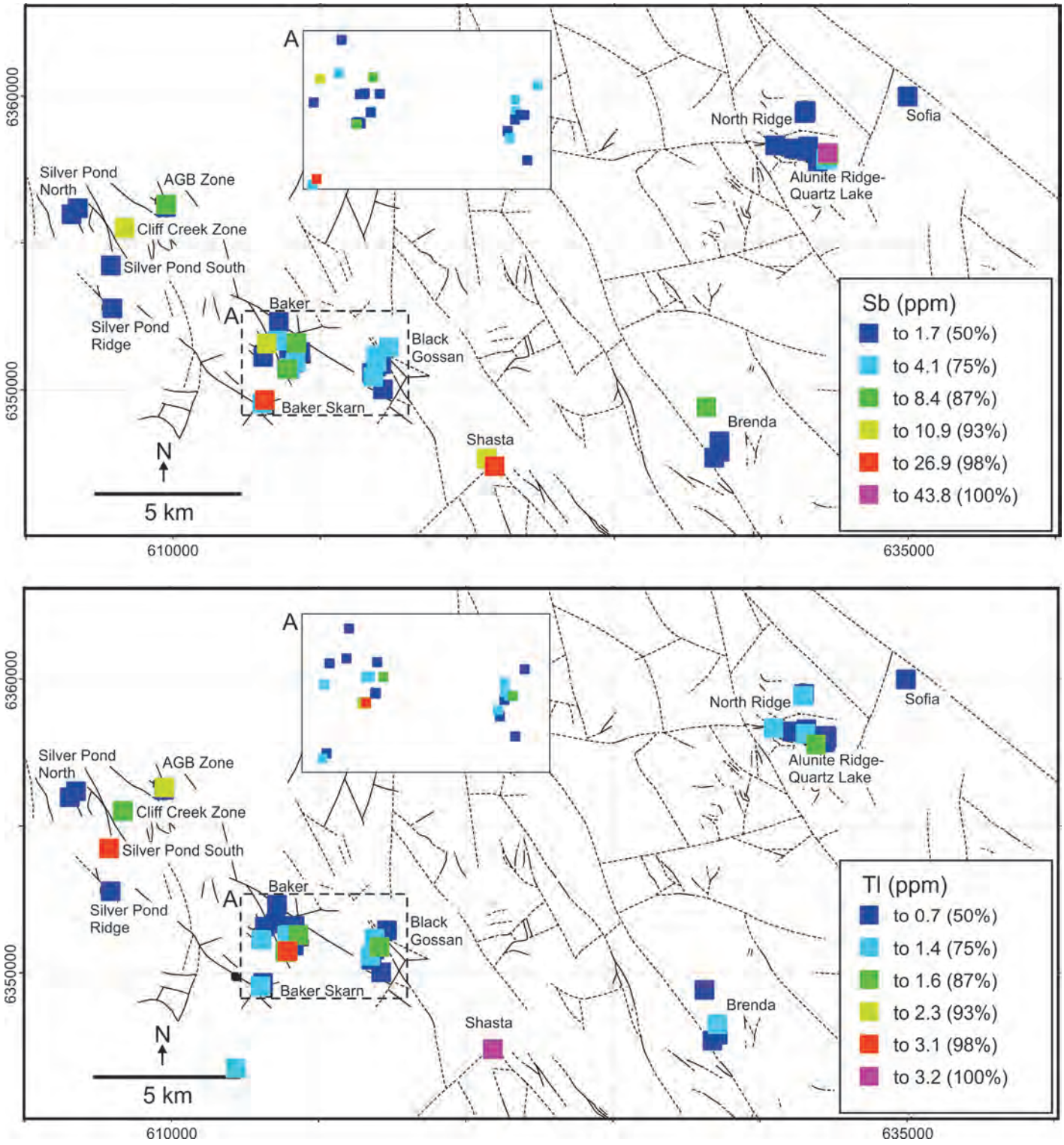

Figure 27: Maps showing concentration distribution of Sb and Tl in select mineralized surface rock samples.

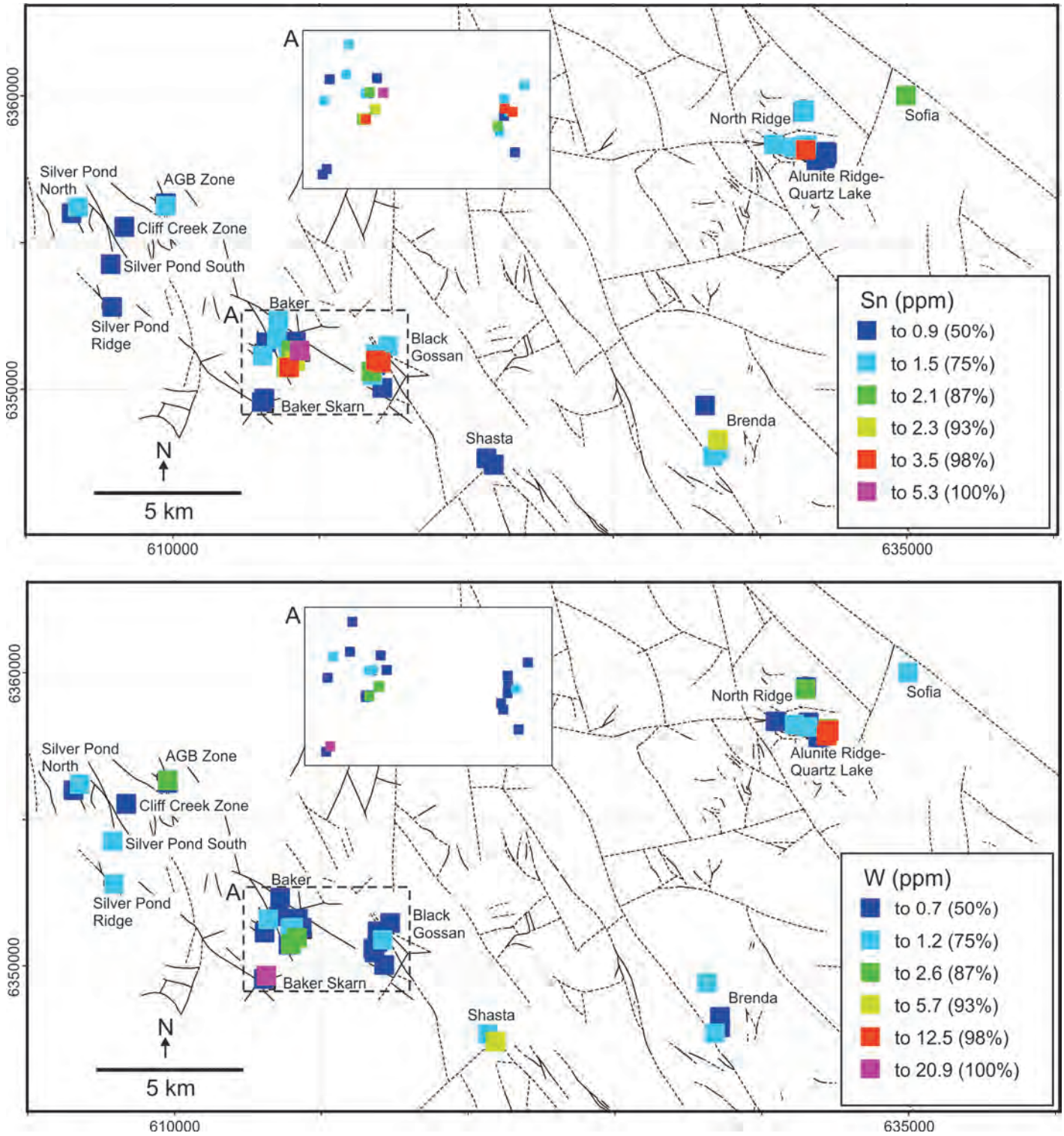

Figure 28: Maps showing concentration distribution of Sn and W in select mineralized surface rock samples.

elevated arsenic concentrations (~10 ppm). Antimony occurs with quartz-alunite alteration at Alunite Ridge (~40 ppm) and Brenda (~5 ppm). Sulfide ore at Shasta and Cliff Creek contain 10-25 ppm Sb. At Lawyers AGB zone, antimony occurs with the banded amethyst veins (~8 ppm). At Baker, weak antimony (5-10 ppm) occurs largely with chlorite-pyrite alteration either in the Takla Group or porphyry unit (Fig. 27).

Other elements that occur with modestly anomalous trace concentrations with the mineralization are Tl, W and Sn (Figures 26 and 27). Thallium occurs with the quartz-sericite-pyrite alteration at Baker and Silver Pond South (2-3 ppm). Tungsten occurs with the skarn-type mineralization at Baker (~20 ppm) but also with the quartz-dickite-diaspore alteration at the Alunite Ridge (5-12 ppm).

Geochemical Index for Porphyry to Epithermal Mineralization

Porphyry and related epithermal deposits have vertical and lateral alteration mineral zoning (e.g., Sillitoe, 2010). Trace metals in these deposits are also zoned upward and outward from the >0.1 wt.% Cu zone in the general sequence Mo, W, Sn, Se, Te, Bi, Sb, As, Li, and Tl (Halley et al., 2015). Similar to the alteration studies, this zonal arrangement of metals can be used to estimate the vertical level of porphyry mineralization and inform decision-making to vector towards mineralization.

To discriminate between those localities that characterize porphyry/proximal from more distal/shallow mineralizing environments, those key metallic elements that define each environment (based on Halley et al., 2015) were considered. More specifically, elements that are enriched at the core of the porphyry deposit such as Cu, Mo, W, Sn were summed and ratioed against those formed at shallow environments such as As, Sb, Ag, Tl, Li. Element concentrations were normalized by multiplying or dividing to a factor such that all of elements have approximately a similar effect on the ratio (Fig. 29).

Results provide a range of ratios from <1 to 5.5, which are herein defined as MPIx (MDRU Porphyry Index) and is utilized to compare the vertical level of exposure of mineral prospects in Toodoggone district as an indicator of proximity to porphyry copper mineralization. A higher MPIx number indicates closer proximity to porphyry-type mineralization.

The Sofia prospect has the highest MPIx of 5.5 (Fig. 29). This is very well supported by field observations of K-silicate alteration and quartz-magnetite veins indicating mineralization that represents proximity to the core of a porphyry centre. The quartz-feldspar porphyry at Baker has an MPIx of 2.5 to 3 associated with strong quartz-sericite-pyrite alteration and contains quartz-molybdenite-pyrite veins typical of the shallower parts of a porphyry deposit. The Baker skarn has also a similar MPIx. This is followed by mineralization at Shasta and Cliff Creek (MPIx = 2 to 2.5) which contains mostly vein type quartz-sulfide veins that also indicate the shallow parts of porphyry system. Strong quartz-sericite alteration at Black Gossan and North Ridge with pyrophyllite at Alunite Ridge has an MPIx of 1.5 to 2 which represents even shallower parts of porphyry system. Those other

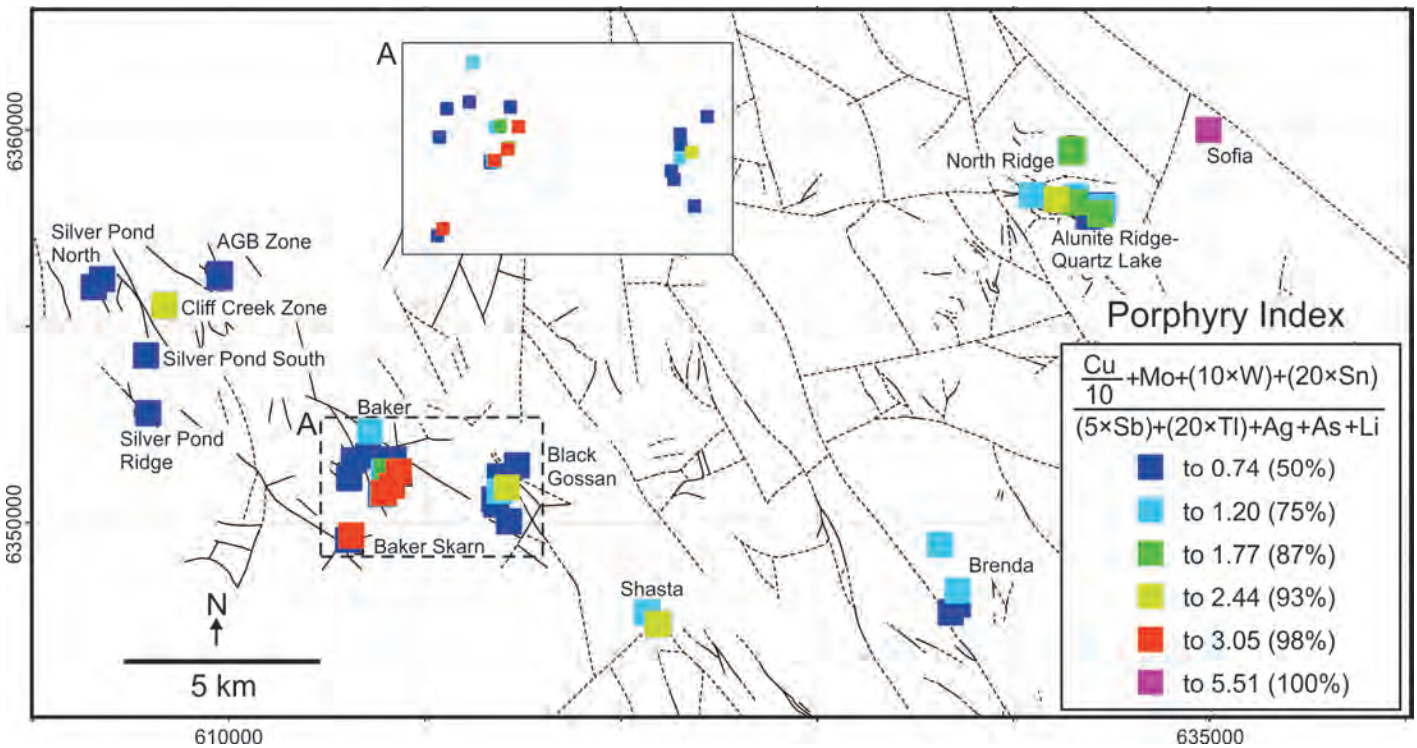

Figure 29: Geochemical index ratios indicating the footprint of porphyry mineralization.

mineralized zones in the Lawyers area, as well as at Brenda, have MPIX values of ~1 or <1 and represent gold mineralization that is distal to the porphyry core and are clearly in the epithermal realm.

FLUID INCLUSIONS

Previous fluid inclusion studies in the Toodoggone area (e.g., Thiersch et al., 1997, Duuring et al., 2009a) characterized those veins that were largely related to the epithermal veins. This study carried out reconnaissance fluid inclusion evaluations of porphyry-type quartz veins are acquired and compared them to the epithermal veins and prospects. More specifically, results from Baker and Black Gossan K-silicate alteration zones located at lower elevations were compared to the quartz-sericite alteration situated at higher elevations. Similarly, fluid inclusion characteristics of K-silicate-altered Sofia porphyry prospect are compared with results from Alunite Ridge.

Petrography

Fluid inclusions were commonly small (< 10 microns) and most of the measurements were on inclusions ~5 microns, using a 100X lens. Thermometry results were only collected for those fluid inclusions that allowed reliable observation on both ice melting, salt dissolution, and vapor homogenization. Results are shown in Appendix 4.

Fluid inclusions were classified into liquid-vapor-salt (LVS) and two-phase liquid-rich with vapor (LV) or vapor-rich with liquid phase (VL). Fluid inclusion populations that formed trails that cross-cut quartz crystal boundary were assumed to be secondary and not representative of the quartz-depositing fluid chemistry, and thus were avoided. Fluid inclusions that formed in crystal growth zones are recognized as strong evidence for primary origin, but these were rare. In most cases, fluid inclusions occur in isolation or as trails within the crystal and were assumed to be primary or pseudo-secondary.

The abundant VL inclusions coexist with the LV inclusions and therefore may constitute an assemblage. VL and LV inclusions also occur together with LVS inclusions but given the limited observations there was no convincing evidence to prove their relationship.

Microthermometry Results

Baker K-silicate Alteration: Sample TD084 from drill core (see Appendix 1) is a quartz-feldspar porphyry with pervasive K-feldspar alteration cut by irregular shaped quartz-magnetite±pyrite±chalcopyrite and quartz-pyrite-chlorite-epidote-chalcopyrite veins. Polyphase LVS inclusions (Fig. 30a) are common and occur with two-phase vapor-rich (VL) inclusion but it is not certain that they formed at the same time. VL inclusions occur with the liquid-rich (LV) inclusion in the same trail. LVS inclusions (n=6) have Th = 310 to 556 °C and salinities of 39.0 to 50.8 wt.%. NaCl equiv.

Baker Phyllic Alteration: Sample TD078 is a quartz-feldspar porphyry from the pit with intense pervasive quartz-sericite-pyrite alteration that is cut by a quartz-pyrite-molybdenite vein. Abundant two-phase LV and VL inclusions occur together (Fig. 30b) typically in euhedral quartz crystals. Most of these inclusions are very small (<3 microns) and larger (~5 microns) inclusions suitable for thermometry are not common. The results for the LV inclusions (n=5) have Th = 196 to 358°C and salinity 0.5 to 2.6 wt.% NaCl equiv.

Black Gossan K-silicate Alteration: Sample TD051 is from a small quartz-monzonite porphyry body that occurs at the lower elevations near the river valley at Black Gossan. It is characterized by K-feldspar alteration that contains quartz-magnetite-pyrite±chalcopyrite veins. Moderate patchy chlorite±epidote

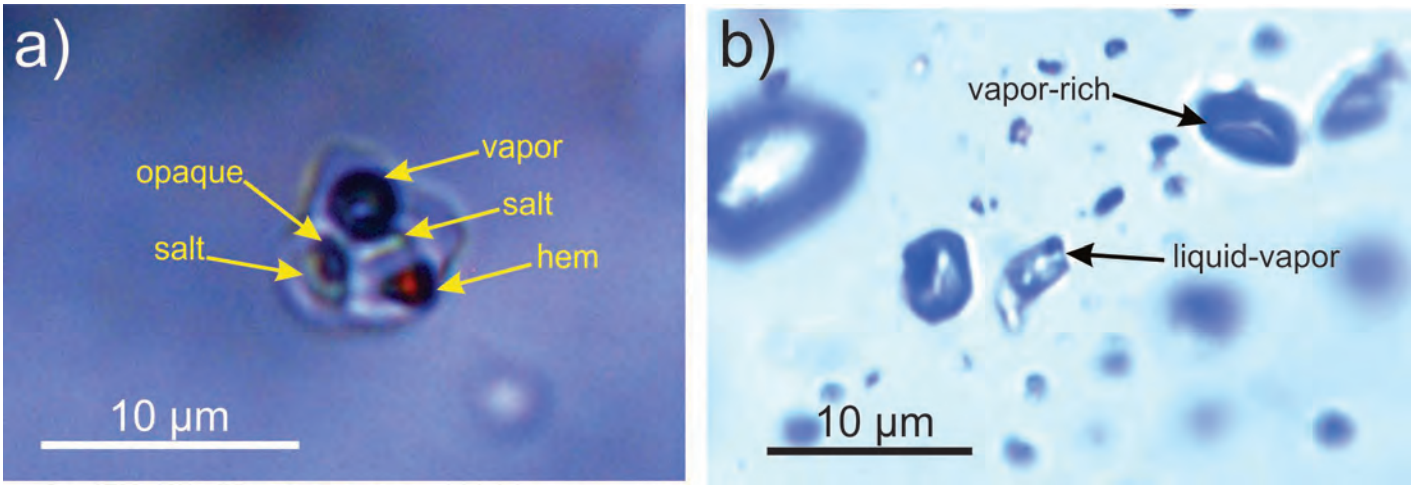

Figure 30: Examples of fluid inclusion types: a) LVS inclusion from the Baker K-silicate alteration containing a red (hematite) and black (chalcopyrite or magnetite) opaque phase. b) LV inclusion occurring with several vapor-rich inclusions (from Black Gossan quartz-sericite-clay altered zone).

alteration overprints the potassic alteration. The quartz-magnetite vein contains LVS fluid inclusions containing halite cubes, yellowish sylvite and locally reddish hematite or chalcopyrite solid phases. Two-phase VL and LV fluid inclusions are abundant. Salt-bearing LVS inclusions (n=3) had Th of 266 to 456°C with salinities of 36.3 to 46.5 wt.% NaCl equiv. whereas the LV inclusions (n=5) had Th of 245 to 313°C, with salinities of 0.9 to 4.0 wt.% NaCl equiv.

Black Gossan Phyllic-Clay Alteration: Sample TD049 is from andesite porphyry at the upper levels of Black Gossan hill with pervasive quartz-sericite-clay alteration cut by narrow quartz-sericite-(pyrite) veins. The quartz has euhedral comb textures and open spaces and cavities in the center of the vein and hosts rare very small (<3 microns) LVS and abundant two-phase LV and VL inclusions. Most inclusions are very small (<2 microns) and rare larger inclusions that were selected for analysis. The LV inclusions (n=5) showed Th = 278 to 397°C with salinities of 0.5 and 8.1 wt.% NaCl equiv.

Sofia K-silicate Alteration: Sample TD123 of granodiorite from the Sofia prospect has been affected by strong K-feldspar alteration and is cut by quartz-magnetite veins. The K-feldspar alteration is overprinted by chlorite-sericite alteration. Magnetite and minor chalcopyrite are disseminated in the rock and in the quartz vein. The quartz-magnetite vein hosts randomly distributed LVS fluid inclusions. Opaque phases resembling hematite (red) and/or chalcopyrite (triangular shape) occur locally. Two-phase LV or VL are abundant. LVS inclusions (n=2) have Th of 460 to 570°C and salinities of 48.8 to 46.8 wt.% NaCl equiv. LV inclusion (n=3) have lower Th (160 to 199°C) and salinities (3.6 to 5.0 wt.% NaCl equiv.).

Quartz Lake Epithermal: Sample TD121 is fine-grained dacitic tuff from Quartz Lake, located about 600 m higher in elevation above the Sofia prospects. It is characterized by quartz-sericite-clay alteration that is cut by a crustiform quartz vein. The quartz vein hosts two phase LV coexisting with VL inclusions suggesting a boiling assemblage. LV inclusions (n=4) exhibited Th = 148 to 343°C with salinities of 0.0 to 4.0 wt.% NaCl equiv.

Fluid Inclusion Interpretation

Homogenization and salinity measurements for all samples are in Fig. 31. Results indicate the occurrence of at least two types of fluid inclusions: Type 1) higher-density, saline (36 to 50 wt.% NaCl), hot (up to 570°C) fluids that are in early quartz veins that are related to K-silicate alteration at Sofia, Baker, and Black Gossan. Type 2) lower density liquid-rich, dilute (0 to 8.1 wt.% NaCl), moderate to low homogenization temperature (148 to 397°C) fluids dominate with the quartz-sericite-(clay) alteration that is well developed in the shallow parts of Baker, Black Gossan and at Quartz Lake. The deep fluids show a trend of cooling (to < 266°C) and dilution (to < 36 wt.% NaCl). Type 2 fluid inclusions occur within the samples containing Type 1 fluid inclusions. This suggests that type 2 fluids have overprinted and probably mixed with the type 1 fluids. This is supported by field observation that the early K-silicate alteration is commonly overprinted by sericite-chlorite alteration assemblage.

Boiling probably occurred in both fluid type 1 and 2 since low-density fluid inclusions occur in each of them, but further measurements that indicate that VL display similar Th is required for confirmation. Data suggest that at least some of the type 1 inclusions did not boil. Seven of the 11 measured LVS inclusions

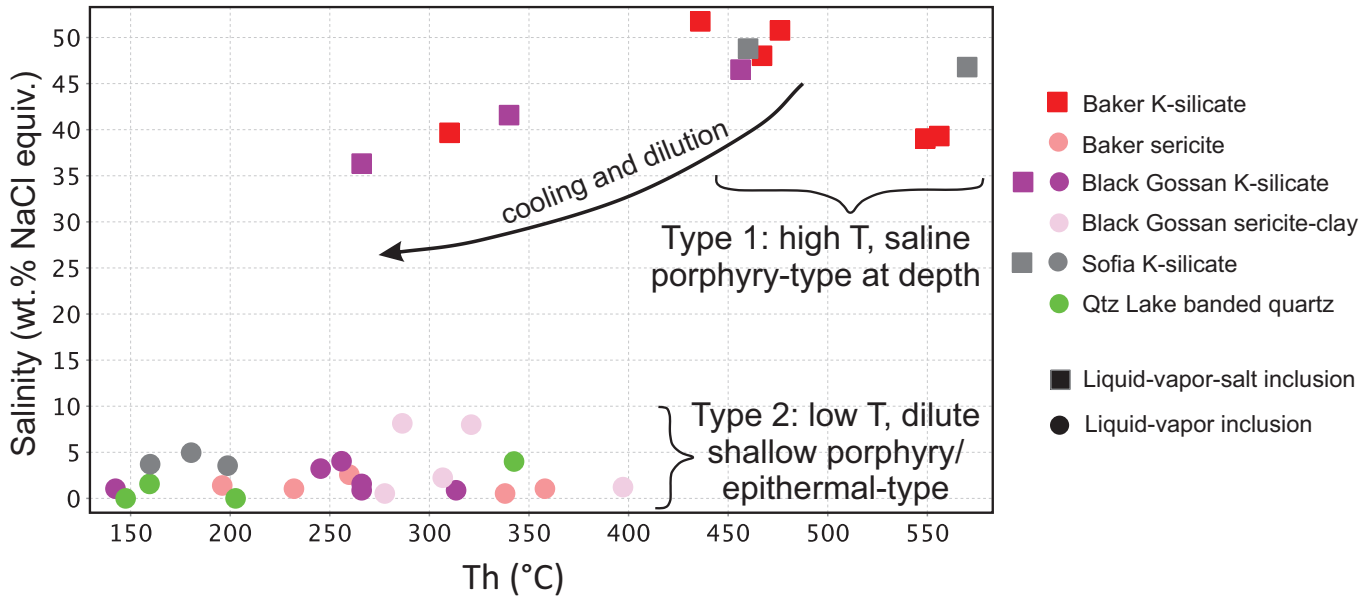

Figure 31: Homogenization temperature (Th) and salinity data for fluid inclusions from Toodoggone district showing two types of fluids related to deep and shallow parts of porphyry systems.

displayed final homogenization by salt dissolution. These fluid inclusions are interpreted to have formed at high pressure under lithostatic conditions (Cline and Bodnar, 1994) or as a result of cooling of a boiling assemblage (Bouzari and Clark, 2006).

We interpret that the type 1 fluids represent fluids generated from a porphyry center at depth. These hot and saline fluids caused K-silicate alteration and potentially copper mineralization at depth. As these fluids rose, they cooled, probably partly boiled and became diluted as they mixed with the lower temperature fluids at shallower levels which caused phyllic and advanced argillic alteration.

DISCUSSION: EVIDENCE OF PORPHYRY-TYPE MINERALIZATION IN CENTRAL TOODOGGONE DISTRICT

The Toodoggone district consists of a thick (>2 km) succession of sub-areal volcanic and comagmatic felsic intrusive rocks that were deposited and emplaced in an elongated volcano-tectonic depression during Late Triassic-Early Jurassic (Diakow et al., 1991). The district's distribution was probably influenced by extensional structures that controlled the ascent of magma to subvolcanic levels (Diakow et al., 1993). Subsequent deformation displaced blocks along major faults. The combination of thick volcanic host rock sequences, coeval felsic intrusions and an active structural environment provided a favourable environment for the generation of porphyry copper and related epithermal deposits.

Preserved Jurassic Epithermal Deposits

The Toodoggone district, with the exception of few other notable occurrences (e.g., Brucejack: Tombe, 2015), is the only region in BC where Early Jurassic epithermal mineralization is well-preserved, leading to the suggestion that other systems may have since been eroded. Preservation of the shallow Toodoggone district may be related to post-mineralization extension and burial by the thick Bowser Basin and Sustut Basin clastic packages which currently crop out to the west and north of the Toodoggone district (Fig. 2; Diakow et al., 1991). Although post-depositional deformation and subsequent uplift led to the erosion of the overlying Bowser Basin sedimentary strata, the underlying Jurassic with older strata and epithermal mineralization were protected from erosion.

All of the deposits and prospects in the central and northern parts of the Toodoggone, except Sofia, have been classified as epithermal type gold-silver deposits (Duuring et al., 2009a) although major late Triassic porphyry-type deposits such as Kemess occur in the southern part of the district. Variable degrees of erosion in the district likely played a role in exposure and preservation of porphyry and epithermal deposits. However, as presented above, the occurrence of many porphyry-type alteration and mineralization features suggests that the historically mined and explored epithermal deposits are part of larger porphyry systems (sensu Sillitoe, 2010) which are largely still preserved.

Host Rocks and Age Relationships

Volcanic rocks of the Takla Group and Lower Toodoggone Formation host the intrusions and mineralization. These volcanic and intrusive rocks show geochemical features indicative of porphyry fertile magmas, except for a dacite unit (see above). The fertile rocks are characterized by weak LREE and MREE enrichment suggesting that hornblende crystallization in a hydrous magma (>4% water) controlled REE distribution. Moreover, these units lack a significant Eu anomaly (Eun/Eu* > 0.5) suggesting high magmatic oxidation state and/or magmatic water content (Richards, 2012; Loucks, 2014). Therefore, magmatic conditions remained favorable for generating porphyry copper and epithermal deposits throughout much of Late Triassic – Early Jurassic.

More significant is the correlation between the timing of emplacement of felsic intrusions, porphyry-type alteration and epithermal mineralization. Age relationships show that epithermal-type mineralization at Alunite Ridge occurred in two episodes (196.9 ± 2.2 Ma and 190.0 ± 1.3 Ma; Diakow et al., 2006); one that was coeval with the emplacement of phases of the Jock Creek pluton (196.7 ± 0.3 Ma; Diakow et al., 2006) and the other with porphyry-type mineralization at Sofia (189.6 ± 2.1 Ma). Similarly, mineralization at the Baker mine (193.8 ± 0.8 Ma) was coeval with the emplacement of a K-silicate altered quartz monzonite at nearby Black Gossan (193.8 ± 0.8 Ma). Further data is required to provide a genetic links between the K-silicate altered porphyry intrusions at depth and shallow-level gold mineralization but the data suggest that epithermal-type mineralization in the area was coeval with the porphyry-type alteration at depth.

The geochronological data from the Toodoggone district suggest that at least from the time of porphyry-type mineralization at ca. 201 Ma at Kemess (201.1 ± 1.2 Ma, Kemess South Re-Os age; Duuring et al., 2009a) to the time of epithermal-type mineralization at Lawyers (ca. 188 Ma) there was no significant hiatus in magmatic-hydrothermal mineralization. These new data also suggest that porphyry-type mineralization was coeval with, and below, argillic and advanced argillic alteration zones and epithermal mineralization over the entire timespan.

Alteration Features

Advanced argillic alteration with abundant clay minerals typically forms in epithermal environments above the porphyry deposits (Sillitoe, 2010). Several deposits in the studied area however, display pervasive quartz-sericite-pyrite alteration locally with pyrophyllite. Sericite alteration without kaolinite occurs at the

Baker mine, Black Gossan and Sofia. Moreover, the white micas in these areas are well-crystalline (>1.75) and K-rich (muscovitic) on the basis of SWIR data (Fig. 21). Such sericitic alteration is typical in the shallow-levels of porphyry deposits. Further pH decreases at shallower levels will transition to typical advanced argillic alteration. Sericite alteration occurs at Alunite Ridge, North Ridge, and Cliff Creek with relatively low crystallinity index, and locally with dickite, in contrast with the absence of sericite at Lawyers AGB and Silver Pond North which represent more distal mineralization. The sericite crystallinity and abundance of pervasive quartz-sericite alteration increases towards the east and north in the Alunite Ridge area, which indicates a trend towards a potential porphyry mineralization at depth.

Pyrophyllite with sericitic alteration suggests a deeper assemblage than the advanced argillic assemblage. Pyrophyllite can form in two distinct settings: ground-water absorption of volcanic vapor from very acidic water producing silicic and quartz-alunite alteration (Hemley et al., 1969) in the halo of high-sulfidation ore bodies and simple cooling of a fluid isotopically stable in equilibrium with sericite (Hedenquist et al, 1997). The latter probably explains the occurrences of pyrophyllite with sericite alteration at Brenda suggesting more similarity with the alteration at shallow levels of porphyry deposits.

At greater depth, sericite with chlorite and K-feldspar or biotite alteration is expected. This type of alteration occurs in drill core samples from the Baker mine which provides additional evidence for a vertical transition to higher temperature porphyry-type alteration assemblages.

Vein Types

Porphyry copper deposits, particularly calc-alkalic types, are essentially stockwork-hosted deposits that record a history of veining events that are typically classified from early to late (e.g., Sillitoe, 2010). The veins are usually quartz-dominant and their textures provide reliable clues to the mineralization even where associated pervasive alteration has been destroyed by superimposing hypogene or supergene assemblages. The evidence for porphyry-type veining events is best developed at the Baker mine where quartz-sericite-pyrite stockwork veinlets host molybdenite and minor chalcopyrite at shallow levels, whereas at deeper levels (>100 m below the topographic surface), quartz-magnetite veins with K-feldspar alteration indicate a transitional zone to the deeper parts of a porphyry system. Similar quartz-sericite veins also occur at Black Gossan although are less dense where exposed. At the Shasta and Cliff Creek occurrences, multiple vein stages from early quartz-pyrite-chalcopyrite to later quartz-sphalerite-pyrite-galena indicates the evolution from an early, probably higher temperature porphyry environment to a later, lower temperature epithermal period. In contrast, the typical low- to intermediate sulfidation types of deposits such as the AGB zone at Lawyers are characterized by open space filling comb-texture quartz veins.

Geochemical Footprint

Porphyry copper deposits have a geochemical footprint of trace metal zonation that is upward and outward from the deeper central copper zone in the general sequence of Mo, W, Sn, Se, Te, Bi, Sb, As, Li and Tl (Emmons, 1917; Halley et al., 2015). Therefore, higher concentrations of elements in the core of the porphyry system relative to those that are enriched at shallower levels can indicate proximity to porphyry mineralization. These element abundances and ratios characterize the Baker mine and the Sofia prospect as porphyry proximal regions. This approach also highlights the porphyry affinities of Cliff Creek, Black Gossan, Shasta and Alunite Ridge. These geochemical patterns are supported by field and mineralogical observations.

Hydrothermal Fluids

The occurrence of high fluid inclusion homogenization temperatures (up to 556 °C) and salinities (up to 50 wt.% NaCl equiv.) at the Baker mine are strong evidence for the presence of porphyry-type fluids. More importantly, these fluids occur only 100-200 m below the present surface where lower temperature (<358°C) and dilute (<2.6% wt.% NaCl equiv.) fluids caused pervasive sericite alteration and quartz veins that host epithermal gold mineralization. This indicates that areas of quartz-sericite-pyrite alteration in the district are directly connected and are proximal to the higher temperature and slightly deeper porphyry-type alteration. Similar, low to moderate temperature and low salinity fluids characterize the sericite alteration at Black Gossan and Alunite Ridge. Therefore, the mixing of dominantly low temperature and low density fluids with hotter and saline fluids is evidence supporting that these advanced argillic zones are likely transitional to porphyry mineralization at depth, such as that described at the Far South-East porphyry and Lepanto deposits in Philippines (Hedenquist et al., 1997).

EXPLORATION IMPLICATIONS

Mineralization in the central Toodoggone district constitutes a range of mineral deposit types that characterize the broader porphyry system environment. This includes both deep- and shallow-level porphyry copper mineralization such as Sofia and Baker/Black Gossan, intermediate to high-sulfidation-type epithermal veins with some porphyry affinities such as Shasta and Cliff Creek, high-sulfidation-type epithermal with advanced argillic alteration such as at Brenda and Alunite Ridge, and low-sulfidation- type epithermal mineralization such as at Lawyers' AGB zone. The approximate locations of these deposits relative to a generalized cross-section of a typical porphyry system model is shown in Fig. 32. Several key conclusions can be extracted from our observations and their relative position within this model that provides important guides for exploration in the region:

1. Whereas advanced argillic alteration and epithermal-type veins are common features, our identification of porphyry-level

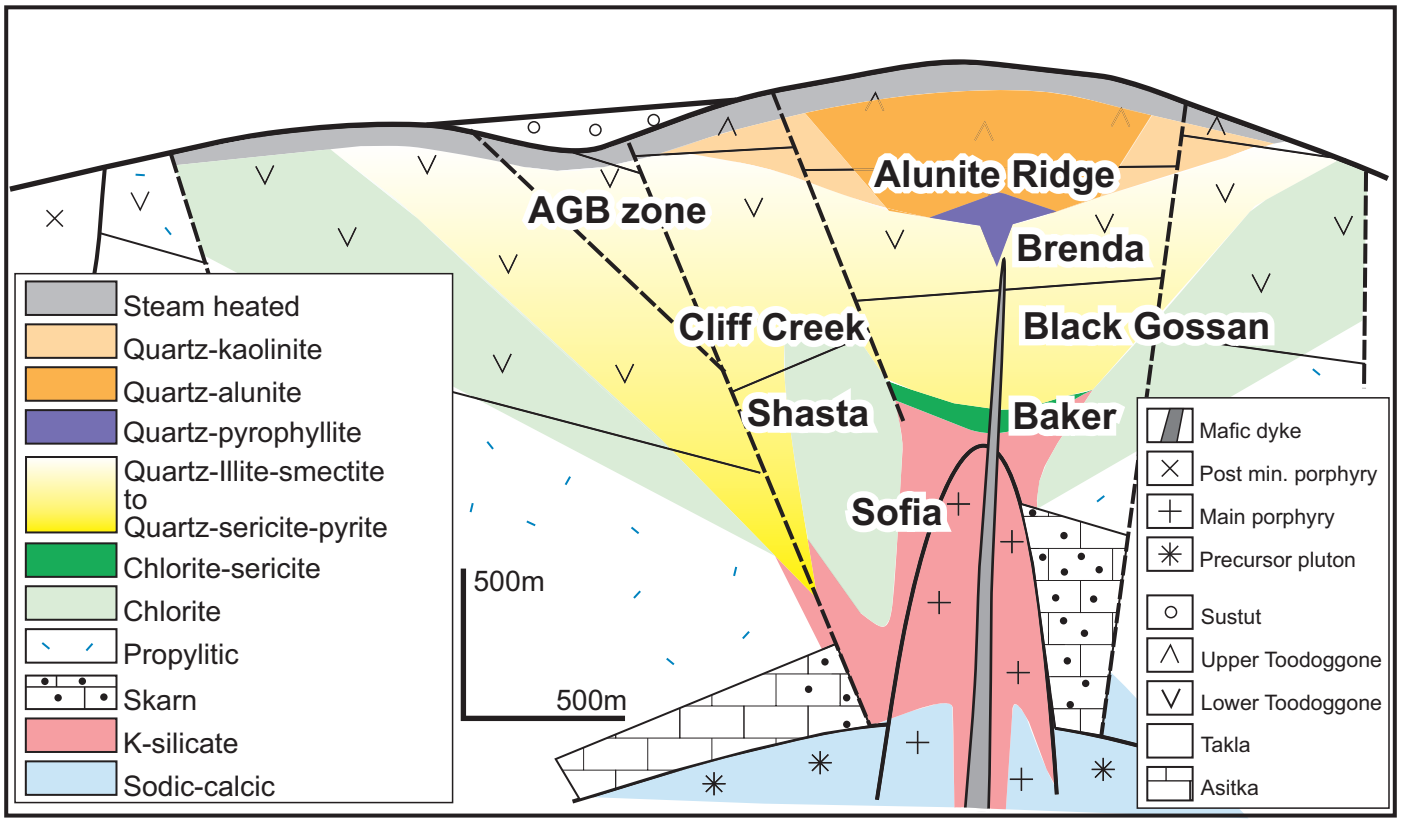

Figure 32: Generalized cross section of the Toodoggone district (based on Diakow et al., 1993) showing location of the mineral deposits and prospect relative to the typical porphyry alteration zoning (based on Sillitoe, 2010).

exposures provides new opportunities for successful exploration of porphyry-type copper deposits in the Toodoggone district.

2. Evidence suggesting that specific Upper Triassic – Early Jurassic Toodoggone district plutons are not porphyry fertile (e.g., Duncan, Duuring et al., 2009a) does not exist. Field, REE geochemical and geochronology data presented herein indicate that the large plutons such as Duncan and Jock Creek are composed of several, different intrusive phases. Emplacement conditions associated with the plutons may have varied. For example, Duncan pluton marginal phases near the Baker mine formed skarn and probably porphyry-type mineralization whereas the central pluton may represent phases emplaced too deep to form porphyry mineralization.

3. Both advanced argillic and K-silicate alteration occurs within the Toodoggone district. These distinct alteration assemblages probably formed contemporaneously as a result of rising hot magmatic fluids that progressively cooled due to dilution and mixing with meteoric water. Therefore, exploration for porphyry copper mineralization benefits from detailed characterization of the alteration assemblages and vein types to correctly identify the appropriate vertical levels of exposure (e.g. Watanabe et al., 2001). In particular, identification of quartz-sericite alteration and pyrophyllite related to shallow porphyry alteration, and distinguishing them from assemblages that formed in advanced argillic zones is fundamental. Use of techniques such as SWIR to characterize sericite crystallinity will provide vectoring trends. The application of trace metal elements and their deep vs shallow porphyry ratios will also be useful to identifying and vectoring towards porphyry centers.

4. Characterizing the paleo-hydrologic controls on the distribution of alteration and mineralization in the epithermal environment is critical (Hedenquist et al., 1998, Bissig et al., 2015). The abundance and densities of normal faults and the existence of sub-horizontal Lower Toodoggone Formation influences the geometry of the porphyry-type, relative to the epithermal-type mineralization. Moreover, in areas of high paleo-relief, the porphyry mineralization may not directly lie below the epithermal deposit (Hedenquist and Taran 2013).

ACKNOWLEDGEMENTS

Geoscience BC is thanked for approving this proposed project and providing financial support. AuRico Metals provided logistical support at Kemess. We thank Canasil Resources Inc., Bob Lane (Phoenix Precious Metals Corp) and Richard Billingsley for granting access to their prospects. Stephen Bigsby assisted during the fieldwork. Paul Jago shared his field experience of the region. Luana Yeung helped with rock photography and drafting maps. Bahram Najafian and Ian Betts helped with zircon separation. Marghaleray Amini from the Pacific Center for Isotopic and Geochemical Research (PCIGR) at UBC is

thanked for analytical insights. Christopher Smith studied thin sections from Shasta. Abdul Razique also contributed to thin section petrography. Two anonymous reviewers provided useful comments on an earlier version of this report. We also would like to extend our gratitude to Sara Jenkins for support with the graphic, map and report production, and to Johanna McWhirter for project management support.

REFERENCES

Arancibia, O.N., and Clark, A.H. (1996). Early magnetite-amphibole-plagioclase alteration-mineralization in the Island Copper porphyry copper-gold-molybdenum deposit, British Columbia. Economic Geology, v. 91, p. 402-438.

Arribas, A., Jr., Hedenquist, J.W., Itaya, T., Okada, T., Concepción, R.A., and García, J.S., Jr. (1995). Contemporaneous formation of adjacent porphyry and epithermal Cu-Au deposits over 300 ka in northern Luzon, Philippines. Geology, v. 23, p. 337-340.

Bissig, T., and Cooke, D.R. (2014). Introduction to the special issue devoted to alkalic porphyry Cu-Au and epithermal Au deposits. Economic Geology, v. 109, p. 819–825.

Bissig, T., Clark, A.H., Rainbow, A., and Montgomery, A. (2015). Physiographic and tectonic settings of high-sulfidation epithermal gold–silver deposits of the Andes and their controls on mineralizing processes. Ore Geology Reviews. v. 65. p. 327-364

Bissig, T., Leal-Mejia, H., Roger, B.S., and Hart, C. (2017). High Sr/Y Magma Petrogenesis and the link to porphyry mineralization as revealed by garnet-bearing I-Type granodiorite porphyries of the middle Cauca Au-Cu belt, Colombia. Economic Geology, v. 112. P. 551-568.

Bodnar, R.J. (1994). Synthetic fluid inclusions: XII. The system H2O-NaCl. Experimental determination of the halite liquidus and isochores for a 40 wt% NaCl solution. Geochimica et Cosmochimica Acta, v. 58, p. 1053-1063.

Bouzari, F., and Clark, A.H. (2006). Prograde evolution and geothermal affinities of a major porphyry copper deposit: The Cerro Colorado hypogene protore, I Region, northern Chile. Economic Geology, v. 101, p. 95-134.

Bouzari, F., and Hart, C.J.R. (2019). Assessing British Columbia porphyry fertility using zircons; in Geoscience BC Summary of Activities 2018: Minerals and Mining, Geoscience BC, Report 2019-1, p. 45–54.

Burnham, A.D., Berry, A.J., Halse, H.R., Schofield, P.F., Cibin, G., and Mosselmans, J.F.W. (2015). The oxidation state of Eu in silicate melts as a function of oxygen fugacity, composition and temperature. Chemical Geology, v. 411, 248–259.

Carter, N.C. (1988). Report on the 1987 exploration program Chappelle gold project; for Multinational Mining Inc. 17p.

Clark, J.R., and Williams-Jones, A.E. (1991). $^{40}Ar/^{39}Ar$ ages of epithermal alteration and volcanic rocks in the Toodoggone Au–Ag district, north-central British Columbia (94E). British Columbia Ministry Energy, Mines and Petroleum Research, Geological Fieldwork 1990, Paper 1991-1: 207–216

Cline, J.S., and Bodnar, R.J. (1994). Direct evolution of brine from a crystallizing silicic melt at the Questa, New Mexico, molybdenum deposit. Economic Geology, v. 89, p. 1780-1802.

Cohen, J.F. (2012). Compositional variation in hydrothermal white mica and chlorite from wall-rock alteration at the Ann-Mason porphyry copper deposit, Nevada. Unpublished M.Sc. thesis, Corvallis, Oregon, Oregon State University, 138 p.

Cunningham, C.G., Austin, G.W., Naeser, C.W., Rye, R.O., Ballantyne, G.H., Stamm, R.G., and Barker, C.E. (2004). Formation of a paleothermal anomaly and disseminated gold deposits associated with the Bingham Canyon porphyry Cu-Au-Mo system, Utah. Economic Geology, v. 99, p. 789-806.

Deer, W.A., Howie, R.A., and Zussman, J. (2003). Rock-forming minerals: Micas, The Geological Society, London, edited by M.E. Fleet, 2nd ed., v. 3A, 758 p.

Diakow, L.J. (1990). Volcanism and evolution of the Early and Middle Jurassic Toodoggone Formation, Toodoggone mining district, British Columbia. Unpublished Ph.D. thesis, The University of Western Ontario, 178 p.

Diakow, L.J., Panteleyev, A., Schroeter, T.G. (1991). Jurassic epithermal prospects in the Toodoggone river area, northern British Columbia: examples of well preserved, volcanic-hosted, precious metal mineralization. Economic Geology, v. 86, p. 529–554

Diakow, L.J., Panteleyev, A., Schroeter, T.G. (1993). Geology of the early Jurassic Toodoggone Formation and gold–silver deposits in the Toodoggone river map area, northern British Columbia. British Columbia Ministry of Energy, Mines and Petroleum Resources, Bulletin 86, 72 pp.

Diakow, L.J., Nixon, G.T., Rhodes. R., van Bui, P. (2006). Geology of the central Toodoggone River map area, north-central British Columbia (parts of NTS 94E/2, 6, 7, 10 and 11). British Columbia Ministry of Energy, Mines and Petroleum Resources, Open file map 2006-6, 1:50 000 scale

Duuring, P., Rowins, S.M., McKinley, B.S.M., Dickinson, J.M., Diakow, L.J., Kim, Y-S., Creaser, R.A. (2009a). Examining potential genetic links between Jurassic porphyry Cu-Au±Mo and epithermal Au±Ag mineralization in the Toodoggone district of North-Central British Columbia, Canada. Mineralium Deposita. v. 44, p. 463-496.

Duuring, P., Rowins, S.M., McKinley, B.S.M., Dickinson, J.M., Diakow, L.J., Kim, Y.S., and Creaser, R. (2009b). Magmatic and structural controls on porphyry-style Cu–Au–Mo mineralization at Kemess South, Toodoggone District of British Columbia, Canada. Mineralium Deposita. v. 44. p. 435-462

Emmons, W.H. (1918). Principles of Economic Geology, 1st ed., New York, McGraw-Hill, 550 p.

Gromet, L.P., and Silver, L.T. (1987). REE Variations across the Peninsular Ranges batholith: Implications for batholithic petrogenesis and crustal growth in magmatic arcs. Journal of Petrology, v. 28, p. 75–125.

Gustafson, L.B., and Hunt, J.P. (1975). The porphyry copper deposit at El Salvador, Chile. Economic Geology, v. 70, p. 857-912.

Halley, S., Dilles, J.H., and Tosdal, R.M. (2015). Footprints: Hydrothermal alteration and geothermal dispersion around porphyry copper deposits: Society of Economic Geologists Newsletter, no. 100, p. 1, 12-17.

Hedenquist, J. W. and Taran, Y. A. (2013). Modeling the formation of advanced argillic lithocaps: volcanic vapor condensation above porphyry intrusions. Economic Geology, v. 108, p. 1523–1540.

Hedenquist, J.W., Arribas, A., Jr., and Reynolds, T.J. (1998). Evolution of an intrusion-centered hydrothermal system: Far Southeast-Lepanto porphyry and epithermal Cu-Au deposits, Philippines. Economic Geology, v. 93, p. 373-404

Hemley, J.J., Hostetler, P.B., Gude, A .J., and Mountjoy, W.T. (1969). Some stability relations of alunite. Economic Geology, v. 64, p. 599-612.

Kay, S. M., and Mpodozis, C. (2001). Central Andean ore deposits linked to evolving shallow subduction systems and thickening crust, GSA Today, 11, p 4.

Lane, R.A. (2017). NI 43-101 Technical Report on the Brenda gold-copper proect. Report prepared for Canasil Resources Inc. 99 p. [http://canasil.com/_resources/brenda/Brenda_43-101_Report_09_12_2017%20Final_Rev_03.pdf]

Lang, J.R. and Titley, S.R. (1998). Isotopic and geochemical characteristics of Laramide magmatic systems in Arizona and implications for the genesis of porphyry copper deposits. Economic Geology, v. 93, p. 138–170.

Loucks, R.R. (2014). Distinctive composition of copper-ore-forming arc magmas. Australian Journal of Earth Sciences, v. 61, p. 5–16.

Marsden, H., Moore, J.M. (1990). Stratigraphic and structural setting of the Shasta Ag–Au deposit (94E). British Columbia Ministry Energy, Mines Petroleum Research, Geological Fieldwork 1989, Paper 1990-1, p. 305–314

Meyer, C., and Hemley, J.J. (1967). Wall Rock alteration, in Barnes, H.L., ed., Geochemistry of hydrothermal ore deposits: New York, Holt, Rinehart and Winston, p. 166-235.

Parry, W.T., Ballantyne, J.M., and Jacobs, D.C. (1984). Geochemistry of hydrothermal sericite from Roosevelt Hot Springs and the Tintic and Santa Rita porphyry copper systems, Economic Geology, v. 79, p. 72-86.

Richards, J. (2012). High Sr/Y magmas reflect arc maturity, high magmatic water content, and porphyry Cu ± Mo ± Au potential: examples from the Tethyan arcs of central and eastern Iran and western Pakistan. Economic Geology, v. 107, p. 295–332.

Sillitoe, R.H. (2010). Porphyry copper systems. Economic Geology, v. 105, p. 3-41.

Sillitoe, R.H., and Gappe, I.M., Jr. (1984). Philippine Porphyry Copper Deposits; Geologic Setting and Characteristics: Committee for Co-Ordination of Joint Prospecting for Mineral Resources in Asian Offshore Areas, UNDP technical support for regional offshore prospecting in East Asia, 89 p.

Sun, S.S., and McDonough, W.F. (1989). Chemical and isotopic systematics of oceanic basalts: implications for mantle composition and processes, in Saunders, A.D., and Norry, M.J., eds., Magmatism in the oceanic basin. Geological Society of London Special Publication 42, p. 313–345.

Thiersch, P.C., Williams-Jones, A.E., Clark, J.R. (1997). Epithermal mineralization and ore controls of the Shasta Au–Ag deposit, Toodoggone District, British Columbia, Canada. Mineralium Deposita, v. 32, p. 44–57

Titley, S.R., Thompson, R.C., Haynes, F.M., Manske, S.L., Robison, L.C., and White, J.L. (1986). Evolution of fractures and alteration in the Sierrita-Esperanza hydrothermal system, Pima County, Arizona. Economic Geology, v. 81, p. 343-370.

Tombe, S.P. (2015). Age and origin of the Brucejack epithermal Au-Ag deposit, northwestern British Columbia, Unpublished M.Sc. thesis. Department of Earth and Atmospheric Sciences, University of Alberta, 178 p.

Watanabe, Y., and Hedenquist, J.W. (2001). Mineralogic and stable isotope zonation at the surface over the El Salvador porphyry copper deposit, Chile. Economic Geology, v. 96, p. 1755-1797.

Woodsworth, G.J., Anderson, R.G., Brookfield, A. and Tercier, P. (1988). Distribution of Plutonic Suites in the Canadian Cordillera, Geological Survey of Canada, Open File 1982

APPENDICES

Appendix 1: Field Sample Description

Appendix 2: Petrographic Atlas

Appendix 3: Re-Os Age Dating of Molybdenite

Appendix 4: Shortwave Infrared (SWIR) TerraSpec Data

Appendix 5: Whole Rock Geochemical Data

Appendix 6: Fluid Inclusion Data

Appendix 7: GIS dataset for geologic information in the central Toodoggone District (digital Appendix only)

APPENDIX 1: Field Sample Descriptions

Sample ID	UTM_E	UTM_N	Elevation (m)	Datum	Area/prospect	Rock Type	Alteration	Description
TD001	609781	6356260	1687	NAD83, Zone 9	Lawyer's	Feldspar Porphyry		Plag-rich, dacitic crystal tuff with some lithic fragments. Not welded
TD002	609786	6356346	1696	NAD83, Zone 9	Lawyer's	Feldspar Porphyry	kaolinite	Quartz vein with greenish material at the margin cutting hematitic altered dacitic crystal tuff. Some amethyst in veins and ankeritic alteration halo
TD003	609786	6356346	1696	NAD83, Zone 9	Lawyer's	Takla Group volcanic		Banded amethist vein with white bands which may be adularia, from float
TD004	609534	6356458	1804	NAD83, Zone 9	Lawyer's	Takla Group volcanic	kaolinite	Vein and quartz-cemented breccia with white clay (?) alteration in clasts
TD005	609534	6356458	1807	NAD83, Zone 9	Lawyer's	Takla Group volcanic		Banded amethist vein with white bands which may be adularia. Small piece from float
TD006	613971	6350783	1740	NAD83, Zone 9	Baker	Quartz-Feldspar Porphyry	quartz-sericite-chlorite	QFP, sericite-quartz-pyrite altered
TD007	613971	6350783	1740	NAD83, Zone 9	Baker	Takla Group volcanic	chlorite-sericite	Darker material adjacent to rock representing TD006, likely Takla group volcanic
TD008	613957	6350793	1735	NAD83, Zone 9	Baker	Quartz-Feldspar Porphyry	quartz-sericite	QFP with sericite-quartz-pyrite alterationand small quartz-pyrite-molybdenite veins
TD009	613957	6350793		NAD83, Zone 9	Baker	Quartz-Feldspar Porphyry	quartz-sericite	QFP with quartz-pyrite-molybdenite vein and sericite alteration around
TD010	613957	6350793		NAD83, Zone 9	Baker	Quartz-Feldspar Porphyry	quartz-sericite	Molybdenite-pyrite-quartz veins in intense phyllic altered QF porphyry.
TD011	613927	6350792	1722	NAD83, Zone 9	Baker	Quartz-Feldspar Porphyry	quartz-sericite	Quartz-plagioclase porphyry with intense sericite alteration
TD012	613927	6350792		NAD83, Zone 9	Baker	Quartz-Feldspar Porphyry	quartz-sericite	Small sample of quartz vein cutting quartz-feldspar porphyry
TD013	613975	6350767	1726	NAD83, Zone 9	Baker	Quartz-Feldspar Porphyry	quartz-sericite	Slightly fresher but still quartz-sericite-pyrite altered quartz-feldspar porphyry, here quartz more evident than in previous samples. From float
TD014	613900	6350754	1720	NAD83, Zone 9	Baker	Takla Group basaltic andesite	chlorite	Dark green, Takla group pyroxene phyric basalt. chlorite altered with disseminated pyrite
TD015	613915	6350781	1708	NAD83, Zone 9	Baker	Quartz-Feldspar Porphyry	quartz-sericite	Intense stockwork veining in QF porphyry
TD016	613893	6350778	1712	NAD83, Zone 9	Baker	Takla Group volcanic	sericite	Yellowish weathering rock, probably Takla, has pale greenish sericite
TD017	613868	6350768	1718	NAD83, Zone 9	Baker	Takla Group basaltic andesite	chlorite	Takla group basalt, chlorite-sericite-pyrite alteration
TD018	613868	6350768		NAD83, Zone 9	Baker	Takla Group basaltic andesite	chlorite	Takla group basalt fresher looking but disseminated pyrite and chlorite
TD019	613821	6350693	1707	NAD83, Zone 9	Baker	Takla Group basaltic andesite	chlorite	Mafic finegrained dyke sample, cuts intensely quartz-sericite altered rock
TD020	613821	6350693		NAD83, Zone 9	Baker	Quartz-Feldspar Porphyry	quartz-sericite	White clayish soapy alteration mineral near quartz veinlets in intensely sericite altered rock (from boulder)
TD021	613813	6350678		NAD83, Zone 9	Baker	Takla Group basaltic andesite	sericite	Pale green finegrained sericite altered Takla group basalt. Some 10 m SW from mafic dyke
TD022	613813	6350678		NAD83, Zone 9	Baker	Takla Group basaltic andesite	sericite	Same location as TD021 but slightly darker greenish
TD023	614182	6350994	1755	NAD83, Zone 9	Baker	Takla Group basaltic andesite	chlorite-sericite	Fine-grained dark greenish-grey rock, likely Takla group basalt. Altered to chl-ser-py and diss cpy, but locally magnetitic alteration preserved.
TD024	614168	6350976	1750	NAD83, Zone 9	Baker	Breccia		Subvertical breccia vein strikes approx 120°
TD025	614062	6351051	1743	NAD83, Zone 9	Baker	Honblened Plagioclase Porphyry	chlorite	Plag-hlbd phyric porphyry, fresh, not veined but late pyrite on fractures.
TD026	614341	6351333	1778	NAD83, Zone 9	Baker	Quartz-Feldspar Porphyry	quartz-sericite	Feldspar porphyry with intense sericite-quartz alteration intruding Takla group basalt
TD027	614341	6351333		NAD83, Zone 9	Baker	Takla Group basaltic andesite		Takla group pyroxene phyric basalt. Some disseminated pyrite
TD028	614569	6351078	1901	NAD83, Zone 9	Baker	Takla Group basaltic andesite	chlorite-epidote	Fresh Takla group basalt, some epidote-chlorite alteration but little pyrite
TD029	613961	6351322	1821	NAD83, Zone 9	Baker	Honblened Plagioclase Porphyry	chlorite-sericite	Feldspar-hornblende porphyry, here crowded, almost equigranular and coarse. Feldspars are pinkish, mafics chloritized , diss pyrite.

Sample ID	UTM_E	UTM_N	Elevation (m)	Datum	Area/prospect	Rock Type	Alteration	Description
TD030	614033	6351324	1820	NAD83, Zone 9	Baker	Honblened Plagioclase Porphyry	chlorite-sericite	Relatively fresh plagioclase porphyry, hematite dusting?
TD031	614055	6351343	1813	NAD83, Zone 9	Baker	Quartz-Feldspar Porphyry	quartz-sericite	Quartz-sericite altered QF porphyry.
TD032	613985	6351341	1830	NAD83, Zone 9	Baker	Quartz-Feldspar Porphyry	quartz-sericite	Similar to TD031
TD033	614060	6351415	1838	NAD83, Zone 9	Baker	Takla Group basaltic andesite		Dark-green pyroxene phyric Takla group rock with minor diss pyrite
TD034	613762	6351510		NAD83, Zone 9	Baker	Quartz-Feldspar Porphyry	epidote-sericite	Fine-grained plag-hbld porphyry, chlorite-epidotealteration with diss py
TD035	613558	6351725	1863	NAD83, Zone 9	Baker	Quartz-Feldspar Porphyry	carbonate	Rubble-crop of sparsely plag-qtz porphyritic rock, rel fresh, late porphyry phase?
TD036	613408	6351619	1801	NAD83, Zone 9	Baker	Takla Group volcanic	chlorite-sericite	Volcanic rock highly altered to chrlorite-green sericite-pyrite
TD037	613201	6351620	1780	NAD83, Zone 9	Baker	Quartz-Feldspar Porphyry	chlorite-epidote	QF porphyry with ep-chl alteration and pinkish feldspars
TD038	612923	6351445	1808	NAD83, Zone 9	Baker	Quartz-Feldspar Porphyry	chlorite-epidote	Same rock type as TD037
TD039	613081	6351168	1811	NAD83, Zone 9	Baker	Quartz-Feldspar Porphyry	chlorite-sericite	Same rock type as TD037
TD040	618768	6338922	1181	NAD83, Zone 9	Sturdee	Granodiorite	Kspar-magnetite, sericite, epidote-albite	Equigranular granodiorite to quartz monzonite cut by epidote-albite +/- chlorite, quartz veinlets with pink K-feldspar halo, cutting earlier K-feldspar and magnetite (-actinolite?) veins. FB took fertility sample
TD041	616778	6350623	1574	NAD83, Zone 9	Black Gossan	Takla Group basaltic andesite	chlorite-sericite	Pyroxene phyric Takla group basalt, pyroxenes are chlorite and pyrite altered, groundmass is greenish sericite. Here abundant disseminated pyrite (~10%)
TD042	616821	6350491	1586	NAD83, Zone 9	Black Gossan	Feldspar porphyry	epidote-sericite	Fine-grained rock, unlcear protolith but likely a feldspar and hornblende porphyry. Pale green alteration containing epidote-sericite-chlorite with <1% diss pyrite.
TD043	616833	6350454	1587	NAD83, Zone 9	Black Gossan	Takla Group volcanic	epidote-sericite	Fragmental rock (polymictic conglomerate or breccia), covering what looks like Takla group sandstone, hematite dusing?
TD044	616841	6350536		NAD83, Zone 9	Black Gossan	Takla Group volcanic?	chlorite-sericite	Fine-grained rock with greenish sericite +/- chlorite and disseminated pyrite alteration
TD045	616929	6350997	1662	NAD83, Zone 9	Black Gossan	Takla Group volcanic?	magnetite, chlorite-sericite	Green, fine-grained rock, likely Takla group volcaniclastic, Chlorite-magnetite +/- sericite altered with ~1% diss pyrite
TD046	616921	6351213	1680	NAD83, Zone 9	Black Gossan	Takla Group volcanic?	chlorite-sericite	Intense grey sericite-pyrite-quartz altered rock, unclear protolith
TD047	617020	6350930	1712	NAD83, Zone 9	Black Gossan	Takla Group volcanic?	quartz-sericite	Intense grey sericite-pyrite-quartz altered rock, pyrite ~3%, unclear protolith
TD048	617149	6350066	1763	NAD83, Zone 9	Black Gossan	Takla Group volcanic	chlorite-sericite	Takla group pyroxene phyric basalt intensely altered to sericite +/- chlorite, pyrite.
TD049	617098	6350928		NAD83, Zone 9	Black Gossan	Feldspar Porphyry	sericite	Intensely sericite altered rock, looks like may have been feldspar porphyry. Sample includes a silicified vein.
TD050	617349	6351493	1710	NAD83, Zone 9	Black Gossan	Feldspar Porphyry	chlorite-epidote	Plag-hbld-phyric dacite (coherent), minor chlorite and epidote replacing mafics. Sample from mass waste deposit below mountain
TD051	616917	6350841	1635	NAD83, Zone 9	Black Gossan	Quartz monzonite	Ksapr-magnetite, epidote-sericite	quartz monzonite porphyry (?) cut by magnetite vein. Alteration: pink K-feldspar, +/- epidote-chlorite
TD052	614150	6351238	1784	NAD83, Zone 9	Baker	Feldspar Porphyry	chlorite-sericite, carbonate	Intensely quartz-sericite-pyrite altered sparsely plag porphyritic rock, some feldspars pale pink.
TD053	613611	6352362	1845	NAD83, Zone 9	Baker	Feldspar Porphyry		Sample of plagioclase porphyry with some eutaxitic texture. Essentially fresh with biotite and hornblende preserved
TD054	620940	6347454	1270	NAD83, Zone 9	Shasta	Takla Group volcanic	sericite	Pink-greenish altered volcaniclastic sandstone cut by a 2 cm thick quartz-carbonate-pyrite vein, diss pyrite in wallrock. From Muckpile outside the mine (only general coordinates)
TD055	620940	6347454	1270	NAD83, Zone 9	Shasta	Takla Group volcanic	chlorite-sericite	Chlorite altered wallrock cut by pink veinlets (K-spar), which were cut by quartz veins
TD056	620940	6347454	1270	NAD83, Zone 9	Shasta	Breccia	chlorite-sericite	Breccia containing angular brownish weathered, K-spar altered clasts, cemented by quartz. Matrix of breccia is greenish. From Muckpile outside the mine (only general coordinates)

Sample ID	UTM_E	UTM_N	Elevation (m)	Datum	Area/prospect	Rock Type	Alteration	Description
TD057	620940	6347454	1270	NAD83, Zone 9	Shasta	Breccia	carbonate	Breccia with pervasively pink K-feldspar altered clasts cemented by quartz with disseminated pyrite and chalcopyrite. From Muckpile outside the mine (only general coordinates)
TD058	620940	6347454	1270	NAD83, Zone 9	Shasta	Breccia	sericite	Breccia with chlorite altered clasts (heterolithic), cemented by quartz-pyrite-chalcopyrite. From Muckpile outside the mine (only general coordinates)
TD059	620940	6347454	1270	NAD83, Zone 9	Shasta	Tuff	carbonate, sericite	Dark grey-greenish quartz vein with pyrite and chalcopyrite. From Muckpile outside the mine (only general coordinates)
TD060	620940	6347454	1270	NAD83, Zone 9	Shasta		carbonate, sericite	Dark grey greenish part of a large vein with abundant chalcopyrite. From Muckpile outside the mine (only general coordinates)
TD061	620940	6347454	1270	NAD83, Zone 9	Shasta		sericite, carbonate	Same vein as sample TD060 but white-grey quartz and disseminated sulfides (py +/- cpy)
TD062	620940	6347454	1270	NAD83, Zone 9	Shasta		carbonate	Banded vein of galena-sphalerite, intergrown with carbonate. From Muckpile outside the mine (only general coordinates)
TD063	628398	6347747	1555	NAD83, Zone 9	Brenda	Feldspar Porphyry	pyrophyllite	Quartz-biotite-plagioclase porphyritic rock moderately altered to quartz-sericite, minor pyrite. Drill platform of 96-03 -65°, Az 055°
TD064	628398	6347819	1576	NAD83, Zone 9	Brenda	Monzonite	epidote-sericite	Plagioclase porphyritic rock, altered to chlorite-epidote-sericite, no veins, minor diss py.
TD065	628462	6347902	1606	NAD83, Zone 9	Brenda	Monzonite	epidote-sericite	Relatively fresh plagioclase-porphyritic rock. Chlorite-epidote relpace mafics, feldspars are pink (K-spar?)
TD066	628576	6347947	1622	NAD83, Zone 9	Brenda	Honblened Plagioclase Porphyry	sericite, carbonate	Relatively fresh hornblende-plagioclase porphyry, minor chlorite replacing hornblende, same or different from TD065?
TD067	628616	6348269	1542	NAD83, Zone 9	Brenda	Feldspar Porphyry	quartz-sericite	Quartz-sericite-pyrite altered plagioclase-porphyry. Rubbly outctrop
TD068	628570	6348302	1526	NAD83, Zone 9	Brenda	Feldspar Porphyry	quartz-sericite	Intensely quartz-sericite-pyrite altered rock, probably the feldspar porphyry.
TD069	628128	6349469	1218	NAD83, Zone 9	Brenda	Feldspar Porphyry	quartz-alunite-kaolinite	Feldspar porphyitic rock intensely quartz-sericite-pyrite altered, more pyrite than other samples collected from Brenda.
TD070	607909	6354275	1863	NAD83, Zone 9	Silver Pond S	Feldspar Porphyry	montmorillonite	Small exposure of argillically altered fine-grained rock. Thin quartz stringers (rhyolite flow/dyke?), weathered out sulfides
TD071	607726	6352847	1745	NAD83, Zone 9	Silver Pond Ridge	Feldspar Porphyry	sericite, carbonate	Pink K-fsp disseminated sulfides in an otherwise fresh rock. From Core-grave yard, unclear drilling location (Hole DDH88-131; coordinates are of core grave yard)
TD072	607961	6352822	1772	NAD83, Zone 9	Silver Pond Ridge	Feldspar Porphyry	chlorite-sericite	Plag-biotite phyric dacite, chlorite-sericite-diss pyrite altered. Location some 200 m E of core-grave yard. Not where Minfile ocurrence for Silver Pond Ridge located (that one shows no evidence of hydrothermally altered rocks)
TD073	608374	6355548	1750	NAD83, Zone 9	Cliff Creek		sericite, carbonate	Vein material with dark sooty quartz and white quartz. Dark grey material has py-cpy and fine-grained silvery mineral (galena?). From muck pile outside the mine
TD074	608374	6355548	1750	NAD83, Zone 9	Cliff Creek	Feldspar Porphyry	kaolinite	Rock showing early sooty quartz cut by white quartz with amethyst. From muck pile outside the mine
TD075	608374	6355548	1750	NAD83, Zone 9	Cliff Creek	Feldspar Porphyry	sericite-dickite, carbonate	Brecciated dacitic host-rock with disseminated, fine-grained pyrite and oxidized dark brown material, cut by grey quartz and later milky-white quartz and amethyst. From muck pile outside the mine
TD076	606788	6356217		NAD83, Zone 9	Silver Pond N	Takla Group volcanic	dickite-kaolinite	White intensely clay altered rock, fine-grained texture, unclear protolith. Clay alteration could be supergene.
TD077	606578	6356012	1750	NAD83, Zone 9	Silver Pond N	Feldspar Porphyry	quartz-dickite	Quartz-sericite altered porphyry with very finegrained pyrite. Unlike the rest around here, less oxidized.
TD078	613927	6350792	1722	NAD83, Zone 9	Baker	Quartz-Feldspar Porphyry	sericite	Rock with thin veinlet of quartz-py-cpy with secondary chalcosite. Veinlet "pinches and swells", could be early A-vein.

Sample ID	UTM_E	UTM_N	Elevation (m)	Datum	Area/prospect	Rock Type	Alteration	Description
TD079	612186	6349941	1817	NAD83, Zone 9	Baker W	Quartz-Feldspar Porphyry	quartz-sericite, carbonate	Intensely quartz sericite-pyrite alterd feldspar porphyritic rock, pyrite disseminated and on fracture surfaces. Plag slightly pinkish sericitized
TD080	612213	6349896	1815	NAD83, Zone 9	Baker W	Takla Group basaltic andesite	sericite	Green chlorite +/- pyrite altered aphanitic mafic rock, likely Takla group. Fault contact to dacite (TD079).
TD081	612213	6349896	1815	NAD83, Zone 9	Baker W	Takla Group basaltic andesite		Small fragment with white to beige or pink fracture coating.
TD082					Baker	Quartz-Feldspar Porphyry	Kspar-magnetite-actinolite, carbonate	Quartz-magnetite vein cut by chalcopyrite vein in Talka group rock (greenish), some K-feldspar alteration in halo to cpy viens. Year drilled 87, hole ID 25 (+/- 2), depth 356 feet (exact hole ID not preserved)
TD083					Baker	Takla Group basaltic andesite	chlorite-sericite	Sericite-chlorite-clay (SCC) altered piece of fragmental mafic volcaniclastic (Takla likely). 87-Hole 25 (+/-2) at 596 feet approx
TD084					Baker	Granodiorite	Kspar, chlorite-epidote	Finegrained granodiorite with K-feldspar alteration and quartz-magnetite-cpy veins. 87, hole 25 +/-2 at 380 feet.
TD085	614211	6351646	1772	NAD83, Zone 9	Baker	Takla Group basaltic andesite	epidote, carbonate	Takla group volcanic rock, chlorite-pyrite +/- epidote altered. Cut by quartz-pyrite vein
TD086	614211	6351646	1772	NAD83, Zone 9	Baker	Takla Group basaltic andesite	epidote, carbonate	Quartz-pyrite vein with chlorite-sericite alteration cutting Takla group volcanic rock. 15 cm wide
TD087	613335	6349334		NAD83, Zone 9	Baker skarn		quartz-sericite	Siliceous vein with pyrite and galena (?) cutting marble. From block from mass waste deposit
TD088	613053	6349593	1719	NAD83, Zone 9	Baker skarn	Granodiorite	Kspar, epidote-sericite, carbonate	Equigranular hornblende bearing granodiorite or similar (Black Lake pluton) in contact with marble. Alteration variable but includes K-feldspar, diopside, epidote, possibly garnet.
TD089	613067	6349745	1730	NAD83, Zone 9	Baker skarn		epidote-diapside-garnet?	Brecciated fractured rock, common black and brown oxides in fractures. Rock is altered to quartz-epidote-diopside(?) garnet(?).
TD090	613137	6349707		NAD83, Zone 9	Baker skarn		epidote-diapside-garnet?	Assorted pieces of skarn material from bottom of scree slope: including: vein with magnetite, quartz-pyrite +/- chalcopyrite; coarse galena in strongly oxidized rock; green skarn with diopside, garnet, epidote(?)
TD091	612202	6346812	1460	NAD83, Zone 9	Shasta		sericite, carbonate	Quartz vein with chalcopyrite-pyrite-chalcocite and silvery mineral (galena?)
TD092				NAD83, Zone 9	Shasta		chlorite-sericite, carbonate	Pink alteration halo around calcite vein, cutting monzonite or similar rock. Carbonate alteration? DDH89-??-30.9-36.6 m
TD093	631912	6357806	1740	NAD83, Zone 9	Alunite Ridge		sericite	Fine-grained aphanitic +/- flowbanded rock, brown-greenish alteration, likely chlorite-sericite, minor pyrite, cut by white quartz veins with late carbonate.
TD094	631948	6357812	1744	NAD83, Zone 9	Alunite Ridge	Takla Group volcanic	sericite, carbonate	Piece of banded chalcedony vein, with pinkish wall-rock alteration (K-feldspar?)
TD095	631954	6357826	1740	NAD83, Zone 9	Alunite Ridge	Granodiorite	chlorite-sericite-epidote	Equigranular intrusive rock (diorite to granodiorite), mafics replaced by epidote and chlorite, feldspars are pinkish (K-feldspar?).
TD096	632206	6357883	1804	NAD83, Zone 9	Alunite Ridge	Dacite Porphyry	quartz-dickite-kaolinite	Grey to orange-brown weathering rock. Protolith unidentifyable but possibly a fragmental volcanic rock. Alteration is grey, quartz-sericite
TD097	632193	6357871	1801	NAD83, Zone 9	Alunite Ridge	Dacite Porphyry	quartz-dickite-diaspore	Similar to TD096. Alternate sample to identify alteration mineralogy by SWIR
TD098	632196	6357891	1805	NAD83, Zone 9	Alunite Ridge	Dacite Porphyry	quartz-dickite-kaolinite	Similar to TD096. Alternate sample to identify alteration mineralogy by SWIR
TD099	632228	6357919	1808	NAD83, Zone 9	Alunite Ridge	Dacite Porphyry	quartz-dickite-diaspore	Similar to TD096. Alternate sample to identify alteration mineralogy by SWIR
TD100	632273	6357946	1800	NAD83, Zone 9	Alunite Ridge	Dacite Porphyry	quartz-dickite-kaolinite	Siliceous material with fine-grained clay-like alteration. May be kaolinite with alunite and quartz.

Sample ID	UTM_E	UTM_N	Elevation (m)	Datum	Area/prospect	Rock Type	Alteration	Description
TD101	632275	6358025	1802	NAD83, Zone 9	Alunite Ridge	Dacite Porphyry	quartz-dickite-kaolinite	Pale grey silica rich rock. Undetermined protolith but around here some fragments seen (fragmental volcanic rock)
TD102	632263	6358056		NAD83, Zone 9	Alunite Ridge	Dacite Porphyry	quartz-dickite-kaolinite	Similar material to samples 96 to 101
TD103	632251	6358096	1800	NAD83, Zone 9	Alunite Ridge	Dacite Porphyry	quartz-alunite	Somewhat more siliceous but otherwise similar material to samples 96 to 101
TD104	632245	6358144	1780	NAD83, Zone 9	Alunite Ridge	Takla Group basaltic andesite	chlorite-sericite-kaolinite	Finegrained green-brownish-grey altered rock. Likely chlorite-sericite altered
TD105	632239	6358266	1750	NAD83, Zone 9	Alunite Ridge	Monzonite	sericite	Finegrained, pink K-feldspar-rich rock, mapped as syenite dyke.
TD106	631465	6359753		NAD83, Zone 9	North Ridge	Dacite Porphyry	quartz-sericite	Feldspar phyric volc (?) rock intensely silica altered, feldspars replaced by white mineral. Mafics oxidized to goethite-jarosite
TD107	631487	6359724	1724	NAD83, Zone 9	North Ridge	Dacite Porphyry	quartz-sericite	Siliceous, white weathering zone, protolith may be fragmental volcanic but difficult to see. Apart from silica, some soft white material (check by SWIR)
TD108	631532	6359635	1739	NAD83, Zone 9	North Ridge	Dacite Porphyry	quartz-sericite	Pale greenish-grey altered fine-grained rock, likely illiite with quartz. Minor partially leached pyrite
TD109	631507	6359581	1744	NAD83, Zone 9	North Ridge	Dacite Porphyry	quartz-sericite	Fine-grained rock with white material with silky luster
TD110	631506	6359524	1745	NAD83, Zone 9	North Ridge	Dacite Porphyry	quartz-sericite	Fine-grained rock with white material with silky luster
TD111	631483	6359452	1755	NAD83, Zone 9	North Ridge	Dacite Porphyry	quartz-sericite	Pale brownish siliceous rock. Looks like feldspars may have been replaced by sericite
TD112	631461	6359448	1750	NAD83, Zone 9	North Ridge	Dacite Porphyry	quartz-sericite	Flow banded (or stratified?) rock intensely altered to quartz and greenish illite (?)
TD113	631008	6358242	1702	NAD83, Zone 9	North Ridge	Dacite Porphyry	quartz-pyrophyllite	From white to greenish altered strongly Fe oxide bearing zone in steep slope. Pale greenish alteration, unknown protolith but likely andesite volcaniclastic
TD114	631100	6358250	1660	NAD83, Zone 9	North Ridge	Dacite Porphyry	quartz-pyrophyllite	Pale yellow greenish sericite, brecciated looking with dark reddish to black matrix and veinlets (MnOxides?). From float but similar to stuff in outcrop at TD113. Approx location.
TD115	630464	6358354		NAD83, Zone 9	North Ridge	Takla Group volcanic	chlorite-sericite	Greenish quartz sericite altered sample with fine-grained disseminated pyrite
TD116	631587	6358323	1576	NAD83, Zone 9	Quartz Lake	Takla Group volcanic	sericite	Chlorite-sericite-pyrite altered fine-grained rock
TD117	631551	6358165	1595	NAD83, Zone 9	Quartz Lake	Takla Group volcanic	sericite-kaolinite	Disseminated fine-grained pyrite in sericite +/- chlorite altered
TD118	631462	6357988	1600	NAD83, Zone 9	Quartz Lake	Takla Group volcanic	chlorite-sericite	Late quartz veins with late amethyst. DDH SG-04-18, ~ 13 m. Coord of core yard
TD119	631462	6357988	1600	NAD83, Zone 9	Quartz Lake	Takla Group volcanic	sericite-kaolinite, epidote	Pale greenish +/- pinkish fragmental volcanic rock cut by dark soothy quartz + white quartz vein and grey quartz veins. Late thin oxidized pyrite stringers cut everything. DDH SG 04 18-44.6 m, coord of core yard
TD120	631462	6357988	1600	NAD83, Zone 9	Quartz Lake	Takla Group volcanic	sericite, carbonate	Grey to white quartz vein with greenish wallrock alteration. DDH SG 04 18-68 m
TD121	631462	6357988	1600	NAD83, Zone 9	Quartz Lake	Takla Group volcanic	sercite-kaolinite	Banded grey + white quartz vein in pale brown beige altered and silicified wallrock. DDH SG 04 18-97 m
TD122	631462	6357988	1600	NAD83, Zone 9	Quartz Lake	Takla Group volcanic	sericite-chlorite, carbonate	Greenish altered wallrock cut by quartz veins. Litho probably a feldspar crystal tuff or dacite flow. DDH SG 04 18-202 m
TD123	634963	6360017	1048	NAD83, Zone 9	Sofia	Granodiorite	sericite	Fine to medium grained granodiorite cut by early quartz-magnetite and later quartz veins. Minor chalcopyrite is present (presence of minor Cu oxides).
TD124	634963	6360017	1048	NAD83, Zone 9	Sofia	Takla Group volcanic	chlorite-sericite	Late veins/fractures affected by chlorite-sericite alteration and pyrite-chalcopyrite mineralization in mafic host-rock. These structures have more Cpy than early porphyry veins.

APPENDIX 2: Petrographic Atlas

Petrographic Atlas

Host-rock, Alteration and Mineralization

Toodoggone District

Abbreviations:

aca = acanthite, carb = carbonate, chl = chlorite, cpy = chalcopyrite, gln = galena, hlbd = hornblende, kspar = K-feldspar, moly = molybdenite, plag = plagioclase, PPL = plane-polarized light, py = pyrite, QFP = quartz-feldspar porphyry, qtz = quartz, RL = reflected light, ser = sericite, sph = sphalerite, XPL = crossed-polarized light

Baker Mine

Rock type: Quartz-Feldspar Porphyry
Alteration: quartz-sericite-pyrite
Vein types: quartz-pyrite-(molybdenite)
Mineralization: pyrite with trace molybdenite

Sample no: TD08
UTM-east: 613957
UTM-north: 6350793
Elevation: 1735m

Hand Sample:

Quartz-feldspar porphyry (QFP) with abundant feldspar and sub-rounded quartz phenocrysts with pervasive quartz-sericite-pyrite alteration and cut by quartz-pyrite-(molybdenite) veins with straight to irregular boundaries.

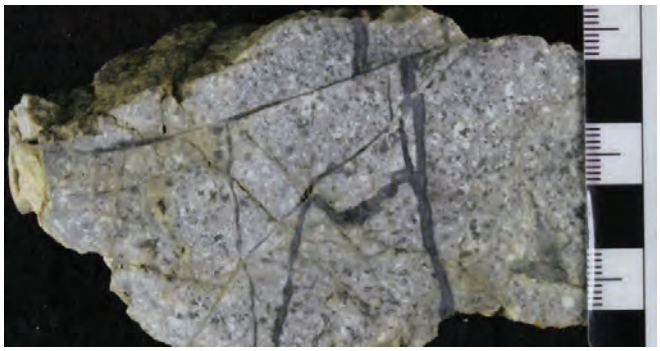

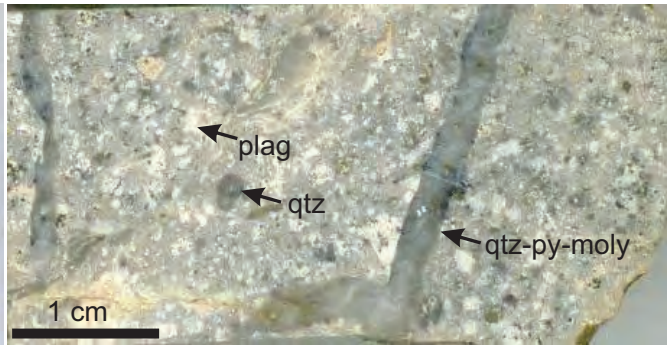

Thin Section:

Rock type: Light cream-grey rock with porphyry texture. Contains ca. 40% plagioclase (1-3mm) and ca. 10% quartz (2-4mm) phenocrysts with <5% mafic (hornblende?) phases strongly altered. The groundmass is a fine-grained mixture of quartz and sericite with abundant pyrite.

Alteration: Intense quartz-sericite-pyrite alteration. Plagioclase phenocrysts are replaced by pale-white soapy muscovite. The groundmass is flooded by a mosaic of fine-grained hydrothermal quartz, sericite and pyrite.

Mineralization: Pyrite occur 3-4%, disseminated and locally in veinlets partially oxidized to reddish hematite. Trace of molybdenite occurs in veinlets.

Vein types: Thin (1-5m) quartz veinlets with tabular molybdenite.

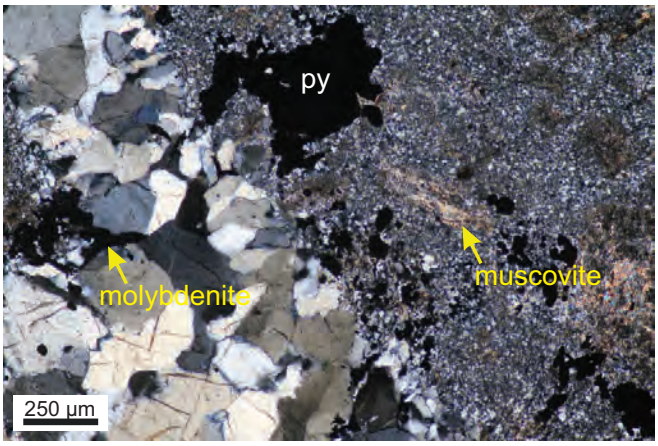

QFP with intense pervasive fine-grained quartz-sericite-pyrite alteration cut by a quartz vein with molybdenite (XPL, 10X)

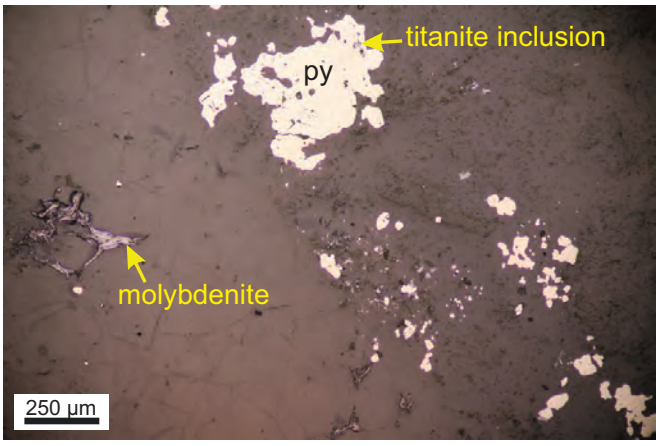

Same area but in RL showing disseminated pyrite and molybdenite in the quartz vein. Pyrite has inclusions of titanite (RL, 10X)

Interpretation:

Host rock is quartz-plagioclase porphyry stock which is intensely altered to quartz-sericite-pyrite representing phyllic alteration and cut by quartz-molybdenite veins, comparable to B-veins, occurring at the shallow parts of porphyry deposit.

Baker Mine

Rock type: Quartz-Feldspar Porphyry
Alteration: quartz-sericite-pyrite
Vein types: quartz-pyrite-(molybdenite)
Mineralization: pyrite with molybdenite and trace chalcopyrite

Sample no: TD010
UTM-east: 613957
UTM-north: 6350793
Elevation:

Hand Sample:

Quartz-feldspar porphyry (QFP) with abundant feldspar and sub-rounded quartz phenocrysts with pervasive quartz-sericite-pyrite alteration and cut by quartz-pyrite-molybdenite) veins.

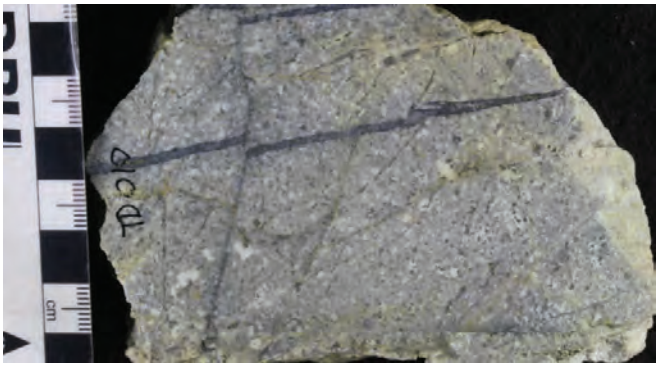

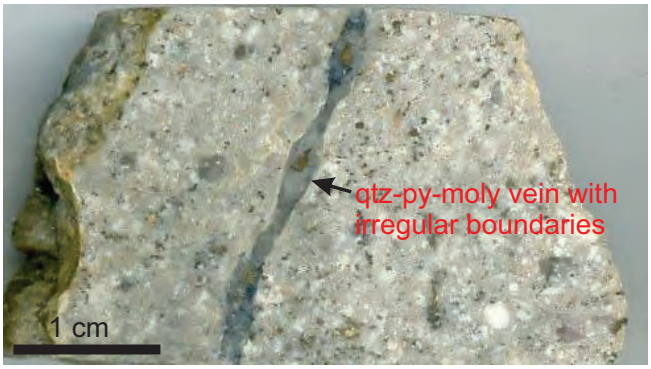

Thin Section:

Rock type: Light cream-grey rock with porphyry texture. Contains ca. 40% plagioclase (1-3mm) and ca. 10% quartz (2-4mm) phenocrysts with <5% mafic (hornblende?) phases strongly altered. The groundmass is a fine-grained mixture of quartz and sericite with abundant pyrite.

Alteration: Intense quartz-sericite-pyrite alteration. Plagioclase phenocrysts are replaced by pale-white soapy muscovite. The groundmass is flooded by a mosaic of fine-grained hydrothermal quartz and sericite.

Mineralization: Pyrite occur 3-4% with trace chalcopyrite, disseminated and in veinlets partially oxidized to reddish hematite. Trace of molybdenite occurs with pyrite in veinlets.

Vein types: Thin (1-5m) quartz veinlets with straight to irregular boundaries containing pyrite and molybdenite.

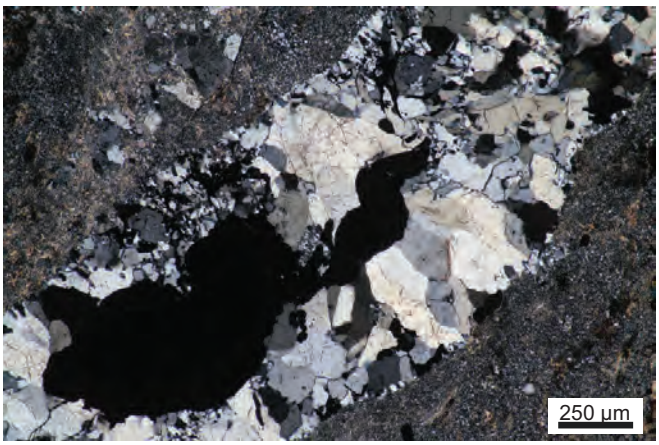

QFP with intense quartz-sericite-pyrite alteration cut by quartz-pyrite-molybdenite vein (XPL, 5X)

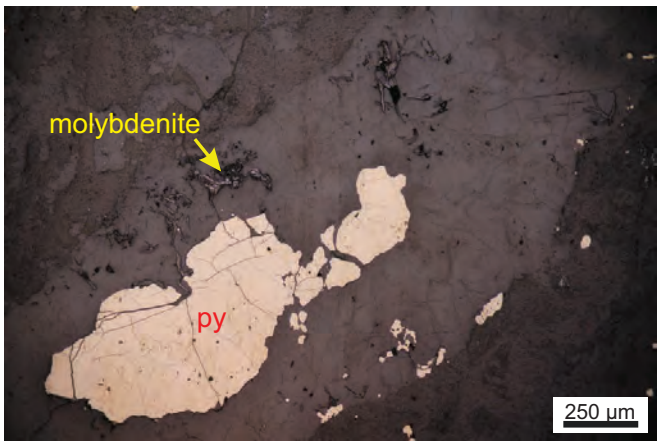

Quartz vein with pyrite and molybdenite commonly occurring near vein margin (RL, 5X)

Interpretation:

Host rock is quartz-plagioclase porphyry stock which is intensely altered to quartz-sericite-pyrite representing phyllic alteration occurring at the shallow parts of porphyry deposit cut by quartz-pyrite-molybdenite veins. The irregular shape of veins suggest early type of veins.

Baker Mine

Rock type: Quartz-Feldspar Porphyry
Alteration: quartz-sericite-pyrite
Vein types: quartz-pyrite-(molybdenite)
Mineralization: pyrite with molybdenite and trace chalcopyrite

Sample no: TD010 (cont.)
UTM-east: 613957
UTM-north: 6350793
Elevation:

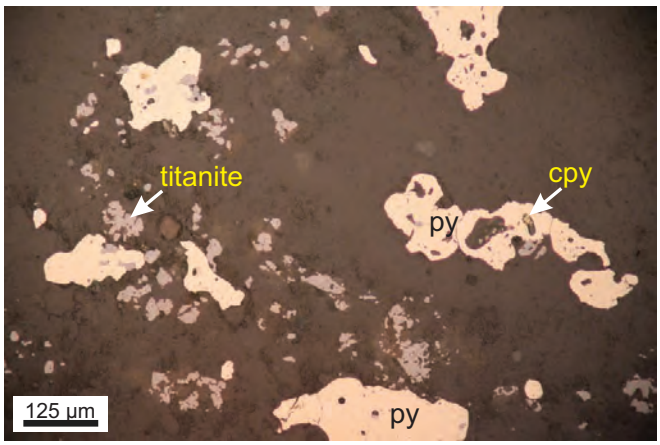

Pyrite with trace chalcopyrite inclusions and titanite. Cluster of titanite near and within pyrite suggests replacement site of a mafic mineral (RL, 20X)

QFP with sub-rounded quartz phenocrysts and some irregular margins in a matrix of quartz-sericite-pyrite (XPL, 5X).

Baker Mine

Rock type: Quartz-Feldspar Porphyry
Alteration: quartz-sericite-pyrite
Vein types: quartz-pyrite-(molybdenite)
Mineralization: pyrite with trace molybdenite

Sample no: TD013
UTM-east: 613975
UTM-north: 6350767
Elevation: 1726m

Hand Sample:

Quartz-feldspar porphyry (QFP) with abundant feldspar and sub-rounded quartz phenocrysts with pervasive quartz-sericite-pyrite alteration and cut by quartz-pyrite-(chalcopyrite-molybdenite) veins.

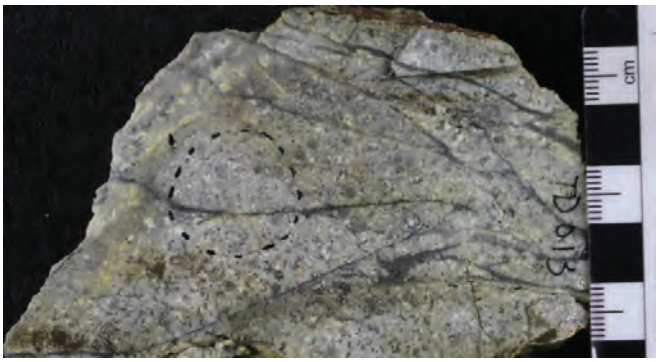

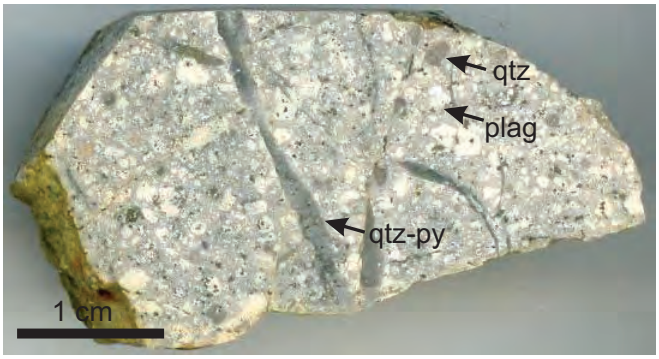

Thin Section:

Rock type: Light cream-grey rock with porphyry texture. Contains ca. 40% plagioclase (1-3mm) and ca. 10% quartz (2-4mm) phenocrysts with <5% mafic (hornblende?) phases strongly altered. The groundmass is a fine-grained mixture of quartz and sericite with abundant pyrite.

Alteration: Intense quartz-sericite-pyrite alteration. Plagioclase phenocrysts are replaced by pale-white soapy muscovite. The groundmass is flooded by a mosaic of fine-grained hydrothermal quartz and sericite.

Mineralization: Pyrite occur 3-4%, disseminated and in veinlets partially oxidized to reddish hematite. Trace of molybdenite occurs with pyrite in veinlets.

Vein types: Thin (1-5m) quartz veinlets and locally bodies with abundant fine grained pyrite and trace of moly.

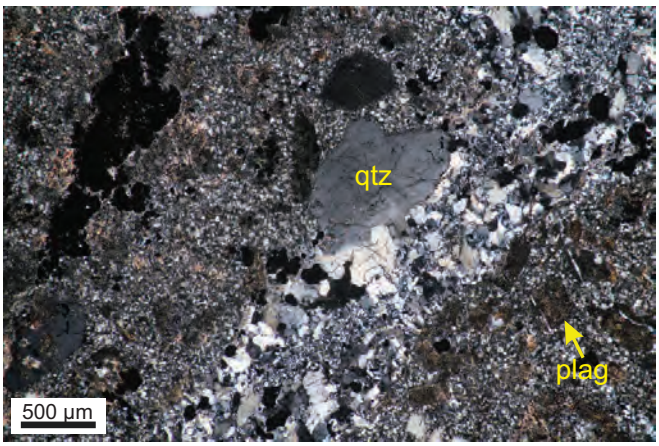

QFP with quartz and plag phenocrysts. Plag altered to fine-grained muscovite. Groundmass is fined-grained muscovite and quartz (XPL, 5X)

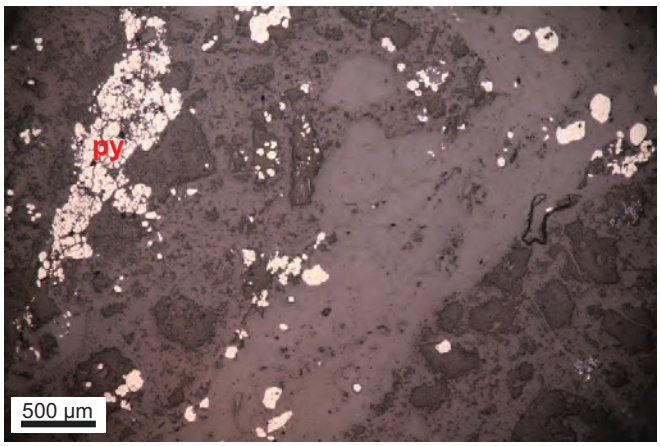

Abundant (3-4%) pyrite in vein and disseminated (RL 5X)

Interpretation:

Host rock is quartz-plagioclase porphyry stock which is intensely altered to quartz-sericite-pyrite representing phyllic alteration occurring at the shallow parts of porphyry deposit.

Baker Mine

Rock type: Basaltic andesite (Takla Group)
Ateration: chlorite-sericite-pyrite-epidote
Vein types: quartz-pyrite-chlorite-epidote and late calcite
Mineralization: pyrite and trace chalcopyrite

Sample no: TD023
UTM-east: 614182
UTM-north: 6350994
Elevation: 1755m

Hand Sample:
Fine-grained dark greenish rock, likely Takla group basaltic andesite. Altered to chl-ser-py and trace disseminated chalcopyrite locally magnetite preserved, cut by quartz-pyrite veins.

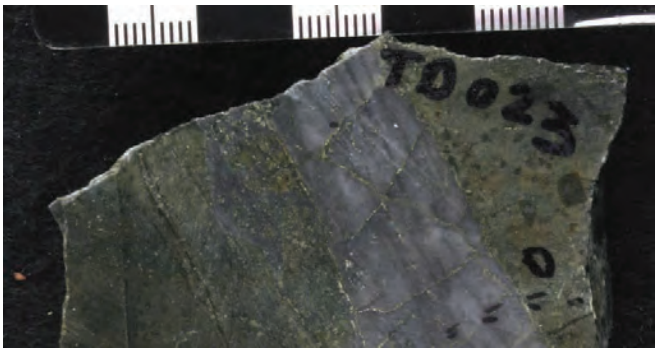

Thin Section:
Rock type: Basaltic andesite with >50% euhedral to sub-hedral phenocrysts of plagioclase (<1mm), hornblende and biotite(?) embedded within an aphanitic groundmass.

Alteration: Pervasive and veinlet controlled chlorite-sericite alteration and patchy epidote locally with calcite. Most mafic minerals altered to chlorite, plagioclase to sericite and magnetite to cluster of titanite-(rutile) locally with sulfides.

Mineralization: Pyrite occur 3-4%, disseminated and in veinlets, locally with trace chalcopyrite.

Vein types: Quartz veins with banded texture cut the pervasive alteration and is cut by chlorite-epidote and late calcite vein.

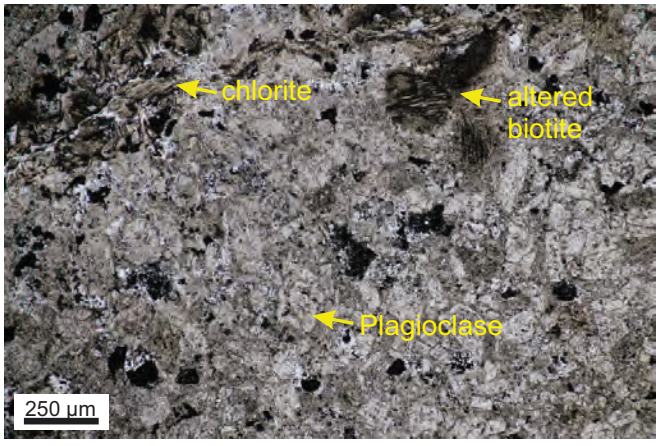

Basaltic andesite with abundant plagioclase, hornblende and biotite(?) altered to chlorite (PPL, 10X).

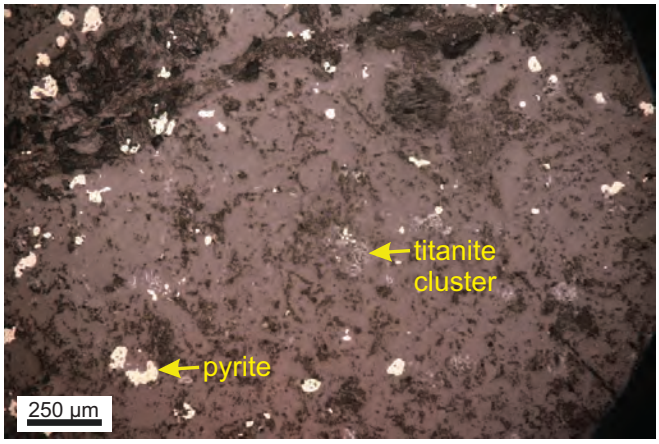

Same area but in RL showing disseminated pyrite and cluster of titanite after hornblende (RL, 10X).

Interpretation:
Basaltic andesite of Takla Group near the QPF stock is altered to chlorite-sericite-pyrite-(epidote) with trace of chalcopyrite and is largely a chlorite alteration halo around the sericite zone. Given the more mafic nature of the rock, there is more chalcopyrite deposited with the basaltic andesite.

Baker Mine

Rock type: Basaltic andesite
Alteration: chlorite-sericite-pyrite-epidote
Vein types: quartz-pyrite-chlorite-epidote and late calcite
Mineralization: pyrite and trace chalcopyrite

Sample no: TD023 (cont.)
UTM-east: 614182
UTM-north: 6350994
Elevation: 1755m

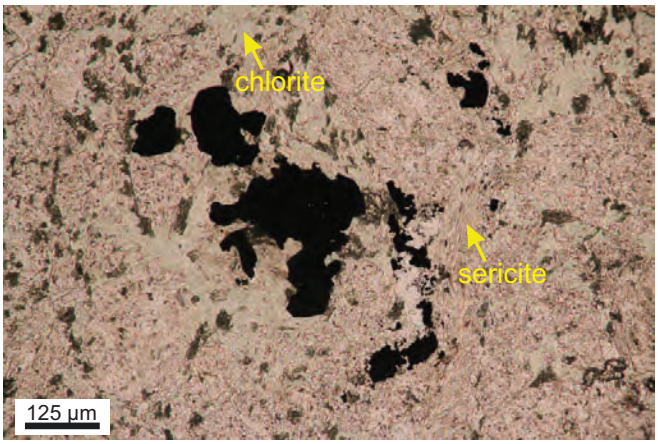

Pervasive chlorite-sericite alteration with sulfide mineralization (PPL, 20X)

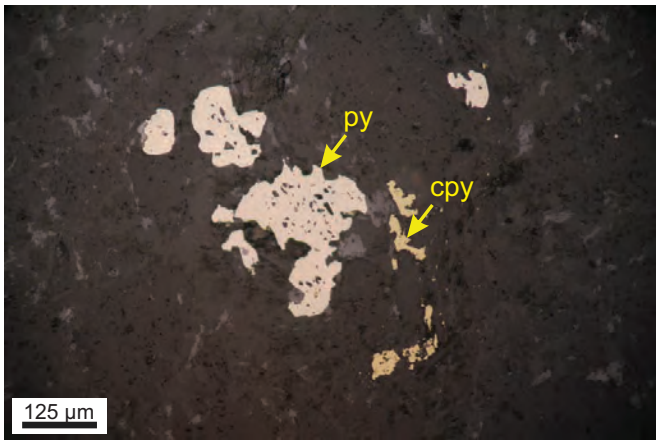

Pyrite with chalcopyrite with the chlorite-sericite (see image on the left) alteration (RL, 20X)

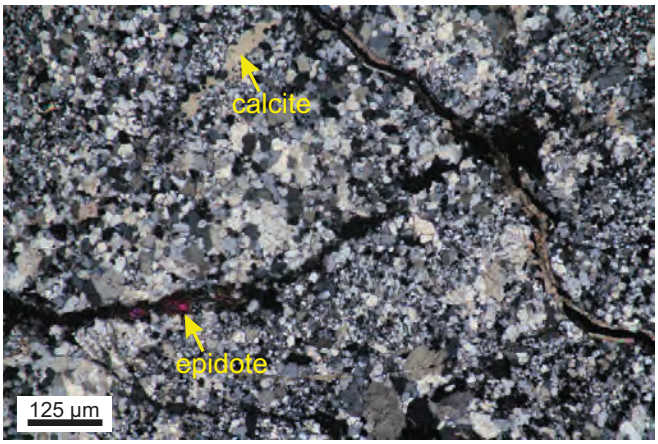

Quartz vein cut by chlorite-epidote-pyrite veinlets and in turn by late calcite veinlets (XPL, 20X)

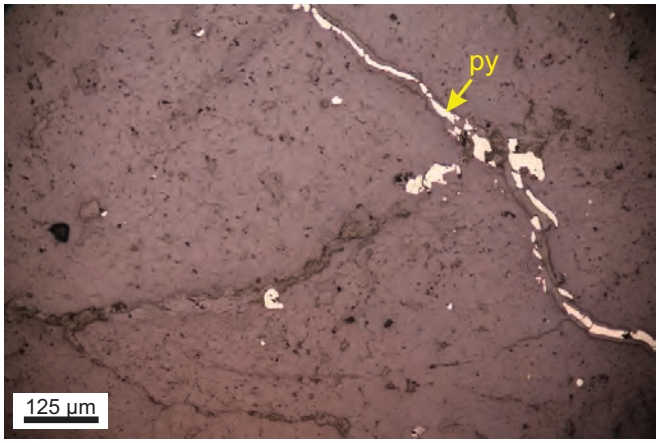

Pyrite veinlets with chlorite-epidote (see image on the left) (RL, 20X)

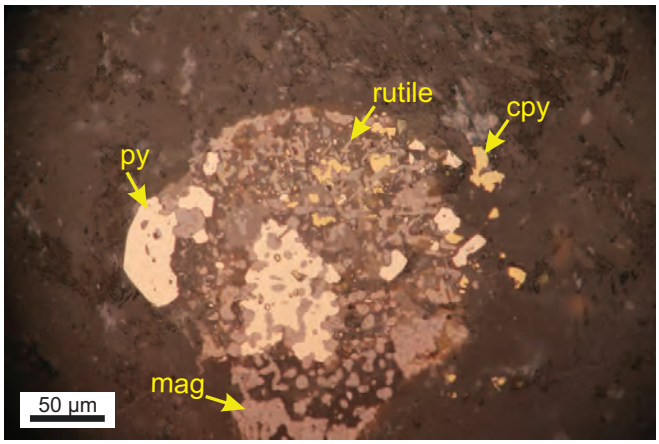

Pyrite and chalcopyrite with a cluster of magnetite and titanite (RL, 50X). Sulfides replacing magnetite and titanite and rutile forming after.

Baker Mine

Rock type: Quartz-Feldspar Porphyry
Alteration: quartz-sericite-pyrite
Vein types:
Mineralization: pyrite

Sample no: TD026
UTM-east: 614341
UTM-north: 6351333
Elevation: 1778m

Hand Sample:

Quartz-feldspar porphyry (QFP) with abundant feldspar and sub-rounded quartz phenocrysts with pervasive quartz-sericite alteration and disseminated pyrite.

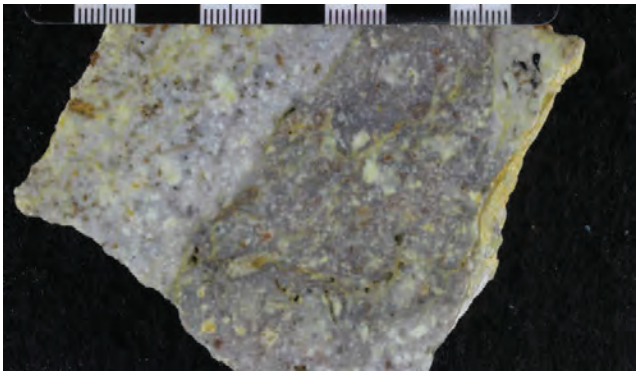

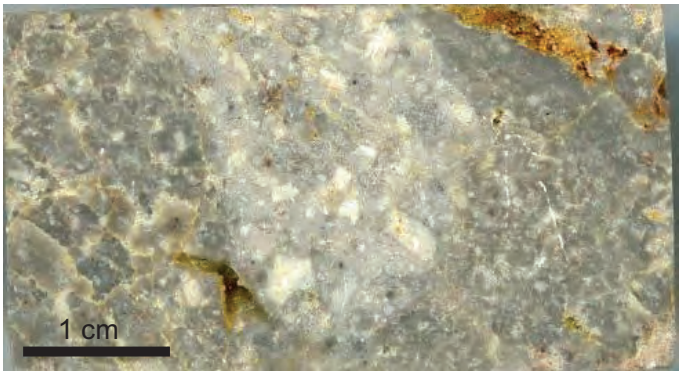

Thin Section:

Rock type: Pale-grey QFP with subhedral phenocrysts of plagioclase (2-8mm), quartz (2-5mm), remnants of amphiboles in a silicified groundmass.

Alteration: Intense quartz-sericite alteration with pyrite. Plagioclase phenocrysts are replaced by pale-white soapy muscovite. Abundant quartz with finer muscovite in the groundmass.

Mineralization: Pyrite (ca 1%) is disseminated and fine-grained and mostly oxidized to jarosite-hematite.

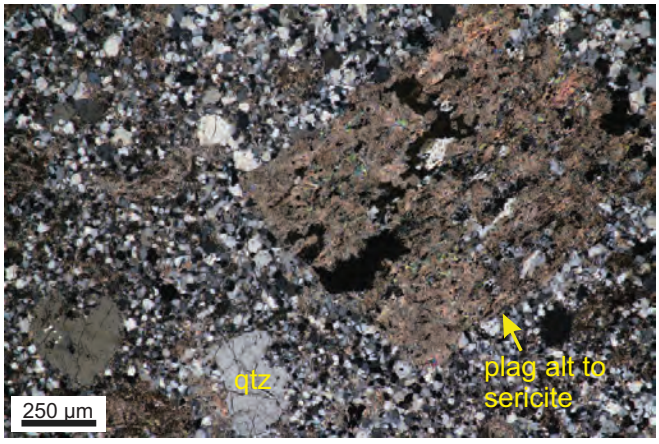

QFP with quartz and plag phenocrysts. Plag altered to fine-grained muscovite. Groundmass is fined-grained muscovite and quartz (XPL, 10X)

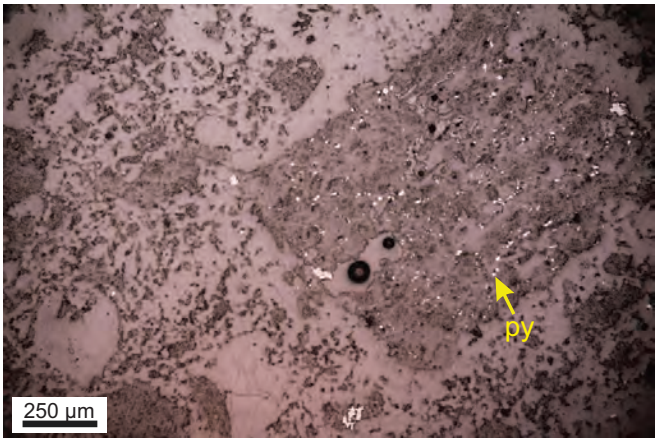

RL image of QFP showing fine-grained pyrite with the sericite alteration. (10X)

Interpretation:

Host rock is quartz-plagioclase porphyry stock which is intensely altered to quartz-sericite-pyrite representing phallic alteration occurring at the shallow parts of porphyry deposit.

Baker Mine

Rock type: Basaltic andesite (Takla Group)
Alteration: chlorite-(sericite)
Vein types:
Mineralization: pyrite with trace of chalcopyrite

Sample no: TD027
UTM-east: 614341
UTM-north: 63513333
Elevation: 1778m

Hand Sample:
Takla Group hornblende-plagioclase-phyric basalt with abundant disseminated coarse pyrite .

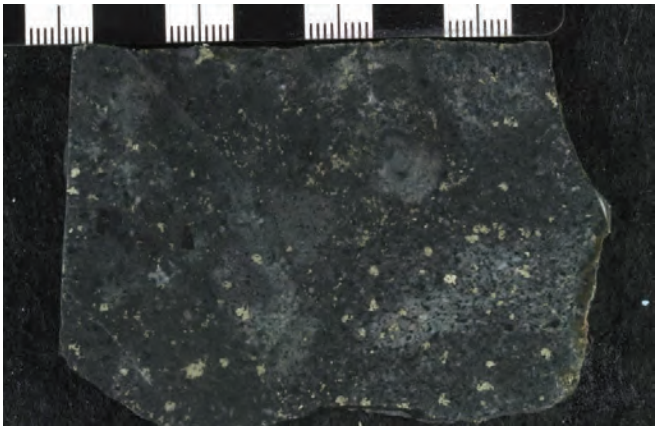

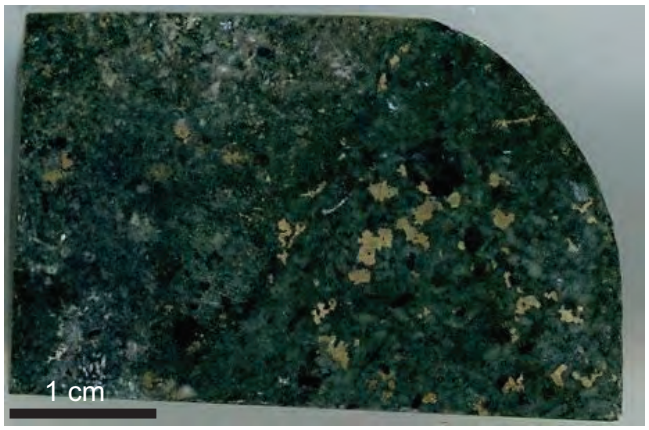

Thin Section:
Rock type: Basaltic andesite with weakly altered plagioclase (1mm) and hornblende in a plagioclase rich groundmass.

Alteration: Weak chlorite alteration of hornblende and sericite after plagioclase.

Mineralization: Pyrite occur 2-3%, disseminated, locally with trace of chalcopyrite.

Vein types: no veins.

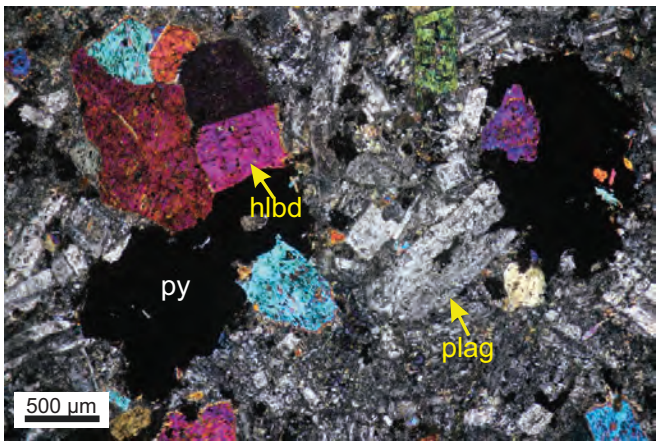

Basaltic andesite with abundant plagioclase and hornblende weakly altered to chlorite and sericite (XPL, 5X)

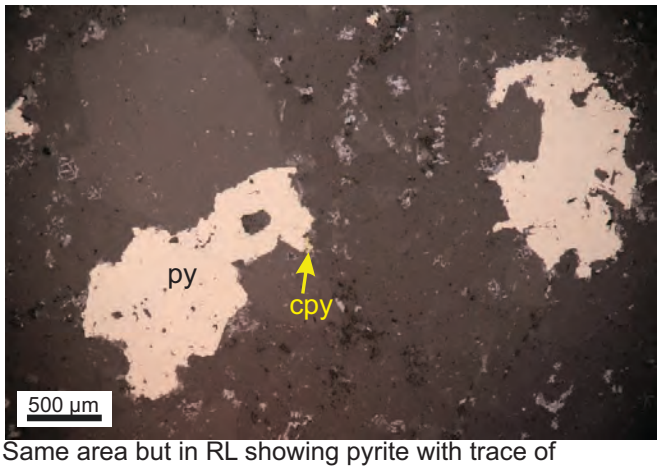

Same area but in RL showing pyrite with trace of chalcopyrite (RL, 5X)

Interpretation:
Weakly altered basaltic andesite of Takla Group with alteration largely developed in groundmass which deposited pyrite with trace of chalcopyrite distal to the main mineralization center.

Baker Mine

Rock type: Takla Group volcanic (andesite?)
Alteration: chlorite-sericite-clay
Vein types: quartz-chlorite-sericite-clay-sulfide
Mineralization: pyrite and chalcopyrite with trace molybdenite

Sample no: TD083
UTM-east:
UTM-north:
Elevation:

Hand Sample:

Takla Group volcanic (andesite?) with intense sericite-chlorite-clay (SCC) alteration occurring as pale soft green dissemination or in narrow veinlets containing pyrite and chalcopyrite. Remnants of earlier K-feldspar and hematite dusting alteration. Sample from DDH87- hole 25 at 596 feet.

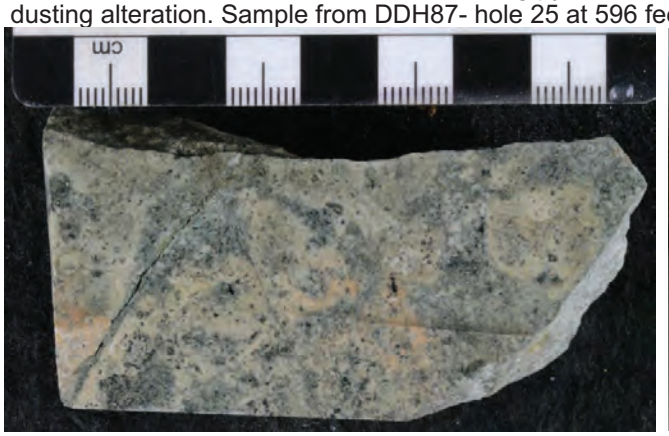

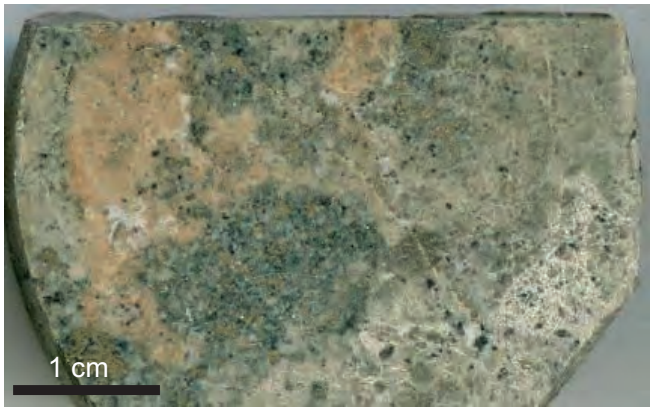

Thin Section:

Rock type: Light greenish grey, plagioclase, hornblende phyric andesite within fragmental texture. Disseminated and veinlet 4-5% pyrite, traces of chalcopyrite and molybdenite.

Alteration: Intense sericite-chlorite-clay (SCC) alteration. Plagioclase are replaced by fine-grained sericite (muscovite), locally superimposed by white argillic alteration whereas hornblende is replaced by chlorite-muscovite. Locally, SCC altered andesite is subsequently overprinted by epidote most commonly along mafic sites.

Mineralization: Disseminated and veinlet 3-4% pyrite, traces of chalcopyrite and molybdenite.

Vein types: Thin (1-2mm) veinlets of chlorite-sericite-clay with sulfides occurring as stockwork.

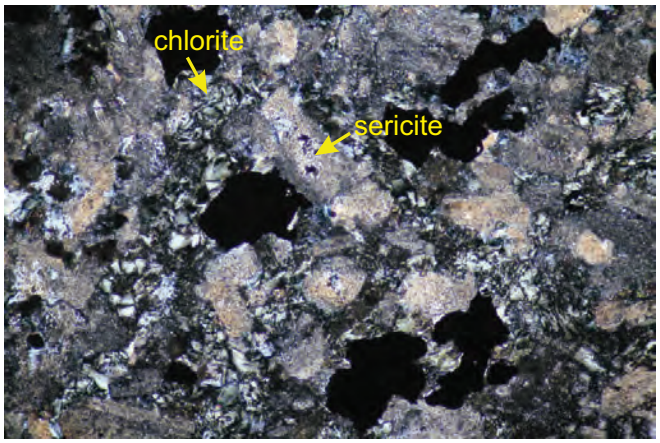

Volcanic rock with sericite and clays alteration after plagioclase and chlorite occurring with sericite along veinlets with disseminated sulfides (XPL, 10X)

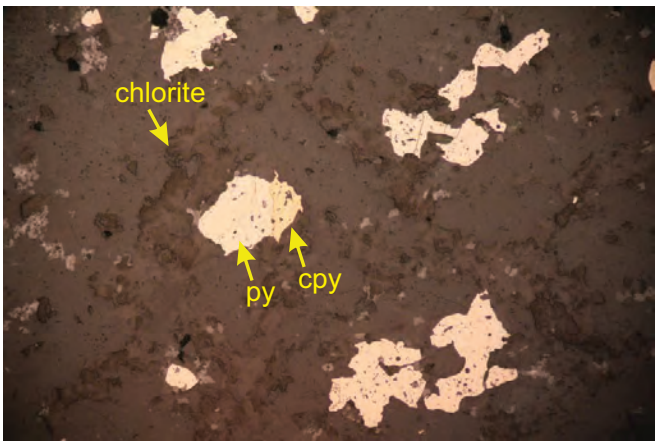

RL showing pyrite and chalcopyrite occurring with the sericite-chlorite alteration (RL, 10X)

Interpretation:

The host rock is probably an andesite of Takla Group which is intensely altered sericite-chlorite-clay (SCC) with pyrite-chalcopyrite mineralization. Given its location at depth (ca. 180 m) it probably represents the SCC zone below the sericite zone outcropped at the surface.

Shasta

Rock type: Breccia ore
Alteration: K-feldspar, qtz-carbonate, epidote
Vein types: quartz-carbonate
Mineralization: pyrite, chalcopyrite, sphalerite, galena, electrum

Sample no: TD056
UTM-east: 620940*
UTM-north: 6347454*
Elevation: 1270m

* coordinate of muckpile

Hand Sample:

Breccia containing angular brownish weathered, K-spar altered clasts, cemented by quartz containing sulfides. Matrix of breccia has greenish alteration of chlorite and epidote.

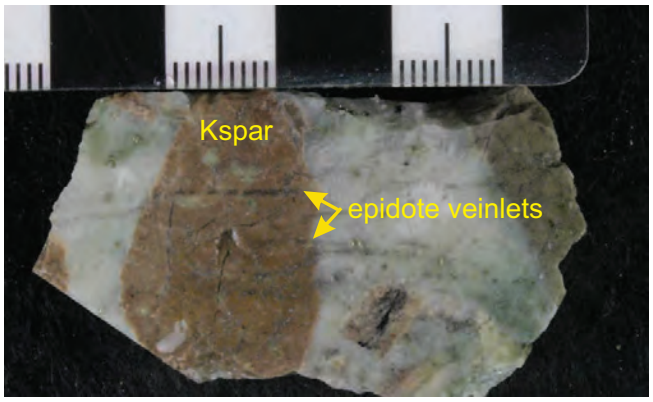

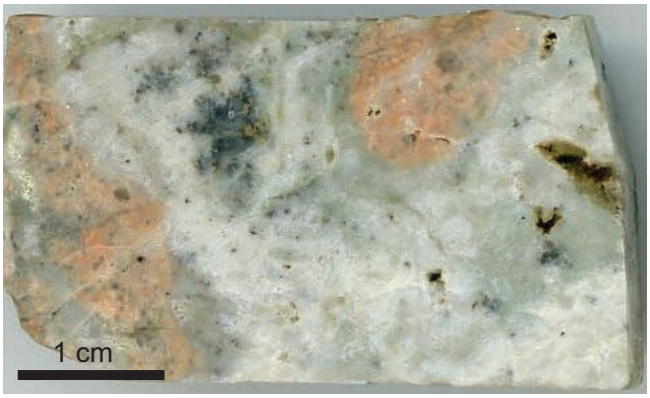

Thin Section:

Rock type: Breccia with angular, irregular clasts of Tabla andesite cemented by hydrothermal quartz, carbonate and sulfides.

Alteration: Clasts are altered to fine-grained pervasive pink K-feldspar overprinted by small patches of chlorite-sericite and cut by veinlets of epidote.

Mineralization: The quartz cement contains pyrite, sphalerite, galena, chalcopyrite and trace electrum.

Vein types: Quartz-carbonate breccia vein with sulfides.

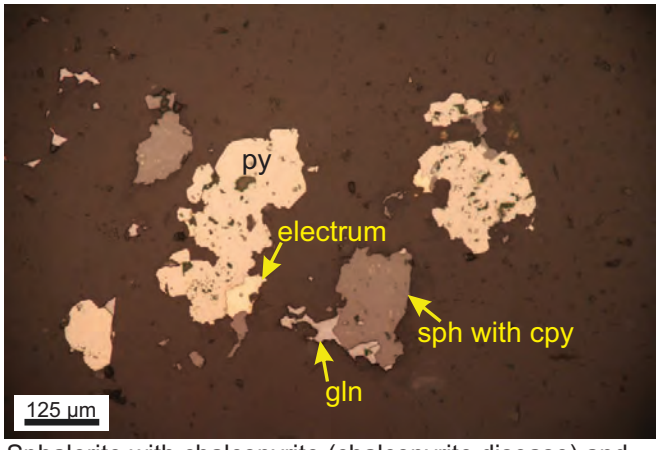

Sphalerite with chalcopyrite (chalcopyrite disease) and galena (gln) and electrum in quartz cement. (RL, 20X)

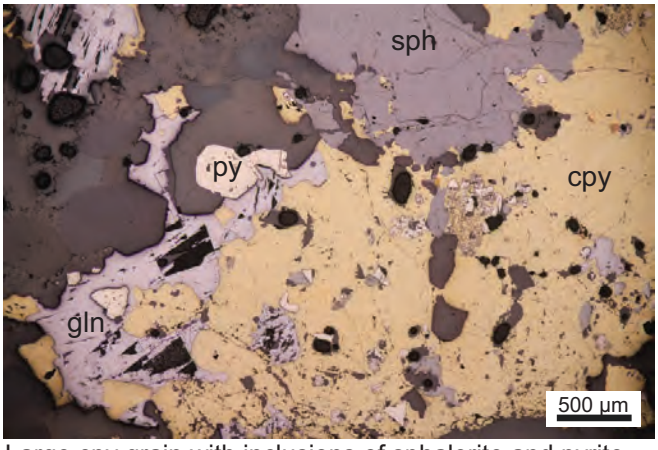

Large cpy grain with inclusions of sphalerite and pyrite (RL, 5X)

Interpretation:

This sample represent a breccia ore. Clasts are K-feldspar altered andesite cemented in quartz can carbonate. Epidote veinlets cut the clasts and cement suggesting some late alteration. Ore is largely pyrite and chalcopyrite with some sphalerite and galena and trace of electrum representing the early stage mineralization.

Shasta

Rock type: Breccia ore
Alteration: chlorite
Vein types: quartz-carbonate
Mineralization: pyrite, chalcopyrite, sphalerite

Sample no: TD058
UTM-east: 620940*
UTM-north: 6347454*
Elevation: 1270m

* coordinate of muckpile

Hand Sample:
Dark grey fine-grained tuff cut by grey-greenish quartz vein with pyrite and chalcopyrite.

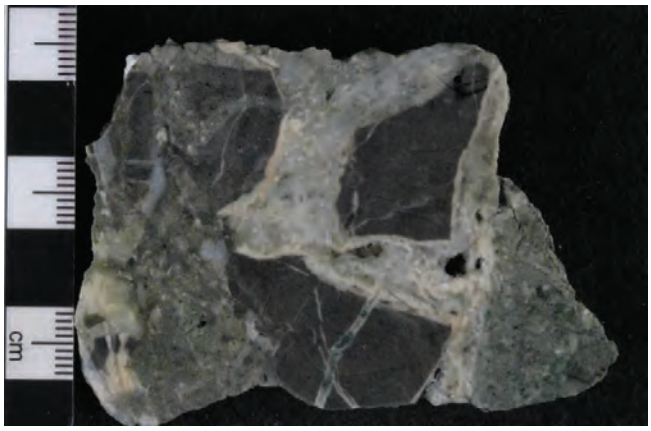

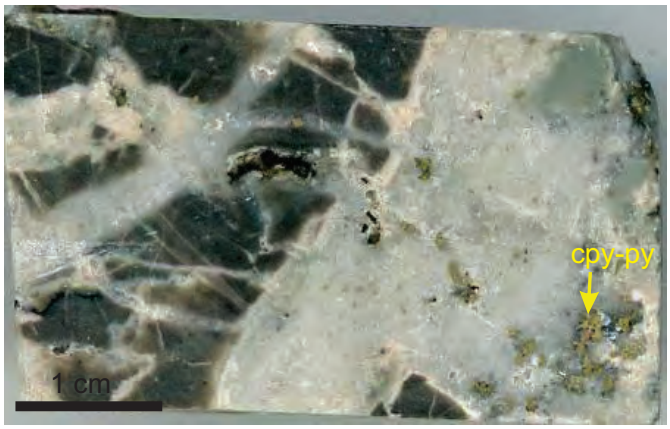

Rock type: Breccia with angular, irregular clasts of andesite tuff cemented by hydrothermal quartz, carbonate and sulfides.

Alteration: Clasts are altered to fine-grained pervasive chlorite.

Mineralization: The quartz veins contain pyrite, chalcopyrite and sphalerite.

Vein types: Quartz-(carbonate) veins with sulfides.

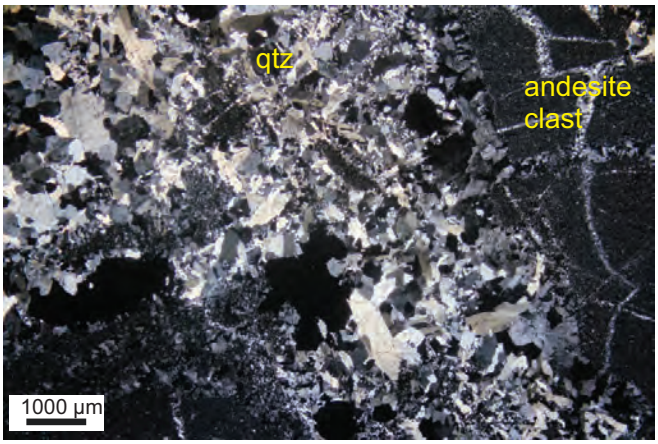

Andesitic tuff cut by quartz vein with sulfides (XPL, 5X)

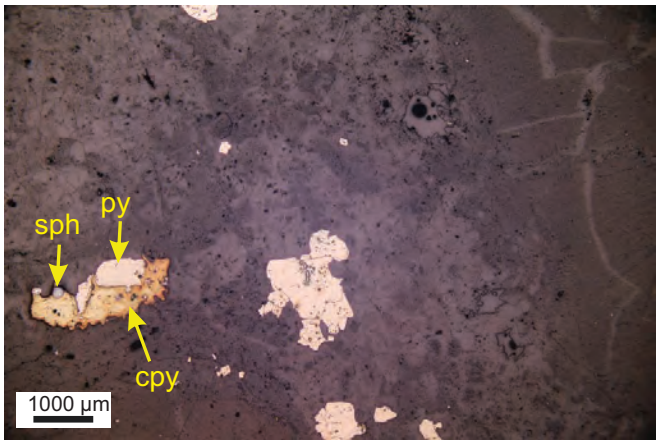

Pyrite, chalcopyrite and sphalerite in quartz veins (RL, 2X).

Interpretation:
This sample represent early quartz vein with pyrite-chalcopyrite-sphalerite mineralization.

Shasta

Rock type: Crystal tuff
Alteration: silicification, sericite
Vein types: quartz
Mineralization: pyrite, chalcopyrite, sphalerite, electrum

Sample no: TD059
UTM-east: 620940*
UTM-north: 6347454*
Elevation: 1270m

* coordinate of muckpile

Hand Sample:
Dark grey tuff cut by grey-greenish quartz vein with pyrite and chalcopyrite which is commonly tarnished.

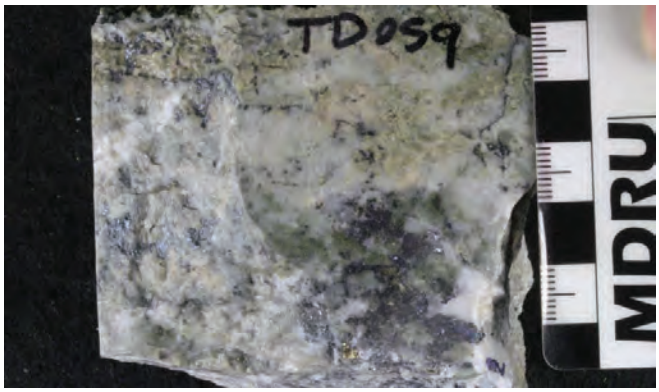

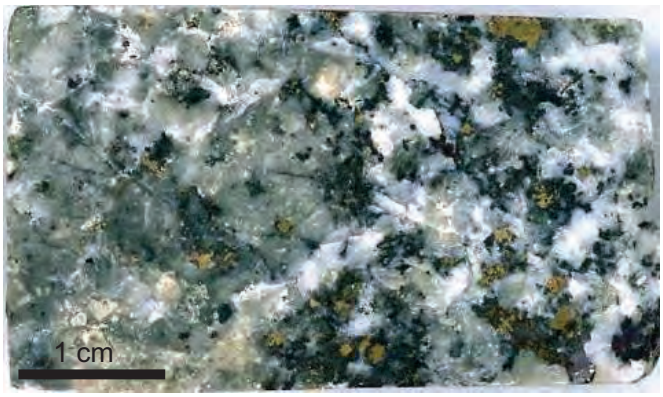

Rock type: Crystal tuff with small (<1mm) angular crystals of quartz and feldspar cemented in finer quartz and feldspar.

Alteration: Pervasive quartz, sericite alteration with minor chlorite.

Mineralization: Pyrite, chalcopyrite, sphalerite and minor electrum occurring with the silicification.

Vein types: Quartz veins with sulfides.

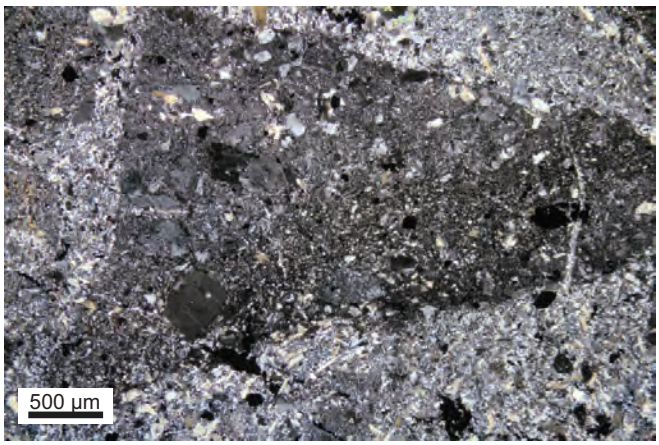

Crystal lithic tuff with silicification and sericite alteration (XPL, 5X)

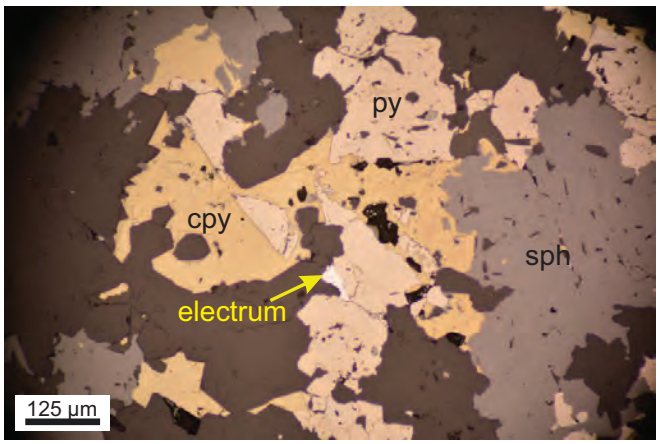

Sulfide mineralization in quartz bodies with abundant chalcopyrite, pyrite, sphalerite and trace of electrum (RL, 20X)

Interpretation:
This sample represent early quartz vein with pyrite-chalcopyrite-sphalerite mineralization.

Shasta

Rock type: Vein material
Alteration: silicification, sericite
Vein types: quartz-sericite
Mineralization: pyrite, sphalerite, galena

Sample no: TD060
UTM-east: 620940*
UTM-north: 6347454*
Elevation: 1270m

* coordinate of muckpile

Hand Sample:
Dark grey greenish part of a large vein with abundant sulfide.

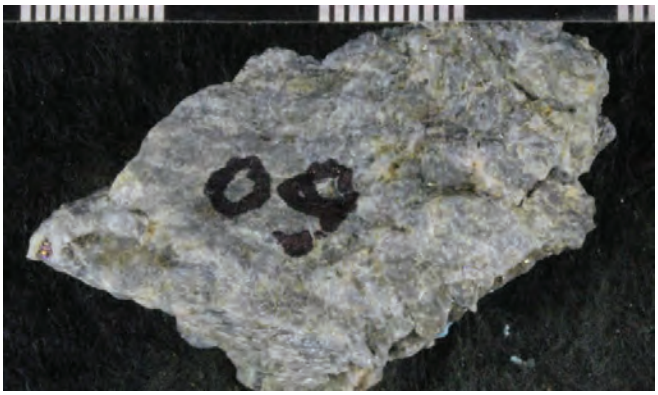

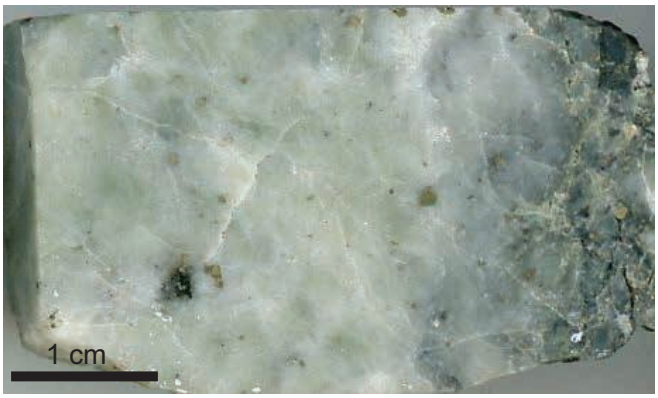

Rock type: Vein material.

Alteration: Quartz, sericite alteration with minor chlorite.

Mineralization: Pyrite (ca. 2%) with traces of sphalerite and galena.

Vein types: Quartz-sericite veins with sulfides.

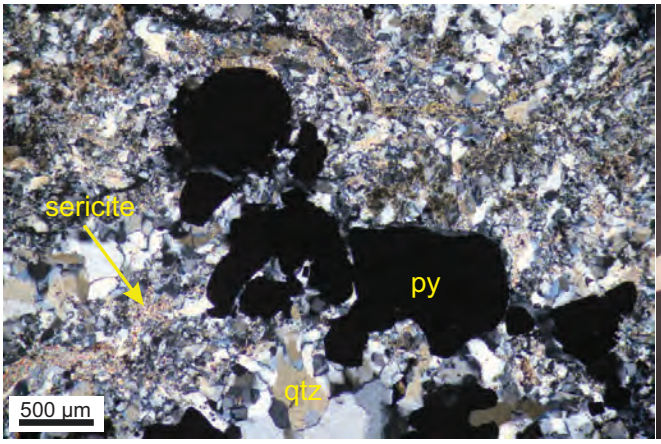

Pervasive quartz and sericite alteration with sulfide mineralization (XPL, 5X)

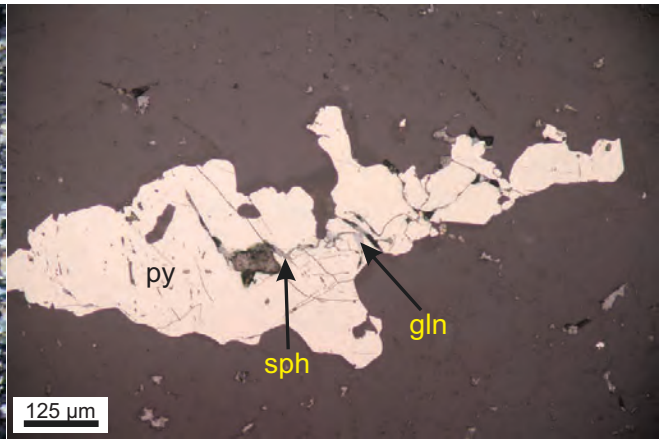

Sulfide are mostly pyrite with traces of sphalerite and galena (RL, 20X)

Interpretation:
This sample represent a later quartz vein with abundant sericite and pyrite and some sphalerite and galena but chalcopyrite does not occur.

Shasta

Rock type: Vein material
Alteration: silicification, sericite
Vein types: quartz-sericite
Mineralization: pyrite, sphalerite, galena, chalcopyrite

Sample no: TD061
UTM-east: 620940*
UTM-north: 6347454*
Elevation: 1270m

* coordinate of muckpile

Hand Sample:
Dark grey greenish part of a large vein with abundant sulfide.

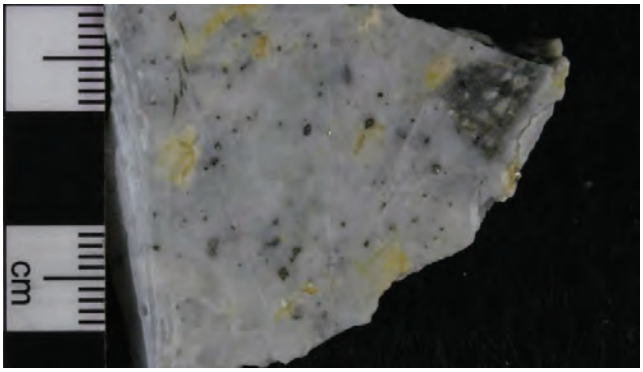

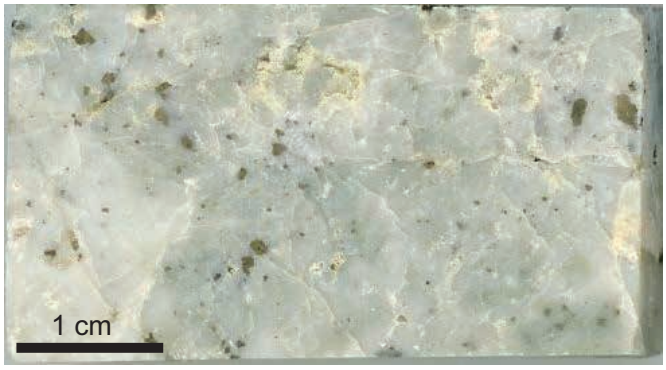

Thin Section:
Rock type: Protolith hosting the vein is not known but probably a volcanic with plagioclase phenocrysts e.g., andesite tuff.

Alteration: Pervasive quartz, sericite alteration.

Mineralization: Pyrite (ca. 2%) with traces of sphalerite and galena and chalcopyrite.

Vein types: Quartz-sericite veins with sulfides.

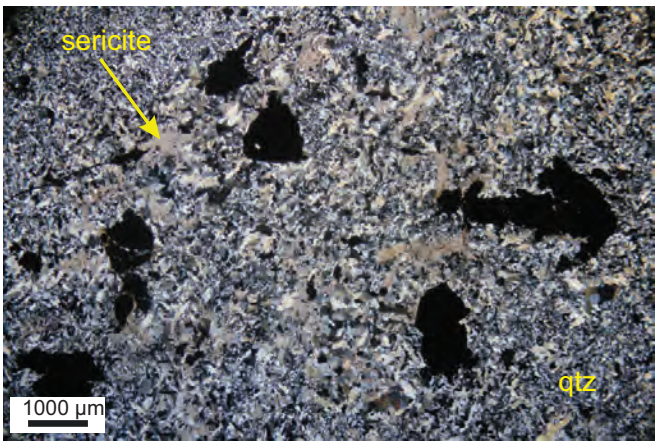

Pervasive quartz and sericite alteration with sulfide mineralization (XPL, 2X)

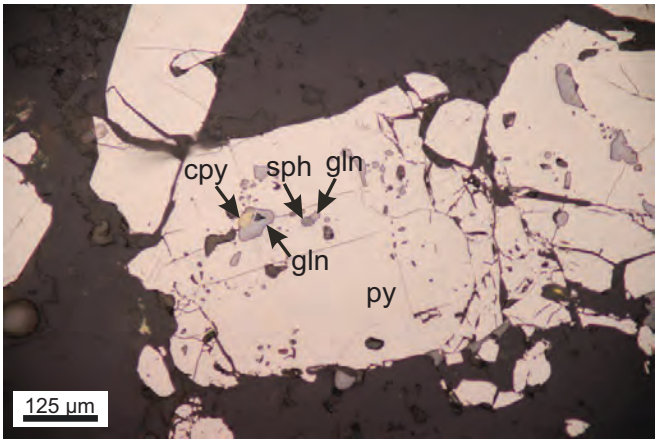

Sulfide are mostly pyrite with traces of sphalerite, galena and chalcopyrite (RL, 20X)

Interpretation:
This sample represents a later quartz vein with abundant sericite and pyrite and some sphalerite and galena, trace of chalcopyrite.

Shasta

Rock type: Vein material
Alteration: carbonate, quartz
Vein types: carbonate-quartz
Mineralization: Sphalerite, galena, pyrite, chalcopyrite, acanthite

Sample no: TD062
UTM-east: 620940*
UTM-north: 6347454*
Elevation: 1270m

* coordinate of muckpile

Hand Sample:
Banded vein of galena and sphalerite intergrown with carbonate.

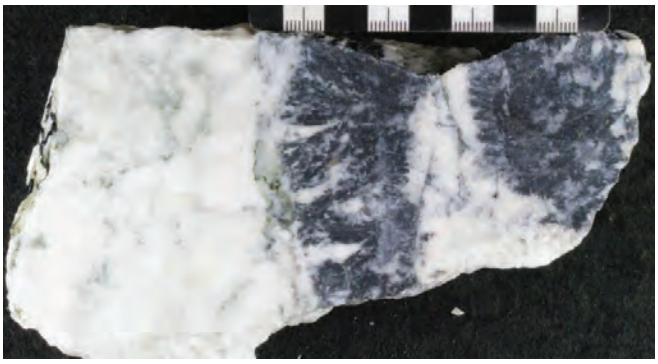

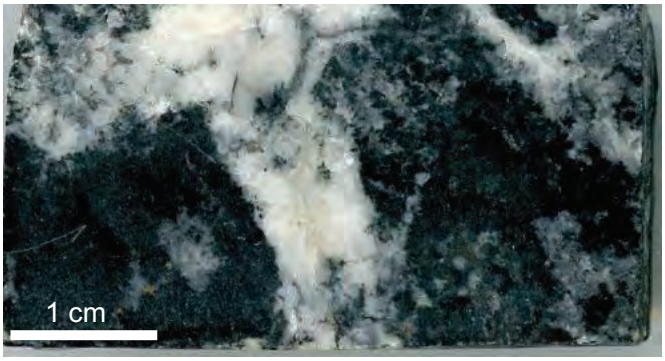

Thin Section:
Rock type: host rock is not known.

Alteration: Quartz-carbonate.

Mineralization: Massive galena-sphalerite-calcite with elongated bands of steel-grey galena intergrown by dark-grey sphalerite, silver sulfide acanthite (Ag_2S), pyrite and chalcopyrite. Acanthite AgS occur as small grains and locally nucleated within galena. Some sphalerite grains contain disseminated inclusion of chalcopyrite (cpy disease).

Vein types: Quartz-carbonate veins with sulfides.

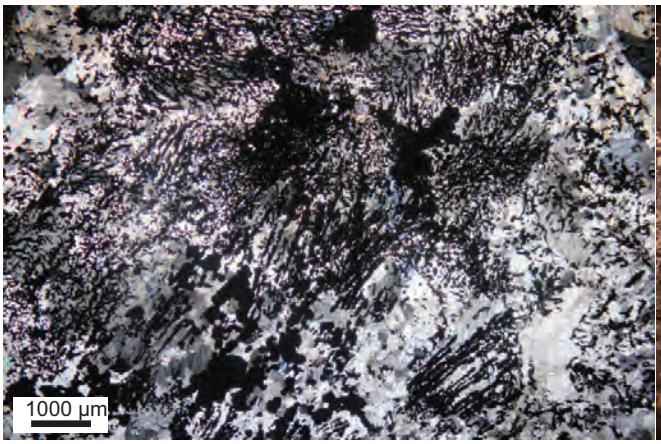

Carbonate vein with bands of sulfide (XPL, 2X)

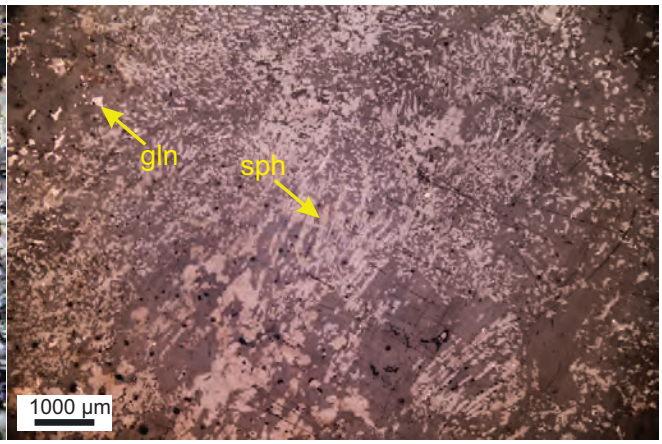

Sulfides have banded texture and are abundant sphalerite, locally with chalcopyrite inclusions, galena and trace of acanthite (RL, 2X)

Interpretation:
This sample represents a later carbonate-quartz vein with abundant sphalerite and galena, trace of chalcopyrite and acanthite.

Shasta

Rock type: Vein material
Alteration: carbonate, quartz
Vein types: carbonate-quartz
Mineralization: Sphalerite, galena, pyrite, chalcopyrite, acanthite

Sample no: TD062 (cont.)
UTM-east: 620940*
UTM-north: 6347454*
Elevation: 1270m

* coordinate of muckpile

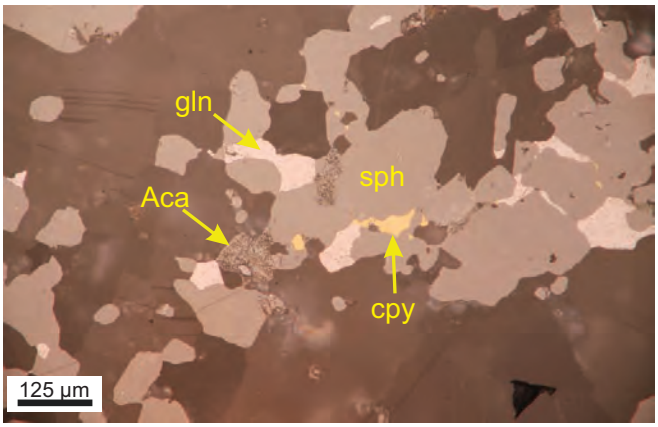

Carbonate vein with sphalerite, galena, acanthite and chalcopyrite (RL, 20X)

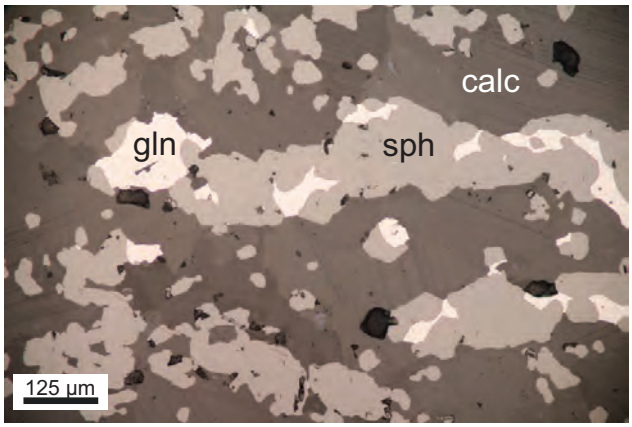

Carbonate vein with bands of sphalerite and galena (RL, 20X)

Brenda

Rock type: Feldspar porphyry
Alteration: quartz, sericite, alunite, kaolinite
Vein types:
Mineralization: pyrite

Sample no: TD069
UTM-east: 628128
UTM-north: 6349469
Elevation: 1218m

Hand Sample:
Feldspar porphyritic rock intensely quartz-sericite-pyrite altered.

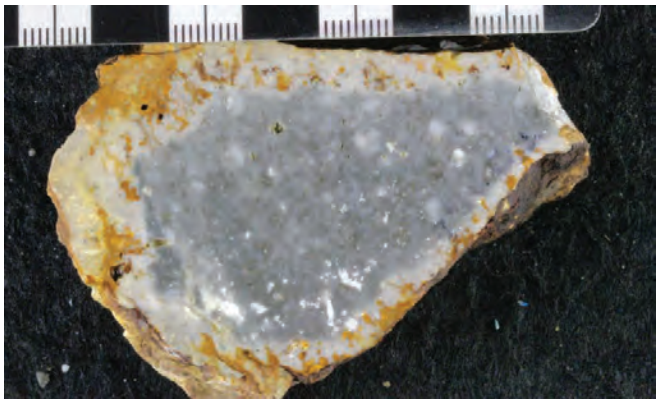

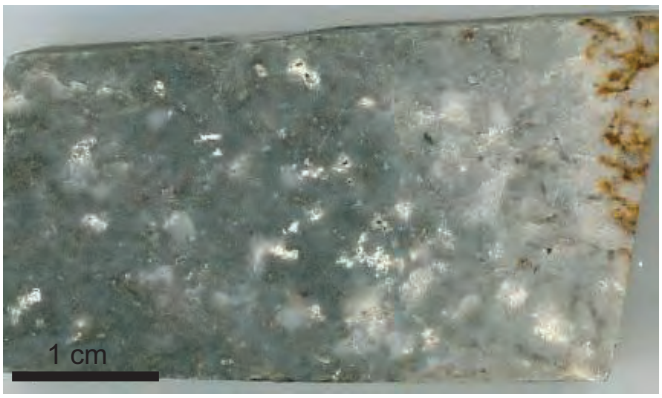

Thin Section:

Rock type: Light grey, rock with porphyry texture, remnants of feldspar phenocrysts in a grey altered groundmass.

Alteration: Pervasive fine-grained quartz, sericite, kaolinite and alunite alteration.

Mineralization: Pyrite (ca. 1%), fine-grained and disseminated.

Vein types:

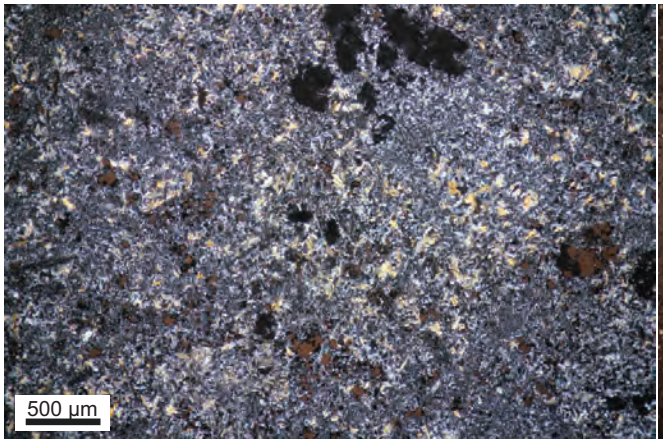

Pervasive quartz, sericite, alunite alteration with sulfide mineralization (XPL, 5X)

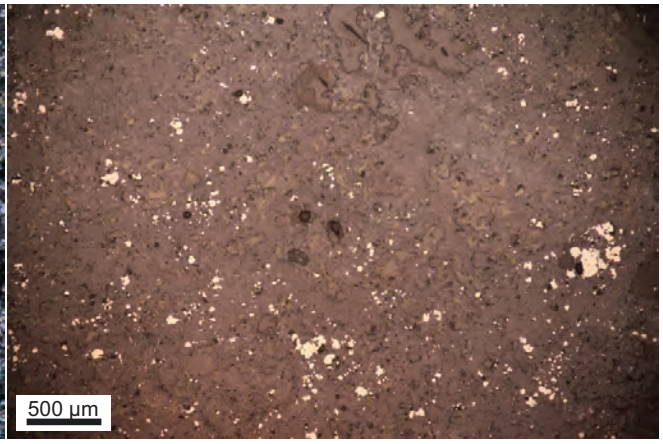

Sulfides are pyrite intergrown with the quartz-sericite-alunite alteration (RL, 5X)

Interpretation:
This sample represents an advanced argillic alteration at shallow levels of Brenda with a mixture containing alunite.

Cliff Creek

Rock type: Vein material
Alteration: quartz, sericite, carbonate
Vein types: Grey quartz
Mineralization: pyrite, chalcopyrite, sphalerite, galena

Sample no: TD073
UTM-east: 608374
UTM-north: 6355448
Elevation: 1750m

Hand Sample:
Vein material of dark sooty quartz with pyrite, chalcopyrite and galena.

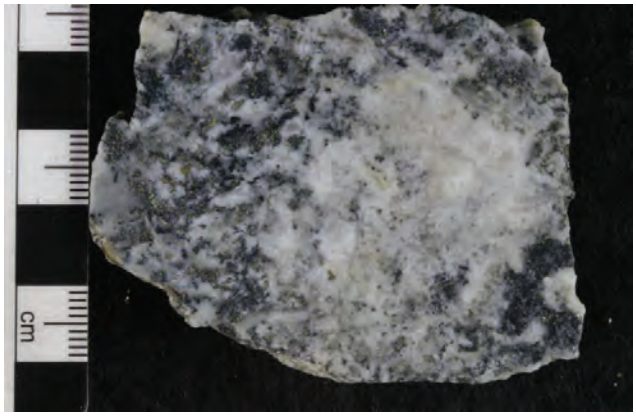

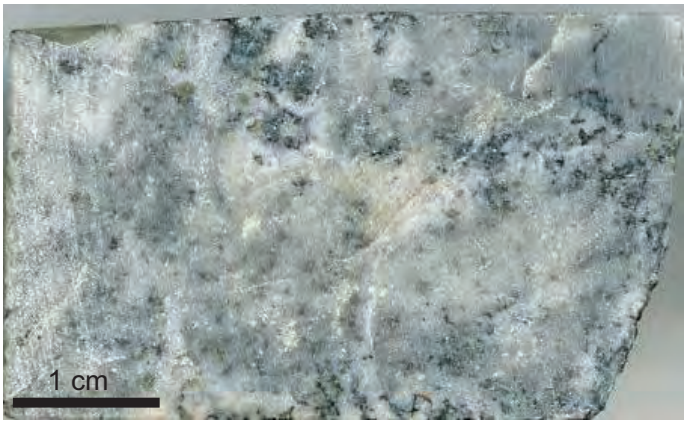

Thin Section:

Rock type: Host rock not known.

Alteration: Coarse quartz, grey colour with abundant fluid inclusions, disseminated sericite and some carbonate.

Mineralization: Disseminated and patches of pyrite, locally cubic, rimmed by chalcopyrite, sphalerite and galena.

Vein types: Light grey, coarse-crystalline quartz vein with sulfides cut by crack infill calcite veins.

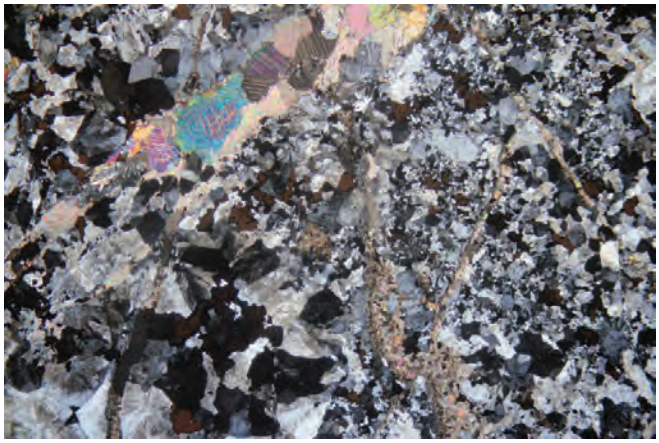

Quartz vein, coarse crystalline with disseminated sericite and sulfides, cut by late calcite veinlets (XPL, 5X)

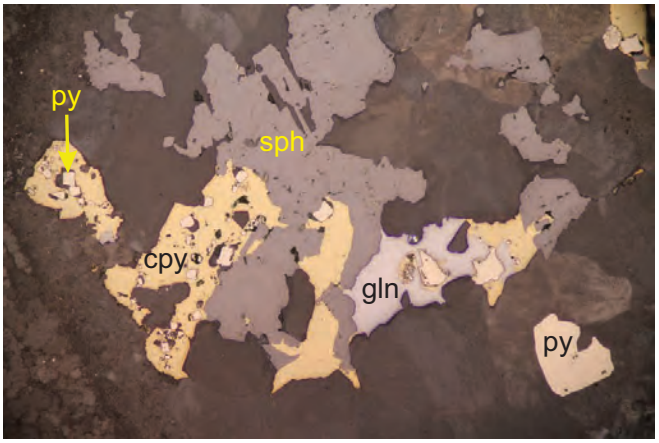

Sulfides are pyrite. locally cubic form, rimmed by chalcopyrite and sphalerite and galena (RL, 10X)

Interpretation:
This sample represents an early stage of mineralization characterized by grey quartz, abundant chalcopyrite, pyrite, sphalerite and galena.

Cliff Creek

Rock type: Dacite porphyry
Alteration: quartz, sericite, dickite, carbonate
Vein types: grey quartz, white quartz-carbonate, and late carbonate
Mineralization: pyrite with trace chalcopyrite overprinted by pyrite

Sample no: TD075
UTM-east: 608374
UTM-north: 6355448
Elevation: 1750m

Hand Sample:

Brecciated dacitic host rock with disseminated, fine-grained pyrite and oxidized dark brown material, cut by grey quartz and later milky-white quartz and amethyst.

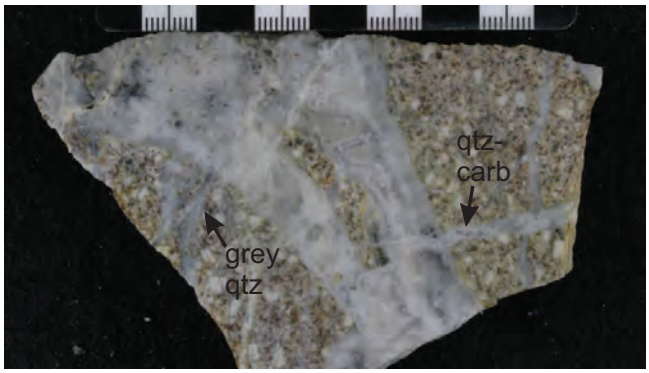

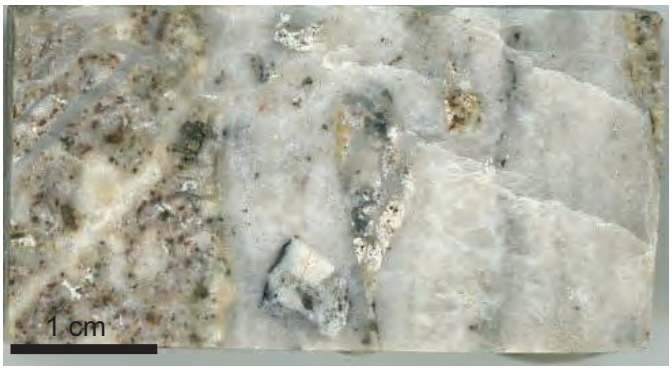

Thin Section:

Rock type: Dacite porphyry with abundant large (up to 0.5cm) feldspar phenocrysts, quartz and remnants of hornblende.

Alteration: Sericite dusting of feldspar with silicification and pervasive clay (dickite) alteration. Rutile and hematite after hornblende.

Mineralization: Pyrite and trace of chalcopyrite in grey quartz veins, disseminated cubic pyrite.

Vein types: Grey quartz veins with pyrite and trace chalcopyrite. Quartz-calcite vein and late dominantly calcite veins.

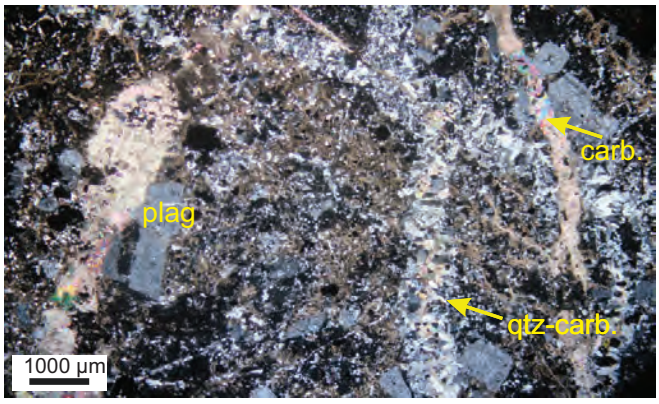

Feldspar porphyry with sericite altered plagioclase, disseminated sericite and carbonate and pyrite cut by quartz-calcite and late calcite veins (XPL, 2X)

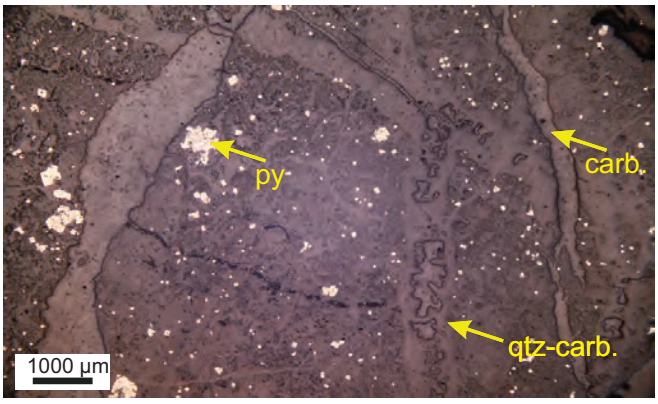

Sulfides are pyrite with the pervasive sericite alteration and cut by late quartz-carb and carb veins. (RL, 2X)

Interpretation:

This sample represents remnants of early stage grey quartz mineralization with pyrite and trace chalcopyrite abundant disseminated cubic pyrite cut by late quartz-carbonate and carbonate veins.

Alunite Ridge

Rock type: Volcanic?
Alteration: quartz, dickite, diaspore
Vein types:
Mineralization: pyrite

Sample no: TD097
UTM-east: 632193
UTM-north: 6357871
Elevation: 1801m

Hand Sample:

Grey to orange-brown weathering rock. Protolith unidentifiable but possibly a fragmental volcanic rock. Alteration is grey quartz-clay.

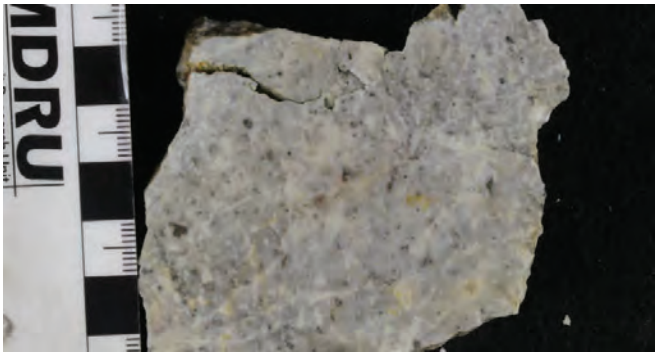

Thin Section:

Rock type: Not known but probably a volcanic rock with ghosts of plagioclase.

Alteration: Pervasive intense fine-grained quartz and clay (dickite) alteration containing clusters of coarse disapore.
.
Mineralization: Trace fine-grained pyrite.

Vein types:

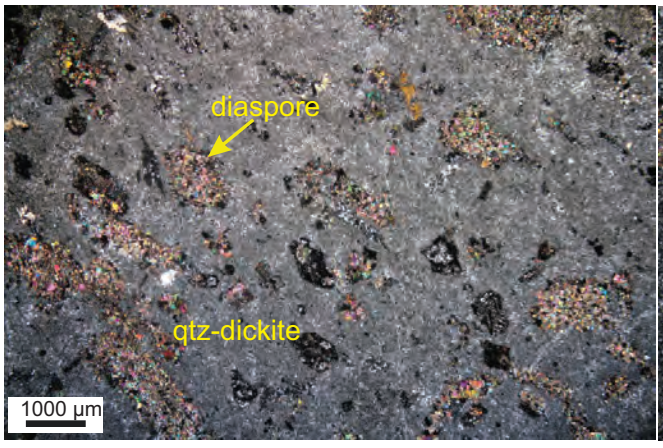

Pervasive intense silicification and clay (dickite) alteration in groundmass with clusters of diaspore and having weakly developed vuggy texture (XPL, 5X)

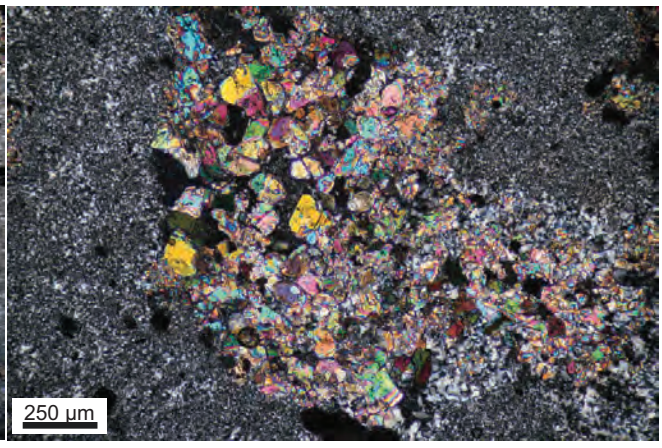

Cluster of coarse grained diaspore in silicified groundmass (XPL, 10X).

Interpretation:

This sample represents intense advanced argillic alteration of the host volcanic rock with abundant quartz-dickite and diaspore.

Alunite Ridge

Rock type: Dacite?
Alteration: quartz, illite, kaolinite, dickite, diaspore
Vein types:
Mineralization: pyrite (oxidized)

Sample no: TD098
UTM-east: 632196
UTM-north: 6357891
Elevation: 1805m

Hand Sample:
Light, pale-grey, highly silicified, felsic rock (dacite?) with remnants of subhedral phenocrysts of plagioclase, clay altered in a siliceous groundmass.

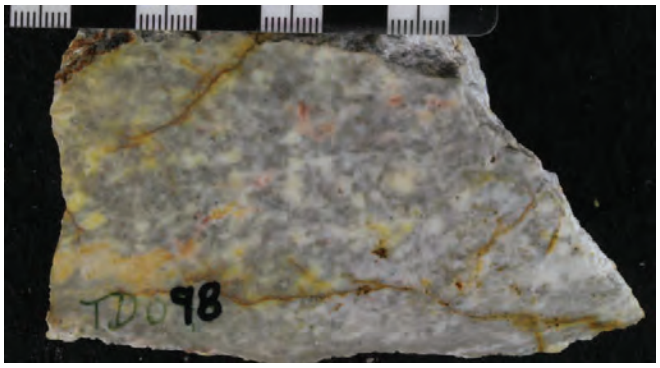

Thin Section:

Rock type: Remnants of plagioclase phenocrysts in a fine-grained groundmass, probably a dacite porphyry.

Alteration: The groundmass is characterized by clusters of quartz and clays. Plagioclase altered to pale-white illite and overprinted by clay minerals (kaolinite-dickite). Contains cluster of disapore.
.
Mineralization: Sparse, patchy and crack infill vein oxides (hematite-jarosite) and traces of pyrite and Cu-oxides (chrysocolla).

Vein types:

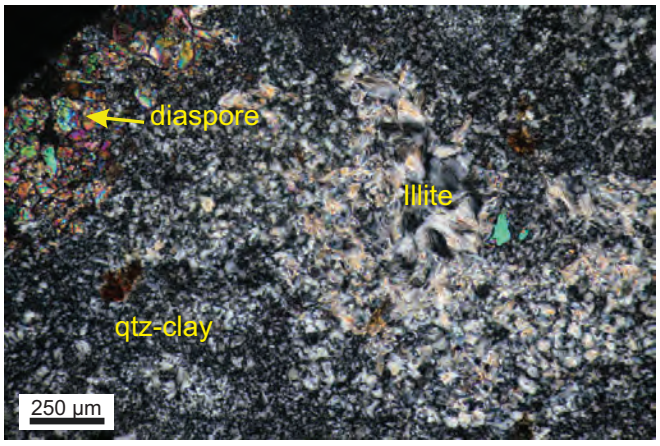

Pervasive intense quartz-clay (kaolinite-dickite) alteration with clusters of diaspore (XPL, 10X)

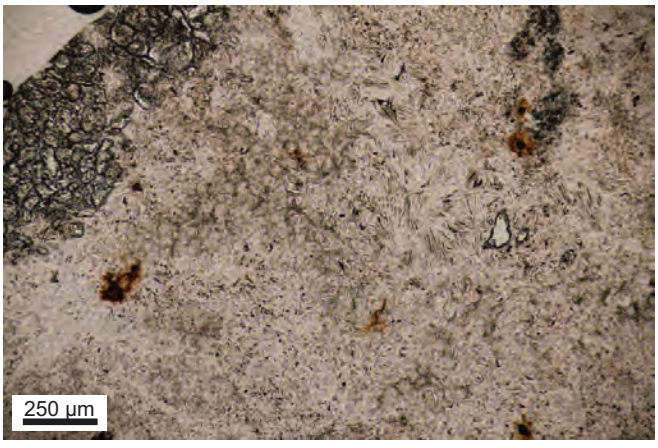

Same field of view but in PPL showing disapore, fine-grained quartz-clay and remnants of reddish iron oxide (PPL, 10X)

Interpretation:
This sample represents intense advanced argillic alteration of the host volcanic rock with abundant quartz, dickite, illite and diaspore.

Alunite Ridge

Rock type: Dacite?
Alteration: quartz, alunite
Vein types:
Mineralization: pyrite (oxidized)

Sample no: TD103
UTM-east: 632251
UTM-north: 6358096
Elevation: 1800m

Hand Sample:
Light, pale-grey, highly silicified, felsic rock (dacite?) with remnants of subhedral phenocrysts of plagioclase, clay altered in a siliceous groundmass.

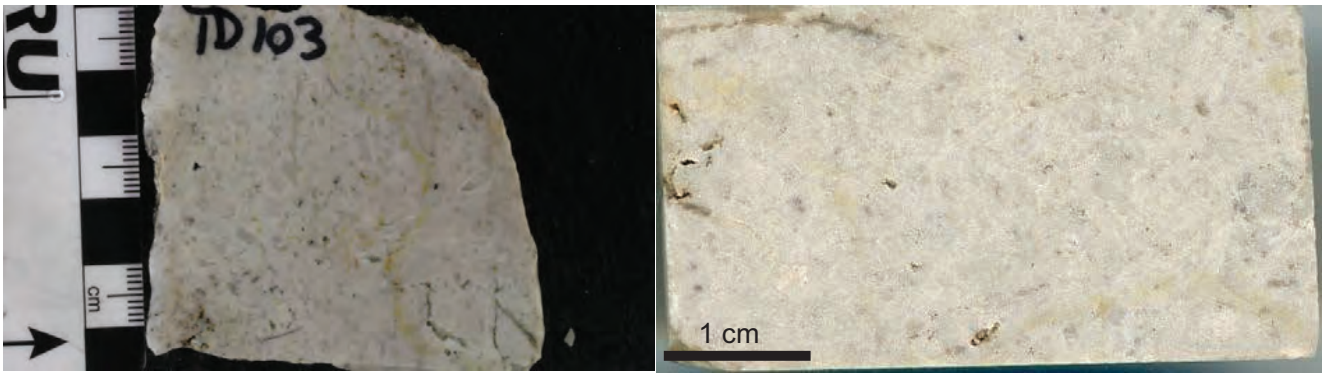

Thin Section:

Rock type: Remnants of plagioclase phenocrysts in a fine-grained groundmass, probably a dacite porphyry.

Alteration: The groundmass is characterized by fine-grained quartz and alunite. Cluster of rutile suggest remnants of hornblende.
.
Mineralization: Trace pyrite.

Vein types:

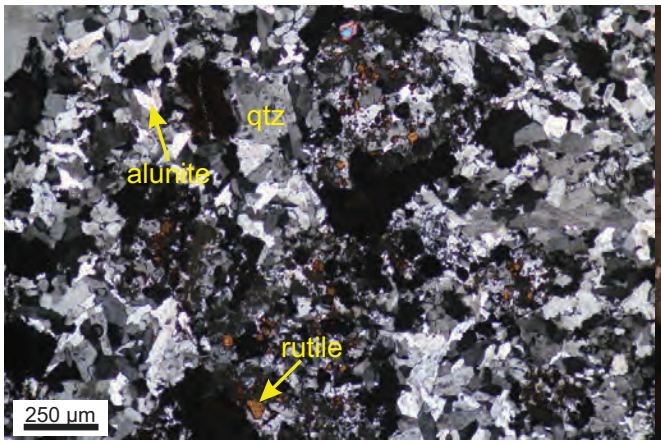

Fine-grained pervasive intense quartz-alunite alteration with rutile after mafic minerals (XPL, 10X)

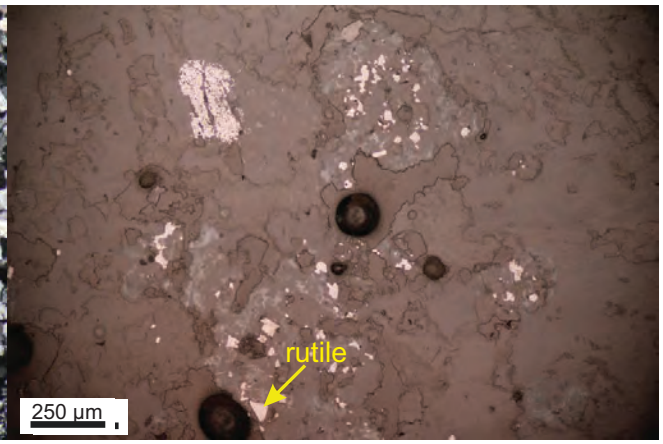

Same field of view but in RL showing cluster of rutile probably after some mafic minerals (RL, 10X)

Interpretation:
This sample represents intense advanced argillic alteration of the host volcanic rock with abundant quartz and alunite.

North Ridge

Rock type: Dacite?
Alteration: quartz, sericite
Vein types:
Mineralization: pyrite (oxidized)

Sample no: TD110
UTM-east: 631506
UTM-north: 6359524
Elevation: 1745m

Hand Sample:
Light, pale-yellow, silicified rock (dacite?) with remnants of subhedral phenocrysts of plagioclase, sericite altered in a siliceous groundmass.

Thin Section:

Rock type: Light, pale-grey dacitic volcanic flow with scattered and locally aligned euhedral phenocrysts of plagioclase, quartz and hornblende set in a fine-grained groundmass.

Alteration: Quartz-sericite altered aphanitic groundmass showing flow banding structures. Dacite is strongly altered to quartz-muscovite and overprinted by white argillic (illite-smectite) minerals. Hornblende altered to muscovite, rimmed and nucleated by clay minerals with a greenish tone (illite). Similarly, cracks and open spaces in plagioclase are filled with muscovite.
.
Mineralization: Traces of pyrite oxidized to orange-red jarosite-hematite also in the cracks.

Vein types:

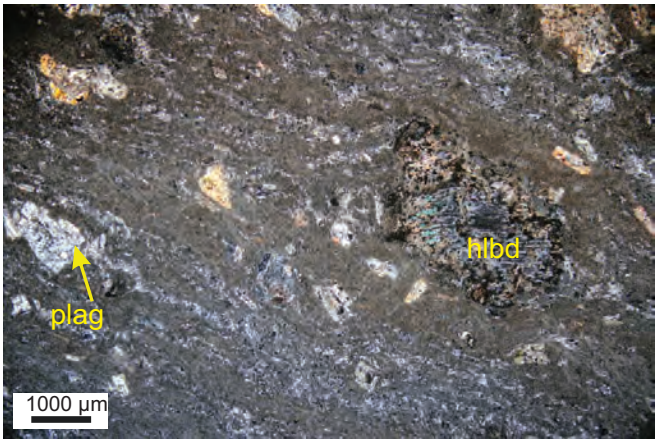

Plagioclase altered to sericite, remnants of hornblende with sericite and iron oxide in a fine quartz-sericite-clay altered groundmass (XPL, 2X)

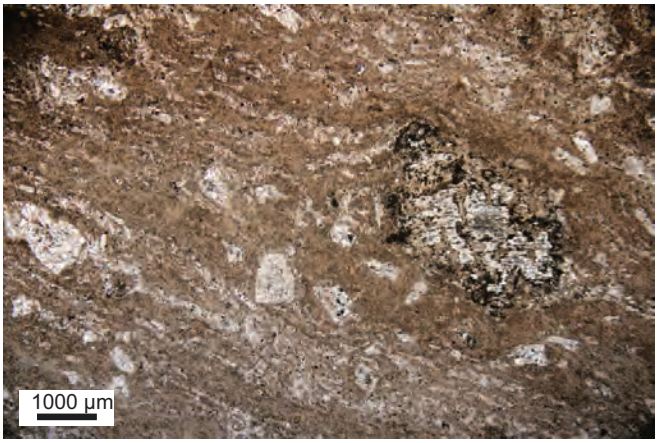

Same field of view showing light brown altered groundmass of quartz and sericite (PPL, 2X)

Interpretation:
This sample represents quartz-sericite alteration of the host volcanic rock probably below the advanced argillic alteration.

North Ridge

Rock type: Dacite?
Alteration: quartz, sericite
Vein types:
Mineralization: pyrite (oxidized)

Sample no: TD112
UTM-east: 631461
UTM-north: 6359448
Elevation: 1750m

Hand Sample:
Flow banded volcanic rock intensely altered to quartz and greenish sericite.

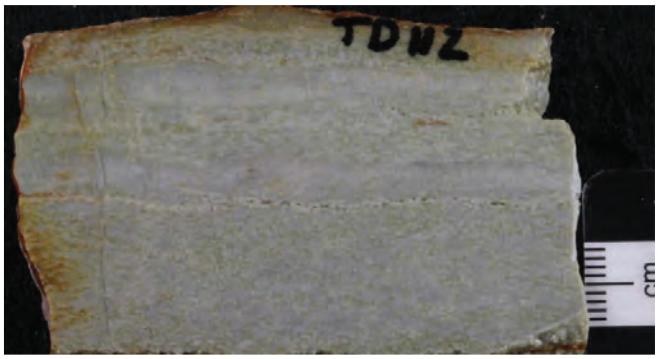

Thin Section:

Rock type: Light, pale-grey, green, flow band textured rock with alternating bands of weak and intense quartz-sericite alteration.

Alteration: Pervasive quartz and pale green sericite alteration. The cubic shaped vugs appear black in XP and bright in PP reflect leaching of pyrite and remanent hematite.
.
Mineralization: Traces of pyrite oxidized to orange-red jarosite-hematite.

Vein types:

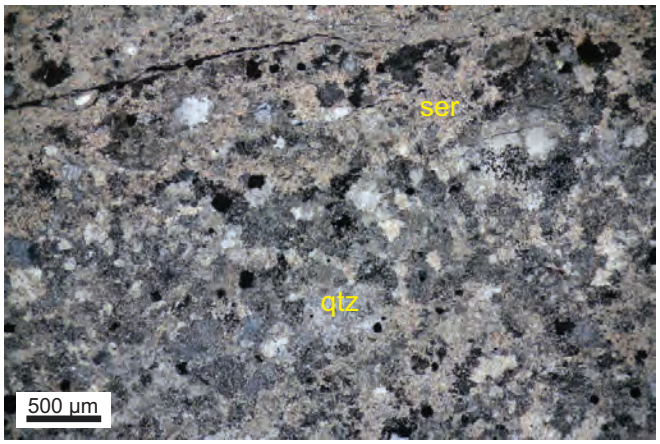

Hostrock intensely altered to quartz and sericite (XPL, 5X)

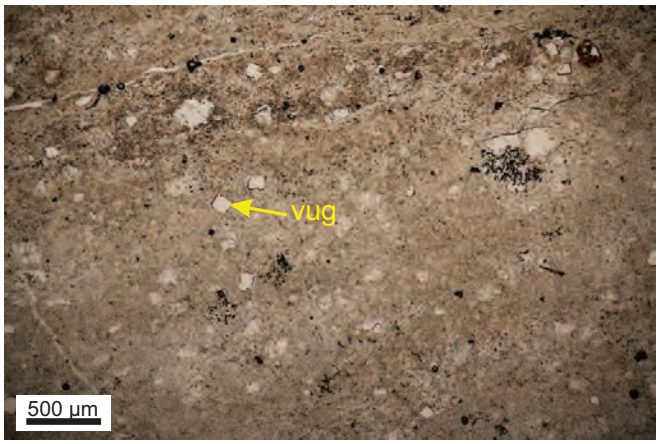

Same field of view showing light brown altered groundmass of quartz and sericite and cubic vugs probably after pyrite (PPL, 5X)

Interpretation:
This sample represents quartz-sericite alteration of the host volcanic rock probably below the advanced argillic alteration.

Sofia

Rock type: Basaltic andesite (Takla Group)
Alteration: chlorite, sericite
Vein types: chlorite-sericite-pyrite-chalcopyrite
Mineralization: pyrite-chalcopyrite

Sample no: TD124
UTM-east: 634963
UTM-north: 6360017
Elevation: 1048m

Hand Sample:

Basaltic andesite, probably Takla Group, near contact with granodiorite with intense chlorite alteration and pyrite-chalcopyrite mineralization.

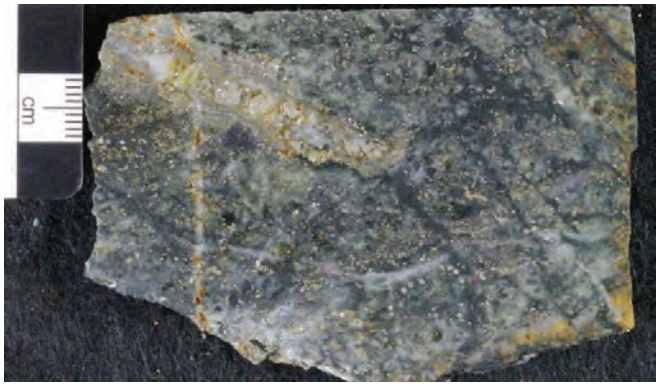

Thin Section:

Rock type: Fine-grained basaltic andesite with remnants of small (<1mm) plagioclase and intense chlorite alteration.

Alteration: Intense chlorite-sericite alteration with disseminated granular pyrite and intergrown chalcopyrite (9:1). Chlorite appear dark-blue in XP and green in PP replacing biotite (early-dark-mica) and amphiboles.

.

Mineralization: Pyrite (ca. 4%) and < 0.5% chalcopyrite.

Vein types: Chlorite-sericite-pyrite.

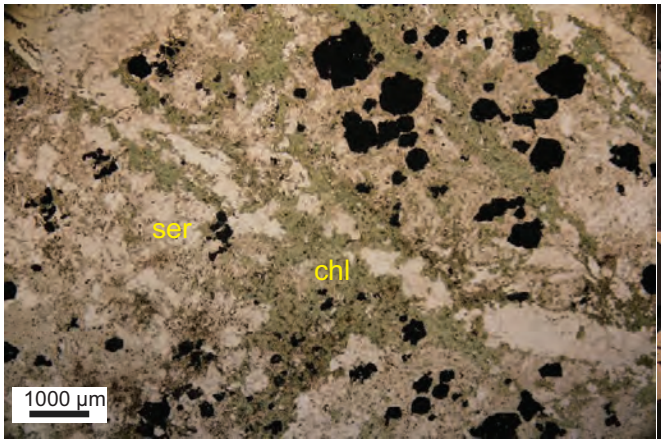

Pervasive and veinlet controlled chlorite alteration and patchy sericite (XPL, 2X)

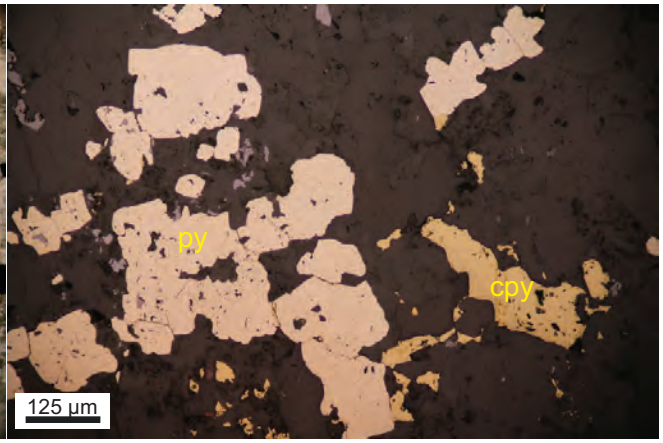

Closer view in RL showing pyrite and lesser chalcopyrite mineralization (RL, 20X)

Interpretation:

This sample represents volcanic rock at the contact with granodiorite with intense chlorite-sericite alteration typical of deeper portion of porphyry deposits.

APPENDIX 3: Re-Os Age Dating of Molybdenite

One molybdenite-bearing rock sample (TD-010) was processed for Re-Os age dating at the University of Alberta. The sample was processed by metal-free crushing followed by gravity and magnetic concentration methods described in detail by Selby and Creaser (2004) to prepare a molybdenite mineral separate. The ^{187}Re and ^{187}Os concentrations in molybdenite were determined by isotope dilution mass spectrometry using Carius-tube, solvent extraction, anion chromatography and negative thermal ionization mass spectrometry techniques. A mixed double spike containing known amounts of isotopically enriched ^{185}Re, ^{190}Os, and ^{188}Os analysis is used (Markey et al. 2007). Isotopic analysis used a ThermoScientific Triton mass spectrometer by Faraday collector. Total blanks for Re and Os are less than <3 picograms and 2 picograms, respectively, which are insignificant for the Re and Os concentrations in molybdenite. The molybdenite powder HLP-5 (Markey et al., 1998), is analyzed as a standard, and over a period of two years an average Re-Os date of 221.1 ± 1.0 Ma (1SD uncertainty, n=12) is obtained. This Re-Os age date is identical to that reported by Markey et al. (1998) of 221.0 ± 1.0 Ma.

The result of the Re-Os age determination is given below in Table 1. The age uncertainty is quoted at 2σ level, and includes all known analytical uncertainty, including uncertainty in the decay constant of ^{187}Re. The analysis showed no Common Os above blank levels.

Table 1: Re-Os isotopic and age data

Sample	Re ppm	±2σ	^{187}Re (ppm)	±2σ	^{187}Os (ppb)	±2σ	Model Age (Ma)	±2σ (Ma)
TD-010	2810	8	1766	5	5713	4	193.8	0.8
TD-010 Rpt	4095	12	2574	7	8332	7	194.0	0.8

ppb = parts per billion, ppm = parts per million. All uncertainties are quoted at the 2 sigma level of precision. Rpt = replicate analysis of the same molybdenite mineral separate.

References

RJ Markey, HJ Stein and JW Morgan "Highly precise Re-Os dating for molybdenite using alkaline fusion and NTIMS". Talanta (1998) 45, 935–946.

RJ Markey, HJ Stein, JL Hannah, D Selby and RA Creaser "Standardizing Re-Os geochronology: A new molybdenite Reference Material (Henderson, USA) and the stoichiometry of Os salts". Chemical Geology (2007), 244, 74-87.

D Selby and RA Creaser "Macroscale NTIMS and microscale LA-MC-ICP-MS Re-Os isotopic analysis of molybdenite: Testing spatial restrictions for reliable Re-Os age determinations, and implications for the decoupling of Re and Os within molybdenite". Geochimica et Cosmochimica Acta (2004), 68, 3897-3908.

APPENDIX 4: Shortwave Infrared (SWIR) TerraSpec Data

Sample ID	UTM_E	UTM_N	Elevation (m)	Datum	Area/prospect	Mineral 1	Mineral 2	Mineral 3
TD001	609781	6356260	1687	NAD 83, Zone 9	Lawyer's	Opal		
TD002	609786	6356346	1696	NAD 83, Zone 9	Lawyer's	Kaolinite	Opal	Halloysite
TD003	609786	6356346	1696	NAD 83, Zone 9	Lawyer's	Muscovite		
TD004	609534	6356458	1804	NAD 83, Zone 9	Lawyer's	Kaolinite		
TD005	609534	6356458	1807	NAD 83, Zone 9	Lawyer's	Illite		
TD006	613971	6350783	1740	NAD 83, Zone 9	Baker	Illite	Brucite	Ankerite
TD007	613971	6350783	1740	NAD 83, Zone 9	Baker	IntChlorite	Illite	
TD008	613957	6350793	1735	NAD 83, Zone 9	Baker	Muscovite		
TD009	613957	6350793		NAD 83, Zone 9	Baker	Muscovite		
TD010	613957	6350793		NAD 83, Zone 9	Baker	Muscovite		
TD011	613927	6350792	1722	NAD 83, Zone 9	Baker	Muscovite		
TD012	613927	6350792		NAD 83, Zone 9	Baker	Muscovite		
TD013	613975	6350767	1726	NAD 83, Zone 9	Baker	Illite		
TD014	613900	6350754	1720	NAD 83, Zone 9	Baker	IntChlorite		
TD015	613915	6350781	1708	NAD 83, Zone 9	Baker	Muscovite		
TD016	613893	6350778	1712	NAD 83, Zone 9	Baker	Muscovite		
TD017	613868	6350768	1718	NAD 83, Zone 9	Baker	Ankerite	Palygorskite	
TD018	613868	6350768		NAD 83, Zone 9	Baker	Siderite		
TD019	613821	6350693	1707	NAD 83, Zone 9	Baker	Aspectral		
TD020	613821	6350693		NAD 83, Zone 9	Baker	Muscovite		
TD021	613813	6350678		NAD 83, Zone 9	Baker	Illite	Phengite	
TD022	613813	6350678		NAD 83, Zone 9	Baker	Muscovite		
TD023	614182	6350994	1755	NAD 83, Zone 9	Baker	Palygorskite		
TD024	614168	6350976	1750	NAD 83, Zone 9	Baker	Palygorskite		
TD025	614062	6351051	1743	NAD 83, Zone 9	Baker	IntChlorite	Illite	
TD026	614341	6351333	1778	NAD 83, Zone 9	Baker	Illite	Paragonite	
TD027	614341	6351333		NAD 83, Zone 9	Baker	Aspectral		
TD028	614569	6351078	1901	NAD 83, Zone 9	Baker	MgChlorite	Hornblende	epidote
TD029	613961	6351322	1821	NAD 83, Zone 9	Baker	IntChlorite	Illite	
TD030	614033	6351324	1820	NAD 83, Zone 9	Baker	Muscovite	IntChlorite	
TD031	614055	6351343	1813	NAD 83, Zone 9	Baker	Illite		
TD032	613985	6351341	1830	NAD 83, Zone 9	Baker	Illite	Paragonite	
TD033	614060	6351415	1838	NAD 83, Zone 9	Baker	Actinolite		
TD034	613762	6351510		NAD 83, Zone 9	Baker	Illite	Epidote	
TD035	613558	6351725	1863	NAD 83, Zone 9	Baker	Ankerite		
TD036	613408	6351619	1801	NAD 83, Zone 9	Baker	IntChlorite	Illite	
TD037	613201	6351620	1780	NAD 83, Zone 9	Baker	IntChlorite	Epidote	
TD038	612923	6351445	1808	NAD 83, Zone 9	Baker	IntChlorite	Epidote	
TD039	613081	6351168	1811	NAD 83, Zone 9	Baker	Muscovite	FeChlorite	
TD040	618768	6338922	1181	NAD 83, Zone 9	Sturdee	Illite	Prehnite	
TD041	616778	6350623	1574	NAD 83, Zone 9	Black Gossan	MgChlorite	Illite	siderite
TD042	616821	6350491	1586	NAD 83, Zone 9	Black Gossan	Epidote	Illite	
TD043	616833	6350454	1587	NAD 83, Zone 9	Black Gossan	Illite	Epidote	
TD044	616841	6350536		NAD 83, Zone 9	Black Gossan	IntChlorite	Illite	epidote
TD045	616929	6350997	1662	NAD 83, Zone 9	Black Gossan	IntChlorite	Muscovite	
TD046	616921	6351213	1680	NAD 83, Zone 9	Black Gossan	Illite	Halloysite	ankerite
TD047	617020	6350930	1712	NAD 83, Zone 9	Black Gossan	Muscovite		
TD048	617149	6350066	1763	NAD 83, Zone 9	Black Gossan	IntChlorite	Illite	ankerite
TD049	617098	6350928		NAD 83, Zone 9	Black Gossan	Muscovite		
TD050	617349	6351493	1710	NAD 83, Zone 9	Black Gossan	IntChlorite	Epidote	
TD051	616917	6350841	1635	NAD 83, Zone 9	Black Gossan	Illite	Epidote	
TD052	614150	6351238	1784	NAD 83, Zone 9	Baker	IntChlorite	Illite	ankerite
TD053	613611	6352362	1845	NAD 83, Zone 9	Baker	Illite		
TD054	620940	6347454	1270	NAD 83, Zone 9	Shasta	Muscovite		

Sample ID	UTM_E	UTM_N	Elevation (m)	Datum	Area/prospect	Mineral 1	Mineral 2	Mineral 3
TD055	620940	6347454	1270	NAD 83, Zone 9	Shasta	IntChlorite	Illite	
TD056	620940	6347454	1270	NAD 83, Zone 9	Shasta	IntChlorite	Muscovite	
TD057	620940	6347454	1270	NAD 83, Zone 9	Shasta	Illite		ankerite
TD058	620940	6347454	1270	NAD 83, Zone 9	Shasta	Muscovite		siderite
TD059	620940	6347454	1270	NAD 83, Zone 9	Shasta	Ankerite	Illite	
TD060	620940	6347454	1270	NAD 83, Zone 9	Shasta	Siderite	Illite	
TD061	620940	6347454	1270	NAD 83, Zone 9	Shasta	Muscovite	Ankerite	
TD062	620940	6347454	1270	NAD 83, Zone 9	Shasta	Calcite		
TD063	628398	6347747	1555	NAD 83, Zone 9	Brenda	Pyrophyllite	K_Alunite	
TD064	628398	6347819	1576	NAD 83, Zone 9	Brenda	Epidote	Illite	
TD065	628462	6347902	1606	NAD 83, Zone 9	Brenda	Illite	Epidote	
TD066	628576	6347947	1622	NAD 83, Zone 9	Brenda	Illite	Ankerite	siderite
TD067	628616	6348269	1542	NAD 83, Zone 9	Brenda	Illite	Jarosite	
TD068	628570	6348302	1526	NAD 83, Zone 9	Brenda	Illite	Phengite	jarosite
TD069	628128	6349469	1218	NAD 83, Zone 9	Brenda	Na_Alunite	Kaolinite	
TD070	607909	6354275	1863	NAD 83, Zone 9	Silver Pond S	Montmorillonite		
TD071	607726	6352847	1745	NAD 83, Zone 9	Silver Pond Ridge	Calcite	Illite	
TD072	607961	6352822	1772	NAD 83, Zone 9	Silver Pond Ridge	IntChlorite	Muscovite	
TD073	608374	6355548	1750	NAD 83, Zone 9	Cliff Creek	Siderite	Illite	ankerite
TD074	608374	6355548	1750	NAD 83, Zone 9	Cliff Creek	Kaolinite		
TD075	608374	6355548	1750	NAD 83, Zone 9	Cliff Creek	Ankerite	Dickite	illite
TD076	606788	6356217		NAD 83, Zone 9	Silver Pond N	Dickite	Kaolinite	
TD077	606578	6356012	1750	NAD 83, Zone 9	Silver Pond N	Dickite		
TD078	613927	6350792	1722	NAD 83, Zone 9	Baker	Muscovite		
TD079	612186	6349941	1817	NAD 83, Zone 9	Baker W	Illite	Ankerite	
TD080	612213	6349896	1815	NAD 83, Zone 9	Baker W	Illite		siderite
TD081	612213	6349896	1815	NAD 83, Zone 9	Baker W	Palygorskite		
TD082					Baker	IntChlorite	Hornblende	dolomite
TD083					Baker	IntChlorite	Muscovite	
TD084					Baker	Zoisite		
TD085	614211	6351646	1772	NAD 83, Zone 9	Baker	Siderite		
TD086	614211	6351646	1772	NAD 83, Zone 9	Baker	Epidote		siderite
TD087	613335	6349334		NAD 83, Zone 9	Baker skarn	Prehnite	Montmorillonite	siderite
TD088	613053	6349593	1719	NAD 83, Zone 9	Baker skarn	Siderite	Illite	ankerite
TD089	613067	6349745	1730	NAD 83, Zone 9	Baker skarn	IntChlorite	Epidote	
TD090	613137	6349707		NAD 83, Zone 9	Baker skarn	IntChlorite		epidote
TD091	612202	6346812	1460	NAD 83, Zone 9	Shasta	Siderite	Illite	
TD092					Shasta	IntChlorite	Illite	calcite
TD093	631912	6357806	1740	NAD 83, Zone 9	Alunite Ridge	Muscovite		phengite
TD094	631948	6357812	1744	NAD 83, Zone 9	Alunite Ridge	Muscovite	Ankerite	
TD095	631954	6357826	1740	NAD 83, Zone 9	Alunite Ridge	IntChlorite	Muscovite	epidote
TD096	632206	6357883	1804	NAD 83, Zone 9	Alunite Ridge	Dickite	Kaolinite	
TD097	632193	6357871	1801	NAD 83, Zone 9	Alunite Ridge	Dickite	Diaspore	
TD098	632196	6357891	1805	NAD 83, Zone 9	Alunite Ridge	Dickite		kaolinite
TD099	632228	6357919	1808	NAD 83, Zone 9	Alunite Ridge	Diaspore	Dickite	
TD100	632273	6357946	1800	NAD 83, Zone 9	Alunite Ridge	Dickite	Kaolinite	
TD101	632275	6358025	1802	NAD 83, Zone 9	Alunite Ridge	Dickite	Kaolinite	
TD102	632263	6358056		NAD 83, Zone 9	Alunite Ridge	Dickite	Kaolinite	
TD103	632251	6358096	1800	NAD 83, Zone 9	Alunite Ridge	K_Alunite		
TD104	632245	6358144	1780	NAD 83, Zone 9	Alunite Ridge	FeChlorite	Muscovite	halloysite
TD105	632239	6358266	1750	NAD 83, Zone 9	Alunite Ridge	Muscovite		
TD106	631465	6359753		NAD 83, Zone 9	North Ridge	Phengite	Illite	
TD107	631487	6359724	1724	NAD 83, Zone 9	North Ridge	Muscovite	Opal	
TD108	631532	6359635	1739	NAD 83, Zone 9	North Ridge	Muscovite		

Sample ID	UTM_E	UTM_N	Elevation (m)	Datum	Area/prospect	Mineral 1	Mineral 2	Mineral 3
TD109	631507	6359581	1744	NAD 83, Zone 9	North Ridge	Illite	Phengite	
TD110	631506	6359524	1745	NAD 83, Zone 9	North Ridge	Illite	Phengite	
TD111	631483	6359452	1755	NAD 83, Zone 9	North Ridge	Muscovite	Jarosite	
TD112	631461	6359448	1750	NAD 83, Zone 9	North Ridge	Illite		
TD113	631008	6358242	1702	NAD 83, Zone 9	North Ridge	Paragonite	Pyrophyllite	
TD114	631100	6358250	1660	NAD 83, Zone 9	North Ridge	Pyrophyllite		
TD115	630464	6358354		NAD 83, Zone 9	North Ridge	Illite	IntChlorite	
TD116	631587	6358323	1576	NAD 83, Zone 9	Quartz Lake	Illite		
TD117	631551	6358165	1595	NAD 83, Zone 9	Quartz Lake	Illite		kaolinite
TD118	631462	6357988	1600	NAD 83, Zone 9	Quartz Lake	IntChlorite	Muscovite	
TD119	631462	6357988	1600	NAD 83, Zone 9	Quartz Lake	Kaolinite	Epidote	illite
TD120	631462	6357988	1600	NAD 83, Zone 9	Quartz Lake	Muscovite	Ankerite	
TD121	631462	6357988	1600	NAD 83, Zone 9	Quartz Lake	Muscovite	Halloysite	
TD122	631462	6357988	1600	NAD 83, Zone 9	Quartz Lake	Muscovite	Ankerite	chlorite
TD123	634963	6360017	1048	NAD 83, Zone 9	Sofia	Muscovite	Ankerite	
TD124	634963	6360017	1048	NAD 83, Zone 9	Sofia	Muscovite	IntChlorite	

Sample ID	hqd1900	w2200	hqd2200	width2200	w2250	hqd2250	width2250	w2350	hqd2350	width2350
TD001	0.201	2208.03	0.1							
TD002	0.214	2208.71	0.151							
TD003	0.254	2200.16	0.0386							
TD004	0.137	2208.9	0.0817							
TD005	0.271	2200.46	0.0756							
TD006	0.177	2207.98	0.103	33.894	2252.57	0.053	20.23	2335.2	0.0757	38.276
TD007	0.283	2207.81	0.145	32.599	2250.74	0.0878	20.15	2337.09	0.132	37.969
TD008	0.13	2200.59	0.269	31.387						
TD009	0.171	2201.39	0.289	31.721						
TD010	0.205	2203.02	0.359	31.774						
TD011	0.177	2201.88	0.363	31.636						
TD012	0.174	2201.58	0.248	31.344						
TD013	0.133	2200.07	0.238	31.805						
TD014	0.076				2249.9	0.0509	12.158	2335.79	0.0823	37.166
TD015	0.188	2203.01	0.2	31.527						
TD016	0.086	2207.86	0.142	34.467						
TD017	0.254				2250.14	0.0782	16.721	2325.34	0.121	40.416
TD018	0.0775	2213.52	0.0472							
TD019	0.248	2225.13	0.0166							
TD020		2199.09	0.0585	28.56						
TD021	0.373	2207.53	0.474	36.421						
TD022	0.179	2207.81	0.16	35.993						
TD023	0.197	2209.41	0.0196							
TD024	0.458	2210.66	0.00881							
TD025	0.0899	2207.62	0.0288	34.019	2251.37	0.0495	17.1	2333.14	0.0688	34.824
TD026	0.305	2197.73	0.448	34.282						
TD027		2208.56	0.0551							
TD028	0.0999				2251.64	0.0991	15.618	2320.2	0.191	38.884
TD029	0.242	2209.84	0.119	35.32	2248.65	0.096	19.574	2336.18	0.104	37.15
TD030	0.251	2210.19	0.179	34.744	2247.42	0.115	19.751	2343.07	0.132	38.183
TD031	0.418	2199.06	0.46	34.762						
TD032	0.219	2195.68	0.474	32.92						
TD033	0.0581	2203.05	0.0577							
TD034	0.21	2205.61	0.124	29.801						
TD035	0.05	2200.87	0.0313							
TD036	0.293	2201.96	0.168	33.664	2251.23	0.148	18.513	2342.29	0.165	37.253
TD037	0.152				2253.36	0.179	19.062	2340.27	0.286	38.059
TD038	0.0969				2253.82	0.0943	19.261	2342.09	0.141	38.183
TD039	0.0927	2207	0.146	33.914	2250.91	0.0848	20.91	2350.92	0.121	36.093
TD040	0.178	2198.51	0.153	28.42						
TD041	0.324	2206.28	0.0863	26.53	2248.52	0.0912	16.087	2319.58	0.162	38.922
TD042	0.121	2202.97	0.089	33.425						
TD043	0.252	2206.87	0.07	24.059						
TD044	0.164	2206.15	0.105	33.522	2253.28	0.114	16.5	2343.43	0.202	37.678
TD045	0.17	2207.59	0.101	35.205	2253.44	0.135	17.84	2342.88	0.166	37.062
TD046	0.321	2206.52	0.2	28.038	2245.12	0.0643	19.203	2348.45	0.0647	38.198
TD047	0.166	2207.71	0.349	33.934				2350.68	0.195	38.092
TD048	0.276	2208.67	0.12	32.036	2250.83	0.0861	19.072	2344.33	0.0937	36.039
TD049	0.288	2207.39	0.377	34.256						
TD050	0.0802				2252.61	0.0501	17.939	2343.21	0.0885	37.938
TD051	0.118	2206.52	0.0435	37.129						
TD052	0.0852	2202.95	0.0466	34.178	2252.01	0.0475	17.363	2337.2	0.0754	36.312
TD053	0.169	2185.33	0.0278	34.55						
TD054	0.159	2210.96	0.18	35.244						

Sample ID	hqd1900	w2200	hqd2200	width2200	w2250	hqd2250	width2250	w2350	hqd2350	width2350
TD055	0.0958	2226.99	0.0298	35.391	2251.8	0.0605	18.259	2347.35	0.0796	36.574
TD056	0.102	2212.58	0.0516	35.847	2251.92	0.0751	18.806	2339.86	0.0911	38.505
TD057	0.33	2199.88	0.0968	31.111	2242.83	0.0439	15.618	2341.98	0.0115	33.029
TD058	0.171	2209.58	0.117	35.162						
TD059	0.144	2207.05	0.054	36.47						
TD060	0.165	2203.22	0.046	34.519						
TD061	0.165	2208.71	0.0928	34.535						
TD062	0.0982	2228.34	0.0113							
TD063	0.138									
TD064	0.146	2206.95	0.0695	31.01						
TD065	0.229	2207.62	0.113	34.253						
TD066	0.165	2203.29	0.0648	28.836						
TD067	0.306	2208.18	0.287	32.786						
TD068	0.33	2209.08	0.283	33.35						
TD069	0.0521									
TD070	0.241	2208.12	0.0941							
TD071	0.158	2219.14	0.0562	31.604						
TD072	0.211	2213.23	0.0873	34.75	2253.81	0.087	19.415	2346.47	0.107	36.368
TD073	0.172	2207.16	0.0368	26.488						
TD074	0.116	2209.15	0.0543							
TD075	0.185	2208.85	0.0666	20.476						
TD076	0.0684	2207.53	0.414							
TD077	0.0684	2208.06	0.139							
TD078	0.247	2202.76	0.423	32.827						
TD079	0.326	2209.29	0.202	34.289						
TD080	0.185	2208.38	0.122	30.521						
TD081	0.597	2207.07	0.00483							
TD082	0.219				2252.19	0.0821	20.849	2324.58	0.177	40.74
TD083	0.0684				2250.89	0.085	17.865	2339.54	0.123	36.019
TD084	0.1	2229.97	0.0396							
TD085	0.197	2206.65	0.192							
TD086	0.0753	2224.02	0.0498							
TD087	0.281									
TD088	0.164	2202.72	0.0418	28.452						
TD089	0.118				2254.28	0.161	19.814	2337	0.278	38.436
TD090	0.124				2255.11	0.0963	20.713	2331.51	0.16	38.163
TD091	0.177	2208.63	0.0722	29.152						
TD092	0.252	2210.94	0.152	35.6	2247.14	0.0976	21.477	2341.86	0.143	36.092
TD093	0.139	2209.64	0.103	35.757						
TD094	0.267	2208.94	0.0608	23.491						
TD095	0.155	2224.01	0.0556	36.053	2254.12	0.0914	16.436	2344.84	0.15	37.753
TD096	0.171	2207.95	0.399							
TD097	0.0916	2207.99	0.265							
TD098	0.108	2208.12	0.281							
TD099		2207.99	0.257							
TD100	0.0428	2208.22	0.384							
TD101	0.146	2208.06	0.428							
TD102	0.146	2207.85	0.469							
TD103	0.214									
TD104	0.16	2209.7	0.103	28.639	2242.1	0.0444	20.796	2357.32	0.0687	33.316
TD105	0.21	2209.48	0.229	33.637						
TD106	0.266	2211.01	0.327	34.725						
TD107	0.339	2208.19	0.313	33.724						
TD108	0.348	2208.88	0.366	33.865						

Sample ID	hqd1900	w2200	hqd2200	width2200	w2250	hqd2250	width2250	w2350	hqd2350	width2350
TD109	0.378	2211.33	0.415	34.713						
TD110	0.404	2208.62	0.44	35.26						
TD111	0.297	2207.8	0.304	33.724						
TD112	0.316	2201.72	0.439	34.314						
TD113	0.365	2187.03	0.173	27.323						
TD114	0.228									
TD115	0.116	2200.35	0.0708	27.613	2247.27	0.0416	19.366	2344.64	0.0623	35.019
TD116	0.099	2204.71	0.0982	29.383						
TD117	0.171	2202.43	0.131	31.372						
TD118	0.148	2210.43	0.128	31.274	2253.65	0.0869	19.237	2348.36	0.125	36.26
TD119	0.214	2208.76	0.111	22.69						
TD120	0.134	2209.43	0.113	28.639						
TD121	0.433	2208.65	0.168	27.154						
TD122	0.193	2203.13	0.0569	34.487	2252.11	0.0472	19.146	2345.24	0.0506	39.052
TD123	0.139	2201.74	0.124	29.441						
TD124	0.0773	2213.11	0.144	36.113	2251.75	0.105	20.262	2344.05	0.132	34.248

Sample ID	sericite crystalinity index	kaolinite crystalinity index	actinolite	epidote	chlorite	muscovite	paragonite	illite
TD001								
TD002		0.992						
TD003								
TD004		1.009						
TD005								
TD006	0.584				chlorite			illite
TD007	0.514				chlorite			illite
TD008	2.066					muscovite		
TD009	1.692					muscovite		
TD010	1.747					muscovite		
TD011	2.044					muscovite		
TD012	1.423					muscovite		
TD013	1.792					muscovite		
TD014					chlorite			
TD015	1.064					muscovite		
TD016	1.646					muscovite		
TD017					chlorite			
TD018								
TD019								
TD020						muscovite		illite
TD021	1.271					muscovite		illite
TD022	0.896					muscovite		
TD023								
TD024								
TD025	0.32				chlorite			illite
TD026	1.466						Paragonite	illite
TD027								
TD028			actinolite	epidote	chlorite			
TD029	0.489				chlorite			illite
TD030	0.713				chlorite	muscovite		
TD031	1.1							illite
TD032	2.166					muscovite	Paragonite	
TD033								
TD034	0.588			epidote				illite
TD035								
TD036	0.573				chlorite			illite
TD037				epidote	chlorite			
TD038				epidote	chlorite			
TD039	1.576				chlorite	muscovite		
TD040	0.863					muscovite		illite
TD041	0.266				chlorite			illite
TD042	0.735			epidote				illite
TD043	0.278			epidote				illite
TD044	0.642			epidote	chlorite			illite
TD045	0.593				chlorite			illite
TD046	0.622				chlorite			illite
TD047	2.097				chlorite	muscovite		
TD048	0.436				chlorite			illite
TD049	1.309					muscovite		
TD050				epidote	chlorite			
TD051	0.369			epidote				illite
TD052	0.547				chlorite			illite
TD053	0.165							illite
TD054	1.128					muscovite		

Sample ID	sericite crystalinity index	kaolinite crystalinity index	actinolite	epidote	chlorite	muscovite	paragonite	illite
TD055	0.311				chlorite			illite
TD056	0.506				chlorite	muscovite		
TD057	0.293				chlorite			illite
TD058	0.685					muscovite		
TD059	0.375							illite
TD060	0.279							illite
TD061	0.561					muscovite		
TD062								
TD063								
TD064	0.476			epidote				illite
TD065	0.493			epidote				illite
TD066	0.394							illite
TD067	0.939							illite
TD068	0.859					muscovite		illite
TD069		1.002						
TD070								
TD071	0.356							illite
TD072	0.415				chlorite	muscovite		
TD073	0.214							illite
TD074		0.997						
TD075	0.359							illite
TD076		0.913						
TD077								
TD078	1.714					muscovite		
TD079	0.62							illite
TD080	0.659							illite
TD081								
TD082			actinolite		chlorite			
TD083					chlorite	muscovite		
TD084				epidote				
TD085								
TD086				epidote				
TD087						muscovite		
TD088	0.255							illite
TD089				epidote	chlorite			
TD090				epidote	chlorite			
TD091	0.409							illite
TD092	0.604				chlorite			illite
TD093	0.74					muscovite		
TD094	0.228					muscovite		
TD095	0.357			epidote	chlorite	muscovite		
TD096		0.94						
TD097								
TD098		0.99						
TD099								
TD100		0.926						
TD101		0.929						
TD102		0.9						
TD103								
TD104	0.643	0.987			chlorite	muscovite		
TD105	1.09					muscovite		
TD106	1.23					muscovite		illite
TD107	0.922					muscovite		
TD108	1.05					muscovite		

Sample ID	sericite crystalinity index	kaolinite crystalinity index	actinolite	epidote	chlorite	muscovite	paragonite	illite
TD109	1.097					muscovite		illite
TD110	1.09					muscovite		illite
TD111	1.024					muscovite		
TD112	1.39							illite
TD113	0.474						Paragonite	
TD114								
TD115	0.608				chlorite			illite
TD116	0.992							illite
TD117	0.77	0.973						illite
TD118	0.865				chlorite	muscovite		
TD119	0.518	0.999		epidote				illite
TD120	0.839					muscovite		
TD121	0.387	0.964				muscovite		
TD122	0.295				chlorite	muscovite		
TD123	0.897					muscovite		
TD124	1.86				chlorite	muscovite		

Sample ID	pyrophyllite	White Mica Group	kaoinite	halloysite	Kaolinite Group	montmorillonite	diaspore	dickite
TD001								
TD002			kaolinite	halloysite	kaolinite			
TD003						montmorillonite		
TD004			kaolinite		kaolinite			
TD005						montmorillonite		
TD006		illite						
TD007		illite						
TD008		muscovite						
TD009		muscovite						
TD010		muscovite						
TD011		muscovite						
TD012		muscovite						
TD013		muscovite						
TD014								
TD015		muscovite						
TD016		muscovite						
TD017								
TD018								
TD019								
TD020		muscovite						
TD021		muscovite						
TD022		muscovite						
TD023								
TD024								
TD025		illite						
TD026		muscovite						
TD027								
TD028								
TD029		illite						
TD030		illite						
TD031		muscovite						
TD032		muscovite						
TD033								
TD034		illite						
TD035								
TD036		illite						
TD037								
TD038								
TD039		muscovite						
TD040		muscovite						
TD041		illite						
TD042		illite						
TD043		illite						
TD044		illite						
TD045		illite						
TD046		illite						
TD047		muscovite						
TD048		illite						
TD049		muscovite						
TD050								
TD051		illite						
TD052		illite						
TD053		illite						
TD054		muscovite						

Sample ID	pyrophyllite	White Mica Group	kaoinite	halloysite	Kaolinite Group	montmorillonite	diaspore	dickite
TD055		illite						
TD056		illite						
TD057		illite						
TD058		illite						
TD059		illite						
TD060		illite						
TD061		illite						
TD062								
TD063	pyrophyllite	pyrophyllite						
TD064		illite						
TD065		illite						
TD066		illite						
TD067		muscovite						
TD068		muscovite						
TD069			kaolinite		kaolinite			
TD070						montmorillonite		
TD071		illite						
TD072		illite						
TD073		illite						
TD074			kaolinite		kaolinite			
TD075		illite						dickite
TD076			kaolinite		kaolinite			dickite
TD077								dickite
TD078		muscovite						
TD079		illite						
TD080		illite						
TD081								
TD082								
TD083		muscovite						
TD084								
TD085								
TD086								
TD087		muscovite				montmorillonite		
TD088		illite						
TD089								
TD090								
TD091		illite						
TD092		illite						
TD093		illite						
TD094		illite						
TD095		illite						
TD096			kaolinite		kaolinite			dickite
TD097							diaspore	dickite
TD098			kaolinite		kaolinite			
TD099							diaspore	dickite
TD100			kaolinite		kaolinite			
TD101			kaolinite		kaolinite			
TD102			kaolinite		kaolinite			
TD103								
TD104		illite		halloysite	halloysite			
TD105		muscovite						
TD106		muscovite						
TD107		muscovite						
TD108		muscovite						

Sample ID	pyrophyllite	White Mica Group	kaoinite	halloysite	Kaolinite Group	montmorillonite	diaspore	dickite
TD109		muscovite						
TD110		muscovite						
TD111		muscovite						
TD112		muscovite						
TD113	pyrophyllite	pyrophyllite						
TD114	pyrophyllite	pyrophyllite						
TD115		illite						
TD116		muscovite						
TD117		illite	kaolinite		kaolinite			
TD118		muscovite						
TD119		illite	kaolinite		kaolinite			
TD120		muscovite						
TD121		illite		halloysite	halloysite			
TD122		illite						
TD123		muscovite						
TD124		muscovite						

Sample ID	Clays	jarosite	alunite	ankerite	siderite	calcite	Carbonates	palygorskite	opal
TD001									opal
TD002	kaolinite								
TD003	montmorillonite								
TD004	kaolinite								
TD005	montmorillonite								
TD006									
TD007									
TD008									
TD009									
TD010									
TD011									
TD012									
TD013									
TD014									
TD015									
TD016									
TD017								palygorskite	
TD018									
TD019									
TD020									
TD021									
TD022									
TD023								palygorskite	
TD024								palygorskite	
TD025									
TD026									
TD027									
TD028									
TD029									
TD030									
TD031									
TD032									
TD033									
TD034									
TD035				ankerite			ankerite		
TD036									
TD037									
TD038									
TD039									
TD040									
TD041					siderite				
TD042									
TD043									
TD044									
TD045									
TD046									
TD047									
TD048									
TD049									
TD050									
TD051									
TD052				ankerite			ankerite		
TD053									
TD054									

Sample ID	Clays	jarosite	alunite	ankerite	siderite	calcite	Carbonates	palygorskite	opal
TD055									
TD056									
TD057				ankerite			ankerite		
TD058					siderite				
TD059				ankerite			ankerite		
TD060					siderite				
TD061				ankerite			ankerite		
TD062						calcite	calcite		
TD063									
TD064									
TD065									
TD066				ankerite	siderite		ankerite+siderite		
TD067									
TD068									
TD069	kaolinite		alunite						
TD070	montmorillonite								
TD071						calcite	calcite		
TD072									
TD073				ankerite	siderite		ankerite+siderite		
TD074	kaolinite								
TD075	dickite			ankerite			ankerite		
TD076	dickite-kaolinite								
TD077	dickite								
TD078									
TD079				ankerite			ankerite		
TD080					siderite				
TD081								palygorskite	
TD082				ankerite			ankerite		
TD083									
TD084									
TD085					siderite				
TD086					siderite				
TD087	montmorillonite				siderite				
TD088				ankerite	siderite		ankerite+siderite		
TD089									
TD090									
TD091					siderite				
TD092						calcite	calcite		
TD093									
TD094				ankerite			ankerite		
TD095									
TD096	dickite-kaolinite								
TD097	dickite-diaspore								
TD098	kaolinite								
TD099	dickite-diaspore								
TD100	kaolinite								
TD101	kaolinite								
TD102	kaolinite								
TD103			alunite						
TD104	halloysite								
TD105									
TD106									
TD107									
TD108									

Sample ID	Clays	jarosite	alunite	ankerite	siderite	calcite	Carbonates	palygorskite	opal
TD109									
TD110									
TD111		jarosite							
TD112									
TD113								palygorskite	
TD114									
TD115									
TD116									
TD117	kaolinite								
TD118									
TD119	kaolinite								
TD120				ankerite			ankerite		
TD121	halloysite								
TD122				ankerite			ankerite		
TD123				ankerite			ankerite		
TD124									

APPENDIX 5: Whole Rock Geochemical Data

	Mo	Cu	Pb	Zn	Ag	Ni	Co
method	**MA250**	**MA250**	**MA250**	**MA250**	**MA250**	**MA250**	**MA250**
range	**PPM**	**PPM**	**PPM**	**PPM**	**PPB**	**PPM**	**PPM**
detection limit	**0.05**	**0.1**	**0.02**	**0.2**	**20**	**0.1**	**0.2**
Sample#							
TD001	0.34	13.1	7.37	115.7	153	3.2	10.4
TD002	0.22	12	6.28	77.9	8302	2	5.7
TD003	0.17	17.7	22.55	44.4	11772	1.2	1.9
TD006	5.74	80.6	38.3	98.8	2346	1.5	4.6
TD007	1.99	47.3	32.62	105.9	2236	1.6	3.4
TD008	55.8	26.7	10.95	48.8	1622	1	5.1
TD009	4.17	92.9	54.09	85.8	6041	1.7	10.4
TD010	220.16	17.9	13.66	47	1567	1.3	4.8
TD011	2.63	21.9	11.77	34.5	1143	1.6	5.8
TD013	4.22	11.3	9.16	26.8	914	1.9	4.3
TD014	0.37	207.4	74.9	250.5	6579	37.8	35.6
TD016	24.29	28.1	22.12	77.5	1167	79.6	35.8
TD023	20.94	251	86.94	169.3	3502	10	32
TD024	17.68	257.3	54.2	67.2	5270	5.8	19.9
TD026	2.73	18.4	3.43	9.2	123	1	0.3
TD027	0.64	106.8	11.27	87.9	381	23.4	29.3
TD029	3.03	51.2	12.13	59.9	385	3	7.3
TD030	2.54	80.5	13.86	58.2	229	2.1	6
TD031	5.77	11.5	37.28	8.6	1525	0.4	<0.2
TD035	0.57	27.4	9.86	143.1	184	5.8	15.5
TD037	0.23	4.9	10.25	75.3	54	5.3	12
TD039	1.37	48.3	8.89	83.4	168	4.8	11.5
TD040	1.47	4.3	7.88	34.5	36	2.3	6.1
TD041	0.46	14.1	12.27	66.5	140	46.1	19.4
TD042	0.67	29.1	15.98	104	115	2.8	5.7
TD045	1.03	31.6	14.12	90.4	64	5.2	5.6
TD046	1.09	15.3	14.37	44.8	68	4.3	9.6
TD047	2.55	5.4	5.12	11.5	88	0.7	0.4
TD048	2.02	6.7	14.16	48	131	2	3.2
TD049	41.05	6.5	37.04	13.1	212	0.6	<0.2
TD050	0.56	5.1	14.56	108.3	54	1.4	9.2
TD051	1.33	77.3	8.92	176.2	123	2.6	10.2
TD053	0.53	12.1	8.74	74.5	99	3.3	9.4
TD054	0.65	16.8	34.07	47.4	92332	1.7	4.7
TD056	6.47	187.4	85.07	69.7	133248	2.8	4.1
TD057	17.87	33.5	462.81	604.6	135240	1	1.1
TD058	14.32	205.9	174.52	436	98704	3.4	7.3
TD059	17.7	7341.9	8727.17	>10000.0	>200000	1.7	5.9
TD060	489.09	84.8	1442.99	51	>200000	3	6.3
TD061	220.24	47.8	241.33	51	>200000	2	3.2
TD062	10.43	926.2	>10000.00	>10000.0	>200000	<0.1	0.7
TD063	3.36	7.6	201.58	450.7	55820	0.2	<0.2
TD066	1.01	24	31.3	401	16172	3.4	11.7
TD068	1.26	11.4	75.95	83	9573	0.5	<0.2
TD069	1.92	9.6	24.23	11.6	1735	1.3	3.8
TD070	0.5	5.3	28.13	46.1	4218	1.5	1.7
TD072	0.5	19.6	5.59	70.1	510	2.5	5.5
TD073	12.09	7075.1	>10000.00	>10000.0	>200000	1.8	1.1
TD074	20.23	142.7	365.11	693.2	>200000	2.8	5.2

	Mo	Cu	Pb	Zn	Ag	Ni	Co
method	**MA250**	**MA250**	**MA250**	**MA250**	**MA250**	**MA250**	**MA250**
range	**PPM**	**PPM**	**PPM**	**PPM**	**PPB**	**PPM**	**PPM**
detection limit	**0.05**	**0.1**	**0.02**	**0.2**	**20**	**0.1**	**0.2**
Sample#							
TD075	48.55	46.2	68.46	156.4	62468	1.9	4.9
TD076	0.73	4.8	23.99	4.7	1238	0.2	<0.2
TD077	1.45	19.2	8.04	5	609	1.9	10.1
TD083	28.99	246.2	33.82	83.3	1098	11.1	25.2
TD084	8.38	230.3	15.78	64.8	1524	3.8	11.2
TD086	66.33	207.8	171.51	222.9	3262	63.2	33.5
TD088	1.74	13.9	33.57	77.5	1218	2.5	7.7
TD090	17.8	371.8	784.23	840.7	4802	16.1	6
TD091	4.97	3310	>10000.00	8087.7	>200000	1.8	3.8
TD093	0.64	12.7	23.66	47.4	2755	1.2	1.5
TD097	0.66	7.8	92.93	9.8	4110	0.5	<0.2
TD098	3.28	3.2	238.27	1.1	178	0.2	<0.2
TD099	1.88	3.9	322.99	1.8	990	0.3	<0.2
TD101	0.48	4.1	94.87	0.9	252	0.3	<0.2
TD102	1.27	8	123.67	2.2	794	0.5	<0.2
TD103	0.91	3.8	555.6	4.7	3155	0.4	0.2
TD110	0.83	3.5	13.36	20.8	560	1	<0.2
TD111	1.38	10.5	11.9	70.1	870	1.2	2.9
TD112	6.55	5.1	27.4	17.6	827	1	0.5
TD114	1.12	11.7	6.66	<0.2	108	0.8	0.2
TD115	4.3	38.3	10.14	65.5	221	5.8	15.7
TD116	0.24	113.5	7.54	72.2	249	6.6	13.4
TD117	0.47	66.1	14.88	51.6	182	6.3	11.2
TD123	0.51	598.5	6.61	328	1288	7.1	13.2
TD124	1.27	804	16.21	267	5011	5.1	10.8

	Mn	Fe	As	U	Th	Sr	Cd
method	**MA250**	**MA250**	**MA250**	**MA250**	**MA250**	**MA250**	**MA250**
range	**PPM**	**%**	**PPM**	**PPM**	**PPM**	**PPM**	**PPM**
detection limit	**1**	**0.01**	**0.2**	**0.1**	**0.1**	**1**	**0.02**
Sample#							
TD001	649	4.27	7.2	2.2	4.9	306	0.15
TD002	548	2.2	4.3	1.3	3.1	123	0.34
TD003	529	0.7	4.3	0.3	0.5	29	0.07
TD006	738	2.7	13.4	1.4	2.7	122	0.43
TD007	1075	2.88	18.1	1.9	4.2	229	0.36
TD008	153	3.21	7.1	2	2.4	7	0.35
TD009	143	2.43	18	1.3	2.2	8	0.78
TD010	187	3	6.3	2	2.1	7	0.46
TD011	89	4.03	8.3	1.4	2.7	8	0.27
TD013	93	2.43	14.6	1.5	2.7	6	0.1
TD014	4463	6.84	39.2	0.3	0.8	384	1.21
TD016	243	6.49	26.7	0.5	0.5	40	0.44
TD023	2511	6.05	23.3	0.2	0.3	875	0.73
TD024	1040	3.2	13.4	0.2	0.3	271	0.71
TD026	49	0.76	0.7	0.8	3.7	18	0.08
TD027	2079	6.82	8.3	0.3	0.6	462	0.32
TD029	258	2.56	2	3.6	6.4	179	0.07
TD030	380	2.4	1.6	4.5	8.6	184	0.15
TD031	28	0.24	1.3	2	4.4	26	0.08
TD035	1520	4.2	7	2.3	4.6	397	0.27
TD037	1327	3.22	28.6	2	4.2	345	0.09
TD039	679	4.56	9.3	2.5	3.7	57	0.14
TD040	526	3.14	1.9	3.1	4.3	564	0.18
TD041	1139	6.44	11.7	0.8	1.5	420	0.07
TD042	1421	3.69	18.3	2.5	4.8	462	0.17
TD045	537	4.63	9.3	2.1	4.7	442	0.71
TD046	1194	4.79	36.1	2.6	4.3	326	0.39
TD047	81	1.42	4.7	1.8	2.4	50	0.09
TD048	451	3.45	19.4	1.7	3.1	270	0.03
TD049	86	0.89	3.5	1.3	2.8	7	0.17
TD050	1267	3.69	9.6	2.6	5.2	336	0.17
TD051	1157	5.26	5.8	1.6	5.2	310	1.23
TD053	998	3.66	2	2.9	5.5	538	0.27
TD054	1963	1.78	2.3	1.1	3.3	240	0.09
TD056	815	1.8	8.9	1.6	1.8	63	0.5
TD057	146	0.71	9.1	0.3	0.5	53	7.39
TD058	503	1.57	11.6	1.7	2.3	84	4.71
TD059	978	2.09	2.8	0.8	1.3	63	192.87
TD060	181	5.74	38.9	0.4	0.2	22	1.13
TD061	320	2.32	15.2	0.2	0.2	15	0.71
TD062	7049	0.53	1.8	<0.1	<0.1	393	1690.31
TD063	27	0.09	4.2	1.2	4.7	943	9.63
TD066	991	3.77	5.5	2.6	7.3	637	1.75
TD068	402	2.54	8.1	3.9	3.6	242	1.5
TD069	15	2.39	8.4	2.2	3.9	813	0.11
TD070	244	0.57	2.2	3.5	9.7	159	0.5
TD072	1218	3.85	4	2.5	4.2	255	0.19
TD073	539	1.98	9.6	0.3	0.3	55	250.15
TD074	847	1.88	30.8	1.5	2.2	122	7.39

	Mn	Fe	As	U	Th	Sr	Cd
method	**MA250**	**MA250**	**MA250**	**MA250**	**MA250**	**MA250**	**MA250**
range	**PPM**	**%**	**PPM**	**PPM**	**PPM**	**PPM**	**PPM**
detection limit	**1**	**0.01**	**0.2**	**0.1**	**0.1**	**1**	**0.02**
Sample#							
TD075	851	1.76	14.6	1.8	2.9	104	1.66
TD076	6	0.37	3.4	2.7	5.5	2433	<0.02
TD077	15	3.4	4.6	2.3	5.5	824	<0.02
TD083	1152	5.77	16.7	0.5	0.9	411	0.45
TD084	578	4.06	16.8	1	2.9	187	0.15
TD086	1075	6.46	93	0.7	0.4	255	3.58
TD088	1691	2.61	6.2	4.1	8.9	458	0.52
TD090	5916	6.82	30.4	6.5	1.3	185	8.85
TD091	661	1.53	<0.2	0.5	1	44	96.07
TD093	555	1.14	8.6	2.5	5.5	84	0.24
TD097	10	0.1	2.6	1.3	5.1	1937	0.09
TD098	3	0.13	1.2	1.1	5.6	1909	0.03
TD099	5	0.22	0.6	0.9	5.9	2488	<0.02
TD101	6	0.09	2.6	1.8	5.3	1643	<0.02
TD102	10	0.17	1.7	1.1	4	911	0.02
TD103	13	0.14	15.1	2.3	2.3	579	0.03
TD110	75	0.99	4.6	3.6	7	172	0.1
TD111	65	1.57	1.8	3.9	8.4	221	0.11
TD112	148	0.73	6.8	4.6	9.3	19	0.14
TD114	14	1.07	2.7	0.4	4.6	495	0.03
TD115	115	5.76	8.2	2.7	4.3	435	0.41
TD116	688	7.12	3.6	1.5	3.5	563	0.32
TD117	142	4.82	9.7	2	3.2	218	0.22
TD123	1090	13.11	3.7	0.6	6.7	224	0.06
TD124	2783	13.21	80.4	0.7	1.9	5	0.41

	Sb	Bi	V	Ca	P	La	Cr
method	**MA250**	**MA250**	**MA250**	**MA250**	**MA250**	**MA250**	**MA250**
range	**PPM**	**PPM**	**PPM**	**%**	**%**	**PPM**	**PPM**
detection limit	**0.02**	**0.04**	**1**	**0.01**	**0.001**	**0.1**	**1**
Sample#							
TD001	1.07	0.05	139	0.68	0.109	16.5	16
TD002	3.46	<0.04	106	0.61	0.054	11	12
TD003	8.34	<0.04	38	1.11	0.01	1.9	12
TD006	1.83	0.78	62	0.29	0.08	6.5	8
TD007	2.49	0.61	68	0.64	0.091	22.1	11
TD008	1.66	0.6	70	0.06	0.058	4.1	7
TD009	2.34	0.68	46	0.03	0.014	4.5	17
TD010	2.06	0.54	67	0.06	0.054	3.3	7
TD011	1.12	0.38	73	0.07	0.087	2.5	6
TD013	1.54	0.39	70	0.08	0.058	4	11
TD014	5.01	0.14	323	4.26	0.128	9.8	76
TD016	1.59	0.8	213	0.21	0.052	1.9	100
TD023	2.26	0.24	226	2.67	0.055	4.4	8
TD024	1.04	0.32	123	9.45	0.043	6.1	3
TD026	0.41	0.04	81	0.03	0.04	8.3	5
TD027	0.89	0.22	314	5.6	0.14	11.9	20
TD029	0.44	<0.04	83	0.27	0.059	11	4
TD030	0.34	0.15	83	0.59	0.056	15.7	3
TD031	0.75	0.27	107	0.03	0.016	15.3	2
TD035	2.53	<0.04	142	2.9	0.108	19.1	8
TD037	9.56	<0.04	116	3.16	0.086	14.3	6
TD039	1.02	0.09	121	0.11	0.075	11	20
TD040	0.57	0.06	94	2.72	0.092	15.3	4
TD041	1.34	0.92	209	2.31	0.028	8.7	170
TD042	3.8	0.22	122	2.71	0.065	16.1	7
TD045	1.94	0.15	243	1.06	0.171	19.9	25
TD046	1.92	0.65	117	0.95	0.09	13.9	9
TD047	0.4	0.24	60	0.04	0.007	6.4	3
TD048	0.86	0.19	110	0.2	0.021	7	8
TD049	1.29	0.76	127	0.02	0.083	5.9	9
TD050	3.68	0.1	68	1.75	0.116	17.4	2
TD051	1.19	0.12	121	1.75	0.082	14.5	4
TD053	0.54	0.13	111	2.74	0.084	15.7	4
TD054	3.64	0.13	31	5.37	0.05	10.2	3
TD056	10.85	0.08	32	0.41	0.018	5.9	6
TD057	7.96	<0.04	6	0.2	0.006	2.8	2
TD058	8.11	0.08	33	0.14	0.024	9.8	5
TD059	11.72	0.06	21	3.98	0.022	3.9	4
TD060	26.92	0.06	31	0.24	0.002	0.7	3
TD061	13.68	<0.04	23	0.44	0.001	1.9	3
TD062	3.91	<0.04	5	30.54	<0.001	2.8	<1
TD063	1.45	1.72	199	0.14	0.22	12	2
TD066	0.49	0.09	91	1.26	0.066	17.1	6
TD068	0.61	0.46	117	0.21	0.048	11.2	3
TD069	4.1	0.19	91	0.13	0.097	8.9	3
TD070	1.12	0.06	20	0.07	0.008	14.1	3
TD072	0.69	<0.04	150	0.58	0.078	10.7	4
TD073	8.75	0.04	5	3.36	0.004	2	3
TD074	7.76	0.07	36	0.57	0.035	6.5	5

	Sb	Bi	V	Ca	P	La	Cr
method	**MA250**	**MA250**	**MA250**	**MA250**	**MA250**	**MA250**	**MA250**
range	**PPM**	**PPM**	**PPM**	**%**	**%**	**PPM**	**PPM**
detection limit	**0.02**	**0.04**	**1**	**0.01**	**0.001**	**0.1**	**1**
Sample#							
TD075	4.06	<0.04	41	1.44	0.034	7.1	3
TD076	1.24	0.38	186	0.14	0.181	14.6	2
TD077	0.96	<0.04	131	0.11	0.143	15.7	3
TD083	3.57	0.57	272	2.61	0.115	7.9	11
TD084	1.56	0.19	84	1.35	0.06	8.6	7
TD086	8.27	0.11	162	2.88	0.046	7.2	84
TD088	2.7	0.11	103	3.32	0.073	15.8	6
TD090	11.29	7.48	199	2.21	0.093	9	15
TD091	8.78	0.29	23	0.14	0.014	8.9	3
TD093	1.47	<0.04	25	0.3	0.018	9.9	2
TD097	3.69	<0.04	70	0.06	0.093	23.9	3
TD098	4.04	0.06	158	0.05	0.095	16.9	2
TD099	2.28	0.37	100	0.07	0.143	45.6	1
TD101	7.97	0.12	81	0.05	0.086	17.6	1
TD102	8.4	1.28	80	0.03	0.05	12.2	1
TD103	43.79	1.47	139	0.04	0.074	4.6	3
TD110	0.71	<0.04	39	0.06	0.009	6.2	3
TD111	0.89	0.06	61	0.09	0.032	12.4	3
TD112	0.85	0.15	21	0.03	0.012	6.4	3
TD114	0.47	0.25	85	0.24	0.141	16.1	10
TD115	1.07	0.08	207	1.41	0.101	9.8	6
TD116	0.57	<0.04	194	1.04	0.127	8.9	9
TD117	0.73	<0.04	253	0.45	0.107	10.4	13
TD123	0.18	0.17	212	0.62	0.05	4	4
TD124	0.77	1.81	123	0.09	0.038	0.6	3

	Mg	Ba	Ti	Al	Na	K	W
method	**MA250**	**MA250**	**MA250**	**MA250**	**MA250**	**MA250**	**MA250**
range	**%**	**PPM**	**%**	**%**	**%**	**%**	**PPM**
detection limit	**0.01**	**1**	**0.001**	**0.01**	**0.001**	**0.01**	**0.1**
Sample#							
TD001	1.42	1917	0.417	7.52	3.612	4.36	0.7
TD002	0.64	1047	0.196	4.91	0.585	5.04	1.6
TD003	0.29	186	0.034	0.91	0.063	0.67	0.3
TD006	0.94	78	0.209	6.89	0.725	5.65	1.4
TD007	1.11	486	0.3	7.45	1.068	4.93	2.6
TD008	0.9	33	0.127	6.85	0.128	4.25	0.6
TD009	0.49	24	0.064	4.33	0.077	2.31	0.2
TD010	0.95	43	0.111	6.66	0.119	4.09	0.5
TD011	0.57	27	0.109	7.23	0.137	4.28	0.6
TD013	0.57	47	0.095	5.99	0.112	3.67	0.9
TD014	4.1	845	0.834	7.31	1.557	2.64	0.5
TD016	1.23	13	0.093	5.18	0.838	3.21	0.5
TD023	2.09	56	0.654	5.58	1.776	0.72	2.1
TD024	0.8	54	0.372	8.2	0.051	0.38	2.3
TD026	0.17	730	0.119	6.19	0.145	3.3	0.5
TD027	2.93	271	0.942	9.38	3.107	0.8	0.2
TD029	1.14	96	0.281	6.32	3.19	3.2	0.8
TD030	0.99	177	0.255	6.9	2.766	3.53	0.4
TD031	0.23	159	0.243	7.56	0.196	3.8	1
TD035	1.73	1210	0.452	8.14	3.454	2.77	0.4
TD037	1.26	849	0.361	7.15	2.917	1.52	0.8
TD039	1.3	108	0.235	6.34	1.399	2.41	0.7
TD040	0.97	1620	0.308	7.78	3.359	3.31	0.6
TD041	4.28	247	0.387	7.46	3.237	1.57	0.2
TD042	1.14	1217	0.417	8.24	3.195	2.24	0.6
TD045	2.33	1561	0.586	9.14	4.232	3.29	0.4
TD046	1.41	40	0.268	8.03	2.836	2.68	0.6
TD047	0.57	1089	0.07	6.41	1.528	2.99	0.2
TD048	1.56	427	0.225	6.96	3.56	1.51	0.4
TD049	0.42	428	0.136	6.91	0.089	3.88	0.9
TD050	1	1454	0.365	7.77	4.222	3.12	0.7
TD051	0.88	1575	0.246	7	2.472	3.4	0.6
TD053	1.16	1276	0.298	7.83	2.941	3.05	0.4
TD054	0.46	167	0.198	6.68	0.993	6.4	1.1
TD056	0.48	63	0.175	2.86	0.053	2.69	3
TD057	0.06	120	0.023	1.11	0.028	1.16	0.8
TD058	0.28	90	0.188	4.37	0.082	5.07	5.7
TD059	0.26	128	0.08	2.32	0.037	2.2	2.6
TD060	0.12	22	0.038	1.58	0.022	1.39	3.2
TD061	0.19	28	0.012	0.89	0.012	0.47	0.7
TD062	0.24	8	<0.001	0.21	0.002	0.02	<0.1
TD063	<0.01	168	0.455	5.83	0.207	0.81	1.1
TD066	0.83	1591	0.269	7.8	2.627	3.46	0.6
TD068	0.87	893	0.286	7.31	1.703	3.24	0.4
TD069	<0.01	22	0.081	5.22	0.852	1.14	1.2
TD070	0.06	1841	0.127	5.78	0.171	8.14	1
TD072	1.24	1213	0.348	7.07	2.722	2.85	0.8
TD073	0.3	51	0.019	0.59	0.02	0.36	0.1
TD074	0.49	75	0.172	3.39	0.079	4.2	0.4

	Mg	Ba	Ti	Al	Na	K	W
method	**MA250**	**MA250**	**MA250**	**MA250**	**MA250**	**MA250**	**MA250**
range	**%**	**PPM**	**%**	**%**	**%**	**%**	**PPM**
detection limit	**0.01**	**1**	**0.001**	**0.01**	**0.001**	**0.01**	**0.1**
Sample#							
TD075	0.7	186	0.154	3.38	0.073	4.12	0.5
TD076	<0.01	2036	0.433	10.65	0.017	0.04	1.1
TD077	<0.01	103	0.418	8.43	0.021	0.03	0.7
TD083	2.06	64	0.853	8.86	3.423	1.95	2.2
TD084	0.82	40	0.248	5.66	2.064	2.4	0.7
TD086	1.69	13	0.293	3.12	0.014	0.01	0.4
TD088	0.93	2678	0.262	7.42	2.028	4.99	0.6
TD090	0.91	69	0.19	2.56	0.008	0.03	20.9
TD091	0.53	187	0.044	1.98	0.056	1.62	0.9
TD093	0.25	1696	0.089	4.8	0.562	4.53	0.4
TD097	<0.01	3186	0.145	4.15	0.006	0.02	8.5
TD098	<0.01	58	0.173	10	0.015	0.01	12.5
TD099	<0.01	329	0.079	7.14	0.022	0.03	5.4
TD101	<0.01	348	0.265	5.37	0.009	0.02	6.6
TD102	<0.01	820	0.123	4.81	0.009	0.05	10
TD103	<0.01	21	0.174	6.4	0.238	3.14	2.7
TD110	0.28	2382	0.203	6.83	1.755	4.56	0.5
TD111	0.17	2430	0.255	7.96	2.843	3.93	1.3
TD112	0.22	902	0.135	5.97	0.048	3.42	1.1
TD114	<0.01	623	0.466	5.71	0.069	0.09	0.8
TD115	0.44	30	0.559	11.61	2.997	1.59	0.6
TD116	1.31	137	0.632	8.84	2.357	1.78	0.5
TD117	0.67	56	0.689	8.27	1.182	3.17	0.9
TD123	0.64	1394	0.298	5.9	1.643	3.63	0.3
TD124	1.29	28	0.187	4.92	0.028	2.13	0.8

	Zr	Sn	Be	Sc	S	Y	Ce
method	**MA250**	**MA250**	**MA250**	**MA250**	**MA250**	**MA250**	**MA250**
range	**PPM**	**PPM**	**PPM**	**PPM**	**%**	**PPM**	**PPM**
detection limit	**0.2**	**0.1**	**1**	**0.1**	**0.04**	**0.1**	**0.02**
Sample#							
TD001	34	1	<1	10.3	<0.04	17	29.07
TD002	16.1	0.5	<1	5.6	<0.04	15.1	22.72
TD003	3	0.2	<1	1.3	<0.04	2.6	3.82
TD006	39.6	1	<1	6.6	1.43	9.3	18.36
TD007	43	1.2	<1	7.4	0.46	15.6	45.13
TD008	54.3	2.1	<1	7.9	3.28	9.8	11.44
TD009	34.7	2	<1	5.3	2.54	8.7	11.77
TD010	52.2	1.9	<1	7.9	3.01	8.9	9.09
TD011	53	2.2	<1	8.7	4.24	8.2	6.85
TD013	39.1	3.3	<1	6.3	2.52	10.7	11.04
TD014	24.1	2	1	29.8	1.34	26.6	23.93
TD016	28.6	2.1	<1	22	7.18	8	5.95
TD023	9.4	2.3	<1	20.2	2.88	11	9.39
TD024	8.4	2.1	<1	12.2	2.73	11.2	12.51
TD026	40.8	5.3	<1	4.4	0.1	3.9	15.35
TD027	30.2	1	<1	26.7	2.84	27.1	26.53
TD029	67.7	1.2	<1	7.6	1.29	11.9	21.63
TD030	63.7	0.8	<1	7.1	0.93	13.8	28.06
TD031	73.5	1.6	<1	8.8	<0.04	6.8	26.65
TD035	52.6	1	1	14.8	<0.04	17.8	36.35
TD037	43.7	0.9	1	10.1	0.14	16.5	30.11
TD039	53.9	1	<1	10.4	1.09	10.6	22.34
TD040	16.7	1.1	1	10	<0.04	15.1	29.29
TD041	59.6	1.7	1	28.2	2.98	10.9	18.18
TD042	97.2	1.3	<1	13.3	0.88	23.2	32.98
TD045	94.7	2.9	1	27.9	0.09	19.4	40.04
TD046	98.7	1	<1	12.8	3.81	21.1	32.94
TD047	80.8	1.2	<1	7	0.16	4.8	13.65
TD048	85.2	0.8	<1	11.1	0.75	8.8	15.53
TD049	65.6	3.5	<1	16.3	0.09	4.9	12.28
TD050	58.8	1	<1	8.1	<0.04	18.8	34.24
TD051	53.5	0.9	<1	9.2	<0.04	13.6	29.2
TD053	42.4	1.1	2	9.9	<0.04	16.1	31.37
TD054	22.4	0.8	<1	4.3	1.13	9.3	21.08
TD056	33.8	0.5	<1	5.3	1.16	9.5	12.25
TD057	3.4	0.2	<1	0.7	0.53	1.2	5.07
TD058	48	0.7	<1	6.1	0.92	12.1	20.55
TD059	13.7	0.6	<1	2.3	2.6	8.1	8.08
TD060	8.8	0.3	<1	2.4	5.96	2.2	2.07
TD061	2.8	0.4	<1	1.3	2.17	2.5	3.48
TD062	<0.2	0.1	<1	<0.1	4.55	6.4	3.8
TD063	31.6	1.4	<1	3.7	1.77	3.9	27.12
TD066	67.3	1	<1	9.3	<0.04	15.6	32.43
TD068	77	2.2	<1	11.6	0.69	5.1	22.65
TD069	58.1	0.5	<1	6	6.39	4.2	20.94
TD070	96.4	0.8	<1	1.4	<0.04	9.6	23.48
TD072	63.4	0.6	<1	11.8	0.56	12.5	20.72
TD073	3	0.2	<1	0.6	3.72	1.5	3.26
TD074	25.6	0.5	<1	5	1.57	7.8	13.06

	Zr	Sn	Be	Sc	S	Y	Ce
method	**MA250**	**MA250**	**MA250**	**MA250**	**MA250**	**MA250**	**MA250**
range	**PPM**	**PPM**	**PPM**	**PPM**	**%**	**PPM**	**PPM**
detection limit	**0.2**	**0.1**	**1**	**0.1**	**0.04**	**0.1**	**0.02**
Sample#							
TD075	37.3	0.6	<1	4.3	1.34	7.7	13.89
TD076	63.6	1.4	<1	8.5	0.26	3.9	29.72
TD077	63.9	0.5	<1	12.4	3.72	6.4	32.26
TD083	31.6	2.1	<1	20.6	4.16	20.3	19.08
TD084	50.4	1.2	<1	7.3	2.18	11.5	19.16
TD086	17.9	0.5	<1	16.7	4.15	25.3	16.19
TD088	29.2	0.7	<1	10.3	0.08	12.6	28.3
TD090	38.2	0.8	<1	7.2	1.28	18.3	15.49
TD091	7.3	0.3	<1	1.4	1.15	2.7	12.39
TD093	96	0.7	1	1.6	0.08	7.9	21.39
TD097	46.8	0.2	<1	2.1	0.18	0.8	30.36
TD098	32.8	0.4	<1	2.7	0.13	0.6	24.27
TD099	18.7	0.1	<1	3.6	0.27	0.5	77.58
TD101	56.8	0.7	<1	5.6	0.13	2.2	28.26
TD102	37.6	0.6	<1	2.9	0.1	1	18.82
TD103	55.4	0.7	<1	10.5	5.61	2.9	11.03
TD110	137.9	1	<1	4	0.13	7.6	10.17
TD111	151.8	1.2	<1	4.1	0.33	10.4	24.69
TD112	148.2	0.9	<1	2.4	0.06	9.4	12.31
TD114	26.2	1.4	<1	3.5	0.07	2.2	35.77
TD115	118.8	1.1	<1	16.4	4.91	28.3	23.85
TD116	87.9	1	<1	20.7	2.35	16.7	21.68
TD117	100.7	2.5	1	27	2.24	14.2	23.8
TD123	21.3	1.9	<1	7.8	0.06	8.4	8.24
TD124	15.4	1.5	<1	5.4	9.46	3.8	1.81

	Pr	Nd	Sm	Eu	Gd	Tb	Dy
method	**MA250**	**MA250**	**MA250**	**MA250**	**MA250**	**MA250**	**MA250**
range	**PPM**	**PPM**	**PPM**	**PPM**	**PPM**	**PPM**	**PPM**
detection limit	**0.1**	**0.1**	**0.1**	**0.1**	**0.1**	**0.1**	**0.1**
Sample#							
TD001	3.9	15.7	3.2	0.9	3.2	0.4	3.3
TD002	2.7	10.6	2.5	1	2.6	0.3	2.2
TD003	0.4	1.8	0.4	0.1	0.4	<0.1	0.4
TD006	2.5	10.5	2.2	0.7	1.9	0.2	1.8
TD007	5.5	21.3	4.4	1.6	3.3	0.5	3.2
TD008	1.6	7.2	1.7	0.5	1.6	0.3	2.1
TD009	1.5	6.8	1.2	0.4	1.2	0.2	1.5
TD010	1.2	5.8	1.5	0.5	1.5	0.2	2.1
TD011	1	4.5	1.2	0.4	1.1	0.2	1.4
TD013	1.5	6.3	1.6	0.5	1.6	0.2	2
TD014	3.3	15.8	4.4	1.3	5.2	0.8	5
TD016	0.9	4.4	1.2	0.3	1.4	0.2	1.5
TD023	1.3	6.8	1.8	0.8	2.2	0.3	2.1
TD024	1.8	8.3	2.2	0.8	2.2	0.3	2
TD026	1.7	6.7	1.2	0.3	0.9	<0.1	0.8
TD027	3.9	18	4.5	1.8	5.3	0.8	5.4
TD029	2.5	9.8	2.2	0.7	2	0.3	2.2
TD030	3.5	12.3	2.3	0.7	2.2	0.3	2.4
TD031	2.9	11	1.8	0.3	0.9	0.1	1.1
TD035	4.7	18.4	3.7	1.3	3.7	0.5	3.1
TD037	3.9	15.9	3.1	1.1	3.1	0.4	2.9
TD039	2.8	11.5	2.6	0.9	2	0.3	2.3
TD040	3.5	13.4	2.7	0.9	2.8	0.4	2.5
TD041	2.3	9.6	2.1	0.6	2.2	0.3	1.9
TD042	4.4	18	4.1	1.2	4.1	0.6	4.3
TD045	5	19.9	4.6	1.3	4.2	0.6	3.9
TD046	4.5	19.1	4.6	1.2	4.2	0.6	3.7
TD047	1.7	6.4	1.3	0.3	1	<0.1	1
TD048	1.8	7.7	1.8	0.4	1.5	0.2	1.7
TD049	1.6	6.3	1.3	0.3	1.2	0.1	1
TD050	4.1	16.9	3.3	1.1	3.3	0.5	3.2
TD051	3.5	14.3	2.4	0.6	2.8	0.4	1.9
TD053	3.2	12.8	3.3	0.9	3.6	0.5	3.4
TD054	2.5	10.2	2.1	0.7	1.7	0.2	1.8
TD056	1.6	6.7	1.6	0.4	1.6	0.2	1.6
TD057	0.6	2.5	0.4	0.2	0.3	<0.1	0.2
TD058	2.6	11.2	2.3	0.7	2.2	0.3	2.3
TD059	0.9	4.2	1.1	0.4	1.1	0.1	1.1
TD060	0.2	1.2	0.4	0.1	0.2	<0.1	0.3
TD061	0.3	1.7	0.4	<0.1	0.3	<0.1	0.4
TD062	0.5	1.8	0.6	0.3	0.7	<0.1	0.7
TD063	3.6	14.7	2.5	0.7	2.6	0.3	1.4
TD066	3.8	13.2	3.2	0.8	2.9	0.4	2.7
TD068	2.7	10.1	1.8	0.4	1.3	0.1	1.1
TD069	2.8	10.4	2.5	0.7	1.4	0.1	0.8
TD070	3.2	9	2.6	0.4	1.8	0.3	2.3
TD072	2.4	9.3	1.8	0.6	2.6	0.3	2.7
TD073	0.3	1.5	0.4	0.1	0.3	<0.1	0.3
TD074	1.6	6.3	1.4	0.4	1.4	0.2	1.4

	Pr	Nd	Sm	Eu	Gd	Tb	Dy
method	**MA250**	**MA250**	**MA250**	**MA250**	**MA250**	**MA250**	**MA250**
range	**PPM**	**PPM**	**PPM**	**PPM**	**PPM**	**PPM**	**PPM**
detection limit	**0.1**	**0.1**	**0.1**	**0.1**	**0.1**	**0.1**	**0.1**
Sample#							
TD075	1.6	6.9	1.4	0.4	1.3	0.1	1.3
TD076	3.5	15.3	3.3	0.6	1.7	0.1	0.9
TD077	3.9	16.8	3.2	0.8	2.3	0.2	1.4
TD083	2.8	12.1	3.3	1.5	3.7	0.6	4.2
TD084	2.5	10.5	2.3	0.8	1.8	0.3	2.1
TD086	2.4	11.1	3.4	1	4.3	0.7	4.8
TD088	3.3	12.1	2	0.5	4.5	0.3	2.2
TD090	2.3	9.6	2.5	1	2.4	0.4	2.8
TD091	1.4	4.6	0.8	0.2	0.4	<0.1	0.5
TD093	2.3	7.7	1.2	0.2	2.1	0.2	1.4
TD097	2.5	6.9	0.3	<0.1	0.6	<0.1	<0.1
TD098	2	5.1	0.6	0.1	0.2	<0.1	0.1
TD099	7.9	20.3	1.8	0.4	0.7	<0.1	0.2
TD101	2.8	8.6	1.2	0.3	0.5	<0.1	0.4
TD102	1.8	5	0.5	<0.1	0.1	<0.1	0.2
TD103	1.5	6	1.1	0.3	0.9	<0.1	0.6
TD110	0.9	3.4	0.8	<0.1	1.1	0.1	1.4
TD111	2.8	10.1	1.6	<0.1	1.2	0.2	1.7
TD112	1.2	4.3	1	0.1	1	0.2	1.6
TD114	4.6	20.7	4.2	0.8	2.8	0.3	0.9
TD115	3.3	14.7	4.3	1.2	4.6	0.8	5.9
TD116	2.8	13.6	3.4	1.3	3.4	0.4	3.7
TD117	2.8	11.8	2.7	1	2.2	0.4	3
TD123	1	5.5	1.4	0.4	2	0.2	1.7
TD124	0.2	1.2	0.4	0.1	0.4	<0.1	0.7

	Ho	Er	Tm	Yb	Lu	Hf	Li
method	**MA250**	**MA250**	**MA250**	**MA250**	**MA250**	**MA250**	**MA250**
range	**PPM**	**PPM**	**PPM**	**PPM**	**PPM**	**PPM**	**PPM**
detection limit	**0.1**	**0.1**	**0.1**	**0.1**	**0.1**	**0.02**	**0.1**
Sample#							
TD001	0.6	1.8	0.3	1.8	0.3	1.18	19.5
TD002	0.5	1.4	0.2	1.5	0.2	0.66	29
TD003	<0.1	0.3	<0.1	0.2	<0.1	0.1	45.7
TD006	0.4	1.2	0.2	1.3	0.2	1.36	13.5
TD007	0.6	1.7	0.3	1.8	0.3	1.4	15
TD008	0.5	1.4	0.2	1.4	0.3	1.56	23.5
TD009	0.3	1.1	0.1	1	0.2	1.04	26.3
TD010	0.4	1.3	0.2	1.5	0.2	1.58	24.6
TD011	0.3	1.3	0.2	1.5	0.2	1.54	11.5
TD013	0.4	1.4	0.2	1.3	0.2	1.25	21.9
TD014	1	3	0.4	2.4	0.3	0.85	36.7
TD016	0.3	1.1	0.1	0.9	0.1	0.7	55.8
TD023	0.4	1.1	0.2	1.1	0.1	0.38	25.3
TD024	0.4	1.1	0.1	0.7	0.1	0.23	10.7
TD026	0.2	0.5	<0.1	0.5	<0.1	1.23	13.5
TD027	1	2.7	0.4	2.2	0.3	0.87	11.7
TD029	0.5	1.5	0.3	1.7	0.3	2.05	17.7
TD030	0.5	1.6	0.3	1.7	0.3	2.11	13.7
TD031	0.3	0.9	0.2	1.2	0.2	2.3	3.8
TD035	0.6	2	0.3	1.8	0.3	1.66	17.3
TD037	0.6	1.9	0.3	1.8	0.3	1.56	17.2
TD039	0.5	1.4	0.2	1.4	0.2	1.58	26.8
TD040	0.5	1.6	0.3	1.9	0.2	0.81	2.8
TD041	0.4	1.2	0.2	1.2	0.2	1.66	17
TD042	0.9	2.6	0.4	2.6	0.4	2.63	11.6
TD045	0.8	2.6	0.4	2.7	0.4	2.57	43.3
TD046	0.8	2.4	0.4	2.3	0.4	2.64	24.4
TD047	0.2	0.7	0.1	0.8	0.1	2.17	12.7
TD048	0.4	1.4	0.2	1.6	0.3	2.32	32.7
TD049	0.2	0.8	<0.1	0.8	0.2	1.65	24.9
TD050	0.7	2.1	0.3	2.2	0.3	2.01	11.7
TD051	0.4	1.8	0.2	1.6	0.2	1.71	9.5
TD053	0.7	2.1	0.3	2.1	0.3	1.49	17.1
TD054	0.4	1.1	0.2	1.1	0.2	0.83	9
TD056	0.3	1.2	0.2	1.2	0.2	1.01	43.7
TD057	<0.1	0.1	<0.1	0.1	<0.1	0.14	113.2
TD058	0.4	1.4	0.2	1.4	0.2	1.5	33.9
TD059	0.2	0.7	<0.1	0.7	<0.1	0.47	60.1
TD060	<0.1	0.3	<0.1	0.3	<0.1	0.26	46.1
TD061	<0.1	0.2	<0.1	0.2	<0.1	0.09	63.5
TD062	0.1	0.3	<0.1	0.2	<0.1	<0.02	2.5
TD063	0.2	0.6	0.1	0.7	<0.1	0.94	0.7
TD066	0.6	2	0.3	2.1	0.3	2.29	15.2
TD068	0.2	0.7	0.1	0.8	0.2	2.34	7.5
TD069	0.2	0.6	<0.1	0.8	<0.1	1.68	1.7
TD070	0.5	1.4	0.3	1.8	0.4	2.84	8.8
TD072	0.4	1.6	0.2	1.8	0.3	2.15	38.3
TD073	<0.1	0.2	<0.1	0.2	<0.1	0.12	40.3
TD074	0.3	0.9	0.1	0.8	0.1	0.76	34.8

	Ho	Er	Tm	Yb	Lu	Hf	Li
method	**MA250**	**MA250**	**MA250**	**MA250**	**MA250**	**MA250**	**MA250**
range	**PPM**	**PPM**	**PPM**	**PPM**	**PPM**	**PPM**	**PPM**
detection limit	**0.1**	**0.1**	**0.1**	**0.1**	**0.1**	**0.02**	**0.1**
Sample#							
TD075	0.3	0.9	0.1	0.9	0.1	1.01	27.5
TD076	0.2	0.8	0.1	1	0.2	1.99	78
TD077	0.3	1	0.2	1.1	0.2	1.65	19.5
TD083	0.9	2.4	0.3	1.9	0.3	0.95	37.5
TD084	0.4	1.3	0.2	1.4	0.2	1.44	11.7
TD086	1	2.8	0.3	2.1	0.3	0.57	78.8
TD088	0.5	1.4	0.2	1.9	0.3	1.37	8.4
TD090	0.6	1.9	0.3	1.8	0.3	1.07	19
TD091	<0.1	0.3	<0.1	0.3	<0.1	0.22	42.3
TD093	0.3	0.9	0.2	1.1	0.2	2.65	12.8
TD097	<0.1	0.1	<0.1	0.2	<0.1	1.59	45
TD098	<0.1	0.1	<0.1	0.2	<0.1	0.97	87.2
TD099	<0.1	<0.1	<0.1	0.1	<0.1	0.57	36.6
TD101	<0.1	0.4	<0.1	0.6	0.1	1.78	72.8
TD102	<0.1	0.1	<0.1	0.3	<0.1	1.3	54.8
TD103	0.1	0.4	<0.1	0.6	0.1	1.88	3.4
TD110	0.3	0.9	0.2	1.5	0.2	3.53	2.4
TD111	0.4	1.3	0.2	1.7	0.3	4.08	1.7
TD112	0.4	1.3	0.2	1.8	0.3	3.9	4.7
TD114	<0.1	0.2	<0.1	0.2	<0.1	0.68	11.4
TD115	1.1	3.5	0.5	3.3	0.6	3.29	9.9
TD116	0.7	1.9	0.3	2	0.3	2.56	18.5
TD117	0.7	2	0.3	2.2	0.3	2.83	8
TD123	0.3	1.1	0.1	1	0.1	0.7	2.9
TD124	0.2	0.7	<0.1	0.7	<0.1	0.6	7.5

	Rb	Ta	Nb	Cs	Ga	In	Re
method	**MA250**	**MA250**	**MA250**	**MA250**	**MA250**	**MA250**	**MA250**
range	**PPM**	**PPM**	**PPM**	**PPM**	**PPM**	**PPM**	**PPM**
detection limit	**0.1**	**0.1**	**0.04**	**0.1**	**0.02**	**0.01**	**0.002**
Sample#							
TD001	118.8	0.4	6.06	4.7	15.9	0.06	<0.002
TD002	172.6	0.3	3.37	2.5	9.6	0.03	<0.002
TD003	23.1	<0.1	0.5	1.2	4.19	<0.01	<0.002
TD006	150.8	0.2	3.42	8.5	15.19	0.21	<0.002
TD007	144.7	0.3	4.97	8.7	16.3	0.34	<0.002
TD008	130.4	0.1	1.65	3.7	16.98	0.07	0.444
TD009	88.7	<0.1	0.76	1.9	10.09	0.07	0.004
TD010	120.6	<0.1	1.2	4	16.8	0.06	1.881
TD011	123.8	<0.1	1.19	2.5	14.98	0.06	0.003
TD013	120.5	<0.1	1.23	2	13.65	0.06	0.003
TD014	51.2	0.4	5.96	7.2	16.09	0.3	0.002
TD016	110.6	<0.1	0.52	3.8	12.9	0.02	0.05
TD023	26.3	0.1	3.07	3.1	13.19	0.2	0.016
TD024	13.1	<0.1	1.61	10.9	13.89	0.04	0.042
TD026	101.2	0.1	1.51	1.5	9.07	0.04	<0.002
TD027	25.6	0.4	6.4	3.5	21.95	0.12	0.002
TD029	77.3	0.3	3.71	1.9	14.64	0.02	0.041
TD030	94.6	0.4	4.87	2.9	14.97	0.06	0.016
TD031	85.7	0.2	3.21	2.1	10.05	0.02	<0.002
TD035	77.1	0.4	5.43	1.1	16.45	0.05	<0.002
TD037	37.5	0.4	5.45	1	17.21	0.07	<0.002
TD039	87.2	0.2	2.87	3	15.22	0.06	<0.002
TD040	69.6	0.4	5.73	2	16.69	0.03	<0.002
TD041	49.7	0.2	2.64	4.5	19.64	0.2	<0.002
TD042	44.8	0.3	4.39	1.7	17.43	0.09	<0.002
TD045	82.4	0.5	8.52	6.8	18.8	0.1	0.004
TD046	50	0.2	2.67	5	18.99	0.07	<0.002
TD047	98.1	<0.1	0.63	3.1	14.81	0.1	0.006
TD048	53	0.1	1.63	5.3	17.26	0.04	0.004
TD049	120.6	0.1	1.61	4.3	10.07	0.09	0.018
TD050	67	0.4	6.71	0.4	16.01	0.05	<0.002
TD051	71.6	0.4	4.11	1.7	12.78	0.06	0.005
TD053	68.8	0.5	5.83	1.8	16.78	0.02	0.005
TD054	182.8	0.3	4.35	2.7	10.82	0.03	<0.002
TD056	91.9	0.2	2.49	2.3	5.16	0.02	<0.002
TD057	37.9	<0.1	0.58	1	1.47	0.01	<0.002
TD058	157.5	0.2	2.89	2.7	7.15	0.03	0.004
TD059	79.4	0.1	1.63	2.2	4.66	0.09	0.005
TD060	49.9	<0.1	0.67	1.2	3.33	<0.01	0.043
TD061	20.3	<0.1	0.19	0.8	2.3	<0.01	0.013
TD062	0.9	<0.1	<0.04	<0.1	1.84	0.01	0.005
TD063	0.5	0.6	8.52	<0.1	18.55	<0.01	0.008
TD066	73.1	0.5	5.61	1.6	16.12	0.05	0.007
TD068	100.3	0.4	4.6	4.7	19.18	0.81	0.003
TD069	1.5	0.1	1.19	<0.1	5.75	<0.01	<0.002
TD070	170.1	0.6	5.4	4.5	7.36	0.03	0.013
TD072	64	0.4	4.93	1.8	15.03	0.05	0.006
TD073	11	<0.1	0.29	0.2	0.98	0.03	0.005
TD074	113.1	0.2	2.16	0.7	5.94	0.04	0.004

	Rb	Ta	Nb	Cs	Ga	In	Re
method	**MA250**	**MA250**	**MA250**	**MA250**	**MA250**	**MA250**	**MA250**
range	**PPM**	**PPM**	**PPM**	**PPM**	**PPM**	**PPM**	**PPM**
detection limit	**0.1**	**0.1**	**0.04**	**0.1**	**0.02**	**0.01**	**0.002**
Sample#							
TD075	120	0.2	2.43	0.7	5.35	0.01	0.01
TD076	0.2	0.4	6.31	<0.1	34.2	0.02	0.004
TD077	0.4	0.4	5.54	<0.1	19.26	0.02	0.007
TD083	71	0.4	6.38	2.2	18.65	0.1	0.033
TD084	52.5	0.2	2.7	1.5	12.33	0.06	0.006
TD086	0.5	<0.1	1.53	0.1	9.6	0.04	0.054
TD088	118.9	0.7	6.49	2.5	13.94	<0.01	0.006
TD090	1.4	0.1	1.83	0.1	8.74	0.44	0.008
TD091	54.1	<0.1	0.94	1.8	5.16	0.07	<0.002
TD093	132.8	0.3	3.87	1.2	9.36	0.01	<0.002
TD097	0.5	0.2	2.07	<0.1	7.57	<0.01	0.011
TD098	0.2	0.2	2.19	<0.1	43.4	<0.01	<0.002
TD099	0.2	<0.1	0.98	<0.1	9.55	<0.01	<0.002
TD101	0.3	0.3	3.39	<0.1	14.45	<0.01	<0.002
TD102	0.9	0.2	1.85	<0.1	16.32	<0.01	<0.002
TD103	1.2	0.2	2.51	<0.1	32.47	0.19	<0.002
TD110	115.1	0.4	5.75	1.1	15.05	0.01	0.008
TD111	109.6	0.5	7.2	1.5	18.41	0.03	0.003
TD112	125.8	0.5	5.59	1.8	16.04	0.01	<0.002
TD114	1.8	0.3	5.34	0.2	18.14	0.03	0.007
TD115	44	0.4	6.25	2.5	20.35	0.04	0.018
TD116	52.1	0.3	5.01	2.2	21.22	0.15	0.002
TD117	84.7	0.3	5.82	4.8	19.65	0.13	0.005
TD123	56.5	0.3	3.31	0.8	21.4	0.28	0.005
TD124	44.5	0.2	1.92	0.4	16.22	0.35	0.005

	Se	Te	Tl	Ag	Cu	Pb	Zn
method	**MA250**	**MA250**	**MA250**	**MA401**	**MA401**	**MA401**	**MA401**
range	**PPM**	**PPM**	**PPM**	**PPM**	**%**	**%**	**%**
detection limit	**0.3**	**0.05**	**0.05**	**1**	**0.001**	**0.01**	**0.01**
Sample#							
TD001	<0.3	<0.05	0.71	N.A.	N.A.	N.A.	N.A.
TD002	<0.3	<0.05	1.81	N.A.	N.A.	N.A.	N.A.
TD003	<0.3	0.09	0.23	N.A.	N.A.	N.A.	N.A.
TD006	1	0.19	2.59	N.A.	N.A.	N.A.	N.A.
TD007	<0.3	0.16	3.1	N.A.	N.A.	N.A.	N.A.
TD008	2.6	0.15	2.28	N.A.	N.A.	N.A.	N.A.
TD009	7.4	0.33	1.53	N.A.	N.A.	N.A.	N.A.
TD010	2.6	0.12	2.21	N.A.	N.A.	N.A.	N.A.
TD011	2.2	<0.05	1.59	N.A.	N.A.	N.A.	N.A.
TD013	1.5	0.1	1.8	N.A.	N.A.	N.A.	N.A.
TD014	<0.3	0.46	1.62	N.A.	N.A.	N.A.	N.A.
TD016	3.9	0.14	1.29	N.A.	N.A.	N.A.	N.A.
TD023	<0.3	0.65	0.34	N.A.	N.A.	N.A.	N.A.
TD024	1.1	0.56	0.22	N.A.	N.A.	N.A.	N.A.
TD026	1	<0.05	1.42	N.A.	N.A.	N.A.	N.A.
TD027	<0.3	0.26	0.53	N.A.	N.A.	N.A.	N.A.
TD029	3.6	0.12	0.93	N.A.	N.A.	N.A.	N.A.
TD030	1.2	0.11	0.73	N.A.	N.A.	N.A.	N.A.
TD031	1.5	0.15	0.97	N.A.	N.A.	N.A.	N.A.
TD035	<0.3	0.13	0.61	N.A.	N.A.	N.A.	N.A.
TD037	<0.3	0.13	0.51	N.A.	N.A.	N.A.	N.A.
TD039	<0.3	0.15	1.17	N.A.	N.A.	N.A.	N.A.
TD040	<0.3	0.11	0.33	N.A.	N.A.	N.A.	N.A.
TD041	1.8	0.39	0.8	N.A.	N.A.	N.A.	N.A.
TD042	<0.3	0.42	0.69	N.A.	N.A.	N.A.	N.A.
TD045	<0.3	<0.05	1.36	N.A.	N.A.	N.A.	N.A.
TD046	<0.3	0.58	0.9	N.A.	N.A.	N.A.	N.A.
TD047	1.3	0.09	1.19	N.A.	N.A.	N.A.	N.A.
TD048	0.8	0.17	0.67	N.A.	N.A.	N.A.	N.A.
TD049	3.6	0.17	1.53	N.A.	N.A.	N.A.	N.A.
TD050	<0.3	<0.05	0.47	N.A.	N.A.	N.A.	N.A.
TD051	<0.3	0.05	0.56	N.A.	N.A.	N.A.	N.A.
TD053	<0.3	0.1	0.33	N.A.	N.A.	N.A.	N.A.
TD054	<0.3	0.12	3.16	N.A.	N.A.	N.A.	N.A.
TD056	<0.3	0.06	1.29	129	0.018	<0.01	<0.01
TD057	1.3	0.07	0.63	137	0.003	0.05	0.06
TD058	<0.3	0.08	2.38	111	0.019	0.02	0.04
TD059	17.2	0.12	1.16	>1000	0.71	0.84	1.26
TD060	3.4	0.1	1.41	>1000	0.007	0.13	<0.01
TD061	1.2	<0.05	0.55	476	0.004	0.02	<0.01
TD062	3.7	1.37	<0.05	>1000	0.09	4.3	9.89
TD063	1.2	0.26	<0.05	N.A.	N.A.	N.A.	N.A.
TD066	<0.3	0.06	0.59	N.A.	N.A.	N.A.	N.A.
TD068	1.7	0.62	1.05	N.A.	N.A.	N.A.	N.A.
TD069	2.3	0.72	<0.05	N.A.	N.A.	N.A.	N.A.
TD070	<0.3	<0.05	3.04	N.A.	N.A.	N.A.	N.A.
TD072	<0.3	<0.05	0.61	N.A.	N.A.	N.A.	N.A.
TD073	7.2	0.16	0.19	>1000	0.715	2	3.14
TD074	1.1	<0.05	1.51	389	0.015	0.04	0.07

	Se	Te	Tl	Ag	Cu	Pb	Zn
method	**MA250**	**MA250**	**MA250**	**MA401**	**MA401**	**MA401**	**MA401**
range	**PPM**	**PPM**	**PPM**	**PPM**	**%**	**%**	**%**
detection limit	**0.3**	**0.05**	**0.05**	**1**	**0.001**	**0.01**	**0.01**
Sample#							
TD075	<0.3	<0.05	1.48	N.A.	N.A.	N.A.	N.A.
TD076	1.8	1.1	<0.05	N.A.	N.A.	N.A.	N.A.
TD077	1.5	1.32	<0.05	N.A.	N.A.	N.A.	N.A.
TD083	0.7	0.31	1.3	N.A.	0.023	N.A.	N.A.
TD084	<0.3	0.17	0.72	N.A.	0.021	N.A.	N.A.
TD086	2.3	1.6	0.19	N.A.	N.A.	N.A.	N.A.
TD088	<0.3	0.13	0.9	N.A.	N.A.	N.A.	N.A.
TD090	0.5	0.18	<0.05	4	0.034	0.07	0.08
TD091	7	0.14	0.79	N.A.	N.A.	N.A.	N.A.
TD093	0.4	<0.05	1.44	N.A.	N.A.	N.A.	N.A.
TD097	1.1	<0.05	<0.05	N.A.	N.A.	N.A.	N.A.
TD098	<0.3	0.12	<0.05	N.A.	N.A.	N.A.	N.A.
TD099	0.6	0.12	<0.05	N.A.	N.A.	N.A.	N.A.
TD101	0.3	0.12	<0.05	N.A.	N.A.	N.A.	N.A.
TD102	<0.3	0.15	<0.05	N.A.	N.A.	N.A.	N.A.
TD103	<0.3	0.17	<0.05	N.A.	N.A.	N.A.	N.A.
TD110	0.9	0.08	0.53	N.A.	N.A.	N.A.	N.A.
TD111	<0.3	<0.05	0.9	N.A.	N.A.	N.A.	N.A.
TD112	0.4	0.16	1.21	N.A.	N.A.	N.A.	N.A.
TD114	<0.3	0.47	<0.05	N.A.	N.A.	N.A.	N.A.
TD115	1.8	0.22	0.77	N.A.	N.A.	N.A.	N.A.
TD116	0.7	<0.05	0.41	N.A.	N.A.	N.A.	N.A.
TD117	0.5	<0.05	0.79	N.A.	N.A.	N.A.	N.A.
TD123	0.5	0.15	0.48	N.A.	0.059	N.A.	N.A.
TD124	4.1	3.78	0.59	N.A.	0.079	N.A.	N.A.

All samples were analyzed at Bureau Veritas Minerals, Vancouver, BC with the following methods: **MA250** = multi-acid digestion method and Ultra-trace ICP-ES/MS method for trace elements. **MA401** = Aqua regia and multi-acid digestions with AAS analysis for ore grade samples.

APPENDIX 6: Fluid Inclusion Data

Sample#	Location	Size (microns)	Phases	V/L (%)	Te (°C)	Tm ice (°C)	Tm salt (°C)	Th V-L (°C)	Th (°C)	Salinity (wt%)
TD084	Baker	12	SLV	5	NM		310.1	255.7	310.1	39.66
TD084	Baker	6	SLV	10	-40?		436	355.7	436	51.75
TD084	Baker	6	SLV	20	-45?		407	467	467	48.02
TD084	Baker	8	SLV	2	-42?		476	170	476	50.77
TD084	Baker	3	SLV	15	NM		315	549	549	39.04
TD084	Baker	7	SLV	30	-43?		319	556	556	39.31
TD074	Baker	4.5	LV	20	-43.3	-0.8		196	196	1.4
TD074	Baker	2.5	LV	30	-39.8?	-0.6		232	232	1.05
TD074	Baker	2.5	LV	30	-45.2	-1.5		259.8	259.8	2.57
TD074	Baker	3	LV	30	-39.3	-0.3	358	338	338	0.53
TD074	Baker	3	LV	50	-41.2?	-0.6			358	1.05
TD051	Black Gossan	3.5	LV	10	NM	-0.6		142.4	142.4	1.05
TD051	Black Gossan	6	LV	10	NM			245.4	245.4	3.23
TD051	Black Gossan	5	LV	30	NM	-2.4		255.9	255.9	4.03
TD051	Black Gossan	3	LV	20	-42?	-0.5		266	266	0.88
TD051	Black Gossan	4	LV	10	-45?	-0.9		266	266	1.57
TD051	Black Gossan	7	LV	20	-45?	-0.5		313.4	313.4	0.88
TD051	Black Gossan	7.5	SLV	10	NM		266	218.9	266	36.32
TD051	Black Gossan	7	SLV	5	-52.5?		340	168	340	41.58
TD051	Black Gossan	2	SLV	50	NM		393	456.2	456.2	46.52
TD049	Black Gossan	6.5	LV	10	-43.5	-0.3		277.6	277.6	0.53
TD049	Black Gossan	3	LV	15	NM	-5.2		286.4	286.4	8.14
TD049	Black Gossan	4	LV	25	NM	-1.3		306.7	306.7	2.24
TD049	Black Gossan	6	LV	15	-44.3	-5.1		321	321	8
TD049	Black Gossan	10	LV	10	-51.8	-0.7		397.2	397.2	1.22
TD121	Qtz-Lake	9	LV	10	-40.7?	0.0?		147.5	147.5	0
TD121	Qtz-Lake	6	LV	5	-42.6?	-0.9		159.5	159.5	1.57
TD121	Qtz-Lake	2	LV	40	-36?	0.0?		202.7	202.7	0
TD121	Qtz-Lake	2.5	LV	30	-42?	-2.4		342.5	342.5	4
TD123	Sofia	5	LV	5	-42?	-2.2		159.8	159.8	3.71
TD123	Sofia	9	LV	10	NM	-3		180.4	180.4	4.96
TD123	Sofia	5	LV	5	-44?	-2.1		198.7	198.7	3.55
TD123	Sofia	5.5	SLV	5	-53.6?		460	155	460	48.8
TD123	Sofia	10	SLV	1	-65?	10.8?	>570	180.3	570	46.79

NM = not measured, Te = Temperature of eutectic, Tm ice = temperature of final ice melting, Tm salt = temperature of final salt melting, Th L-V = temperature of liquid-vapore homogenization, Th = temperature of final homogenization.